Dissertation

submitted to the

Combined Faculty of Natural Sciences and Mathematics

of the Ruperto Carola University Heidelberg, Germany

for the degree of

Doctor of Natural Sciences

Presented by

Dipl. Biol. Christina S. Schüßler

born in: Aschaffenburg, Germany

Oral examination: 10.07.2020

No Tertiary relicts? A biogeographical study on the Macaronesian laurel forest species in *Daucus* (Apiaceae), *Geranium* (Geraniaceae), *Gesnouinia* (Urticaceae), *Phyllis* (Rubiaceae), *Semele* (Asparagaceae) and *Visnea* (Pentaphylacaceae)

Referees: Prof. Dr. Marcus A. Koch
PD Dr. Mike Thiv

Contents

Abstract **7**

Summary 7

Zusammenfassung 9

1. General Introduction **11**

1.1. (Oceanic) Islands as biogeographical model systems 11

1.2. Macaronesia and the laurel forest 12

1.2.1. Geological origin of Macaronesia 12

1.2.2. Macaronesian vegetation types 13

1.2.3. Macaronesian laurel forest 15

1.2.4 Biogeographical hypotheses 17

1.3. Model species 19

1.4. Aims of the study 32

2. General Material & Methods **35**

2.1. Sampling 35

2.2. Molecular analysis 35

2.2.1. DNA extraction, PCR and sequencing 35

2.2.2. Phylogenetic inference 38

2.2.3. Molecular dating 38

2.2.4. Ancestral area reconstruction 39

2.3. Morphological and anatomical analyses 41

2.3.1. Microtome sections 41

2.3.2. MicroCT Scans 41

2.3.3. Ancestral character state estimation 41

2.3.4. Phylogenetic analysis 42

2.3.5. Multivariate statistics 42

3. Potential Tertiary relicts: lineages and taxa of Oligocene, Miocene or Early Pliocene origin **43**

3.1. *Visnea mocanera* (Pentaphylacaceae) 45

3.1.1. Specific Material and Methods 45

3.1.2. DNA sequence variation and phylogenies 54

3.1.3. Molecular dating: Oligocene origin and Plio-/Pleistocene diversification 55

3.1.4. Biogeographic reconstructions: Macaronesian, European or Macaronesian-European origin 57

3.1.5. Fruit anatomy: Microtome, hand and MCT sections 57

3.1.6. Phylogenetic analysis of morphological data: Unresolved relationships 67

3.1.7. Multivariate statistics on morphological traits: Possible closeness of *Visnea mocanera* and *V. germanica* 67

3.1.8. Discussion 71
3.2. *Geranium reuteri*, *G. maderense*, *G. palmatum* and *G.yeoi* (Geraniaceae) 79
3.2.1. Specific Material and Methods 79
3.2.2. DNA sequence variation and phylogenies 82
3.2.3. Molecular dating: Late Miocene origin and diversification of the laurel forest lineage 84
3.2.4. Biogeographic reconstructions: Mediterranean origin 87
3.2.5. Discussion 88
3.3. *Semele androgyna* and *S. gayae* (Asparagaceae) 91
3.3.1. Specific Material and Methods 91
3.3.2. DNA sequence variation and phylogenies 94
3.3.3. Molecular dating: Late Miocene stem and Early Pleistocene crown age 95
3.3.4. Biogeograhic reconstruction: Origin in Macaronesia or Eurasia-Macaronesia 96
3.3.5. Discussion 96
3.4. *Daucus elegans* (Apiaceae) 98
3.4.1. Specific Material and Methods 98
3.4.2. DNA sequence variation and phylogenies 100
3.4.3. Molecular dating: Late Miocene origin and Middle Pleistocene diversification 101
3.4.4. Biogeographic reconstruction: Mediterranean or Macaronesian-Mediterranean origin 103
3.4.5. Discussion 103
3.5. *Phyllis nobla* (Rubiaceae) 105
3.5.1. Specific Material and Methods 105
3.5.2. DNA sequence variation and phylogenies 108
3.5.3. Molecular dating: Early Pliocene origin and Middle Pleistocene diversification 110
3.5.4. Biogeography: Macaronesian origin 110
3.5.5. Discussion 112
4. Non-relicts: Pleistocene origin 115
4.1. *Gesnouinia arborea* (Urticaceae) – An example of an insular woody laurel forest species? 115
4.1.1. Specific Material and Methods 115
4.1.2. DNA sequence variation and phylogenies 118
4.1.3. Molecular dating: Early Pleistocene origin and Middle Pleistocene diversification 121
4.1.4. Biogeographic reconstructions: Macaronesian origin 121
4.1.5. Stem sections: Derived woodiness in *G. arborea* and *G. filamentosa* 121
4.1.6. Character state optimization of woodiness: Woody traits already present

prior to colonization of Macaronesia 122
4.1.7. Discussion 125
5. Conclusions 131
References 137
Appendix 151
Acknowledgements 159

List of Figures

Figure 1. Laurel forest habitat 15
Figure 2. *Gesnouinia arborea* and putatively closely related taxa 20
Figure 3. *Visnea mocanera* and related taxa from Pentaphylacaceae s.str. 22
Figure 4.´ Selected laurel forest geraniums and putatively closely related species 25
Figure 5. *Phyllis nobla* and its closest relative 27
Figure 6. *Semele* and closely related species 28
Figure 7. *Daucus elegans* 30
Figure 8. Stem ages of 33 Macaronesian laurel forest species/lineages 43
Figure 9. Crown ages of 26 Macaronesian laurel forest species/lineages 44
Figure 10. Italian *Visnea germanica* fossils 47
Figure 11. Chronograms from stem node and crown node dating in *Visnea* 56
Figure 12. Biogeography of Pentaphylacaceae s.str. 58
Figure 13. Young and more mature fruits of *Visnea mocanera*, sectioned by hand 59
Figure 14. MicroCT images of *Visnea mocanera* 60
Figure 15. MicroCT images of extant Pentaphylacaceae s.str., longitudinal view 62
Figure 16. MicroCT images of extant Pentaphylacaceae s.str., transverse view 63
Figure 17. MicroCT images of *Visnea germanica*, longitudinal view 65
Figure 18. MicroCT images of *Visnea germanica*, transverse view 66
Figure 19. Multidimensional scaling analysis of the metric traits 67
Figure 20. Multidimensional scaling analysis of the ordinal scaled traits 68
Figure 21. Dendrogram from hierarchical cluster analysis using the average linkage method.. 69
Figure 22. Dendrogram from hierarchical cluster analysis using the single linkage method 71
Figure 23. Stem age estimates for *Visnea* 78
Figure 24. Biogeography of *Geranium* subg. *Robertium* 84
Figure 25. Nuclear phylogeny (ETS & ITS) of *Geranium* sect. *Robertium* and *Geranium* sect. *Unguiculata* from ML analysis 85
Figure 26. Chronograms from stem node and crown node dating in *Geranium* 86
Figure 27. Distribution and sampling of *Semele androgyna* and *S. gayae* on the Canary Islands.… 91
Figure 28. Distribution and sampling of *Semele androgyna* on Madeira. 92
Figure 29. Biogeography of Rusceae 94
Figure 30. Chronograms from stem node and crown node dating in *Semele* 95
Figure 31. Biogeography of *Daucus* sect. *Daucus* and *Daucus* sect. *Melanoselinum* .. 101
Figure 32. Chronograms from stem node and crown node dating in *Daucus* 102
Figure 33. Biogeography of Anthospermeae as inferred from BBM analysis in RASP, based on the plastid chronogram 109
Figure 34. Chronograms from stem node and crown node dating in *Phyllis* 111
Figure 35. Biogeography of Parietarieae 119
Figure 36. Chronograms of the perennial clade of Parietarieae 120
Figure 37. Evolution of woody traits (life-form, habit quotient, continuity of wood cylinder throughout the stem) in Parietarieae 125
Figure 38. Biogeographic affinity of Macaronesian laurel forest as inferred from 36 species/lineages 132

List of Tables

Table 1. Fossil record of *Visnea* based on literature 23
Table 2. Markers selected for phylogenetic analyses 35
Table 3. Cycling profiles and primers 36
Table 4. Genera of Pentaphylacaceae s.str. 45
Table 5. Fossils of *V. germanica* analyzed in this study 46
Table 6. MCMC settings for Bayesian analysis of the *Visnea* datasets using MrBayes 48
Table 7. Coding for ancestral area estimation in Pentaphylacaceae s.str. 50
Table 8. Biogeographical models tested for the combined ITS & plastid-dataset of Pentaphylacaceae 51
Table 9. Settings for MCT scanning using the SkyScan 1272 52
Table 10. Coding for morphological analyses in Pentaphylacaceae s.str. 53
Table 11. Sequence characteristics of the Ericales and Pentaphylacaceae s.str. datasets 55
Table 12. Clusters indicated by hierarchical (average linkage, complete linkage, centroid, median and Ward) clustering analyses 68
Table 13. Clusters indicated by hierarchical (single linkage) clustering analysis 70
Table 14. Clusters indicated by two step clustering 70
Table 15. Fossil record of Pentaphylacaceae from literature. 75
Table 16. Geographic sampling of *Geranium robertianum* and *G. purpureum* for phylogenetic analysis 79
Table 17. MCMC settings for Bayesian analysis of the *Geranium* datasets using MrBayes. 80
Table 18. Coding for ancestral area estimation in *Geranium* subg. *Robertium* 82
Table 19. Biogeographical models tested for the plastid-dataset of *Geranium* subg. *Robertium*.. 82
Table 20. Sequence characteristics of the *Geranium* subg. *Robertium* and Geraniaceae datasets 83
Table 21. MCMC settings for Bayesian analysis of the *Semele* datasets using MrBayes 92
Table 22. Coding for ancestral area estimation in Rusceae 93
Table 23. Biogeographical models tested for the plastid dataset of Ruscaceae 93
Table 24. Sequence characteristics of the plastid datasets of Asparagaceae 94
Table 25. MCMC settings for Bayesian analysis of the *Daucus* datasets using MrBayes 98
Table 26. Coding for ancestral area estimation in *Daucus* sect. *Daucus* and *Daucus* sect. *Melanoselinum* 99
Table 27. Biogeographical models tested for the combined ITS & *rps16* data of *Daucus* sect. *Daucus* and *Daucus* sect. *Melanoselinum* 100
Table 28. Sequence characteristics of the Apiaceae and *Daucus* datasets 100
Table 29. MCMC settings for Bayesian analysis of the *Phyllis* datasets using MrBayes . 105
Table 30. Coding for ancestral area estimation in Anthospermeae 107
Table 31. Biogeographical models tested for the plastid dataset of Anthospermeae 108
Table 32. Sequence characteristics of the Rubiaceae, Anthospermeae and Anthosperminae datasets 108
Table 33. MCMC settings for Bayesian analysis of the *Gesnouinia* datasets using MrBayes 116
Table 34. Coding for ancestral area estimation and for ancestral character state reconstruction of woodiness in Parietarieae 117

Table 35. Biogeographical models tested for the Parietarieae plastid dataset 118
Table 36. Sequence characteristics of the Parietarieae and Urticaceae datasets..... 119
Table 37. Stem anatomy of Parietarieae 123
Table 38. Climatic history of the Canary Islands 135

Abstract

Summary

The Macaronesian laurel forest is characterized by humidity-adapted, evergreen trees with glossy, entire and elongated leaves. Based on fossil data, this vegetation type has been regarded as a relict of Tertiary, European/Mediterranean forests since at least the middle of the 19th century. In contrast to that, more recent studies indicate that the Macaronesian laurel forest species may be much younger than previously thought, with the majority of the analyzed species dating to the Plio-/Pleistocene. Furthermore, they recovered a rather heterogeneous geographical origin, suggesting that the Mediterranean region, other Macaronesian vegetation zones as well as tropical areas have served as source areas for the corresponding species. Although previous analyses included quite characteristic taxa, e.g. all of the Macaronesian Lauraceae, only a small number (around 26%) of laurel forest genera has been studied to this day, most of them are woody.

In this dissertation, the biogeography of six typical and widespread Macaronesian laurel forest genera (*Daucus*, *Geranium*, *Gesnouinia*, *Phyllis*, *Semele* and *Visnea*) is studied, covering different life-forms and ecologies. Conducting molecular phylogenetic and dating analyses as well as ancestral area estimations, a) the timeframes for the colonization of Macaronesia and the laurel forest, b) the geographical origin of the colonizers and c) the timeframes for inter-archipelago and inter-island dispersal were studied. Furthermore, the usefulness of stem ages and crown ages for inferring the colonization times is tested. Additional analyses were conducted for *Gesnouinia* and *Visnea*. In *Gesnouinia*, the wood anatomy was studied as the genus was considered as potentially insular woody in previous studies, which would contradict a relict status. For *Visnea*, fossils of the extinct *V. germanica* from the Miocene to Pliocene of Germany and Italy were analyzed regarding their affinity to laurel forest *V. mocanera* using MicroCT scans.

The results obtained here provide further support for the heterogeneous origin of the Macaronesian laurel forest and indicate that stem ages should be preferred over crown ages for inferring the relict status. A relict origin of *Visnea* (Oligocene age) and the laurel forest taxa of *Geranium* (Miocene age) is very likely, whereas the situation is ambiguous in *Semele* and *Daucus*. The latter two are of Miocene age, but their phylogenetic position is poorly resolved. Laurel forest *Gesnouinia* and *Phyllis* originated within Macaronesia and are clearly no relicts from the Tertiary by their source area. Dispersal from or into the dry infra-Canarian vegetation is indicated for both genera, with the time frames differing. In *Phyllis*, dispersal falls into the Early Pliocene, whereas in *Gesnouinia*, an overlap with range-shifts associated with the Pleistocene glaciation cycles is recovered. The non-relictual trait of insular woodiness could not be unambiguously inferred for *Gesnouinia*. While woodiness in *Gesnouinia* probably is derived, it may have evolved prior to island colonization. Inter-archipelago colonization between Madeira and the Canary Islands is inferred to be young in most taxa, overlapping with Pleistocene sea-level fluctuations and the timeframes recovered for species from other Macaronesian vegetation zones. The same is found for inter-island colonization within the archipelagos.

For the Macaronesian laurel forest as a whole, the newly generated data as well as literature data indicate that there is likely no obvious relationship between time of colonization and life-form or time of colonization and the extant ecological niche occupied within the forest. Instead, data points towards a link between time of colonization and the main source area of the colonizers. In the humid climate of the Late Miocene, habitat conservative dispersal from the Mediterranean/Europe to newly emerged islands and habitat space created by catastrophic events seems to have predominated. In the still humid Early Pliocene, the influx from the Mediterranean/Europe decreased and the majority of colonizers originated within Macaronesia. During the Late Pliocene climatic deterioration (cooler, drier and increasing seasonal), dispersal from the Mediterranean, probably non-habitat conservatively, was prevalent. In the course of the Pleistocene (Early and Middle), climatic changes and range shifts associated with the glaciation cycles possibly promoted the arrival of a large amount of Macaronesian taxa. Pleistocene establishment is also indicated for a number of Mediterranean/European taxa, but restricted to the Early Pleistocene. Colonization events from Asia, the New World and (Eastern) Africa seem to be rare and likely occurred prior to the Pleistocene. They may have been facilitated by the lack of e.g. climatic, tectonic or marine barriers during certain periods of time.

Zusammenfassung

Der makaronesische Lorbeerwald zeichnet sich durch das Vorhandensein an Feuchtigkeit angepasster, immergrüner Bäume mit glänzenden, ganzrandigen und länglichen Blättern aus. Er wird seit mindestens Mitte des neunzehnten Jahrhunderts auf Grundlage von Fossilfunden als Relikt tertiärer, europäischer Wälder angesehen. Neuere Studien zeigen jedoch, dass die Mehrheit der Pflanzenarten im makaronesischen Lorbeerwald auf das Plio- oder Pleistozän zurückgeht und damit deutlich jüngeren Ursprungs ist als bislang angenommen. Des Weiteren finden sie einen relativ heterogenen geografischen Ursprung des Lorbeerwaldes, der darauf hinweist, dass der Mittelmeerraum, andere Vegetationszonen innerhalb Makaronesiens und tropische Gebiete als Quelle für seine Besiedlung fungierten. Obwohl diese Studien sehr charakteristische Taxa betrachten, insbesondere alle makaronesischen Lauraceae, beinhalten sie nur ca. 26% aller Lorbeerwaldgattungen, der Großteil davon ist holzig.

Die vorliegende Dissertation präsentiert Studien zur Biogeographie sechs typischer und weitverbreiteter Lorbeerwaldgattungen mit unterschiedlicher Lebensform und Ökologie (*Daucus*, *Geranium*, *Gesnouinia*, *Phyllis*, *Semele* und *Visnea*). Mit Hilfe molekularer phylogenetischer Analysen, molekularer Datierung und Rekonstruktionen des ursprünglichen Verbreitungsgebiets wurden a) die Zeitrahmen für die Besiedlung Makaronesiens und des Lorbeerwaldes, b) der geografische Ursprung der kolonisierenden Art und c) die Zeitrahmen für die Verbreitung zwischen den Archipelen und den Inseln ermittelt. Weiterhin wurde die Rolle von Stamm- und Kronenalter bei der Abschätzung des Zeitpunkts der Besiedlung überprüft. Zusätzliche Analysen wurden für *Gesnouinia* und *Visnea* durchgeführt. An *Gesnouinia* wurde die Holzanatomie untersucht, da die Gattung in älteren Studien als mögliches Beispiel für die Evolution von Holzigkeit auf Inseln genannt wurde; dies würde einem Reliktstatus widersprechen. Bei *Visnea* wurden verfügbare Fossilien der ausgestorbenen Art *V. germanica* aus dem Miozän und Pliozän von Italien und Deutschland untersucht, indem ihre Affinität zur Lorbeerwaldart *V. mocanera* mit Hilfe von MicroCT Scans eingeschätzt wurde.

Die Ergebnisse der vorliegenden Arbeit unterstützen den sich bereits in vorausgegangenen Studien abzeichnenden heterogenen Ursprung des makaronesischen Lorbeerwaldes und sprechen dafür, dass für die Beurteilung des Reliktstatus das Stammalter dem Kronenalter vorgezogen werden sollte. Ein Reliktcharakter der Lorbeerwaldarten der Gattungen *Visnea* (oligozäner Ursprung) und *Geranium* (miozäner Ursprung) ist sehr wahrscheinlich, wohingegen sich die Situation bei *Semele* und *Daucus* als nicht eindeutig darstellt. Der Ursprung der beiden letzteren wurde auf das Miozän geschätzt, allerdings wäre aufgrund der schlecht aufgelösten phylogenetischen Position auch ein jüngeres Alter denkbar. Die Lorbeerwaldarten von *Gesnouinia* und *Phyllis* sind innerhalb Makaronesiens entstanden und wegen ihres Ursprungsgebiets keine Relikte. Für beide zeigt sich, dass sie vermutlich entweder den Lorbeerwald aus der trockenen infra-kanarischen Vegetation besiedelt haben oder umgekehrt. Die Zeitfenster für diese Besiedlung unterscheiden sich jedoch. Bei *Phyllis* fand sie während des frühen Pliozäns statt, bei *Gesnouinia* überlappt sie mit den Arealverschiebungen durch die Kalt- und Warmzeitzyklen des frühen Pleistozäns.

Ob die Holzigkeit von *Gesnouinia* auf Inseln entstanden ist, was ebenfalls gegen einen Reliktcharakter sprechen würde, konnte nicht abschließend geklärt werden. Die Holzigkeit der Gattung ist zwar vermutlich sekundär entstanden, möglicherweise jedoch bereits vor einer Inselbesiedlung.

Die Ausbreitung aller untersuchten Lorbeerwaldgattungen zwischen den Archipelen (Madeira und Kanaren) ist größtenteils jung und überschneidet sich sowohl mit den Meeresspiegelschwankungen des Pleistozäns als auch mit den Zeitfenstern, die für Arten aus anderen Vegetationszonen gefunden wurden. Dasselbe ist für die Ausbreitung zwischen den Inseln innerhalb der Archipele der Fall.

Für den makaronesischen Lorbeerwald in seiner Gesamtheit ergibt sich aus der Kombination der neuen Daten mit der bestehenden Literatur, dass es keinen deutlich sichtbaren Zusammenhang zwischen Kolonisationszeitpunkt und Lebensform oder Kolonisationszeitpunkt und gegenwärtiger ökologischer Nische innerhalb des Waldes gibt. Stattdessen deutet sich an, dass die geographische Region, aus der der Großteil der besiedelnden Arten stammt, über die Zeit hinweg wechselte. Während des humiden Klimas des späten Miozäns fand vermutlich hauptsächlich eine habitatkonservative Besiedlung von neu aus dem Meer auftauchenden Inseln und von neuem, durch Katastrophen entstandenem Habitat durch Arten aus dem Mittelmeerraum/Europe statt. Im weiterhin warmen, frühen Pliozän hingegen waren die meisten kolonisierenden Arten wahrscheinlich makaronesischen Ursprungs. Als sich das Klima im späten Pliozän zu kühler und trockener mit ausgeprägten Jahreszeiten veränderte, könnte wieder Besiedlung aus dem Mittelmeer/Europa dominiert haben. Diese war vermutlich nicht mit Habitatkonservativität verbunden. Im sich anschließenden Pleistozän (Frühes und Mittleres) förderten möglicherweise Arealverschiebungen durch die Zyklen von Kalt- und Warmzeiten die Ausbreitung von makaronesischen Arten aus anderen Vegetationszonen in den Lorbeerwald. Eine pleistozäne Besiedlung findet sich auch für eine Reihe von Arten aus dem Mittelmeer/Europa, könnte jedoch hier auf das frühe Pleistozän beschränkt sein. Kolonisation des Lorbeerwaldes aus Asien, der neuen Welt und (Ost-) Afrika scheint relativ selten zu sein und fand wahrscheinlich vor Beginn des Pleistozäns statt. Sie wurde vermutlich durch die Abwesenheit klimatischer, tektonischer und mariner Barrieren innerhalb bestimmter Zeiträume befördert.

1. General Introduction

1.1. (Oceanic) Islands as biogeographical model systems

The text of the following paragraph is derived and extended from Schüßler, Bräuchler, Reyes-Betancort, Koch, & Thiv (2019) and has been originally written by myself:

Islands are biogeographical model systems for colonization, speciation and evolution, e.g. MacArthur & Wilson (2001), Whittaker, Triantis, & Ladle (2008), Fernández-Palacios et al. (2015) and Otto et al. (2016). Based on the mode and degree of isolation, Wallace (1902) and Whittaker & Fernández-Palacios (2007) recognize three types of islands, i.e., oceanic islands, continental fragment islands and continental islands. Of those, oceanic islands are especially interesting for the study of evolution and speciation. They are of volcanic origin, have never been connected to mainland, e.g. the Macaronesian Islands, Hawaii and Galapagos (Whittaker & Fernández-Palacios, 2007), and constitute isolated systems that usually contain high levels of endemism (Whittaker & Fernández-Palacios, 2007). Thus, long distance dispersal (LDD) plays an important role in their colonization, with founder event speciation as the main mode of building up the basis of species composition (Carlquist, 1974; Whittaker & Fernández-Palacios, 2007). LDD can be facilitated by wind and marine currents, e.g. in case of Macaronesia northeastern trade winds and the cool Canarian current, or low Pleistocene sea levels (Whittaker & Fernández-Palacios, 2007). Support for the presence of LDD comes from the disharmony of the island floras, which means that certain taxonomic groups are under- or overrepresented due to the polar island climate and the water barrier acting as filter for colonization and establishment (Carlquist, 1974). As an alternative to LDD, vicariance, i.e. the emergence of a barrier (e.g, climatic or tectonic) splitting a continuous range in two or more parts, has also been suggested by some authors, e.g. Grehan (2017). In contrast to that, Whittaker & Fernández-Palacios (2007) argue that both LDD and vicariance likely play a role in the colonization of oceanic islands, as barriers between island and source area may have varied in their strength throughout time. For the geographic origin of colonizers, it is often observed that different areas serve as source pools (Renvoize, 1979; Whittaker & Fernández-Palacios, 2007). Temporally, distinct windows of time for colonization have been indicated by e.g. Kim et al. (2008). These windows are usually inferred from stem ages. A recent study by García-Verdugo, Caujapé-Castells, & Sanmartín (2019), however, suggests crown ages to be a more appropriate measurement, as species often diversify shortly after colonization. Subsequent to colonization, species are often found to strongly differ morphologically from their mainland relatives because of adaptation and processes linked to geographic isolation. For example, island species differ from mainland relatives by insular woodiness, dwarfism and gigantism, e.g., Carlquist (1974), Meiri, Cooper, & Purvis (2008) and Losos & Ricklefs (2009).

1.2. Macaronesia and the laurel forest

The biogeographic region of Macaronesia was named by Philip Barker Webb in 1845. The term is derived from the Greek and means “Islands of the Blessed”, likely referring to the Roman name of the Canary Islands, i.e. Insulae Fortunatae (Stearn, 1973). Macaronesia comprises the Canary Islands, Madeira, the Salvage Islands, the Azores, the Cape Verde Islands and an enclave on the African mainland (Sunding, 1979; Takhtajan, 1986). Thus, it extends from 40°N to 15°N and covers a range of climates from cool-oceanic to an oceanic tropical monsoon-drift climate (Whittaker & Fernández-Palacios, 2007). The distance of the islands to the mainland varies between ca. 96 km to ca. 1370 km (Whittaker & Fernández-Palacios, 2007). Based on shared elements of the flora, Kunkel (1993) distinguishes Central Macaronesia (Canary Islands and Madeira), Lauri Macaronesia (Canary Islands, Madeira, Azores and an enclave on the Iberian Peninsula) and Great Macaronesia (all of Macaronesia). The term Macaronesia, however, is likely not appropriate for all organisms. For example, it has recently been proposed to replace Macaronesia with Webbnesia, a region comprising Madeira, the Salvage Islands and the Canary Islands, in marine taxa (Freitas et al., 2019).

1.2.1. Geological origin of Macaronesia

The Macaronesian archipelagos comprise volcanic islands of different ages and stages in their life cycle (Fernández-Palacios et al., 2011). The majority of them originated from volcanism within the African Plate, whereas the Azores formed due to volcanism in the mid-atlantic ocean ridge (Whittaker & Fernández-Palacios, 2007). Although the Canary Islands and Madeira have their origin within the same plate, they were built by separate hotspot systems (Geldmacher, Hoernle, Bogaard, Duggen, & Werner, 2005).

Islands above sea level are found in the Macaronesian region at least since 60 million years ago [mya](Fernández-Palacios et al., 2011). In the timeframe of 60-25 mya, further paleo-Macaronesian islands emerged and submerged again (Fernández-Palacios et al., 2011; Geldmacher et al., 2005; Geldmacher, Hoernle, van den Bogaard, Zankl, & Garbe-Schönberg, 2001). The oldest of the current Macaronesian islands, Selvagem Grande, emerged 27 mya (Fernández-Palacios et al., 2011; Geldmacher et al., 2001). Between 21-1.1 mya, the extant Canary Islands rose above sea-level. Ca. 14 mya, Porto Santo, and ca. 5 mya, the main island of Madeira and Desertas emerged (Geldmacher, van den Bogaard, Hoernle, & Schmincke, 2000).

The different life stages represented by the Canarian, Madeiran and Salvage Islands are described by Fernández-Palacios et al. (2011) and Fernández-Palacios & Whittaker (2010). According to their data, an island in the stage of underwater birth and construction (stage A) is exemplified in the Canarian hotspot by Las Hijas, located southwest of El Hierro. The stage of island emergence and continuing construction above sea-level (stage B) is found in e.g. La Palma, El Hierro and Tenerife. Examples for stage C, in which erosion and dismantling prevail, are Madeira, Gran Canaria and La Gomera. A flattened plain (stage D) is observed in Porto Santo and Selvagem Grande. In stage E, the island submerges, like e.g. Selvagem Pequena and Ilheu de Fora. In the final stage, stage F, the island is reduced to a

seamount with flattened summit, as observed in the palaeo-madeiran Seine, Coral Patch and Unicorn and the palaeo-canarian Amanay, Conception and Dacia.

1.2.2. Macaronesian vegetation types

In the following, the vegetation zones of the laurel forest harboring Macaronesian archipelagos will be described.

Canary Islands

The vegetation of the Canary Islands can be divided in three major zones, 1) beneath the clouds (infra-canarian), 2) within the clouds (thermo- and meso-canarian) and 3) above the clouds (supra-canarian and oro-canarian; Hohenester & Welss, 1993). Not all of the zones are found on every Canarian Island, e.g. the third zone is missing on the more eroded eastern islands of Lanzarote and Fuerteventura as well as on the western islands of Gran Canaria, La Gomera and El Hierro (Schönfelder & Schönfelder, 1997).

The infra-canarian zone comprises dune and coastal vegetation as well as the succulent scrub. The first, i.e. coastal and dune vegetation, is characterized by dryness and salinity and provides a habitat to species like *Astydamia latifolia* Baill., *Limonium pectinatum* Kuntze, *Traganum moquinii* Webb ex Moq. and *Euphorbia aphylla* Brouss. (Schönfelder & Schönfelder, 1997). The second, i.e. the succulent scrub, is a rather dry habitat with 100-245 mm precipitation per year (Ehrig, 1998). It extends to an elevation of ca. 100-200 mm, on the easternmost islands even to 800 m (Schönfelder & Schönfelder, 1997). Typical species are e.g. *Kleinia neriifolia* Haw., *Euphorbia canariensis* L. and *Plocama pendula* Aiton (Ehrig, 1998).

The thermo-canarian zone includes thermophilous woodlands and laurel forests. Thermophilous woodlands are found at an elevation at ca. 200 m on the north sides and at ca. 900 m on the south sides and harbor species like *Olea europaea* subsp. *cerasiformis* (Webb & Berthel.) G.Kunkel & Sunding, *Juniperus turbinata* subsp. *canariensis* (Guyot) Rivas Mart., Wildpret & P.Pérez and *Pistacia atlantica* Desf. (Schönfelder & Schönfelder, 1997). Laurel forests occur at ca. 500-1100 m elevation (minimum 200 m; Schönfelder & Schönfelder, 1997). It is restricted to the north sides of Gran Canaria, Tenerife, La Gomera, La Palma and El Hierro (Hohenester & Welss, 1993) and will be described later on in more detail.

The meso-canarian zone is build up by pine forest. On the north sides, it is found at an elevation of 900-2000 m, on the south sides at 600-900 m (Schönfelder & Schönfelder, 1997). The precipitation is higher on the north sides (ca. 700 mm) and lower on the south sides (ca. 469 mm; Ehrig, 1998) but in general lower than in the laurel forerst (Schönfelder & Schönfelder, 1997). The only tree growing in this type of vegetation is *Pinus canariensis* C.Sm. ex DC. (Kunkel, 1993).

The supra-canarian zone is restricted to Tenerife and La Palma, where it occurs at ca. 2000-3000 m altitude (Hohenester & Welss, 1993; Schönfelder & Schönfelder, 1997). It is of subalpine nature and characterized by rather extreme climatic temperature, i.e. -13°C in the winter and up to 58°C in the summer, and a high intensity of UV radiation (Schönfelder & Schönfelder, 1997). Taxa tolerating this kind of habitat are e.g. *Spartocytisus supranubius*

(L.f.) A.Santos, *Pterocephalus lasiospermus* Link and *Echium wildpretii* H.Pearson ex Hook.f. (Hohenester & Welss, 1993).

The oro-canarian zone is only found on the summit of Tenerife, at an altitude of more than 2600-3100 m (Ehrig, 1998). It is built up by a few herbaceous plants like *Viola cheiranthifolia* Bonpl. (Schönfelder & Schönfelder, 1997).

Madeira

The island of Madeira was originally dominated by forest (Capelo, Sequeira, Jardim, Mesquita, & Costa, 2005). Today, Press & Short (1994) recognize three main vegetation types, i.e. coastal vegetation, laurel forest and upland vegetation. These three types can be subdivided further, see e.g. Capelo et al. (2005).

The coastal vegetation occurs from sea level up to an elevation of 100 m in the North and up to an elevation of 300 m in the South (Press & Short, 1994). It is mainly built up by herbs and shrubs, e.g. *Globularia salicina* Lam., *Euphorbia piscatoria* Aiton and *Echium nervosum* W.T.Aiton, but also includes trees, e.g *Sideroxylon mirmulans* R.Br. and *Helichrysum melaleucum* Rchb. (Capelo et al., 2005; Press & Short, 1994).

The Madeiran laurel forest originally comprised a drier and a humid part (Press & Short, 1994). Now, it is reduced to its humid part at an altitude of 300-1300 m on the North side and 700-1200 m on the South side (Press & Short, 1994). Therein, species like *Laurus novocanariensis* Rivas Mart., Lousã, Fern.Prieto, E.Días, J.C.Costa & C.Aguiar, *Persea indica* Spreng., *Ocotea foetens* (Aiton) Baill. and *Clethra arborea* Aiton, are found (Press & Short, 1994).

The upland vegetation is recovered in elevations above the laurel forests. Its characteristic species include *Erica arborea* L., *Vaccinium padifolium* Sm. and *Erica cinerea* L. (Press & Short, 1994).

Azores

As none of the species analyzed in this dissertation is distributed on the Azores, their vegetation will only be described briefly. Like Madeira, the Azores were nearly completely covered in wood once (Dias, Mendes, Melo, Pereira, & Elias, 2005). Due to extensive forestry, native vegetation is mostly restricted to remote areas, volcanic craters, cliffs on the coast and steep hills in the mountains (Schäfer, 2005).

The vegetation types on the Azores have been divided differently by e.g. Dias et al. (2005) and Schäfer (2005). Dias et al. (2005) distinguish coastal vegetation, humid vegetation, forests, atlantic heathlands, grasslands and formations of recent lavas. Natural Azorean vegetation types according to Schäfer (2005) are 1) coastal vegetation dominated by *Festuca petraea* Guthn. ex Seub. 2) natural pastures above 700 m and in craters (*Festuca jubata* Lowe, *Holcus rigidus* Hochst. ex Seub., *Deschampsia foliosa* Hack.) 3) peat bogs (*Sphagnum* spec., *Eleocharis multicaulis* (Sm.) Desv.), 4) marshland, 5) laurel forest (*Laurus azorica* (Seub.) Franco, *Frangula azorica* Grubov, *Picconia azorica* (Tutin) Knobl., *Erica azorica* Hochst. ex Seub. and *Vaccinium cylindraceum* Sm.) and 6) juniper forest (*Juniperus brevifolia* Antoine, *Sphagnum spec.*).

1.2.3. Macaronesian laurel forest

Laurel forests constitute world-wide distributed plant communities of differing species composition. They are characterized by evergreen trees with laurophyllous (glossy, entire and elongated) leaves and occurs in humid, mostly frost free areas (Pott, 2005; Walter & Breckle, 1999). Although laurel forests were widely spread in the Tertiary (66.0-2.6 mya), today they occur in globally scattered fragments so that less than 1% of the area occupied by forests worldwide contains laurel forest now (Lüpnitz, 1995; Mai, 1989; Pott, 2005). One of these fragments can be found in Macaronesia. It occurs mainly on the north-facing sides of the higher, less eroded islands, where cloud formation is induced by humid, north-eastern trade winds during the late morning to early evening (Schönfelder & Schönfelder, 1997; Fig. 1A). The climate inside the laurel forest is moderate and sub-humid to humid, with the Canaries being drier than the Azores and Madeira. For the Canarian laurel forest (Fig. 1B), an air humidity of 80% and a mean annual temperature of 13-14°C in the upper and 16-17°C in the lower part are reported (Ehrig, 1998). The annual precipitation ranges from 500-800 mm (Gran Canaria) to 750-1200 mm (La Palma; Ehrig, 1998). In the laurel forest of the Azores, a mean annual temperature of 18°C and a precipitation of 1500 m are found by Dias et al. (2005). On Madeira, a humidity of 85%, a mean annual temperature of 10-16°C and a mean annual precipitation of 1800 mm (maximum 3000 mm) are described for the laurel forest by Boieiro et al. (2013) and Claudino-Sales (2019). The area occupied by laurel forest has decreased on all Macaronesian archipelagos, mainly due to human activities (Dias et al., 2005; Kunkel, 1993; Press & Short, 1994). Easily accessible parts of the forest have been severely deforested several times and true primary laurel forest is mainly found in less

Figure 1. Laurel forest habitat. **A** Cloud layer created by the trade winds at the Northern side of Tenerife; **B** Laurel forest in the Teno mountains, Tenerife.

accessible ravines (Kunkel, 1993). For example, the Madeiran laurel forest has been reduced to 27% of its original area of distribution (Press & Short, 1994). The situation reported for Gran Canaria by Kunkel (1993) was even more dramatic, with the forest being reduced to less than 1% of its original distribution.

According to Kondraskov, Schütz, et al. (2015), 100 genera, characteristic as well as non-characteristic ones, are found in the Macaronesian laurel forest. The majority of those are either shared between the Canary Islands and Madeira (38%) or shared between the Canary Islands, Madeira and the Azores (30%; Kondraskov, Schütz, et al., 2015). Only 1% of the genera occur exclusively on both the Canary Islands and the Azores and only 3% exclusively on both Madeira and the Azores (Kondraskov, Schütz, et al., 2015). The rest of the genera is restricted to one archipelago, i.e. 12% to the Canary Islands, 9% to Madeira and 7% to the Azores (Kondraskov, Schütz, et al., 2015).

The Canarian laurel forests are especially well-studied. Their tree layer comprises of ca. 20 species of 10-30 m height (Kunkel, 1993; Lüpnitz, 1995). In those, hygromorphic as well as xeromorphic adaptations are found according to Lüpnitz (1995). As xeromorphic adaptations, he considers e.g. glossy and reflecting leaves with a dense venation, a thick epidermis, a less developed spongy parenchyma and a well-developed palisade parenchyma. These features occur e.g. in the Lauraceae, *Prunus lusitanica* L. (Rosaceae) and *Visnea mocanera* L.f. (Pentaphylacaceae). The Lauraceae are characteristic for this forest type and are present with four species, which are also found in the Madeiran laurel forest (Hohenester & Welss, 1993; Press & Short, 1994). The most frequent of those is *Laurus novocanariensis*, growing in forest with closed canopy as well as in open or degraded forest (Lüpnitz, 1995; Schönfelder & Schönfelder, 1997). *Ocotea foetens* is bound to areas with high precipitation and high ground humidity (Kunkel, 1993). *Apollonias barbujana* (Cav.)Bornm. also prefers soaked ground, but rather grows on warm hills of lower elevations within the laurel forest (Lüpnitz, 1995; Schönfelder & Schönfelder, 1997). *Persea indica* is interspersed throughout the whole forest but rather forms stands in very humid localities (Lüpnitz, 1995). Further tree species include e.g. *Picconia excelsa* (Aiton) DC. (Oleaceae), *Rhamnus glandulosa* Aiton (Rhamnaceae), *Prunus lusitanica* subsp. *hixa* (Willd.) Franco (Rosaceae), *Heberdenia excelsa* Banks ex Roem. & Schult. and *Pleiomeris canariensis* (Willd.) DC. (Primulaceae) and *Visnea mocanera* (Pentaphylacaceae; Hohenester & Welss, 1993; Kunkel, 1993). The shrub layer comprises taxa like e.g. *Viburnum rigidum* Vent. (Adoxaceae), *Euphorbia mellifera* Aiton (Euphorbiaceae), *Sambucus palmensis* Link (Adoxaceae) and *Isoplexis canariensis* (L.) Don (Plantaginaceae; Kunkel, 1993; Lüpnitz, 1995). Species of lianoid growth-form are also observed in the laurel forest, e.g. *Semele androgyna* Kunth (Asparagaceae), *Smilax aspera* L. and *S. canariensis* Willd. (Smilacaceae), *Rubus bollei* Focke (Rosaceae) and *Convolvulus canariensis* L. (Convolvulaceae; Ehrig, 1998; Schönfelder & Schönfelder, 1997). Exclusive epiphytes are not found, but e.g. *Aichryson* spec. (Crassulaceae), *Davallia canariensis* (L.) Sm. (Davalliaceae) and *Polypodium macaronesicum* A.E. Bobrov (Polypodiaceae) often grow epiphytically (Kunkel, 1993; Schönfelder & Schönfelder, 1997). The composition of the herbaceous layer differs between the islands and is largely dominated by ferns, e.g. *Davallia canariensis* (Davalliaceae), *Hymenophyllum tunbrigense* (L.) Sm. (Hymenophyllaceae), *Asplenium*

adiantum-nigrum L. (Aspleniaceae) and *Woodwardia radicans* (L.) Sm. (Blechnaceae; Lüpnitz, 1995).

Widespread angiospermous elements include e.g. *Ixanthus viscosus* Griseb. (Gentianaceae), *Canarina canariensis* (L.) Vatke (Campanulaceae), *Dracunculus canariensis* Kunth (Araceae), *Geranium reuteri* Aedo & Muñoz Garm. (Geraniaceae) and *Ranunculus cortusifolius* Willd. (Ranuculaceae; Kunkel, 1993). In the upper dry edge of the laurel forest and in localities with more extreme climatic conditions as well as rocks exposed to wind, a community by the name of Fayal-brezal is found (Ehrig, 1998; Schönfelder & Schönfelder, 1997). It is characterized by the trees *Erica arborea* (Ericaceae) and *Myrica faya* Aiton (Myricaceae), which may be associated with *Ilex canariensis* Poir. (Aquifoliaceae), *Rhamnus glandulosa* (Rhamnaceae), *Isoplexis canariensis* (Plantaginaceae) and *Cedronella canariensis* (L.) Webb & Berthel. (Lamiaceae; Ehrig, 1998; Schönfelder & Schönfelder, 1997).

1.2.4 Biogeographical hypotheses

The following sections are derived and extended from Schüßler et al. (2019) and have been originally written by myself:

The Macaronesian flora, including laurel forest and non-laurel forest species, has been proposed to be closely linked to the Mediterranean flora. However, affinities to other regions, e.g. East/South Africa and America have also been suggested (Andrus, Trusty, Santos-Guerra, Jansen, & Francisco-Ortega, 2004; Kondraskov, Schütz, et al., 2015; Pokorny et al., 2014). Concerning the number of colonization events within lineages, one colonization event or multiple colonization events to Macaronesia have been indicated (Carine, Russell, Santos-Guerra, & Francisco-Ortega, 2004; Silvertown, 2004; Silvertown, Francisco-Ortega, & Carine, 2005). Additionally, back-colonization to the continent has been found (Carine et al., 2004; Caujapé-Castells, 2004), and a role of the islands as glacial refugia has been suggested (Laenen et al., 2011). Island colonization has been proposed to be linked to discrete time frames when habitat spaces became available, e.g. by climatic or volcanic events (island colonization hypothesis; e.g. Carine, 2005; Kim et al., 2008; Navarro-Pérez et al., 2015). For inter-archipelago colonization, it has been recovered that the Canary Islands often served as stepping stone for the colonization of Madeira and that dispersal between the two archipelagos coincides with the Pleistocene glaciations, e.g. Kim et al. (2008) and Spalik & Downie (2007). Intra-archipelago colonization is present and may follow various patterns, e.g. a sequence from the oldest (easternmost) to the youngest (westernmost) island (progression rule; Hess, Kadereit, & Vargas, 2000) or an East-West pattern with Tenerife (central) as starting point (Mairal, Sanmartín, et al., 2015). Within the archipelago/islands, cladogenesis as well as anagenetic speciation (Stuessy et al., 2006) may be found and have resulted in the evolution of insular woodiness in, e.g., ca. 40% of the Canarian endemic species (Lens, Davin, Smets, & del Arco, 2013).

Relict hypothesis

The Macaronesian laurel forest is commonly regarded as a Tertiary (66.0-2.6 mya) relict of the European/Mediterranean laurophyllous vegetation which gradually disappeared due to

climatic deteriorations in the Neogene (23.0-2.6 mya; Engler, 1879; Hooker, 1867; D. H. Mai, 1989). The fossil record of laurophyllous taxa in Europe and Macaronesia has been summarized in Kondraskov, Schütz, et al. (2015). It shows that *Laurus* L., *Ocotea* Aubl., *Persea* Mill. and several other Macaronesian laurel forest genera were present in Europe from the Oligocene to the Plio-/Pleistocene boundary. A colonization of Macaronesia during the Plio- or Pleistocene at the latest is indicated by the Madeiran fossil record (Kondraskov, Schütz, et al., 2015, and references therein). However, Kondraskov, Schütz, et al. (2015) discovered in an analysis on eighteen representative and mostly woody laurel forest species that the majority of them are too young to be relicts from the Tertiary.

Insular woodiness

Insular woodiness is considered as non-relictual and has been recovered for ca. 40% of the Canarian endemic species (Lens et al., 2013). Genera which evolved insular woodiness and comprise laurel forest species include e.g. *Argyranthemum* Webb, *Ixanthus* Griseb., *Sideritis* L., *Echium* L. and *Pericallis* D.Don (Lens et al., 2013). Still, the term “insular woodiness” is not strictly defined and its usage varies among authors. Carlquist (1974) and Dulin & Kirchoff (2010) refer to two concepts of insular woodiness. The first one is relictual, i.e., the woodiness is retained from ancestrally (primary) woody continental species. The second one evolved from herbaceous continental ancestors on islands and thus developed a derived (secondary) type of woodiness on the islands (Carlquist, 1974; Dulin & Kirchoff, 2010). Lens et al. (2013) only apply the term “insular woodiness” to taxa meeting the criteria of the second concept. Here, we follow the definition of insular woodiness by Lens et al. (2013). Furthermore, we use the term “derived woodiness” instead of secondary woodiness to avoid confusion with secondary xylem and, correspondingly, the term “ancestral woodiness” instead of primary woodiness.

In derived woody taxa, anatomical features like raylessness or rays with mainly square to upright cells and flat or decreasing length-on-age curves for vessel elements are found (Carlquist, 1974; Lens et al., 2013). However, the terms “woodiness” and “herbaceousness” are not strictly defined as many herbs, even annual ones, produce limited amounts of wood in their stems (Dulin & Kirchoff, 2010; Lens, Eeckhout, Zwartjes, Smets, & Janssens, 2012). To distinguish between the different scenarios, various approaches have been used. For instance, a habit quotient obtained from the ratio of the double wood cylinder thickness and stem diameter was proposed by Lens et al. (2012). Lens et al. (2013) and Kidner et al. (2015) recognized taxa with a distinct wood cylinder extending into the upper parts of the stem or the upper branches as woody. In contrast to that, Dulin & Kirchoff (2010) suggested discarding the terms “woody” and “herbaceous” to describe the growth form of plants and to use the Raunkiær classification based on perennation strategies instead.

The trigger for the evolution of this trait is still not understood (Lens et al., 2013), but potential causes may include improved competitiveness of woody taxa, higher seed production due to longevity, seasonality release and absence of herbivores or drought (Carlquist, 1974; Lens et al., 2013). Furthermore, insular woodiness has been recovered as prerequisite for plant radiations (Nürk, Atchison, & Hughes, 2019).

1.3. Model species

Woody as well as herbaceous species are studied in this dissertation, setting a special focus on the laurel forest species of *Gesnouinia* Gaudich., *Visnea* L.f. and *Geranium* L.

1) *Gesnouinia arborea*

Gesnouinia arborea (L.f.) Gaud. (Urticaceae, tribe Parietarieae), called Estrelladera or Ortegón de los montes in Spanish, is a shrub with a maximum height of 6 m (Hohenester & Welss, 1993; Fig. 2A). It is endemic to the Canary Islands and found on Gran Canaria, Tenerife, La Gomera and El Hierro (Arechavaleta, Rodríguez, Zurita, & García, 2010). The plants growing on Tenerife and El Hierro have been found to be of a more tree-like habit than on the other islands (Martín Osorio, 2008). A detailed description of the wood of *G. arborea* has been provided by Bonsen & ter Welle (1984). They found features associated with derived woodiness by Carlquist (1974) and Lens et al. (2013), e.g. square to upright ray cells. Accordingly, Carlquist (1974) treats the species as an example of an insular woody lineage. Lens et al. (2013), however, note that the species might be ancestrally woody instead.

The entire and evergreen leaves of *G. arborea* lack the thick cuticle found in Lauraceae but they show adaptation to the laurel forest habitat by possessing large palisade cells and an abaxially multilayered epidermis (Barry, 1977). In contrast to that, other closely related species from Urticaceae tribe Parietarieae, i.e. *Parietaria officinalis* L., *P. judaica* L., *P. cryptorum* K.Koch, *P. debilis* G.Forst., *P. serbica* Pančić, possess only a single layer of epidermis (Vasilevskaya & Oganesyan, 1978). The red, terminal inflorescences are paniculate and consist of monoecious flowers (Weddell, 1857). The typical condition of the genus, one female flower sharing an involucre with two male flowers, is found (Weddell, 1857). The perianth of the flowers is tetramerous (Weddell, 1857). In the male flowers, four stamens and a rudimentary ovary are present (Friis, 1993). The female flowers contain an ovary with a linear stigma (Friis, 1993) and are pollinated by wind (Martín Osorio, 2008). The fruit is an achene with no obvious adaptations to dispersal (Martín Osorio, 2008).

Gesnouinia arborea occupies open eutrophic areas of the laurel forest (Hohenester & Welss, 1993), e.g. in the undergrowth of humid ravines and fissures (Martín Osorio, 2008). It is classified as vulnerable by the Red List Spain (Martín Osorio, 2008). The species is endangered by human activities that reduce humidity in forest, e.g. draining of ground water and alterations in the courses of rivers. Further threats are exotic species reducing subterranean water, e.g. *Eucalyptus* L'Hér., deforestation, the construction of roads or recreational areas in proximity of the species, severe weather and fire.

Gesnouinia arborea is often considered the only species in genus *Gesnouinia*, e.g. Bramwell & Bramwell (1974), Hohenester & Welss (1993) and Schönfelder & Schönfelder (1997). However, some authors also attribute *Parietaria filamentosa* Webb & Berthel., a species growing rather xerophytically as half-shrub on cliffs of the Canary Islands (Tenerife, La Gomera, La Palma), to the genus (Friis, 1993; Weddell, 1857; Fig. 2B). As closest relative of Canarian endemic *Gesnouinia*, Schenck & Schimper (1907) proposed the Mediterranean endemic herb *Soleirolia* Gaudich. (Fig. 2C), considering both genera as possible Tertiary

relicts. A different hypothesis comes from Engler (1879), who assumes that *Gesnouinia* is close to the Mediterranean species in *Parietaria* L. (Fig. 2D).

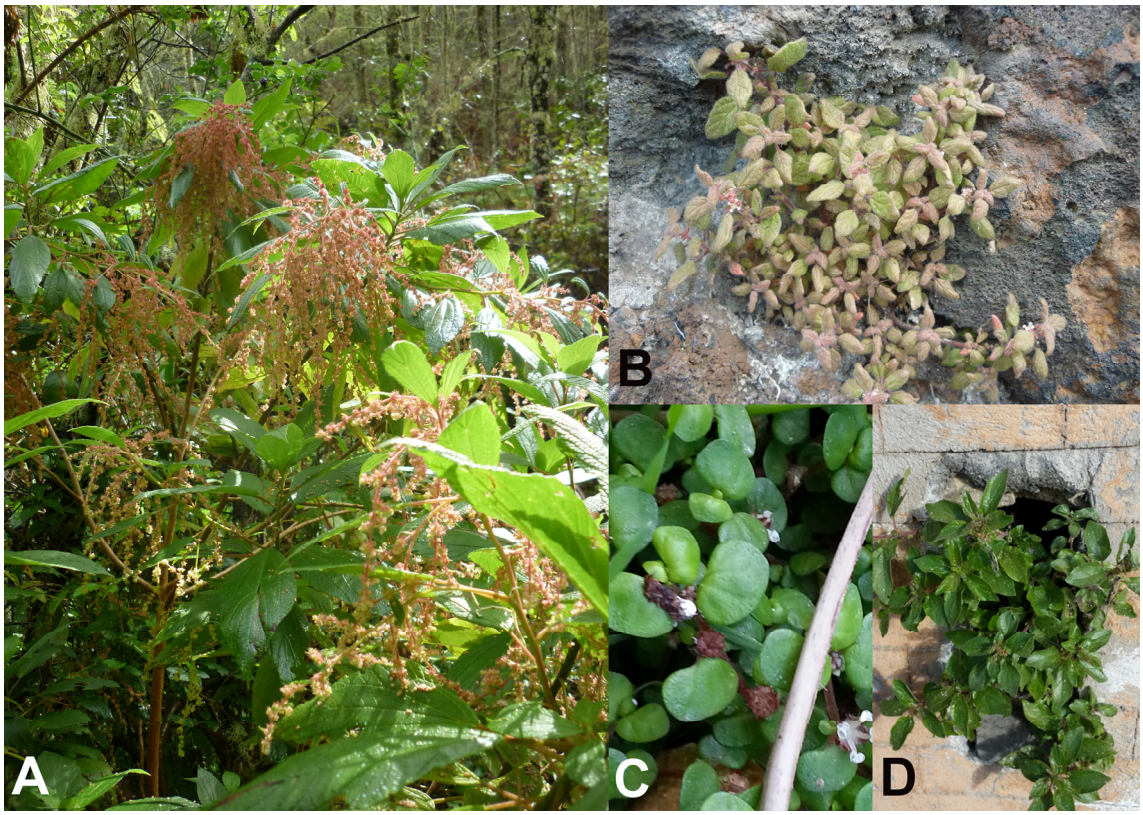

Figure 2. *Gesnouinia arborea* and putatively closely related taxa. **A** *G. arborea*; **B** *G. filamentosa*; **C** *Soleirolia soleirolii* (photo by M. Thiv); **D** *Parietaria spec.*

2) *Visnea mocanera*

Visnea mocanera (Pentaphylacaceae, tribe Freziereae DC.)., also known as Mocán in Spanish and Mocano in Portugese, occurs on the Canary Islands (Fuerteventura, Gran Canaria, Tenerife, La Gomera, La Palma, El Hierro) and the main island of Madeira (Arechavaleta et al., 2010; Borges et al., 2008). On the Canary Islands, the species mainly inhabits lower elevations of the laurel forest and can also be found in the thermophilous scrub (Hohenester & Welss, 1993; Schönfelder & Schönfelder, 1997). On Madeira, *V. mocanera* is very rare and mainly known to grow on banks and steep rocks (Press & Short, 1994).

The life-form of the species is shrub- to tree-like, reaching a maximum height of 15 m (Hohenester & Welss, 1993; Press & Short, 1994). The wood of *V. mocanera* consists of square to upright ray cells (Keng, 1962). Being nested in a family comprising only shrubs and trees (Weitzman, Dressler, & Stevens, 2004), the species is not listed as insular woody or potentially insular woody by Carlquist (1974) and Lens et al. (2013).

The leaves of *V. mocanera* are evergreen, serrate and possess a thickened cuticle (Hohenester & Welss, 1993; Keng, 1962; Fig. 3A). The flowers are fragrant, white, hermaphroditic and pendulant in groups of one to three (Schönfelder & Schönfelder, 1997). They are characterized by pentamerous sepals and petals, ten or more stamens and a half-inferior, three-locular ovary with three free styles (Keng, 1962; Schacht, 1859; Weitzman et al., 2004). Per locule, two to three anatropous ovules are present (Schacht, 1859). The fruit is a dehiscent capsule coated by the fleshy calyx which is, like the style, persistent (Bramwell & Bramwell, 1974; Schacht, 1859; Fig. 3A,B). Within one fruit, usually only one to four seeds are developed (Schacht, 1859). The exotesta of the seeds is brown and its cells comprise a lignified and thickened inner wall and strongly thickened anticlinal walls (Corner & Corner, 1976). The embryo is J-shaped (Weitzman et al., 2004).

Although *V. mocanera* is the only extant species of *Visnea*, fruits of three extinct *Visnea* species have been recovered from the Cretaceous to the Pliocene of Europe (Mai, 1971; Table 1). Of these fossil taxa, *Visnea minima* Knobloch & Mai is only known from the Upper Cretaceous (Maastrichtian, 72.1-66.0 mya; Table 1). In contrast to that, records of *Visnea germanica* Menzel range from the Late Eocene to the Late Pliocene (37.8-2.6 mya; Table 1) and records of *Visnea hordwellensis* (Chandler) Mai from the Late Eocene to the Middle Miocene (37.8-28.1 mya; Table 1). According to Mai (1971) and Knobloch & Mai (1986), the three species are mainly distinguished by the number of seeds developed (five to eight in *V. hordwellensis* and *V. minima*, three to five in *V. germanica*), the size of the fruits (exclusive pedicel and style: *V. minima* 2-3 mm, *V. hordwellensis* 4-5 mm, *V. germanica* 4-7 mm) and the attachment of the seeds to each other (*V. germanica* strongly, *V. minima* and *V. hordwellensis* loosely). Furthermore, the seeds of *V. germanica* usually almost grow to reach the length of the locule (Mai, 1971), whereas the seeds within fruits of *V. minima* and *V. hordwellensis* differ in size and only some of them reach locule length (Knobloch & Mai, 1986).

Regarding the closest relative of extant *Visnea*, several hypotheses have been proposed. Engler (1879) suggested Malaysian *Anneslea* Wall. (Fig. 3C), whereas Schenck & Schimper (1907) were in favor of European fossils of *Eurya* Thunb. (Fig. 3E). In support of the latter are

Figure 3. *Visnea mocanera* and related taxa from Pentaphylacaceae s.str. **A** *V. mocanera*, branches with fruits and serrate leafs (Tenerife, Teno); **B** *V. mocanera*, fruit; **C** *Anneslea fragrans* var. *lanceolata*, fruit; **D** *Ternstroemia gymnanthera*, fruit; **E** *Eurya gungshanensis*, fruit; **F** *Adinandra formosana,* fruit; **G** *Freziera undulata,* fruit; **H** *Cleyera japonica,* fruit.

the findings by Zhang & Schönenberger (2014), who discovered similar patterns of floral development and organization in *Visnea* and Asian *Eurya*. Phylogenetic analysis of morphological data only (Luna & Ochoterena, 2004) rather suggests a close relationship of *Visnea* and New World genus *Symplococarpon* Airy Shaw. More recent molecular phylogenetic analysis by Rose et al. (2018) and Tsou, Li, & Vijayan (2016) placed *Visnea*

either in a close relationship with Asian *Eurya* (indicated by *trnL-trnF* spacer) and *Euryodendron* Hung T.Chang or as sister to all other Freziereae (Fig. 3A-B,E-H; ITS or combination of nuclear, plastid and mitochondrial data). Biogeographically, a Paleoarctic-Indomalaysian origin during the Early Eocene has been proposed by Rose et al. (2018) based on an Ericales dataset comprising ten species of Pentaphylacaceae.

Table 1. Fossil record of *Visnea* based on literature.

Species	**Structure**	**Location**	**Age**	**Time scale (mya)**	**Reference**
Visnea germanica Menzel	Fruits	Germany, Italy, France (Type: Germany)	Upper Eocene to Upper Pliocene (Type: Upper Miocene)	37.8-2.6 (Type: 11.6-5.3)	Basilici, Martinetto, Pavia, & Violanti (1997); Bertoldi & Martinetto (1995); Ferguson, Pingen, Zetter, & Hofmann (1998); Ferrero, Merlino, Provera, & Martinetto (2005); Gregor (1978); Gregor (1990); Kovar-Eder, Kvaček, Martinetto, & Roiron (2006); Mai (1971); Martinetto, Monegato, Irace, Vaiani, & Vassio (2015); Martinetto, Pavia, & Bertoldi (1997); Martinetto & Ravazzi (1997); Martinetto, Scardia, & Varrone (2007) (Type: Menzel, 1913)
Visnea hordwellensis (Chandler) Mai	Fruits	UK, Germany, Denmark (Type: UK)	Upper Eocene to Middle Miocene (Type: Upper Eocene)	37.8-11.6 (Type: 37.8-33.9)	Friis, (1979); Mai, (1971); Mai (1998) (Type: Chandler, 1925 and Chandler, 1961)
Visnea minima Knobloch & Mai	Fruits	Germany (Type: Germany)	Maastrichtian (Type: Maastrichtian)	72.1-66.0 (Type: 72.1-66.0)	Knobloch, Kvaček, Bůžek, Mai, & Batten (1993); Knobloch & Mai (1991) (Type: Knobloch & Mai, 1986)

3) *Geranium reuteri, G. maderense, G. palmatum* and *G. yeoi*

The analyzed laurel forest species of *Geranium* L. (Fig. 4A-C; Geraniaceae) are closely related herbs (Fiz et al., 2008; Pokorny et al., 2014) and have been included in *Geranium* sect. *Ruberta* Dumort. among Mediterranean and widespread taxa by Aedo (2017). The close relationship between *Geranium reuteri* and Mediterranean/European taxa like *Geranium robertianum* L. has already been pointed out by Engler (1879) and Schenck & Schimper (1907). The Macaronesian laurel forest geraniums share e.g. a pachycaul habit (with exception of the more herbaceous *Geranium yeoi* Aedo & Muñoz Garm.), a palmately five-lobed leaf shape, the basic flower shape and the dispersal of their seeds as individual carpels (Yeo, 1973). Their flowers are pink, hermaphroditic and have pentamerous calyxes and petals (Yeo, 1973). Compared to the closely related widespread *G. robertianum* (Fig. 4D) and *Geranium purpureum* Vill. (Fig. 4E), the flowers of *G. reuteri* (Fig. 4B), *Geranium palmatum* Cav. (Fig. 4C) and *Geranium maderense* Yeo are large, the ones of *G. yeoi* medium-sized (Yeo, 1973). Reproductive isolation in the Madeiran species is likely achieved by adaptation to different pollinators and by placing the pollen on different body parts of the animals (Yeo, 1973). In the following, the species will be described in more detail.

Geranium reuteri, Pata de gallo in Spanish*,* reaches a height of up to 1 m and is a perennial with a slightly woody base (Fig. 4A,B; Hohenester & Welss, 1993; Schönfelder & Schönfelder, 1997). It is endemic to the Canary Islands (Gran Canaria, Tenerife, La Gomera, La Palma, El Hierro) and occurs in the undergrowth of older laurel forests and in the shade of fayal brezal (Arechavaleta et al., 2010; Hohenester & Welss, 1993; Schönfelder & Schönfelder, 1997). The flowers of *G. reuteri* possess a light colored throat, white to red stamen filaments and reddish anthers (Yeo, 1973). The species is pollinated by insects, most likely *Lepidoptera* (Yeo, 1973). Its chromosome number is 2n=128 (Yeo, 1973).

Geranium palmatum, in Portugese Gerânio folha-de-anémona, is a perennial with a more or less woody stem and reaches a maximum height of 1 m (Fig. 4C; Press & Short, 1994). It is endemic to the main island of Madeira and grows in the laurel forest, on shady and humid cliffs and close to streams (levadas; Aedo, 2017; Borges et al., 2008; Press & Short, 1994). The flower of *G. palmatum* is lilac with a dark throat (Press & Short, 1994; Yeo, 1973). The stamen filaments are dark red to pinkish and longer than the sepals, the anthers pale pink and show the color of the orange pollen (Aedo, 2017; Yeo, 1973). As pollinators, Yeo (1973) suggests *Lepidoptera*. The number of chromosomes is 2n = 68 (Van Loon, 1984; Widler-Kiefer & Yeo, 1987; Yeo, 1973).

Geranium maderense, also called Pássaras in Portugese, is a monocarpic plant with a more or less woody stem up to 1 m in height (Press & Short, 1994). Endemic to the main island of Madeira, it can be found in the laurel forest and on humid cliffs (Aedo, 2017; Borges et al., 2008; Press & Short, 1994). Its flower is purplish pink and has a dark throat (Press & Short, 1994; Yeo, 1973). The blackish-purple to dark-red stamen filaments are shorter than those of *G. palmatum*, the anthers are of dark red color (Aedo, 2017; Yeo, 1973). Possible pollinators are light-weighted and short-tongued bees (Yeo, 1973). Like in *G. maderense*, the chromosome number 2n = 68 (Widler-Kiefer & Yeo, 1987; Yeo, 1973).

Geranium yeoi is a biennial that grows up to 0.75 m in height (Yeo, 1973). Yeo (1973) compares it to a large *G. robertianum*. The species is also endemic to the main island Madeira and inhabits laurel forests, grassy banks and areas close to levadas (Aedo, 2017; Borges et al., 2008; Press & Short, 1994). Its flowers are mauve-pink and dark throated, its stamen filaments white or pink and its anthers orange-pink (Aedo, 2017; Press & Short, 1994; Yeo, 1973). The flowers are likely pollinated by *Bombus* (Yeo, 1973). The number chromosome is 2n = 128, equaling the number in *G. reuteri* (Widler-Kiefer & Yeo, 1987; Yeo, 1973).

Within *Geranium* sect. *Ruberta*, speciation by hybridization and autopolyploidization was suggested for the origin of some taxa. For example, the Madeiran taxa *G. maderense* and *G. palmatum* (former sect. *Anemonifolia* Knuth) may be the result of hybridization between widespread *G. purpureum* (2n = 32) or an unknown *Geranium* species and the Mediterranean species *Geranium cataractarum* Coss. (2n = 36; Widler-Kiefer & Yeo, 1987; Yeo, 1973). Widespread *G. robertianum* (2n = 64) was proposed to be the result of hybridization between *G. purpureum* and an unknown species (Widler-Kiefer & Yeo, 1987; Yeo, 1973). Subsequent autopolyploidization in *G. robertianum* might have led to Madeiran *G. yeoi* (Widler-Kiefer & Yeo, 1987; Yeo, 1973). The only proposed scenario for the origin of Canarian *G. reuteri* is rather speculative. According to Widler-Kiefer & Yeo (1987), it would involve a polyphyletic origin of *G. robertianum*, followed by polyploidization by two different strains of *G. robertianum* hybridizing.

Figure 4. Selected laurel forest geraniums and putatively closely related species. **A, B** *G. reuteri*; **C** *G. palmatum* (photo by M. Thiv); **D** *G. robertianum*; **E** *G. purpureum*.

4) *Phyllis nobla*

Phyllis nobla L. (Rubiaceae), called Capitana, Cachimbera or Mato negro in Spanish and Cabreira, Seisim or Seisinho in Portugese, is a half-shrub reaching a height of over 1 m (Fig. 5A; Hohenester & Welss, 1993; Press & Short, 1994; Schönfelder & Schönfelder, 1997). Like *Visnea*, *P. nobla* occurs on two Macaronesian archipelagos, i.e. the Canary Islands (Gran Canaria, Tenerife, La Gomera, La Palma, El Hierro) and Madeira (Madeira, Porto Santo, Desertas; Arechavaleta et al., 2010; Borges et al., 2008; Hohenester & Welss, 1993). On the Canary Islands, it occupies edges of or clearings within the laurel forest (Hohenester & Welss, 1993; Schönfelder & Schönfelder, 1997). For Madeira, it is reported from rocky ground of cliffs, and banks as well as from walls of levadas (Press & Short, 1994). Morphologically, *P. nobla* is characterized by a woody base, its slightly branched habit, long paniculate inflorescences without innovation and by possessing entire leafs (Bramwell & Bramwell, 1974; Mendoza Heuer, 1972). The species is monoecious, with both hermaphroditic flowers and unisexual flowers occurring on the same plant. The petals are tetra- or pentamerous and whitish to pale green, a calyx is not visible (Schönfelder & Schönfelder, 1997). The fruit is dry, ovate, glabrous and splits into two indehiscent mericarps (Mendoza-Heuer, 1977; Puff, 1982; Schönfelder & Schönfelder, 1997).

The genus is not listed as potentially insular woody by Carlquist (1974) and Lens et al. (2013), although Koek-Noorman & Puff (1983) note the presence of rays with square to upright cells. Derived woodiness has also been proposed as likely in some closely related genera, e.g. *Nenax* Gaertn., *Carpacoce* Sond. and some species of *Anthospermum* L. (Koek-Noorman & Puff, 1983). The remainder of species in *Anthospermum* are ancestrally woody or herbaceous (Koek-Noorman & Puff, 1983), whereas *Galopina* Thunb. consists of perennial herbs (Puff, 1986). Still, the half-shrub habit of *Phyllis* L. makes the interpretation of woodiness difficult, see Lens et al. (2013).

Phyllis nobla is one of the two species in *Phyllis* (Mendoza Heuer, 1972). The second species of the genus, *P. viscosa* Christ, is morphologically very similar (Fig. 5B; Bramwell & Bramwell, 1974). It is endemic to the Canary Islands and grows on cliffs of the succulent scrub of La Gomera, Tenerife and La Palma (Bramwell & Bramwell, 1974; Hohenester & Welss, 1993). As regards the phylogenetic relationships of the genus, Engler (1879) indicates a closeness of *Phyllis* to South African taxa of Rubiaceae tribe Anthospermeae Cham. & Schltdl., of which Schenck & Schimper (1907) single out *Galopina.* Mendoza Heuer (1972) suggests *Anthospermum* instead. Molecular analysis (Anderson, Rova, & Andersson, 2001; Bremer & Eriksson, 2009; Thureborn, Razafimandimbison, Wikström, Khodabandeh, & Rydin, 2019) shows that *Phyllis* is nested in subtribe Anthosperminae Benth. A sister group relationship of *Phyllis* and *Galopina* or *Phyllis* and *Anthospermum* is not supported by molecular data and *Phyllis* may rather be sister to the remainder of Anthosperminae (Thureborn et al., 2019).

Figure 5. *Phyllis nobla* and its closest relative. **A** *Phyllis nobla*; **B** *Phyllis viscosa*.

5) *Semele androgyna* and *S. gayae*

Semele androgyna, (Fig. 6A) and *S. gayae* (Webb) Sventenius & G.Kunkel (Fig. 6B; Asparagaceae, tribe Rusceae Dumort.) are known as gibalbera, alicacán (Schönfelder & Schönfelder, 1997) or zarzaparrilla macho in Spanish (Navarro, 2004) and as alegra campo in Portuguese (Press & Short, 1994). They grow as climbing shrubs up to 10 m in height (Arber, 1924; Schönfelder & Schönfelder, 1997). *Semele androgyna* inhabits the laurel forests of the Canary Islands (Gran Canaria, Tenerife, La Gomera, La Palma, El Hierro) and Madeira (Madeira, Porto Santo, Desertas; Arechavaleta et al., 2010; Borges et al., 2008). On Madeira, the species also extends into more xerophytic, lower elevations (Lucas, Pinheiro de Carvalho, & Paiva, 1998).

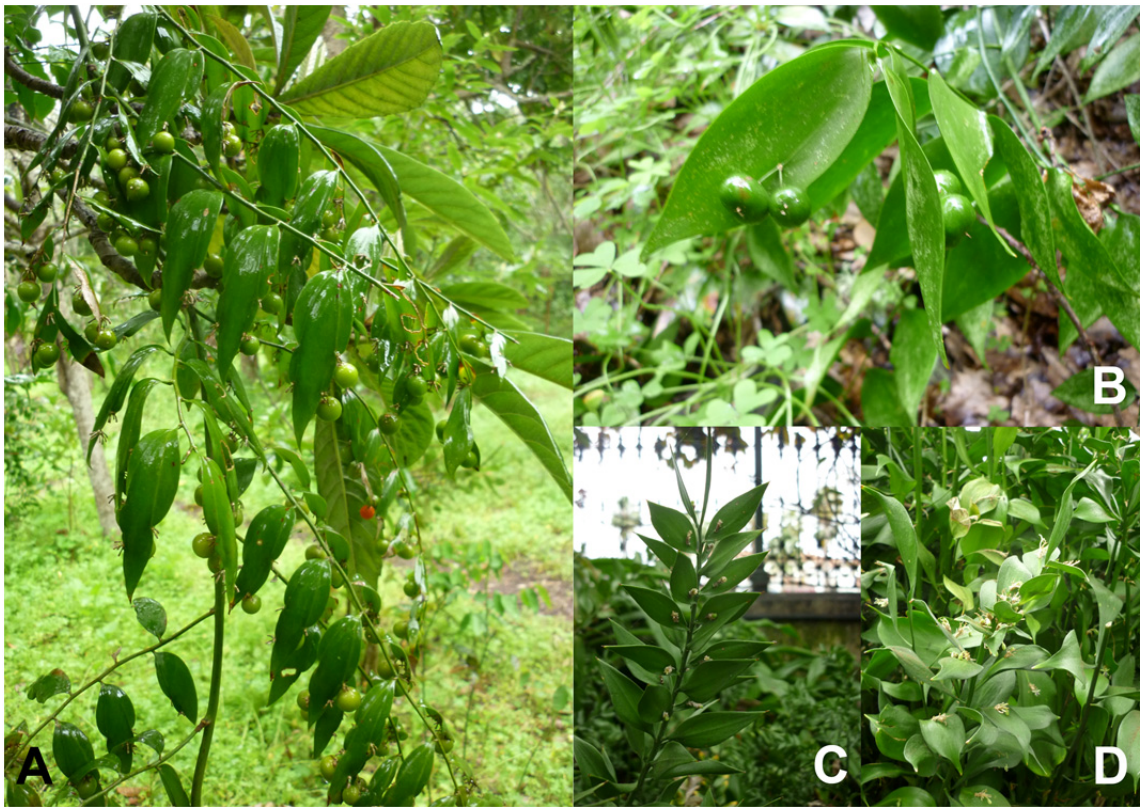

Figure 6. *Semele* and closely related species. **A** *Semele androgyna*; **B** *Semele gayae*; **C** *Ruscus aculeatus*; **D** *Ruscus hypophyllus*.

Several species and subspecies of *Semele* Kunth have been described for Madeira. Thereof, Pinheiro de Carvalho et al. (2004) only recognize *S. menezesii* Costa as distinct from *S. androgyna* by the habit of the shoots and inflorescence characteristics. In contrast to that, Borges et al. (2008) and Press & Short (1994) treat all of the Madeiran species and subspecies of *Semele* as synonymous to *S. androgyna*. *Semele gayae* is endemic to Gran Canaria and occurs on cliffs and slopes in relictual forests in the potential range of laurisilva (Navarro, 2004). It is classified as vulnerable by the Red List of Spain (Navarro, 2004) and threatened by habitat destruction due to water shortage caused by decline of aquifers, clearing, mowing, fires and landslides, as well as by collection as ornamental flowers.

Semele is characterized by phylloclades bearing clusters of whitish flowers (Arber, 1924; Schönfelder & Schönfelder, 1997). In *S. androgyna*, the flowers are positioned at the margin of the phylloclade (Fig. 6A), whereas in *S. gayae* they are found along the main nerve

(Fig. 6B; Hohenester & Welss, 1993). The flowers are hermaphroditic, but often either the male or the female organs are fully developed (Pinheiro de Carvalho et al., 2004; Lucas et al., 1998). The fruit is a red, globose berry (Schönfelder & Schönfelder, 1997) and dispersed via endozoochory, likely by birds (Navarro, 2004; Yeo, 1998).

As closest relatives of *Semele*, Schenck & Schimper (1907) propose Eurasian distributed Rusceae. Molecular data confirms the placement of *Semele* within Rusceae (Chen, Kim, Chase, & Kim, 2013; Kim, Kim, Forest, Fay, & Chase, 2010; Seberg et al., 2012). Furthermore, a weakly supported sister group relationship to *Ruscus* L. (Fig. 6C,D) is indicated (Kim et al., 2010).

6) *Daucus elegans*

Daucus elegans (Webb ex Bolle) Spalik, Banasiak & Reduron is a biennial herb, reaching a maximum height of ca. 0.5 m (Fig. 7; Schönfelder & Schönfelder, 1997). It is found in shady and humid locations inside the laurel forest of the Canary Islands (Tenerife, La Gomera, La Palma, El Hierro; Arechavaleta et al., 2010; Schönfelder & Schönfelder, 1997)

The species possesses uni- to bipinnate leafs (Schönfelder & Schönfelder, 1997). Its umbels are protruding horizontally and consist of up to ten pedicels (Hohenester & Welss, 1993). The fruits are black, globose and glabrous (Schönfelder & Schönfelder, 1997). They are glabrous and lack spines or wings on the secondary ridges, as well as any secondary appendages (Banasiak et al., 2016). As mode of dispersal, Spalik & Downie (2007) suggest gravity. Being an herb, insular woodiness was not proposed for *D. elegans*, but for the closely related Madeiran *D. decipiens* (Schrad. & J.C.Wendl.) Spalik, Wojew., Banasiak & Reduron and *D. edulis* (Lowe) Wojew., Reduron, Banasiak & Spalik (Carlquist, 1974; Spalik & Downie, 2007).

Figure 7. *Daucus elegans* in a laurel forest within the Teno Mountains, Tenerife.

No biogeographical hypotheses from Engler (1879) and Schenck & Schimper (1907) are available. However, Engler (1879) proposes a close relationship of Madeiran *D. decipiens* and *D. edulis* with Mediterranean *Thapsia* L. Molecular analysis, e.g. Banasiak et al. (2016), do not agree with this and place *D. elegans* among and *D. decipiens* and *D. edulis* close to Mediterranean, European and Macaronesian taxa of *Daucus* L. sect. *Daucus*, e.g. Banasiak et al. (2016) and Spalik & Downie (2007). Although *D. elegans* is recovered close to *D. edulis* and *D. decipiens*, the relationship between the Canarian taxon and the Madeiran species is

poorly resolved (Banasiak et al., 2016; Spalik & Downie, 2007). Including information from fruit morphological data, Banasiak et al. (2016) establish *D. elegans* in *Daucus* sect. *Daucus* and *D. edulis* and *D. decipiens* in *Daucus* sect. *Melanoselinum* (Hoffm.) Spalik, Wojew., Banasiak & Reduron. Spalik & Downie (2007) suggest that the Macaronesian taxa of *D. elegans*, *D. decipiens* and *D. edulis* either evolved within Macaronesia or that they are the result from a dispersal event from the Mediterranean to Macaronesia during the Late Tertiary. They propose the latter as more likely, with Madeira and the Canary Islands being colonized independently (Spalik & Downie, 2007).

1.4. Aims of the study

Although Macaronesian laurel forest species were traditionally regarded as relicts from a Tertiary laurophyllous vegetation in Europe (Mai, 1989), several characteristic species are likely too young to be relicts (Kondraskov, Schütz, et al., 2015). Still, only eighteen of 100 laurel forest inhabiting genera were tested, most of them woody. From other studies, data of only around eight further genera is available (see also Fig. 8). This thesis provides six new studies on the island biogeography of the characteristic laurel forest taxa/lineages of *Gesnouinia*, *Visnea*, *Geranium*, *Daucus*, *Phyllis* and *Semele*. These new model species/lineages are potentially old according to Engler (1879), Rose et al. (2018), Schenck & Schimper (1907) and Spalik & Downie (2007), i.e. they originated within the Tertiary, and they are widely distributed within the Canary Islands or the Canary Islands and Madeira. They include taxa from the tree, shrub and herb layer of five different life-forms, i.e. tree, shrub, half-shrub, herb and climber, as well as one potential example of insular woodiness (*Gesnouinia*). Furthermore, they occupy different niches within the Canarian or Canarian-Madeiran laurel forests, i.e. the lower thermophilous edge, open places (rocky, grassy or close to streams), the shady undergrowth of trees, and/or the Fayal-Brezal. The dissertation thesis presented here aims at identifying the biogeographical patterns in the six model species and providing a time frame for the colonization of the Macaronesian islands as well as for inter-island colonization. The following main questions will be addressed: 1) Are the species/lineages relicts of a European Tertiary laurophyllous vegetation according to their spatial, temporal and habitat origin? 2) Are crown ages useful in evaluating the relict status of laurel forest taxa, e.g. García-Verdugo et al. (2019)? 3) Does speciation within Macaronesia overlap with climatic events, e.g. the Pleistocene glaciation cycles? 4) Was Madeira colonized from the Canary Islands during the Plio-/Pleistocene, as it has been proposed for several other taxa (Kim et al., 2008)?

More specifically, the following will be examined in *Gesnouinia*: A) Is *Gesnouinia arborea* of Mediterranean origin as suggested by Engler (1879) and Schenck & Schimper (1907)? B) What is the relationship of the laurel forest species to Macaronesian *Gesnouinia filamentosa* Wedd., which has been assigned either to *Gesnouinia* or *Parietaria* in recent literature? If there is a close relationship between both species, does the divergence between the taxa overlap with the Pleistocene glaciation cycles? C) Did insular woodiness, which is considered as non-relictual by e.g., Carlquist (1974) and Lens et al. (2013), evolve in the genus?

For *Visnea*, the following will be studied in more detail: A) Did *Visnea* originate in Asia during the Early Tertiary, as suggested by Rose et al. (2018)? B) Can genetic differentiation within and between archipelagos be observed in this putatively ancient species? C) Was Madeira colonized from the Canary Islands? D) Does fruit morphological and anatomical evidence place the Tertiary Mediterranean/European fossil species *V. germanica* close to Macaronesian *V. mocanera*?

The questions specifically addressed in *Geranium* include: A) Did the Macaronesian laurel forest geraniums originate in Europe, as suggested by Engler (1879), Pokorny et al. (2014), Schenck & Schimper (1907)? B) Was Madeira colonized from the Canary Islands?

C) Does molecular data support the patterns of hybridization and auto-polyploidization suggested by e.g. Yeo (1973)?

The specific research questions for *Phyllis* are: A) Can the non-relict origin (from a Tertiary Mediterranean vegetation) indicated by Engler (1879), Schenck & Schimper (1907) and Thureborn et al. (2019) be supported? B) Did laurel forest species *P. nobla* and succulent scrub species *P. viscosa* split during the Pleistocene glaciation cycles? C) Was Madeira colonized from the Canary Islands during the Pliocene?

For *Semele*, the following will be analyzed in detail: A) Did the laurel forest species originate in the Mediterranean, as suggested by Kim et al. (2010) and Schenck & Schimper (1907)? B) Are *S. gayae* and Madeiran distributed *Semele* distinct from Canarian *S. androgyna*? C) Was Madeira colonized from the Canary Islands?

In *Daucus*, it will be specifically analyzed, if the origin within the Mediterranean/Europe during Late Tertiary, as suggested by Spalik et al. (2010), can be confirmed.

To this end, molecular phylogenetic and dating analyses, ancestral area estimations, stem and fruit sections, MicroCT scans and ancestral character state reconstructions were conducted.

2. General Material & Methods

Specific settings and strategies are given in sections 3.1.1. (*Visnea*), 3.2.1 (*Geranium*), 3.3.1 (*Semele*), 3.4.1 (*Daucus*), 3.5.1 (*Phyllis*) and 4.1.1 (*Gesnouinia*).

2.1. Sampling

Sampling strategies are based on published phylogenies of the laurel forest taxa and their closest relatives. From each Macaronesian island of distribution, it was attempted to include at least one accession per species.

2.2. Molecular analysis

The text of the following sections is derived and extended from Schüßler et al. (2019) and has been originally written by myself:

2.2.1. DNA extraction, PCR and sequencing

For silica dried samples, total genomic DNA was isolated applying the CTAB extraction protocol by Ivanova, Fazekas, & Hebert (2008) or the NucleoSpin Plant II kit (Macherey-Nagel). The latter was also used for herbarium material, as it usually allowed to acquire a higher yield of DNA. PCRs for nuclear and plastid markers were performed. Marker selection was based on previously published studies (Table 2). Additionally, for *Geranium*, nuclear and plastid markers with reported high amounts of variability were tested, e.g. Blattner (2016), Cox, Bennett, & Dyer (1992) and Shaw, Lickey, Schilling, & Small (2007). Up to two nuclear markers and up to three plastid markers were chosen per study taxon (Table 2). Primers, reaction mixes and cycling profiles used in PCR are listed in Table 3. PCR products were cleaned up and sequenced by the external sequencing service of LGC Genomics. Sequence editing and assembly was performed in Geneious 7.1.7 (Biomatters). The sequences were aligned using MUSCLE incorporated in PhyDE 0.9971 (Edgar, 2004; Müller, Quandt, Müller, & Neinhuis, 2005). The alignments were checked visually and corrected where algorithm failed to identify gaps.

Table 2. Markers selected for phylogenetic analyses. Markers in brackets have been tested and discarded. The asterisk (*) indicates markers of which no own sequence data was created. nr: nuclear, pt: plastid.

LF taxon/taxa	Markers	References
Gesnouinia	nr: ITS pt: *matK*, *trnL-trnF* spacer	Wu et al. (2013)
Visnea	nr: ITS pt: *trnL-trnF* spacer, *matK*, *psbA-trnH* spacer	Tsou et al. (2016)
Geranium	nr: ETS, ITS (5S NTS, TOPO6) pt: *matK*, *trnL-trnF* spacer, *rbcL** (*3'rps16–5'trnK*$^{(UUU)}$, *psbA-trnH* spacer, *psbJ-petA*)	Blattner (2016); Nishida, Azuma, Naiki, & Ogawa (2012); Shaw et al. (2007)
Phyllis	nr: ITS pt: *rps16* intron, *ndhF**	Anderson et al. (2001); Bremer & Eriksson (2009)
Daucus	nr: ITS pt: *rps16* intron	Banasiak et al. (2013)
Semele	nr: (ITS, 5S NTS, ETS) pt: *matK,* (*rpl32-trnL* spacer), *ndhF**, *atpB**, *rbcL**	Kim et al. (2010); Shaw et al. (2007)

Table 3. Cycling profiles and primers .

Marker	Primer and reference	PCR recipe (µl)	PCR program
ITS	ITSA: 5'-GGA AGG AGA AGT CGT AAC AAG G-3' (Blattner, 1999)	ddH_2O 16.55, PCR buffer(10x) 2.5, dNTPs (2 mM) 2.5, Primer F (10 µM) 1, Primer R (10 µM) 1, Taq Polymerase (5 U/µl) 0.2, BSA (10 mg/ml) 0.25, DNA template 1	95°C for 3 min, 9 cycles of (95°C for 30 s, 60°C* for 30 s, 72°C for 50 s), 29 cycles of (95°C for 30 s, 55°C for 30 s, 72°C for 50 s), 72°C for 10 min *-0.5°C per cycle
	ITSC: 5'-GCA ATT CAC ACC AAG TAT CGC-3' (Blattner, 1999)		
	ITS3: 5'-GCA TCG ATG AAG AAC GCA GC-3' (White, Bruns, Lee, & Taylor, 1990)		
	ITSB: 5'-CTT TTC CTC CGC TTA TTG ATA TG-3' (Blattner, 1999)		
ETS	jkETS–9: 5'-CGT WMA GGY GYA TGA GTG GT-3 ' (Mitchell, Heenan, & Paterson, 2009)	ddH_2O 13.05, PCR buffer(10x) 2.5, dNTPs (2 mM) 2.5, MgCl2 (25 mM) 1.5, Primer F (10 µM) 1, Primer R (10 µM) 1, Taq Polymerase (5 U/µl) 0.2, BSA (10 mg/ml) 0.25, DNA template 3	94°C for 1 min, 40 cycles of (94°C for 50 s, 52°C for 1 min, 72°C for 1 min 20 s), 72°C 10 min
	ETS-18S: 5'-GAG CCA TTC GCA GTT TCA CAG-3' (Wright, Yong, Wichman, Dawson, & Gardner, 2001)		
5S NTS	5S-NTS F: 5'-TGG GAA GTC CTY GTG TTG CA-3' (Cox et al., 1992)	ddH_2O 16.55, PCR buffer(10x) 2.5, dNTPs (2 mM) 2.5, Primer F (10 µM) 1, Primer R (10 µM) 1, Taq Polymerase (5 U/µl) 0.2, BSA (10 mg/ml) 0.25, DNA template 1	95°C for 3 min, 9 cycles of (95°C for 30 s, 64°C* for 30 s, 72°C for 50 s), 29 cycles of (95°C for 30 s, 59°C for 30 s, 72°C for 50 s), 72°C for 10 min *-0.5°C per cycle
	5S-NTS R: 5'-KTM GYG CTG GTA TGA TCG CA-3' (Cox et al., 1992)		
TOPO6 (Exon 2-7)	Top6_2F_305: 5'-CGG AGA ACA AGA AYA TYG CKG G-3' (Blattner, 2016)	ddH_2O 14.125, PCR buffer(10x) 2.5, dNTPs (2 mM) 2.5, $MgCl_2$ (25 mM) 1.5, Primer F (10 µM) 1.25, Primer R (10 µM) 1.25, Taq Polymerase (5 U/µl) 0.25, BSA (20 mg/ml) 0.625, DNA template 1	98°C for 2 min, 45 cycles of (98°C for 30 s, 61°C for 1 min, 72°C for 1 min), 72°C 12 min
	Top6_7R_1308: 5'-GTG TYT GCY TCA ANC CAT AYT TTG-3' (Blattner, 2016)		
trnL-trnF	c: 5'-CGA AAT CGG TAG ACG CTA CG-3' (Taberlet, Gielly, Pautou, & Bouvet, 1991)	ddH_2O 16.33, PCR buffer (10x) 2.5, dNTPs (2 mM) 2.5, $MgCl_2$ (25 mM) 0.5, Primer F (10 µM) 0.94, Primer R (10 µM) 0.94, Taq polymerase (5 U/µl) 0.2, BSA (10 mg/ml) 0.1, DNA template 1	94°C for 1 min, 30 cycles of (94°C for 50 s, 52°C for 1 min, 72°C for 1 min 20 s), 72°C 10 min
	d: 5'-GGG GAT AGA GGG ACT TGA AC-3' (Taberlet et al., 1991)		
	e: 5'-GGT TCA AGT CCC TCT ATC CC-3' (Taberlet et al., 1991)		
	f: 5'-ATT TGA ACT GGT GAC ACG AG-3' (Taberlet et al., 1991)		
matK	-19F: 5'-CGTTCTGACCATATTGCACTATG-3'(Gravendeel et al., 2001)	ddH_2O 16.55, PCR buffer(10x) 2.5, dNTPs (2 mM) 2.5, Primer F (10 µM) 1, Primer R (10 µM) 1, Taq Polymerase (5 U/µl) 0.2, BSA (10 mg/ml) 0.25, DNA template 1	94°C for 3 min, 9 cycles of (95°C for 20 s, 59°C* for 40 s, 72°C for 2 min), 29 cycles of (94°C for 20 s, 54°C for 30 s, 72°C for 2 min), 72°C 10 min *-0.5°C per cycle
	matk-F_uni: 5'-AAT TTA CGA TCH ATT CAT TCM ATW TTT CC-3' (Schaefer et al., 2011)		

	805R/Laur1R: 5‘-GTC TTT GAA CAA CCA TAG GGT-3‘(Rohwer, 2000) matk-R_uni: 5'-AGT TYT ARC ACA AGA AAG TCG AAR TAT ATA-3' (Schaefer et al., 2011)		
rps16 intron	rps16F: 5’-AAA CGA TGT GGT ARA AAG CAA C-3’ (Shaw et al., 2005) rps16R: 5’- AAC ATC WAT TGC AAS GAT TCG ATA-3’ (Shaw et al., 2005)	ddH_2O 12.1, PCR buffer(10x) 2.5, dNTPs (2 mM) 2.5, $MgCl_2$ (25 mM) 1.5, Primer F (10 µM) 2.5, Primer R (10 µM) 2.5, Taq Polymerase (5 U/µl) 0.2, BSA (10 mg/ml) 0.2, DNA template 1	80°C for 5 min, 9 cycles of (94°C for 30 s, 62°C* for 30 s, 72°C for 1 min), 29 cycles of (94°C for 30 s, 57°C for 30 s, 72°C for 1 min), 72°C for 5 min
3’rps16–5’trnK$^{(UUU)}$	rpS16x2F2: 5’-AAA GTG GGT TTT TAT GAT CC-3‘(Shaw et al., 2007) trnK$^{(UUU)}$x1: 5‘-TTA AAA GCC GAG TAC TCT ACC-3’ (Shaw et al., 2007)	ddH_2O 15.375, PCR buffer(10x) 2.5, dNTPs (2 mM) 2.5, $MgCl_2$ (25 mM) 1.5, Primer F (10 µM) 0.625, Primer R (10 µM) 0.625, Taq Polymerase (5 U/µl) 0.25, BSA (20 mg/ml) 0.625, DNA template 1	80°C for 5 min, 35 cycles of (95°C for 1 min, 50°C for 1 min, 65°C for 2 min), 65°C for 5 min
psbJ-petA	psbJ: 5’-ATA GGT ACT GTA RCY GGT ATT-3’ (Shaw et al., 2007) petA: 5’-AAC ART TYG ARA AGG TTC AAT T-3’ (Shaw et al., 2007)	ddH_2O 15.375, PCR buffer(10x) 2.5, dNTPs (2 mM) 2.5, $MgCl_2$ (25 mM) 1.5, Primer F (10 µM) 0.625, Primer R (10 µM) 0.625, Taq Polymerase (5 U/µl) 0.25, BSA (20 mg/ml) 0.625, DNA template 1	80°C for 5 min, 35 cycles of (95°C for 1 min, 50°C for 1 min, 65°C for 2 min), 65°C for 5 min
psbA-trnH	psbA:5’- GTT ATG CAT GAA CGT AAT GCT C-3’ (Sang, Crawford, & Stuessy, 1997) trnH ^{GUG}: 5’-CGC GCA TGG TGG ATT CAC AAT CC-3’ (Tate & Simpson, 2003)	ddH_2O 16.33, PCR buffer (10x) 2.5, dNTPs (2 mM) 2.5, $MgCl_2$ (25 mM) 0.5, Primer F (10 µM) 0.94, Primer R (10 µM) 0.94, Taq polymerase (5 U/µl) 0.2, BSA (10 mg/ml) 0.1, DNA template 1	94°C for 1 min, 30 cycles of (94°C for 50 s, 52°C for 1 min, 72°C for 1 min 20 s), 72°C 10 min

2.2.2. Phylogenetic inference

A maximum likelihood (ML) as well as a Bayesian (BI) approach was used to perform molecular phylogenetic analysis. The substitution models with the best fit according to AIC were determined in jmodeltest 2.1.5 (Darriba, Taboada, Doallo, & Posada, 2012) and analyses were set up accordingly.

For ML analyses, RaxML Blackbox 8.2.10 on CIPRES was used (Miller, Pfeiffer, & Schwartz, 2010; Stamatakis, 2014). Bootstrapping was set to be automatically halted as soon as stable support values were obtained.

BI was conducted with MrBayes v3.2.6. on CIPRES (Miller et al., 2010; Ronquist et al., 2012). Two independent runs were chosen, each run consisting of one cold chain and three heated chains with a heating parameter of 0.2. The total number of generations and sampling frequencies were selected in a way that convergence was reached, indicated by Potential Scale Reduction Factor (PSRF) values close to 1.0 (see specific Material and Methods sections). The default setting of 25% was used for the burn-in and checked in Tracer 1.6 for its appropriateness (Rambaut, Suchard, Xie, & Drummond, 2014). A 50% majority rule consensus tree was generated excluding the burn-in fraction.

In general, molecular phylogenetic analyses were performed for individual markers first. The resulting phylogenies were checked for congruence comparing topologies and support values, regarding bootstrap support values [BS] ≥70% and posterior probabilities [PP] ≥0.95 as significant support (Pirie, 2015). Evolutionary congruence of the datasets was also tested using PartitionFinder v.2.1.1 analysis (Lanfear, Frandsen, Wright, Senfeld, & Calcott, 2016), comparing an unpartitioned scheme to a scheme with partitions defined for the individual markers. When congruence was indicated, the individual markers were combined using SequenceMatrix v.1.7.8 (Vaidya, Lohman, & Meier, 2011). Intra-specific data were removed during concatenation as the combined datasets were to be used in subsequent stem node dating analyses, where an imbalanced mix of species and population data may cause erratic age estimates (Drummond & Bouckaert, 2015; Mairal, Pokorny, Aldasoro, Alarcón, & Sanmartín, 2015).

2.2.3. Molecular dating

All molecular dating analyses were performed in BEAST 2.4.3 or BEAST 2.4.7 (Bouckaert et al., 2014), applying the bmodeltest package for BEAST2 (Bouckaert, 2015) to estimate the substitution model during analysis. The settings for stem and crown node dating differed and are described in the respective sections. To allow for comparisons between the age estimates of all laurel forest taxa analyzed in this thesis with respect to e.g. colonization windows, dating procedures need to be analogous (see Carine, 2005). Thus, the age estimates by Magallón, Gómez-Acevedo, Sánchez-Reyes, & Hernández-Hernández (2015) modelled as uniform calibration priors were used as standard for calibration in stem node dating. Subsequently, the estimates from stem node dating were used as reference for crown node dating. Additionally, dating based on age estimates from other studies was conducted, if available.

Estimation of stem ages

The birth-death model describing the birth death of lineages was set as tree prior. As clock model, a relaxed lognormal molecular clock was chosen. Calibration points were selected from literature (for details see specific material and methods sections) and modelled as uniform distribution priors. The length of the MCMC (Markov Chain Monte Carlo) chain was set for the effective sample size (ESS) to equal or exceeded 200 for all parameters. The sampling frequency was adjusted in a way that 10,000 trees were acquired from analysis. The MCMC output was visualized in Tracer 1.6 (Rambaut et al., 2014) and stationarity of the MCMC chain was determined. Subsequently, 10% of the trees were discarded as burn-in and maximum clade credibility trees were created using TreeAnnotator v 1.8.0 (Rambaut & Drummond, 2013).

Estimation of crown ages

Secondary calibration approaches based on the estimates from stem node dating were conducted. The marker displaying the highest variability in the phylogenetic analyses was chosen. If more than one marker indicated intra-species patterns and no conflict of data was detected, the respective markers were combined. The datasets were reduced to contain mainly intra-species data, since a very unequal mix of species and population data may result in unreliable age estimates (Drummond & Bouckaert, 2015; Mairal, Pokorny, et al., 2015). With the birth-death model being not appropriate for intra-species data, a coalescent tree prior was selected. To test whether a constant population coalescent model was suitable, analysis was run under the exponential growth coalescent model first and checked for the marginal posterior distribution of the growth rate to include zero (Drummond & Bouckaert, 2015). A random local clock was applied instead of a relaxed clock, as recommended by Drummond & Bouckaert (2015).

2.2.4. Ancestral area reconstruction

Bayesian Binary MCMC (BBM) analyses were conducted using RASP 3.2 (Ronquist & Huelsenbeck, 2003; Yu, Harris, Blair, & He, 2015). As input, the dated maximum clade credibility (MCC) trees from stem node dating were used. According to the recommendations in the RASP manual by Yu, Harris, Blair, & He (2014), all outgroups were removed from the input phylogeny with the outgroup-removal tool provided in the program. The maximum number of ranges was set to equal the number of areas coded and nodes supported with pp < 0.90 were excluded from analyses. RASP allows to set up four different models, i.e. JC, JC+Γ, F81 and F81+Γ. As the results obtained under the different models were almost identical, the default setting of fixed state frequencies (JC) with equal among-site variation was chosen. For the MCMC settings, the default was used.

Yu et al. (2015) recommend to test additional biogeographical models. Thus, biogeographical analysis using the BioGeoBEARS R package (Matzke, 2013a; Matzke, 2013b) was conducted on the outgroup-removed phylogenies from RASP analysis. The example script by Matzke (revised and improved version 2015-04-15; available at http://phylo.wikidot.com/biogeobears#script) was modified and used to compare the dispersal-extinction-cladogenesis (DEC) model to a likelihood version of Dispersal-

Vicariance Analysis (DIVALIKE) as well as to the likelihood version of BayArea (BAYAREALIKE). The models were run with and without parameter J, which adds founder event speciation to the analysis (Matzke, 2014). As some species occupy a large number of areas, maximum range size was not restricted and set to the number of areas coded. Since it is not possible to exclude poorly supported nodes or to analyze phylogenies with polytomies in BioGeoBEARS, the suggested model was run as statistical model (S-DEC or S-DIVA) in RASP. S-DEC performs a DEC and S-DIVA a DIVA analysis on a specified number (here 500) of randomly selected phylogenetic trees from the 10,000 trees obtained from molecular dating in BEAST (Beaulieu, Tank, & Donoghue, 2013; Yu, Harris, & He, 2010; Yu et al., 2015).

2.3. Morphological and anatomical analyses

Morphological and anatomical analyses were conducted for *Gesnouinia arborea* and *Visnea mocanera* and served different purposes. In *Gesnouinia*, the wood anatomy and the evolution of woodiness in the stem was of main interest. In *Visnea*, focus lay on studying and comparing the fruit anatomy of extant and fossil representatives of Pentaphylacaceae.

2.3.1. Microtome sections

The text of the following paragraphs is derived and extended from Schüßler et al. (2019) and has been originally written by myself:

Microtome sectioning was performed for stems of *Gesnouinia arborea* and related species as well as for fruits of *Visnea mocanera*. Samples for microtome sectioning were embedded in Technovit 7100 (Heraeus-Kulzer) conducting the following steps. In the case of herbarium material, the samples were soaked in a 10% NH_3 solution for a minimum of 10 days. Fresh material was available from *P. officinalis* and *Soleirolia soleirolii* (Req.) Dandy. For those species, the material was collected and immediately stored in 70% ethanol. All material was dehydrated in an ascending ethanol series (30%, 50%, 70%, 80%, 90% and 96% for herbarium material; 80%, 90% and 96% for fresh material) with 1h incubation time per step. Pre-infiltratation was conducted in vacuum conditions using 1:2, 1:1 and 2:1 solutions of Technovit 7100:ethanol with an incubation time 8-10h of per solution. The subsequent embedding procedure followed the manufacturer's protocol.

The material was sectioned transverse and/or longitudinally at 5 µm, 10 µm or 15 µm using a rotary microtome equipped with a d-profile knife. For staining, either a few drops of Giemsa's azur eosin methylene blue solution (Merck) diluted in dH_2O (3:1) or Astrablue-Safranin (Roth; Schweingruber, 2007) was used. Stained sections were mounted in Euparal (Roth) or RotHistoKitt (Roth) and photographed using the digital microscope Keyence VHX 500-F (Keyence).

2.3.2. MicroCT Scans

MicroCT scans were conducted for *Visnea mocanera* and its closest relatives using the SkyScan 1272 (Bruker) at the State Museum of Natural History Stuttgart. Samples were fixed at their bases to prevent movement during acquisition, using modelling clay or polystyrene. From the projections obtained during the scan, cross section images were reconstructed using NRecon 1.7.1.6 (Bruker).

2.3.3. Ancestral character state estimation

The text of the following paragraphs is derived from Schüßler et al. (2019) and has been originally written by myself:

For character state optimization, Mesquite 3.2 was used (Maddison & Maddison, 2006; Maddison & Maddison, 2017). Maximum likelihood and parsimony analyses were performed, collapsing branches without significant statistical support prior to analysis. For ML analysis, two models were available, i.e. the Mk1 model with one estimated rate of state change and the asymmetrical 2-parameter Markov k-state model with two different estimated rates for

state gain and state loss. Both models were compared performing a likelihood-ratio test in Mesquite. The likelihood of both models did not differ significantly. For this reason, the less complex Mk1 model was selected. Parsimony analysis was conducted under the unordered state model, which assigns the same cost to any state change.

2.3.4. Phylogenetic analysis

Analysis of morphological and anatomical traits of *Visnea* was conducted in PAUP* 4.0a and MrBayes v3.2.6. In PAUP, parsimony analysis was conducted as heuristic search with 100 bootstrap replicates. In MrBayes, analysis was run under the standard discrete model which corresponds to the JC model. The MCMC settings equaled the ones described for molecular analysis (see also section 2.2.2).

2.3.5. Multivariate statistics

Morphological and anatomical traits of *Visnea* were analyzed in SPSS 24 (IBM). Uncategorized data was selected as input (Appendix Table 1) and standardized by z-Transformation prior to analysis.

Principal components analysis (PCA) was conducted to detect autocorrelation between variables and to identify which variables should be analyzed together. Subsequently, multidimensional scaling (MDS) analysis was carried out to graphically visualize the dissimilarities between the analyzed taxa. Additionally, hierarchical and two-step Cluster analyses were run, testing all hierarchical clustering algorithms available in SPSS. For statistical comparison of cluster means, ANOVAs and t-tests were calculated.

3. Potential Tertiary relicts: lineages and taxa of Oligocene, Miocene or Early Pliocene origin

Inferred from this study and previously published data, one third of the laurel forest taxa/lineages have stem ages clearly consistent with the Tertiary relict hypothesis, falling into the span of Oligocene to Miocene (Fig. 8). Amongst those are the species/lineages of *Visnea*, *Geranium*, *Semele* and *Daucus* studied in this dissertation (Fig. 8). Early Pliocene stem ages are found in 15% of cases, e.g. *Phyllis nobla* (Fig. 8). Kondraskov, Schütz, et al. (2015) argue that Pliocene taxa are likely not relictual, as laurel forest was relatively scare in Europe during this time. Yet, laurel forest was likely still widespread in the Early Pliocene, e.g. Kovar-Eder (2003). For this reason, Early Pliocene taxa are treated as potential Tertiary relicts in this dissertation. Putative non-relicts of Late Pliocene or younger stem age make up 52% of species, including *Gesnouinia* (Fig. 8). The latter will be discussed further in chapter 4.

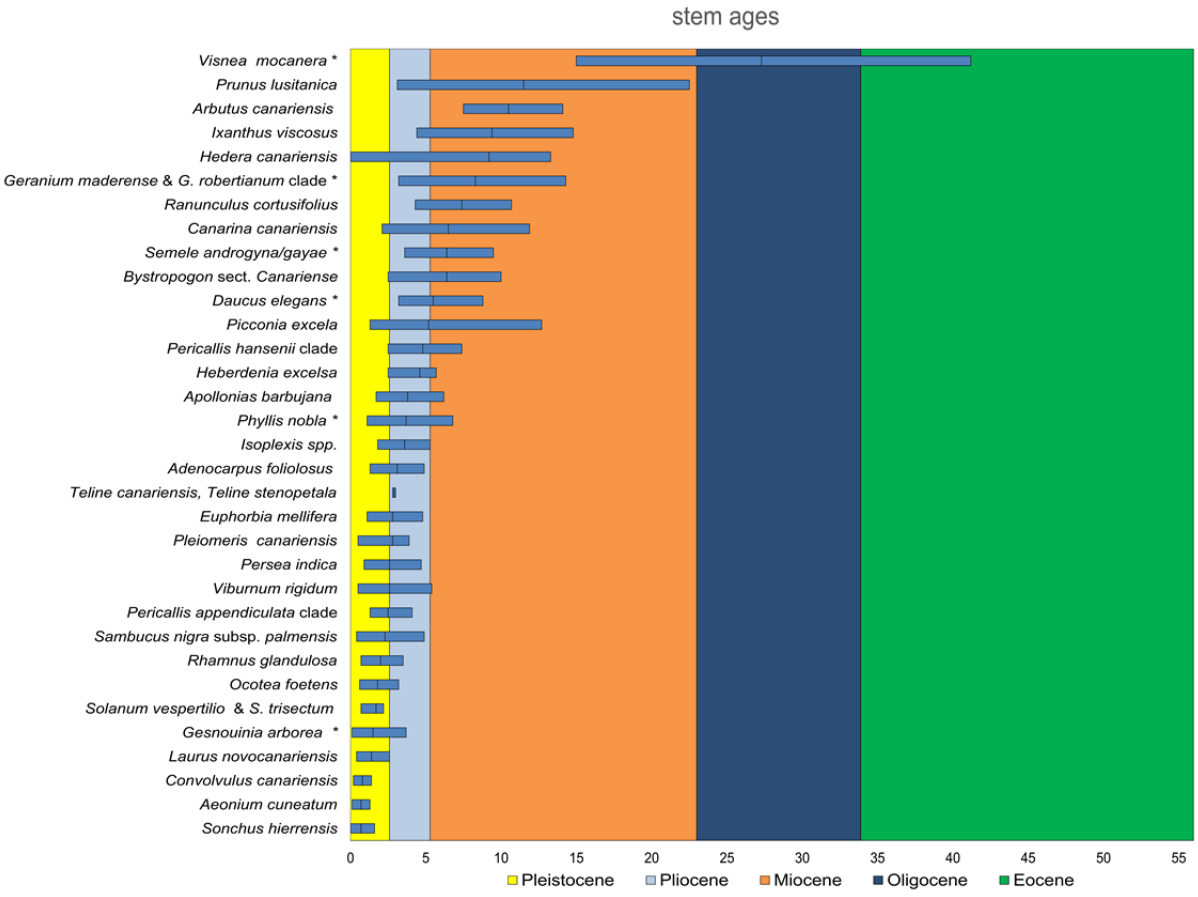

Figure 8. Stem ages of 33 Macaronesian laurel forest species/lineages. Own data is indicated by an asterisk, additional data was obtained from Carine (2005), Cubas, Pardo, Tahiri, & Castroviejo (2010), García-Verdugo et al. (2019), Jones, Reyes-Betancort, Hiscock, & Carine (2014), Kim et al. (2008), Kondraskov, Schütz, et al., (2015), Mairal, Sanmartín, et al. (2015), Percy, Page, & Cronk (2004), Valcárcel, Guzmán, Medina, Vargas, & Wen (2017) and Williams et al. (2015).

According to García-Verdugo et al. (2019), crown ages may be a more suitable measurement for the time of island colonization than stem ages. A Late Miocene/Early Pliocene crown age hinting towards a relict status is only indicated for 12% of the taxa/lineages, e.g. *Geranium* (Fig. 9), whereas 88% are dated to the Late Pliocene or

younger, e.g. *Visnea*, *Semele*, *Daucus*, *Phyllis* and *Gesnouinia*. In the following, time of colonization will be discussed relying on stem ages for the following reasons: 1) crown ages do not consider extinction along long branches and 2) stem ages are a more conservative measurement and decrease the probability that the relict hypothesis is rejected incorrectly.

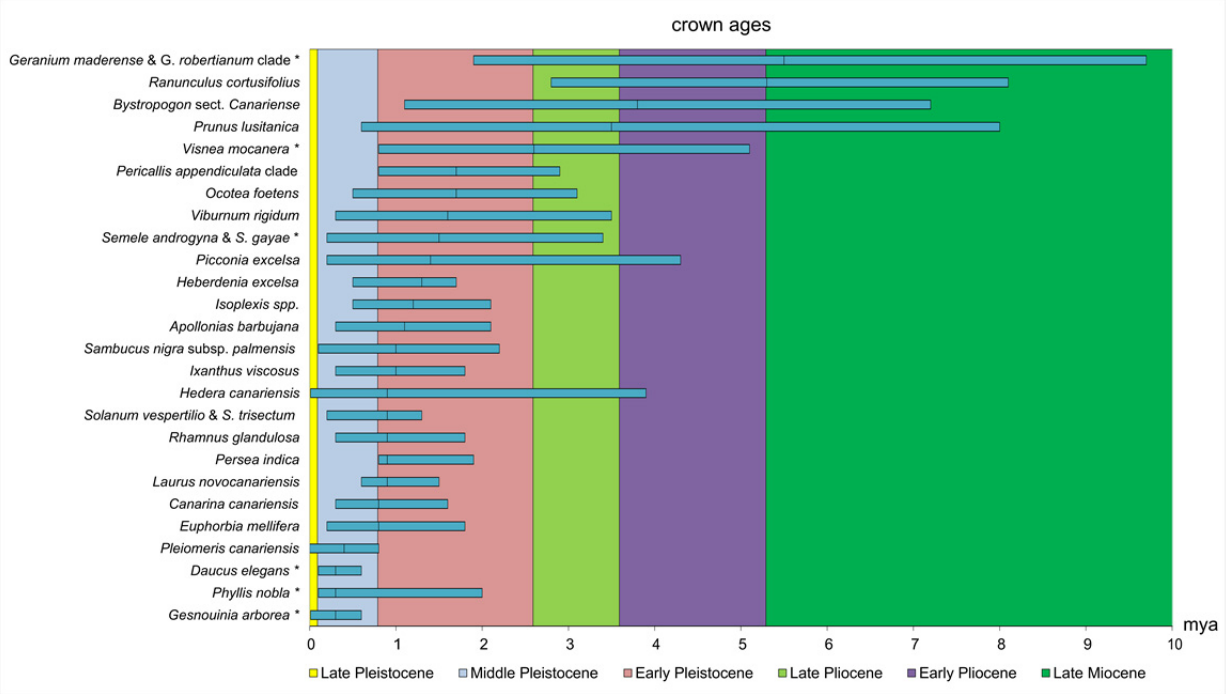

Figure 9. Crown ages of 26 Macaronesian laurel forest species/lineages. Own data is indicated by an asterisk, additional data is obtained from García-Verdugo et al. (2019), Jones et al. (2014), Kim et al. (2008), Kondraskov, Koch, & Thiv, 2015, Kondraskov, Schütz, et al. (2015), Mairal, Sanmartín, et al. (2015), Valcárcel et al. (2017) and Williams et al. (2015).

3.1. *Visnea mocanera* (Pentaphylacaceae)

3.1.1. Specific Material and Methods

Phylogenetic sampling

The phylogenetic sampling is given in Appendix Table S2. According to the molecular phylogenies by Tsou et al. (2016), *Visnea mocanera* is recovered within tribe Freziereae of Pentaphylacaceae s.str. The sister group of the species is ambiguous in the analyses by Tsou et al. (2016). Their nuclear phylogeny indicated *V. mocanera* as basal in tribe Freziereae, whereas their plastid data pointed towards a close relationship of *V. mocanera*, *Euryodendron* and *Eurya*. In the present study, the sampling thus focused on Pentaphylacaceae s.str. Sequences of Pentaphylacaceae s. str. were downloaded from GenBank, attempting to cover the major clades found by Su et al. (2011), Tsou et al. (2016) and Wu, Hsu, & Tsou (2007). New sequences were generated for *Visnea* (25) and *Balthasaria* Verdc. (one). All genera recognized by Weitzman et al. (2004) could thus be represented by at least one sequence, with the exception of *Archboldiodendron* Kobuski, of which no material and sequence was available (Table 4). However, some of the genera within Pentaphylacaceae s.str., i.e. *Ternstroemia* L.f., *Adinandra* Jack, *Eurya* and *Freziera* Willd., are very rich in species. For those, the amount of species covered was often low due to a lack of material (Table 4).

Table 4. Genera of Pentaphylacaceae s.str., number of species, geographic distribution and sampling for this study.

Genus	Distribution genus	Total number of species	Number of species sampled (molecular analysis)	Number of species sampled (fruit anatomy)	Origin samples	References
Adinandra Jack	Asia	ca. 80	9	2	Asia	Weitzman et al. (2004)
Anneslea Wall.	Asia	3	1	1	Asia	Weitzman et al. (2004)
Archboldiodendron Kobuski	Asia	1	-	-	-	Weitzman et al. (2004)
Balthasaria Verdc.	Africa	1?	1	-	Africa	Weitzman et al. (2004)
Cleyera Thunb.	Asia, America	24	2	1	Asia	Min & Bartholomew (2007)
Eurya Thunb.	Asia	ca. 130	23	1	Asia	Min & Bartholomew (2007)
Euryodendron Hung T.Chang	Asia	1	1	-	Asia	Min & Bartholomew (2007)
Freziera Willd.	America	57	3	1	America	Weitzman et al. (2004)
Pentaphylax Gardner & Champ.	Asia	1	1	-	Asia	Weitzman et al. (2004)
Symplococarpon Airy Shaw	America	9	2	-	America	Weitzman et al. (2004)
Ternstroemia L.f.	Asia, America, Africa	ca. 90	4	1	Asia	Min & Bartholomew (2007)
Visnea L.f.	Macaronesia	1	1	1	Macaronesia	Hohenester & Welss (1993)

Intraspecifically, one to three accessions of *V. mocanera* from each island of distribution (Fuerteventura, Gran Canaria, Tenerife, La Gomera, La Palma, El Hierro, Madeira; Arechavaleta et al., 2010; Borges et al., 2008) were sampled.

For molecular dating, the dataset was extended to Pentaphylacaceae s. l. by adding sequences of Sladeniaceae, e.g. Tsou et al. (2016). Additionally, the major families in Ericales as recovered by e.g. Magallón et al. (2015) and Rose et al. (2018) were represented by one to three sequences per family.

Anatomic sampling

For MicroCT scanning, fruits of extant Pentaphylacaceae were obtained. Of the tribe Freziereae *Visnea* is nested in, the following species were included by one sample each: *Adinandra formosana* Hayata, *A. lasiostyla* Hayata, *Cleyera japonica* Thunb., *Eurya acuminata* DC. and *Freziera undulata* Willd. (see Fig. 3F-H). *Visnea mocanera* was represented by four samples (see Fig. 3A,B). No material was available for *Archboldiodendron*, *Balthasaria*, *Euryodendron* and *Symplococarpon*. Two species of tribe Ternstroemieae DC., *Anneslea fragrans* var. *lanceolata* Hayata and *Ternstroemia gymnanthera* (Wight & Arn.) Bedd., were included as outgroup (Fig. 3C,D).

Table 5. Fossils of *V. germanica* analyzed in this study and information about their localities. AT: mean annual temperature, AP: mean annual precipitation.

Sample	Locality	Country	Fruits scanned	Age	Climatic conditions	Vegetation	Reference
Type	Herzogenrath	Germany	1	Late Miocene	AT: 14°C, AP: 1500-2500 mm	Open mixed forest (conifers and angiosperms), nearly one third tropical and subtropical elements	Menzel (1913), Van der Burgh (1973), Van der Burgh (1984)
CI1B5U	Corneliano d'Alba (Ciabot Cagna close to Alba)	Italy	2 and 2 fragments	Lago-Mare episode (5.59–5.33 mya), i.e. around the Pliocene-Miocene boundary	warm-temperate, sub-humid	woody plants and herbs, probably gallery forest along rivers	Kovar-Eder et al. (2006)
SP110	Scipione Ponte (Stirone River, close to Fidenza)	Italy	5	Lago-Mare episode (5.59–5.33 mya), i.e. around the Pliocene-Miocene boundary	unknown	probably similar to Corneliano d'Alba assemblage	Kovar-Eder et al. (2006)
CV12 A0C	Ca' Viettone close to Levone Cavanese	Italy	2	Pliocene thermic optimum (4.7-3.6 mya)	AT: 15-17°C, AP: 1300-2700 mm	forest resembling extant evergreen broad leaved forests in China	Bertoldi & Martinetto (1995); Martinetto (1995)
CV (CV12) A0X	like CV12 A0C	like CV12 A0C	3	like CV12 A0C	like CV12 A0C	like CV12 A0C	like CV12 A0C
BG2A1R	Sento (Val Chiusella)	Italy	2	Pliocene	subtropical	unknown	Basilici et al. (1997)

Fossils of *Visnea germanica* were available from one German and four Italian localities (see also Table 5): 1) Holo-Type from the Late Miocene of Herzogenrath, Germany; 2) BG2A1R (Fig. 10A,B) from the Pliocene of Sento, Italy; 3) CV (CV12) A0X (Fig. 10C-E) and CV12 A0C (Fig. 10F,G) from the Early Pliocene of Ca' Viettone, Italy; 4) SP110 (Fig. 10H-L) from the Miocene-Pliocene boundary of Scipione Ponte, Italy; and 5) CI1 B5U (Fig. 10M-O) from the Miocene-Pliocene boundary of Corneliano d'Alba, Italy.

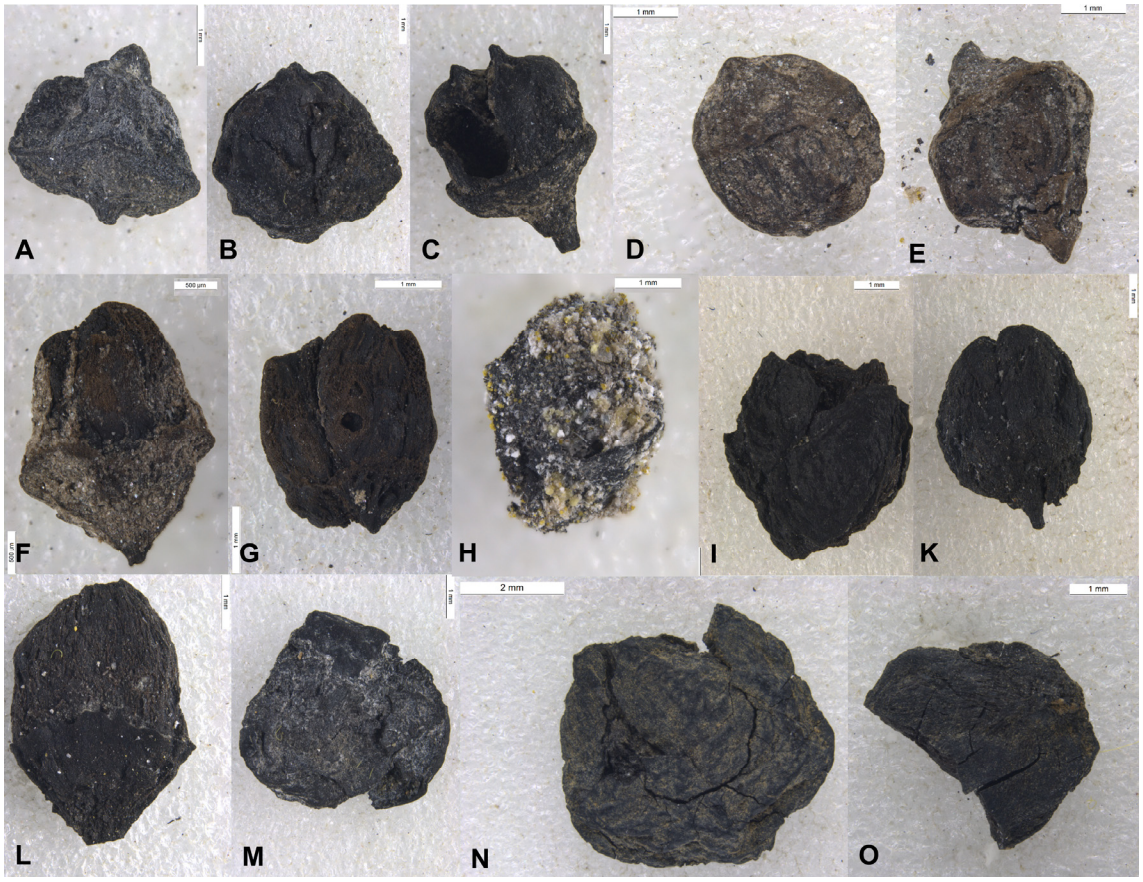

Figure 10. Italian *Visnea germanica* fossils. **A-B** BG2A1R (Sento, Pliocene); **C-E** CV(CV12)A0X (Ca' Viettone, Late Pliocene); **F-G** CV12 A0C (Ca' Viettone, Late Pliocene); **H-L** SP110 (Scipione Ponte, Miocene-Pliocene boundary); **M-O** CI1 B5U (Corneliano d'Alba, Miocene-Pliocene).

Molecular phylogenetic analyses

ML and BI phylogenies were calculated for individual and combined marker datasets spanning Pentaphylacaceae s. str. and different outgroups. MCMC settings for BI are given in Table 6.

Firstly, *trnL-trnF* spacer (t-RNA Leucine and t-RNA Phenylalanine intergenic spacer) and *matK* (maturase K gene) datasets of Ericales were checked for congruence. Statistically supported incongruence was detected within *Fouquieria* Kunth (Fouquieriaceae; Appendix Figs. S1, S2). As the phylogenetic relationships within this genus were of minor interest, the incongruence was ignored and the datasets subsequently combined. Secondly, a concatenated dataset of *trnL-trnF* spacer and *matK* spanning a subset of Ericales (Pentaphylacaceae, Theaceae, ericoids, sarracenioids, styracoids, Primulaceae, Ebenaceae and Sapotaceae; Appendix Fig. S3) was compared to a *psbA-trnH* spacer dataset (photosystem II protein D1 and t-RNA Histidine intergenic spacer; Appendix Fig. S4) covering the same taxonomic level. Both datasets were combined afterwards. Thirdly,

congruence was checked between a Pentaphylacaceae s.str. dataset comprising *trnL-trnF* spacer, *matK* and *psbA-trnH* spacer (Appendix Fig. S5) and an ITS (internal transcribed spacers 1 and 2 of nuclear encoded ribosomal RNA) dataset of Pentaphylacaceae s.str. (Appendix Fig. S6). Those datasets were also concatenated subsequently.

Outgroup selection was phylogenetically informed by the studies of Magallón et al. (2015), Rose et al. (2018) and Tsou et al. (2016). In the case of the Ericales datasets, balsaminoids were used as outgroup; in the case of the subset of Ericales, Primulaceae, Ebenaceae and Sapotaceae were selected. For the Pentaphylacaceae s.str. datasets, tribe Pentaphylaceae P.F. Stevens & A.L. Weitzman was chosen.

Table 6. MCMC settings for Bayesian analysis of the *Visnea* datasets using MrBayes.

	matK [a]	***trnL-trnF*** [a]	***trnL-trnF & matK*** [a]	***trnL-trnF & matK*** [b]	***psbA-trnH*** [b]	***matK & trnL-trnF & psbA-trnH*** [b]	**ITS** [c]	**Plastid** [c]	**Plastid & ITS** [c]
Chain length (million states)	10	10	10	50	10	10	10	10	50
Sample frequency	1000	1000	1000	1000	1000	1000	1000	1000	5000
Number of chains	4	4	4	4	4	4	4	4	4
Number of runs	2	2	2	2	2	2	2	2	2
Heating parameter	0.2	0.2	0.2	0.2	0.2	0.2	0.2	0.2	0.2

[a] Ericales dataset; [b] Ericales subset; [c] Pentaphylacaceae s.str. dataset

Stem age estimation

The estimation of stem nodes was based on a cp-dataset comprising *matK*, *psbA-trnH* spacer and *trnL-trnF* spacer. According to the phylogenies by Magallón et al. (2015) and Rose et al. (2018), sequences of Theaceae, ericoids, sarracenioids and styracoids were included for rooting and Primulaceae, Ebenaceae and Sapotaceae as outgroups. The molecular clock was calibrated setting the stem age of Pentaphylacaceae (92.6-99.7 mya) estimated by Magallón et al. (2015) as uniform prior (calibM). The chain length was set to 50 000 000 and the sampling frequency to 5000. As the mean stem age obtained for *Visnea* was considerably younger (28.5 mya) than the one estimated by Rose et al. (2018; 51.9 mya), two further settings tested were tested here. For these approaches, an Ericales dataset was created by adding sequences of polemonoids and Lecythidaceae for rooting and balsaminoids as outgroup. The following analyses were restricted to *matK* and *trnL-trnF* spacer, as *psbA-trnH* marker was removed due to its high variability and the consecutive difficulties in confidentially aligning the Ericales dataset.

The first calibration alternative (calibL) was based on Landis et al. (2018). Since their analysis only provides mean ages, the following procedure was chosen. The age estimate for the *Actinidia* Lindl. lineage (85.6 mya) was used as minimum and the age estimate for the stem of Ericales (105.7 mya) as maximum to set the age of the split of Ericaceae from Fouquieriaceae as uniform calibration prior. The chain length was increased to 70 000 000, to sampling frequency to 7000.

The second calibration alternative (calibR) was based on Rose et al. (2018), who also provided only mean ages. Correspondingly, the stem age of Lecythidaceae was set as

uniform calibration prior with the mean estimated for this split as minimum (106.6 mya; Rose et al., 2018) and the crown age of Ericales as maximum (110.1 mya; Rose et al., 2018). Additionally, three of the fossils used by Rose et al. (2018) were included to fix further nodes, 1) *Raritaniflora spp.* to set the split of Eriaceae from Clethraceae (89.8–93.9 mya), 2) *Actinocalyx bohrii* Friis for the MRCA (most recent common acenstor) of Diapensiaceae and Styracaceae (84.0–80.6 mya) and 3) *Parasaurauia allonensis* Keller, Herendeen & Crane for the MRCA of *Actinidia* and *Roridula* Burm. ex L. (72.1–83.6 mya). Like in calibL, the chain length equaled 70 000 000, the sampling frequency 7000.

Tip dating

For subsequent ancestral area estimation including the fossil distribution of *V. germanica*, an additional dated phylogeny was created. Using BEAST 2.4.3 and the sampled ancestors package (Gavryushkina, Welch, Stadler, & Drummond, 2014), a tip dating analysis was set up on a combined plastid and ITS dataset of Pentaphylacaceae s.str. For the fossil *Visnea germanica*, the sequence is unknown. Thus, it was included by a sequence only consisting of gaps as suggested by Gavryushkina (2015) and constrained as sister to *V. mocanera*. According to PartitionFinder, two partitions were defined, the first containing ITS and the second plastid data. For both partitions, the substitution model and clock rate were estimated individually. The tip of *V. germanica* was fixed to 3.6 mya (upper boundary of the Zanclean). As a further calibration point, the split of Ternstroemieae from Freziereae was set to 74.4-30.8 mya, as estimated in the previous plastid dating analysis based on Magallón et al. (2015; calibM, Appendix Fig. S7). Like in the previous analysis, the site model was estimated by bmodeltest and a relaxed lognormal clockmodel was applied. As tree prior, the fossilized birth-death model was selected. The chain length set increased to 20 000 000, sampling every 2000th state.

Crown age estimation

Crown node dating was based on an ITS dataset of *Visnea* using three accessions of *Euryodendron* as outgroup. The molecular clock was calibrated with the age estimate for the stem of *Visnea* from stem node dating (41.2-15.0 mya, calibM, Appendix Fig. S7) serving as uniform calibration prior. As tree prior, coalescent constant populations was chosen.

For comparison, a second analysis was run based on the much older stem age estimate by Rose et al. (2018). Their age estimate of 51.9 mya was used as minimum age for the node, the age estimate of the stem of tribe Freziereae, i.e. 66.7 mya, as maximum age. In both approaches, a chain length of 10 000 000 and a sampling frequency of 1000 were set up.

Ancestral area estimation

The combined (ITS, *matK*, *psbA-trnH*, *trnL-trnF*) MCC tree of Pentaphylacaceae s.str. from tip-dating analysis was used as input for biogeographical analysis. Coding of areas was as follows: Macaronesia (A), Asia (B), Europe (C), Neotropical America (D), Paleotropical Africa (E; Table 7).

Table 7. Coding for ancestral area estimation in Pentaphylacaceae s.str. Macaronesia (A), Asia (B), Europe (C), Neotropical America (D), Paleotropical Africa (E).

Species	Area	Reference
Adinandra angustifolia (S.H.Chun ex H.G.Ye) B.M.Barthol. & T.L.Ming	B	Min & Bartholomew (2007)
Adinandra bockiana E.Pritz. ex Diels	B	Min & Bartholomew (2007)
Adinandra dumosa Jack	B	Keng (1990)
Adinandra formosana Hayata	B	Min & Bartholomew (2007)
Adinandra glischroloma Hand.-Mazz.	B	Min & Bartholomew (2007)
Adinandra hainanensis Hayata	B	Min & Bartholomew (2007)
Adinandra lasiostyla Hayata	B	Min & Bartholomew (2007)
Adinandra millettii Benth. & Hook.f. ex Hance	B	Min & Bartholomew (2007)
Adinandra nitida Merr. ex H.L.Li	B	Min & Bartholomew (2007)
Anneslea fragrans Wall.	B	Min & Bartholomew (2007)
Balthasaria schliebenii (Melch.) Verdc.	E	Weitzman et al. (2004)
Cleyera japonica Thunb.	B	Min & Bartholomew (2007)
Cleyera pachyphylla Chun ex Hung T.Chang	B	Min & Bartholomew (2007)
Eurya acuminata DC.	B	Min & Bartholomew (2007)
Eurya acuminatissima Merr. & Chun	B	Min & Bartholomew (2007)
Eurya alata Kobuski	B	Min & Bartholomew (2007)
Eurya chinensis R.Br.	B	Min & Bartholomew (2007)
Eurya ciliata Merr.	B	Min & Bartholomew (2007)
Eurya disticha Chun	B	Min & Bartholomew (2007)
Eurya distichophylla Hemsl. ex F.B.Forbes & Hemsl.	B	Min & Bartholomew (2007)
Eurya emarginata Makino	B	Min & Bartholomew (2007)
Eurya glaberrima Hayata	B	Min & Bartholomew (2007)
Eurya hebeclados Y.Ling	B	Min & Bartholomew (2007)
Eurya japonica Thunb.	B	Min & Bartholomew (2007)
Eurya leptophylla Hayata	B	Min & Bartholomew (2007)
Eurya loquaiana Dunn	B	Min & Bartholomew (2007)
Eurya macartneyi Champ.	B	Min & Bartholomew (2007)
Eurya muricata Dunn	B	Min & Bartholomew (2007)
Eurya nitida Korth.	B	Min & Bartholomew (2007)
Eurya obliquifolia Hemsl.	B	Min & Bartholomew (2007)
Eurya patentipila Chun	B	Min & Bartholomew (2007)
Eurya rubiginosa Hung T.Chang	B	Min & Bartholomew (2007)
Eurya saxicola H.T.Chang.	B	Min & Bartholomew (2007)
Eurya strigillosa Hayata	B	Min & Bartholomew (2007)
Eurya subintegra Kobuski	B	Min & Bartholomew (2007)
Eurya weissiae Chun	B	Min & Bartholomew (2007)
Euryodendron excelsum Hung T.Chang	B	Min & Bartholomew (2007)
Freziera reticulata Bonpl.	D	Ulloa Ulloa & Jørgensen (2004)
Freziera undulata Willd.	D	Ulloa Ulloa & Jørgensen (2004)
Freziera verrucosa (Hieron.) Kobuski	D	Ulloa Ulloa & Jørgensen (2004)
Symplococarpon hintonii (Bullock) Airy Shaw in Hook.	D	Kobuski (1941a)
Symplococarpon purpusii (Brandegee) Kobuski	D	Kobuski (1941a)

Ternstroemia gymnanthera (Wight & Arn.) Bedd.	B	Min & Bartholomew (2007)
Ternstroemia impressa Lundell	D	Kobuski (1942)
Ternstroemia kwangtungensis Merr.	B	Min & Bartholomew (2007)
Ternstroemia luteoflora L.K.Ling	B	Min & Bartholomew (2007)
Ternstroemia microphylla Merr.	B	Min & Bartholomew (2007)
Visnea germanica Menzel	C	Mai (1971)
Visnea mocanera L.f.	A	Hohenester & Welss (1993)

In the MCC tree with mean node heights annotated, negative branch lengths were present within the *Adinandra-Cleyera* clade. In RASP BBM analysis, those were excluded from analysis as they were the product of low phylogenetic resolution.

For BioGeoBEARS analysis, a MCC with the node heights of the best-scoring tree was created. This was necessary as BioGeoBEARS does not allow to analyze trees with negative branch-lengths or to exclude nodes. BioGeoBEARS indicated the recently criticized DEC+J model as best-scoring and significantly different from DEC (one-tailed chi-squared test, df = 1, p = 0.00; Table 8). The second-best scoring model was DIVALIKE+J, also significantly differing from DIVALIKE (one-tailed chi-squared test, df = 1, p = 0.01; Table 8). As neither of the best-scoring models was available for statistical analysis in RASP, no further analyses were conducted.

Table 8. Biogeographical models tested for the combined ITS & plastid-dataset of Pentaphylacaceae and their likelihoods, AICs and AICcs as inferred by BioGeoBEARS (Matzke, 2013a; Matzke, 2013b). The best-scoring model is marked in bold, the second best-scoring model with an asterisk (*).

Model	**Likelihood (LnL)**	**AIC**	**AICc**
DEC	-40.23	84.47	84.72
DEC+J	**-32.81**	**71.62**	**72.14**
DIVALIKE	-36.58	77.15	77.41
DIVALIKE+J*	-33.30*	72.61*	73.13*
BAYAREALIKE	-49.69	103.4	103.6
BAYAREALIKE+J	-33.80	73.61	74.13

Microtome sections

To facilitate identification of structures and tissues in MicroCT Scans, some fruits of *Visnea mocanera* and one of *V. germanica* were sectioned destructively. In *V. mocanera*, the size of the embedding trays restricted microtome sections to longitudinal sections. For this reason, the transverse sections were performed by hand on *V. mocanera* fruits soaked in 70% ethanol for at least seven days. The fossilized fruits of *V. germanica* were not suitable for embedding and microtome sectioning due to their high breakability (communication A. Roth-Nebelsick, Staatliches Museum für Naturkunde Stuttgart). Thus, a longitudinal section of one fruit of *V. germanica* (SP110) was attempted by hand. This, however, resulted in fruit parts crumbling away under the razor blade and was subsequently discontinued.

MicroCT scans

Dried samples of extant Pentaphylacaceae (Table 9) were scanned using the SkyScan 1272. The scan settings followed the default settings of the scanner. Filters were chosen according to the automatic selection function of the scanning program which ensures values higher than 15% for the brightness of the acquired image. The settings for each object are listed in Table 9.

Table 9. Settings for MCT scanning using the SkyScan 1272.

Species	Sample name	Filter	Voltage (kV)	Current (µA)	Exposure (ms)	Rotation (°)	Rotation step (°)	Pixel size (µm)
Adinandra formosana		0.25 mm Al	60	166	2829	180	0.2	13.39
Adinandra lasiostyla		no	50	200	239	180	0.6	15.96
Anneslea fragrans		0.25 mm Al	60	166	2000	180	0.4	20.10
Cleyera japonica		no	50	200	415	180	0.2	8.79
Eurya acuminate		no	50	200	1139	180	0.2	4.19
Freziera undulata		no	50	200	1139	180	0.2	4.00
Ternstroemia gymnanthera		no	50	200	571	180	0.2	11.09
Visnea mocanera	Barone	no	50	200	571	180	0.2	12.04
Visnea mocanera	TF23	no	50	200	330	180	0.1	3.99
Visnea mocanera	2 (91018)	no	50	200	415	180	0.2	9.00
Visnea mocanera	Tf23-2	no	50	200	550	180	0.4	4.33

For the Italian *V. germanica* fossils, test scans using different filters and different voltage-current combinations were at first performed on the SkyScan 1272 (Appendix Table S3). As these scans were poorly resolved, further scanning of the Italian *V. germanica* fossils was conducted by Y. Staedler (University of Vienna) on a MicroXCT-200 (Xradia) and obtained as reconstructed images. Additionally, a reconstructed scan of the type specimen of *V. germanica* was provided by S. Schultka and K. Mahlow (both Museum für Naturkunde Berlin).

All reconstructed scans were visualized in Amira 6.5.0 (Thermo Fisher Scientific). Digital sections were conducted. Structures of interest, e.g. fruits, embryo cavities, raphe cavities and seeds, were segmented using the magic wand tool as well as the brush tool.

For measuring the size of the fruits and the seeds, landmarks were placed in Stratovan Checkpoint v. 2018.09.07.0325 WIN x64 (Stratovan). For length and width measurements of the fruits, style, stalk and sepals were ignored as these structures tended to be damaged in the fossils as well as in some of the dried fruits. The coordinates of the landmarks (p and q) were exported and used to calculate euclidean distances (d).

$d(p,q) = \sqrt{(p_1 - q_1)^2 + (p_2 - q_2)^2 + (p_3 - q_3)^2}$, if p = (p_1, p_2, p_3) and q = (q_1, q_2, q_3).

To approximate the shape of the seeds, fruits and raphe cavities, the circularity [$circularity = 4\pi(\frac{area}{perimeter^2})$] was measured using ImageJ 1.50b. In the measurements of the fruit shape, sepals and petals were excluded due to their poor preservation in the fossils; in the shape measurements of the seed, lateral view was analyzed.

Ancestral character state estimation

Thirteen fruit- and seed-morphological characters were coded: a) Mean fruit length: <4.0 mm (0), 4.0-6.9 mm (1), 7.0-9.9 mm (2), >10.0 mm (3); b) mean fruit diameter: <5.5 mm (0), 5.5-7.9 mm (1), 8.0-10.4 mm (2), >10.5 mm (3); c) fruit shape (circularity): <0.7 (0), 0.8-0.9 (1), 1.0 (2); d) mean seed length: <2.5 mm (0), 2.5-3.9 mm (1), 4.0-5.4 mm (2), >5.5 mm (3); e) mean seed thickness: <0.7 mm (0), 0.7-1.3 mm (1), 1.4-2.0 mm (2), 2.1-2.7 mm (3), >2.8 mm (4); f) mean seed width: <1.4 mm (0), 1.5-2.3 mm (1), 2.4-3.2 mm (2), 3.3-4.1 mm (3), >4.2 mm (4); g) maximum number of seeds developed: one to three (0), four to six (1), seven to nine (2), more than ten (3); h) seed shape (circularity): <0.7 (0), 0.8-0.9 (1), 1.0 (2); i) shape of the embryo cavity: U (0), J (1), straight to bent (2); j) raphe cavity shape (circularity): <1.0 (0), 1.0 (1); k) position of the ovary: superior (0), half-inferior (1), inferior (2); l) maximum number of locules: two (0), three (1), six (2); m) structure of testa: smooth (0), foveate (1; Table 10). Maximum parsimony reconstruction under the unordered state model was conducted on a dated MCC tree (ITS and plastid markers) containing the taxa for which morphological data was measured.

Table 10. Coding for morphological analyses in Pentaphylacaceae s.str. a) Mean fruit length: <4.0 mm (0), 4.0-6.9 mm (1), 7.0-9.9 mm (2), >10.0 mm (3); b) mean fruit diameter: <5.5 mm (0), 5.5-7.9 mm (1), 8.0-10.4 mm (2), >10.5 mm (3); c) fruit shape (circularity): <0.7 (0), 0.8-0.9 (1), 1.0 (2); d) mean seed length: <2.5 mm (0), 2.5-3.9 mm (1), 4.0-5.4 mm (2), >5.5 mm (3); e) mean seed thickness: <0.7 mm (0), 0.7-1.3 mm (1), 1.4-2.0 mm (2), 2.1-2.7 mm (3), >2.8 mm (4); f) mean seed width: <1.4 mm (0), 1.5-2.3 mm (1), 2.4-3.2 mm (2), 3.3-4.1 mm (3), >4.2 mm (4); g) maximum number of seeds developed: one to three (0), four to six (1), seven to nine (2), more than ten (3); h) seed shape (circularity): <0.7 (0), 0.8-0.9 (1), 1.0 (2); i) shape of the embryo cavity: U (0), J (1), straight to bent (2); j) raphe cavity shape (circularity): <1.0 (0), 1.0 (1); k) position of the ovary: superior (0), half-inferior (1), inferior (2); l) maximum number of locules: two (0), three (1), six (2); m) structure of testa: smooth (0), foveate (1).

Taxon	**a**	**b**	**C**	**d**	**e**	**f**	**g**	**h**	**i**	**j**	**k**	**l**	**m**
Adinandra formosana	2	2	2	0	1	1	3	2	0	1	0	2	0
Adinandra lasiostyla	1	0	?	?	?	?	3	?	0	?	0	?	0
Anneslea fragrans	3	3	1	3	4	4	0	1	0	1	2	1	0
Cleyera japonica	1	0	2	0	3	1	0	1	0	1	0	0	1
Eurya acuminata	0	0	2	0	1	1	1	1	2	1	0	1	1
Freziera undulata	0	0	2	?	?	?	3	?	2	?	0	1	?
Ternstroemia gymnanthera	1	1	2	2	2	3	0	1	0	0	0	0	0
Visnea germanica (type)	1	0	0	0	1	1	1	0	1	1	1	1	0
Visnea germanica (BG2 A1R)	0	0	1	0	0	0	2	0	1	1	1	?	0
Visnea germanica (CI1 B5U)	0	0	1	?	?	?	?	?	?	?	1	?	?
Visnea germanica (CV A0X)	0	0	0	0	0	0	1	1	1	1	1	1	0
Visnea germanica (CV12 A0C)	0	0	0	0	0	0	2	0	1	1	1	1	0
Visnea germanica (SP110 A6M)	0	0	1	0	1	0	1	0	1	1	1	?	0
Visnea mocanera	1	0	0	1	2	1	1	1	1	0	1	1	0

Phylogenetic analysis of fruit and seed traits

The Pentaphylacaceae s.str. fruit traits and seed traits possessing a phylogenetic signal in ancestral character state reconstruction (fruit diameter, fruit length, fruit shape, position of the ovary, seed length, seed width, seed shape, shape of the embryo cavity) were selected for Parsimony and Bayesian analysis in PAUP* 4.0a and MrBayes v3.2.6.

Multivariate statistics

Analyses on the phylogenetically relevant, uncategorized z-transformed Pentaphylacaceae s.str. fruit traits (see previous paragraphs) were performed in SPSS 24 (IBM).

Principal components analysis (PCA) was conducted twice. In the first analysis, correlation was indicated between fruit width and fruit length as well as between seed width and seed length. In consequence, fruit length and seed length were excluded from all further analyses. PCA was repeated and extracted only one component, consisting of all input-variables. Subsequently, multidimensional scaling (MDS) analysis was carried out. Metric data (fruit diameter, fruit shape, seed diameter, seed shape) was analyzed separately from ordinal data (position of the ovary, shape of embryo cavity). In both cases, the standard settings were used and Euclidean distances were calculated.

Hierarchical Cluster analysis was run, testing all clustering algorithms available in SPSS. The standardized ordinal variables *shape of the embryo cavity* and *position of the ovary* were treated as metric data and analyzed in combination with *fruit diameter*, *fruit shape*, *seed diameter* and *seed shape*. Distances were calculated as squared Euclidean. The number of clusters was set to range from two to the number of taxa included in analyses. As *Anneslea fragrans* was indicated to be highly deviant from the rest of the taxa in the first clustering analyses (Appendix Fig. S8), it was removed from the dataset and clustering analyses were run anew.

As it is not optimal to treat ordinal data as metric data, a two-step cluster analysis based on log-likelihood distances was conducted in addition. The number of clusters was not fixed and the maximum number of clusters was set to the number of input taxa.

For all clusters indicated, independent two-sample t-tests were calculated. ANOVA was tested for cases where more than two clusters were found, but discarded due to a lack of variance homogeneity.

3.1.2. DNA sequence variation and phylogenies

Twenty-five newly created sequences of *Visnea mocanera* and one of *Balthasaria schliebenii* (Melch.) Verdc. were uploaded to GenBank (Appendix Table S2). Sequence variation of the alignments is provided in Table 11.

The plastid, nuclear and combined phylogenies spanning the different taxonomic levels (Figs. 11, 12; Appendix Figs. S1-7, S9-S11) largely agree with Magallón et al. (2015), Rose et al. (2018) and Tsou et al. (2016). One statistically supported conflict is found in the *matK* Ericales phylogeny (Appendix Fig. S1). It contradicts Magallón et al. (2015) and Rose et al. (2018) with respect to the phylogenetic relationships within sarracenioids, albeit without very strong statistical support (PP < 0.95, BS = 84).

Pentaphylacaceae s.str. are recovered as monophyletic (Appendix Fig. S7), with *Pentaphylax euryoides* Gardner & Champ. as sister to a clade containing the monophyletic tribes Freziereae and Ternstroemieae. *Visnea mocanera* is positioned within Freziereae as sister to all other Freziereae based on the combination of *trnL-trnF* and *matK* for the subset of Ericales (Appendix Fig. S3), on the *psbA-trnH* phylogeny (Appendix Fig. S4), and on the combined plastid (*trnL-trnF*, *matK* & *psbA-trnH*) phylogeny of the subset of Ericales (Appendix Fig. S7). If *Pentaphylax* Gardner & Champ. is used as an outgroup, *V. mocanera* forms a polytomy with *Balthasaria*, a clade comprising species of *Adinandra* and *Cleyera* Thunb. and a clade containing *Eurya*, *Freziera*, *Euryodendron* and *Symplococarpon* (Fig. 12, Appendix Fig. S11). Intraspecific patterns in *V. mocanera* are weakly indicated, with the Madeira accessions proposed as sister to the accession from Gran Canaria (Appendix Fig. S11). Alternatively, *trnL-trnF* spacer hints towards a close relationship of the Tenerife and Madeira accessions (Appendix Fig. S2).

Table 11. Sequence characteristics of the Ericales and Pentaphylacaceae s.str. datasets, i.e. plastid datasets of Ericales (*trnL-trnF*; *matK*; *matK* & *trnL-trnF*), plastid datasets of the Ericales subset (*trnL-trnF* & *matK*; *psbA-trnH*; *trnL-trnF* & *matK* & *psbA-trnH*) and plastid, nuclear and combined datasets of Pentaphylacaceae s.str. (*trnL-trnF* & *matK* & *psbA-trnH*; ITS; ITS & *trnL-trnF* & *matK* & *psbA-trnH*).

	***matK*[a]**	***trnL-trnF*[a]**	***trnL-trnF & matK*[a]**	***trnL-trnF & matK*[b]**	***psbA-trnH*[b]**	***matK & trnL-trnF & psbA-trnH*[b]**	**ITS[c]**	**Plastid[c]**	**Plastid & ITS[c]**
Number of accessions	64	71	55	57	43	64	66	45	60
Total number of characters	770	1259	2029	1876	805	2681	707	2136	2840 (Partition 1: 704; Partition 2: 2136)
Variable characters	51%	49%	42%	36%	21%	32%	35%	9%	15%
Parsimony-informative characters	35%	23%	19%	18%	11%	15%	28%	4%	10%
Substitution model (AIC)	GTR+Γ	GTR +Γ	GTR+Γ	GTR+Γ	GTR +Γ	GTR+Γ +I	GTR+ Γ	GTR+Γ	Partition 1: GTR+Γ+I Partitition 2: GTR+Γ

[a] Ericales dataset; [b] Ericales subset; [c] Pentaphylacaceae s.str.

3.1.3. Molecular dating: Oligocene origin and Plio-/Pleistocene diversification

The results from the three calibration approaches are relatively similar to each other (Fig. 11A, Appendix Fig. S7, S9, S10), with the one based on Rose et al. (2018; calibR) returning slightly older and the one based Landis et al. (2018; calibL) returning slightly younger age estimates than the approach based on Magallón et al. (2015; calibM). For tip dating, the outcomes from analysis are even younger those from calibL (Fig. 12).

Diversification within Pentaphylacaceae started during the Upper Cretaceous (Fig. 11A, calibM: 67.01 mya, 95% HPD 88.62-42.96 mya; calibR: 72.46 mya, 95% HPD 98.47-47.60 mya) to Mid-Paleocene (calibL: 60.13 mya, 95% HPD 83.49-35.76 mya). Subsequently, tribe Freziereae split from Ternstroemieae during the Late Paleocene (calibR: 56.45 mya, 95% HPD 81.64-32.55 mya), Early Eocene (Fig. 11A, calibM: 51.74 mya, 95% HPD 74.40-30.81 mya) or Mid-Eocene (calibL: 46.91 mya, 95% HPD 69.47-25.90 mya). The crown of Freziereae, which is also the stem of Visnea, dates to the Oligocene (calibR: 28.95 mya, 95% HPD 43.10-15.68 mya; Fig. 11A, calibM: 27.26 mya, 95% HPD 41.17-14.97 mya; calibL: 25.70 mya, 95% HPD 40.64-13.66 mya). Within *V. mocanera*, intra-

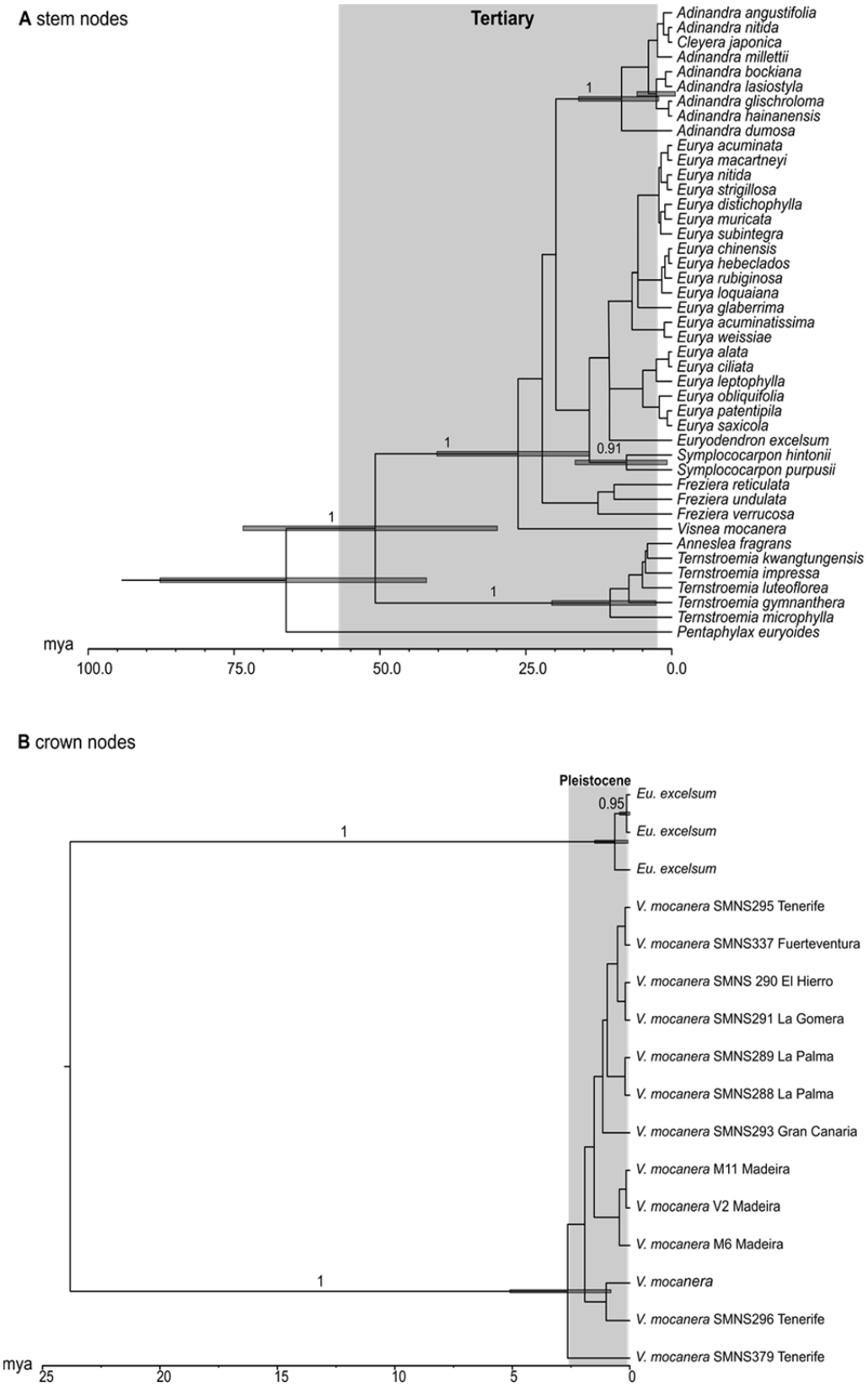

Figure 11. Chronograms from stem node and crown node dating in *Visnea*. Bars at the nodes indicate 95% highest posterior densities; posterior probabilities from BEAST analysis ≥ 0.90 are given above the branches. **A** Stem node dating, plastid data (*trnL-trnF* & *matK* & *psbA-trnH* of the subset of Ericales, calibM); **B** Crown node dating based on ITS data of *Visnea* and *Euryodendron*.

specific diversification occurred during the Pliocene-Pleistocene boundary (2.64 mya, 95% HPD 5.14-0.80 mya; Fig. 11B) based on the outcome of calibM as calibration reference. If the age estimate for the stem of *Visnea* by Rose et al. (2018) is used to calibrate the molecular clock, the crown age of *V. mocanera* increases to the Late Miocene (6.24 mya, 95% HPD 10.55-2.75 mya; Appendix Fig. S12).

3.1.4. Biogeographic reconstructions: Macaronesian, European or Macaronesian-European origin

BBM (Fig. 12) and DIVALIKE+J (Appendix Fig. S13) do not strongly differ in the biogeographical patterns reconstructed.

Both analyses indicate that the MRCA of extant Pentaphylacaceae (Fig. 12, BBM: PP = 1.0; Appendix Fig. S13), the MRCA of Freziereae and Ternstroemieae (Fig. 12, BBM: PP = 0.99; Appendix Fig. S13) as well as the ancestor of genus *Visnea* occurred in Asia (Fig. 12, BBM: PP = 0.97; Appendix Fig. S13). In the MRCA of *V. germanica* and *V. mocanera*, a Macaronesian (Fig. 12, PP = 0.37) or a European distribution (Fig. 12, PP = 0.28) was established according to BBM. DIVALIKE+J suggests a Macaronesian-European distribution instead (Appendix Fig. S13).

3.1.5. Fruit anatomy: Microtome, hand and MCT sections

The observations described here are based on the hand and microtome sections (Fig. 13, Appendix Figs. S14, S15) as well as on the MCT scans (Figs. 14-18, Appendix Fig. S16). In the MCT scans, cells were often not resolved, hampering tissue identification, e.g. of extotesta and mesotesta (Figs. 14-18). In the following, mean values are given for fruit size and seed size. Detailed measurements are available in Appendix Tables S4, S5. Fruit shape is given excluding sepals and style.

Extant Freziereae

***Visnea mocanera*. —** The fruits of *V. mocanera* are enclosed by five fleshy, persistent sepals (Figs. 13, 14, Appendix Fig. S16). The style with three free stylodia is also persistent in fruit (Figs. 13, 14). Including the sepals, the fruit is ovate in shape (Fig. 3A,B, Appendix Fig. S16). Excluding the sepals and styles, its shape is subovate to conical (Figs. 13, 14). In average, the fruits of *V. mocanera* are ca. 4.6 mm long and of ca. 3.6 mm in diameter. The half-inferior ovary is tri-locular (Fig. 13A,C,D). Its septs are easier to detect in young fruits than in more mature ones (Fig. 13A,B). In more mature fruits, the seeds are hard to separate and tend to be attached to each other, the central axis and the pericarp, hampering the identification of the septs. The number of seed developed per fruit ranged from one to six here. The seeds are ca. 3.2 mm long, 1.5 mm thick, ca. 2 mm wide and subtriangular in shape (Appendix Fig. S16). Their testa is uneven and slightly foveate. The cells of the exotesta are large and brownish with thickened cell walls, the mesotesta consists of whitish, small, circular cells with thickened cell walls (Fig. 13B, Appendix Fig. S14). The endotesta could not be unambiguously identified here (Appendix Fig. S14). Endosperm is found in abundance and contains a J-shaped embryo (Fig. 13B, Appendix Fig. S14, Appendix Fig. S16). The raphe cavity is r-shaped or triangular (Appendix Fig. S16).

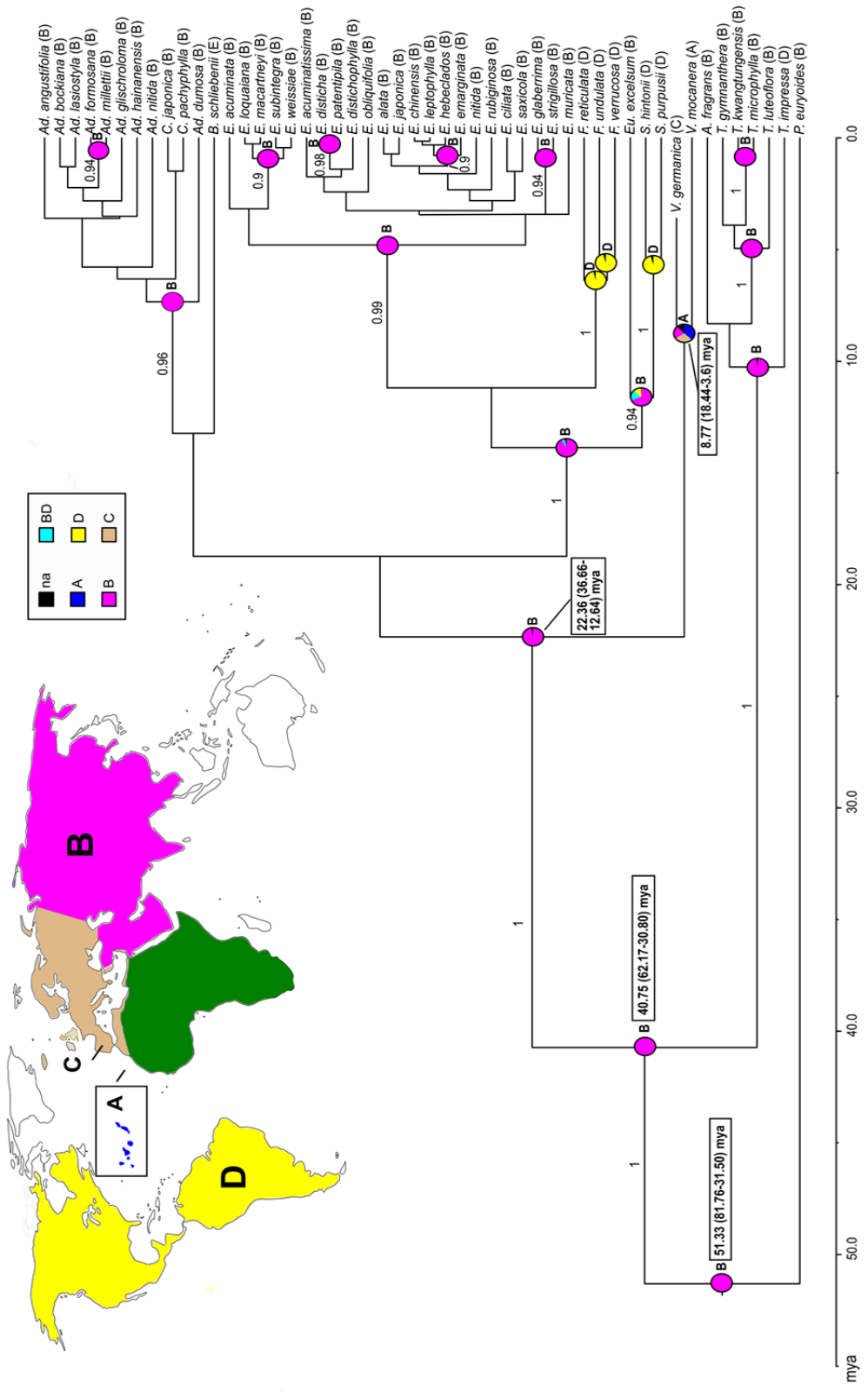

Figure 12. Biogeography of Pentaphylacaceae s.str. as inferred from BBM analysis in RASP, based on the chronogram (ITS, *psbA-trnH*, *trnL-trnF*, *matK*) from tip-dating. Numbers above branches indicate posterior probabilities from MrBayes analysis, bootstrap values from RAxML analysis and posterior probabilities from BEAST analysis. Only posterior probabilities ≥0.90 and bootstrap values ≥80 are shown. On the nodes, the posterior probabilities of the estimated areas/area combinations are indicated by pie charts. Areas coded include Macaronesia (A), Asia (B), Europe and the Mediterranean (C), The New World (D). For nodes of interest, the age estimates from BEAST analysis are given. The world map was modified from https://commons.wikimedia.org/wiki/File:Simplified_blank_world_map_without_Antartica_(no_borders).svg.

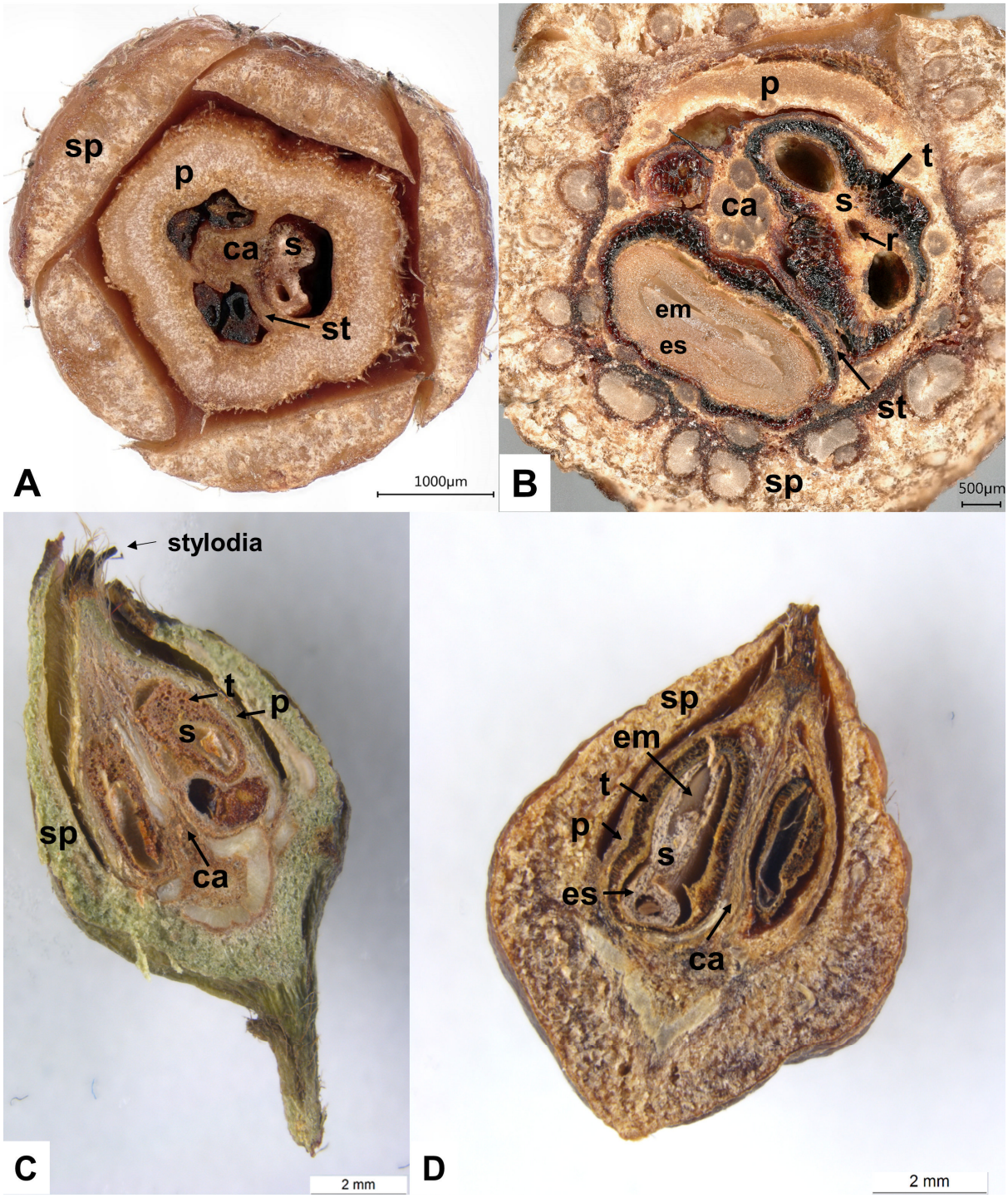

Figure 13. Young and more mature fruits of *Visnea mocanera*, sectioned by hand. **A** Young fruit, transverse section from the middle part; **B** More mature fruit, transverse section from the lower middle part; **C** Young fruit, longitudinal section; **D** More mature fruit, longitudinal section. Abbreviations: ca: central axis, em: embryo, es: endosperm, p: pericarp, r: raphe, s: seed, sp: sepal, st: septum, t: testa.

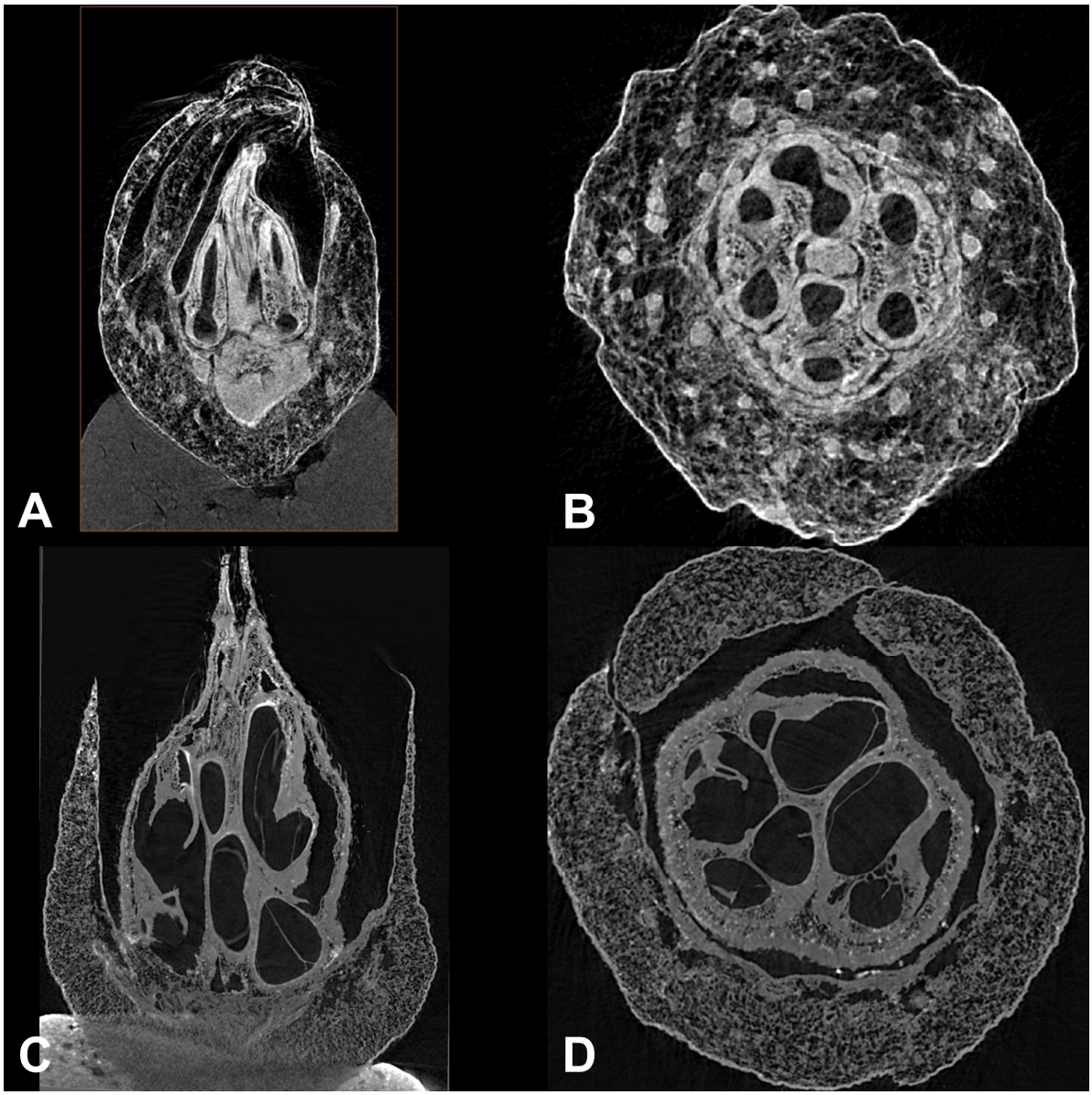

Figure 14. MicroCT images of *Visnea mocanera*. **A** Mature fruit, longitudinal view; **B** Mature fruit, transverse view; **C** Young fruit, longitudinal view; **D** Young fruit, transverse view.

***Adinandra lasiostyla*. —** The scan of this sample was not well-resolved. In consequence, not all traits were analyzable. The fruit is characterized by a superior ovary, longish persistent sepals and a persistent style (Appendix Fig. S16). Its size is ca. 5.2 mm in length and ca. 4.7 mm in diameter. The fruit shape could not be measured due to deformation probably caused by herbarization, but was most likely originally globose (Appendix Fig. S16). The seeds are numerous (more than ten), presumably with a smooth testa.

***Adinandra formosana*. —** Like in *A. lasiostyla*, a superior ovary, longish, persistent sepals and a persistent style can be found (Figs. 3F, 15C, Appendix Fig. S16). With a length of ca. 8.8 mm and a diameter of ca. 9.7 mm, the globose fruit of *A. formosana* is larger than the fruit of *A. lasiostyla*. The ovary is hexa-locular and comprises numerous compressed globose seeds with a smooth testa (Figs. 15C, 16C, Appendix Fig. S16). The seeds are ca. 2 mm long, ca. 1.8 mm wide, ca. 0.8 mm thick and contain a U-shaped embryo and a v-shaped raphe (Appendix Fig. S16).

***Cleyera japonica.* —** This species possesses globose fruits, ca. 6.0 mm in length and ca. 5.1 mm in diameter (Fig. 3H, Appendix Fig. S16). The sepals are short and, like the style, persistent (Fig. 3H). The ovary is superior and bi-locular in the lower part, uni-locular in the upper part (Figs. 15F, 16F). Three developed, compressed ovate to globose seeds were found (Appendix Fig. S16). The size of the seeds is ca. 2.4 mm in length, 2.0 mm in width and ca. 0.9 mm in thickness. Their testa is foveate and contains rounded cells with strongly thickened cell walls (Figs. 15F, 16F, Appendix Fig. S16). Furthermore, a U-shaped embryo and an r-shaped raphe are found (Appendix Fig. S16).

***Eurya acuminata*. —** The fruits of *Eurya acuminate* are globose, with short persistent sepals and persistent styles (Fig. 15D, Appendix Fig. S16). They are of small size, being ca. 2.8 mm long and ca. 2.4 mm wide. The ovary is superior, tri-locular and contains five sub-triangular seeds (Figs. 15D, 16D, Appendix Fig. S16). For the seed size, a length of ca. 1.7 mm, a width of ca. 0.9 mm and a thickness of ca. 0.9 mm were measured. The testa is strongly pitted and consists of funnel-shaped cells (Figs. 15D, 16D). The embryo is slightly curved, the raphe triangular (Appendix Fig. S16).

***Freziera undulata*. —** The analyzed fruit of *Freziera undulata* lacked sepals, but the style was persistent (Fig. 3G, Appendix Fig. S16). The fruit is globose, ca. 3.3 mm long and ca. 3.2 mm wide (Fig. 3G). The ovary is tri-locular and likely superior (Figs. 15E, 16E). Numerous undeveloped seeds are present (Figs. 15E, 16E).

Extant Ternstroemieae

***Anneslea fragrans* var. *lanceolata*. —** The ovate fruit of *A. fragrans* possesses a tri-locular, inferior ovary with persistent sepals (Figs. 3C, 15B, 16B). A persistent style was not observed (Figs. 3C, 15B). The fruit is large, being ca. 13.4 mm long and 10.7 mm wide. One compressed ovate seed of 10.1 mm length, 4.6 mm thickness and 5.9 mm width is developed (Appendix Fig. S16). It is characterized by a fleshy testa, a U-shaped embryo and an arrowhead-shaped raphe cavity (Figs. 15B, 16B, Appendix Fig. S16).

***Ternstroemia gymnanthera*. —** The fruit of *T. gymnanthera* is globose, ca. 5.6 mm in length and 6.2 mm in diameter (Fig. 3D, Appendix Fig. S16). The sepals and the style are persistent (Figs. 3D, 15A, Appendix Fig. S16). The ovary is superior and bi-locular, and contains two developed seeds (Figs. 3D, 15A, 16A). The seeds are compressed ovate to compressed globose (Appendix Fig. S16), ca. 4.7 mm long, ca. 2.3 mm thick and ca. 3.5 mm wide. Their testa is smooth, the embryo U-shaped and the raphe cavity arrowhead shaped (Figs. 15A, 16A, Appendix Fig. S16).

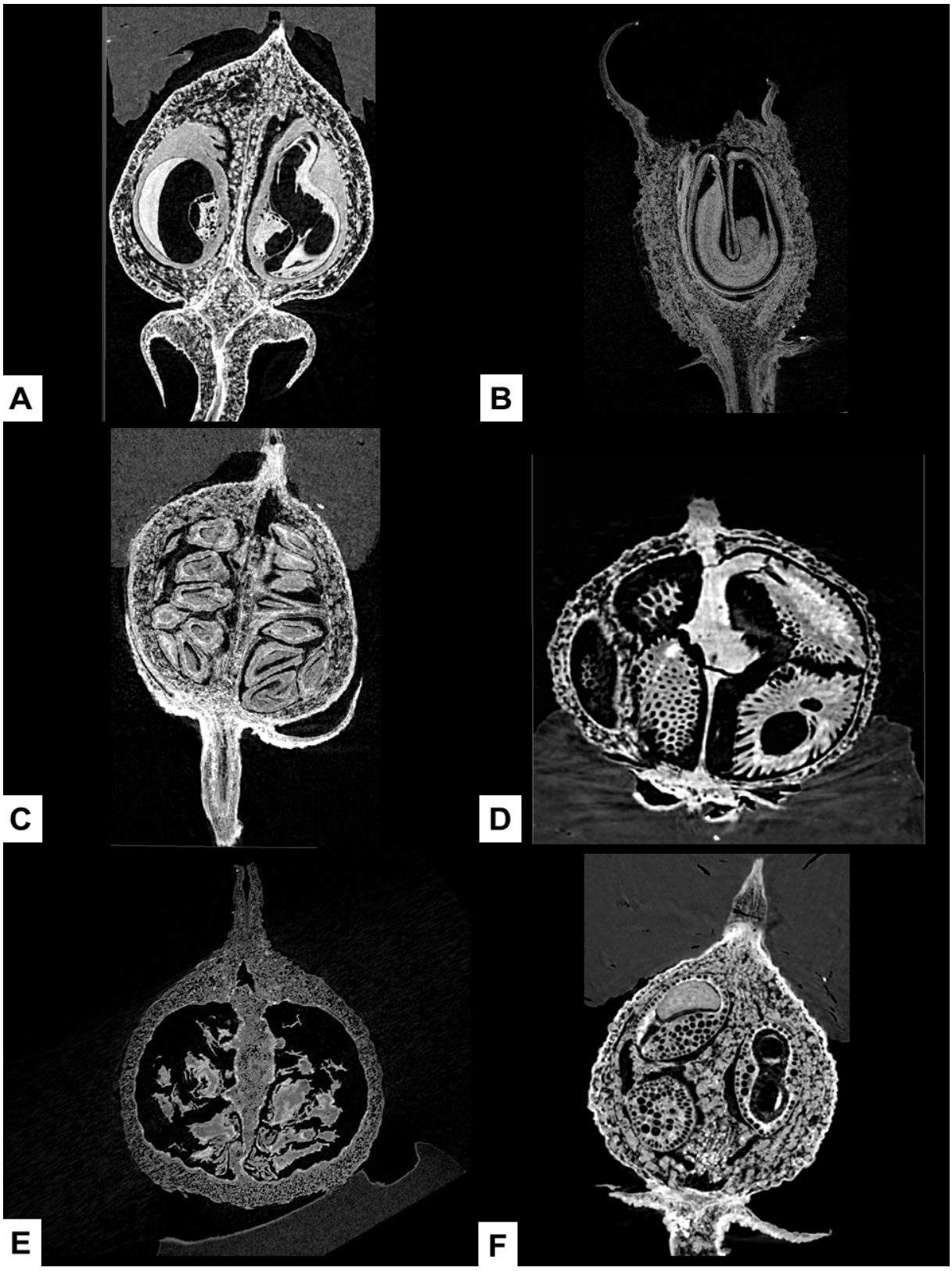

Figure 15. MicroCT images of extant Pentaphylacaceae s.str., longitudinal view. **A** *Ternstroemia gymnanthera*; **B** *Anneslea fragrans*; **C** *Adinandra formosana*; **D** *Eurya acuminate*; **E** *Freziera undulata*; **F** *Cleyera japonica*.

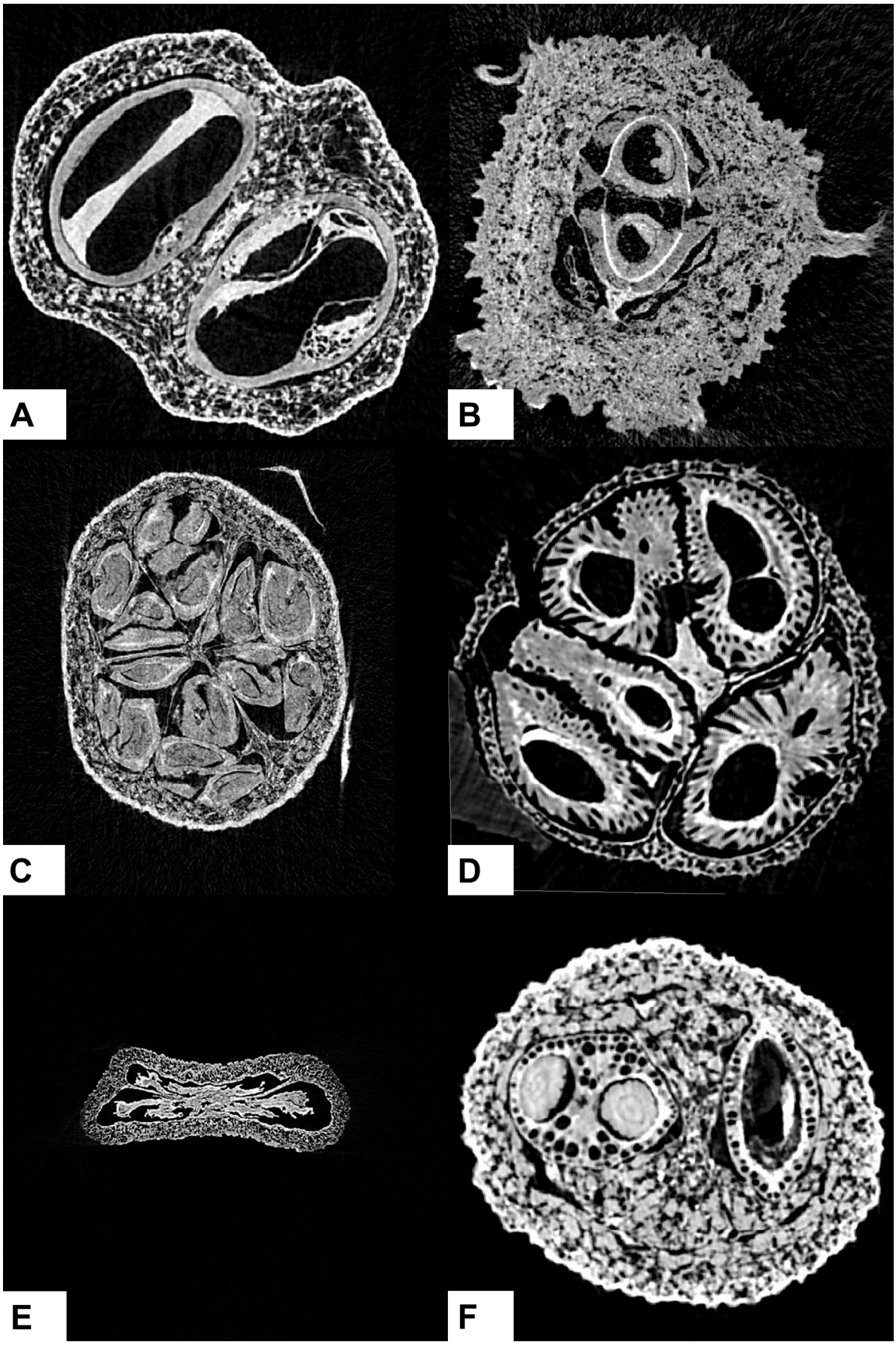

Figure 16. MicroCT images of extant Pentaphylacaceae s.str., transverse view**. A** *Ternstroemia gymnanthera*; **B** *Anneslea fragrans*; **C** *Adinandra formosana*; **D** *Eurya acuminata*; **E** *Freziera undulata*; **F** *Cleyera japonica*.

Fossils of Visnea germanica

Type. — The type specimen of *V. germanica* (Late Miocene of Germany) is ovately shaped (Appendix Fig. S16), with a length of 5.3 mm and a diameter of 4.3 mm. Styles and sepals are strongly abraded but persistent (Fig. 17A, Appendix Fig. S16). The ovary is half-inferior and tri-locular (Figs. 17A, 18A, Appendix Fig. S16). Six crescently shaped seeds of ca. 2.1 mm length, 1.1 mm thickness and 1.7 mm width are developed (Appendix Fig. S16), almost reaching the length of the locule. Their testa is smooth to slightly foveate and contains elongate cells with thickened cell walls (Fig. 17A, Fig. 18A). The embryos are J-shaped and the raphe is r-shaped (Appendix Fig. S16).

CI1 B5U. — Scans of these samples from the Miocene-Pliocene boundary of Italy are poorly resolved and/or only fragments were scanned. The only analyzable sample is ovately shaped, ca. 3.4 mm long, ca. 2.8 mm wide and possesses a half-inferior ovary (Fig. 17B, Appendix Fig. S16). The sepals and the style are largely abraded and persistent (Figs. 10M-O, 17B, 18B, Appendix Fig. S16). The seeds seem to almost reach locule length.

SP110. — These fruits from the Miocene-Pliocene boundary of Italy are ovate to subovate in shape, with persistent, largely abraded sepals and a persistent, largely abraded style (Fig. 10H-L, 17C, Appendix Fig. S16). The fruit length is ca. 2.8 mm, the fruit diameter ca. 3.0 mm. The ovary is half-inferior and contains six developed seeds (Figs. 10H-L, 17C, Appendix Fig. S16). The number of locules cannot be unambiguously inferred (e.g. Fig. 18C). The crescently to ovately shaped seeds are ca. 1.6 mm long, ca. 0.8 mm thick and 1.2 mm wide and almost reach locule length (Appendix Fig. S15). Their testa is presumably slightly foveate and build up by elongate cells with thickened cell walls (Fig. 17C, 18C). The embryos are J-shaped and the raphe cavities r-shaped (Appendix Fig. S16).

CV12 A0C. — In these samples from the Early Pliocene of Italy, no persistent style could be detected (Figs. 10F,G, 17D, Appendix Fig. S16). Largely abraded sepals were found, indicating a half-inferior ovary (Figs. 10F,G, 17D, Appendix Fig. S16). Fruits are subovate to globose in shape (Figs. 10F,G, Appendix Fig. S16), with a length of ca. 2.7 mm and a width of 2.4 mm. The ovary is tri-locular and contains a maximum of eight subtriangular to ovate seeds (Appendix Fig. S16) almost reaching the length of the loculed. The seeds enclose a likely slightly foveate testa with rounded to elongate cells with thickened cell walls, a J-shaped embryo and a presumably r-shaped raphe (Figs. 17D, 18D, Appendix Fig. S16).

CV (CV12) A0X. — These Early Pliocene fossils from Italy possess a persistent, largely abraded style, persistent, largely abraded sepals and are of globose to ovate shape (Fig. 10C-E, Appendix Fig. S16). They are ca. 2.7 mm long and ca. 3.0 mm wide. The ovary is half-inferior, tri-locular and encloses six sub-triangular to ovate seeds (Figs. 17E, 18E, Appendix Fig. S16). Like in sample C12A0C, the seeds are characterized by a likely slightly foveate testa consisting of elongate cells with thickened cell walls, a J-shaped embryo and a r-shaped raphe (Figs. 17E, 18E, Appendix Fig. S16). They are ca. 1.9 mm long, ca. 0.6 mm thick and ca. 0.7 mm wide and almost reach locule length.

BG2A1R. — The fossils from this Pliocene Italian locality are of ovate to sub-ovate shape, ca. 2.8 mm long and ca. 3.9 mm in diameter (Fig. 10A,B, Appendix Fig. S16). Sepals and style are persistent but, like in the other fossils, largely subject to abrasion (Figs. 10A,B, 17F, Appendix Fig. S16). The ovary is half-inferior and contains seven

developed seeds of subtriangular to crescent shape (Figs. 10A,B, 17F, Appendix Fig. S16). The locularity of the ovary cannot be unambiguously inferred from the scans (Fig. 18F). The seeds are ca. 1.3 mm in length, 0.5 mm in thickness and 1.0 mm in width, and almost reach the locule length. Their testa is likely slightly foveate with elongate cells and thickened cell walls, their embryo J-shaped and their raphe r-shaped (Figs. 17F, 18F, Appendix Fig. S16).

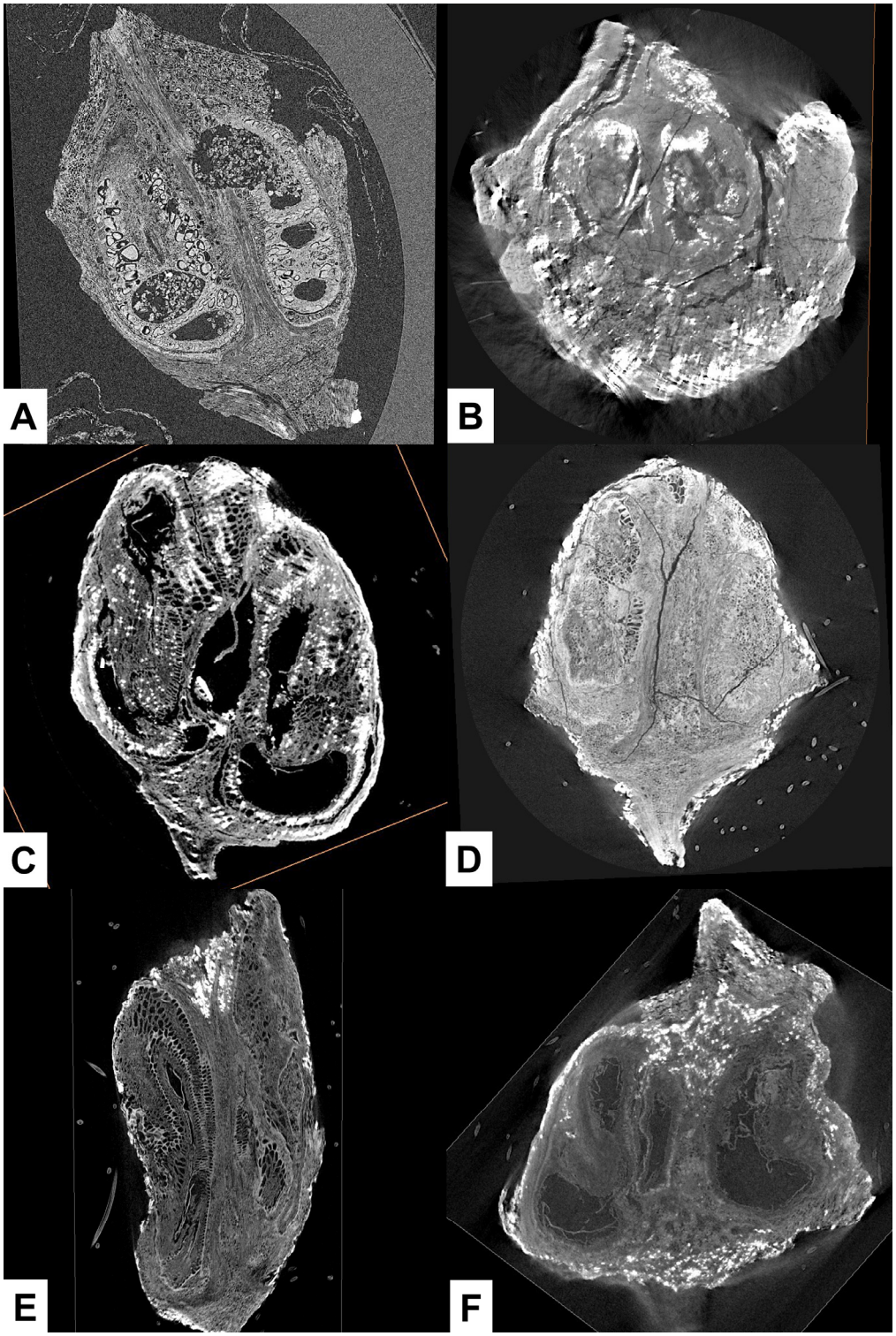

Figure 17. MicroCT images of *Visnea germanica*, longitudinal view. **A** Type (Late Miocene, Germany); **B** CI1 B5U (Miocene-Pliocene, Italy); **C** SP110 (Miocene-Pliocene, Italy); **D** CV12 A0C (Early Pliocene. Italy); **E** CV (CV12) A0X (Early Pliocene, Italy); **F** BG2A1R (Pliocene, Italy).

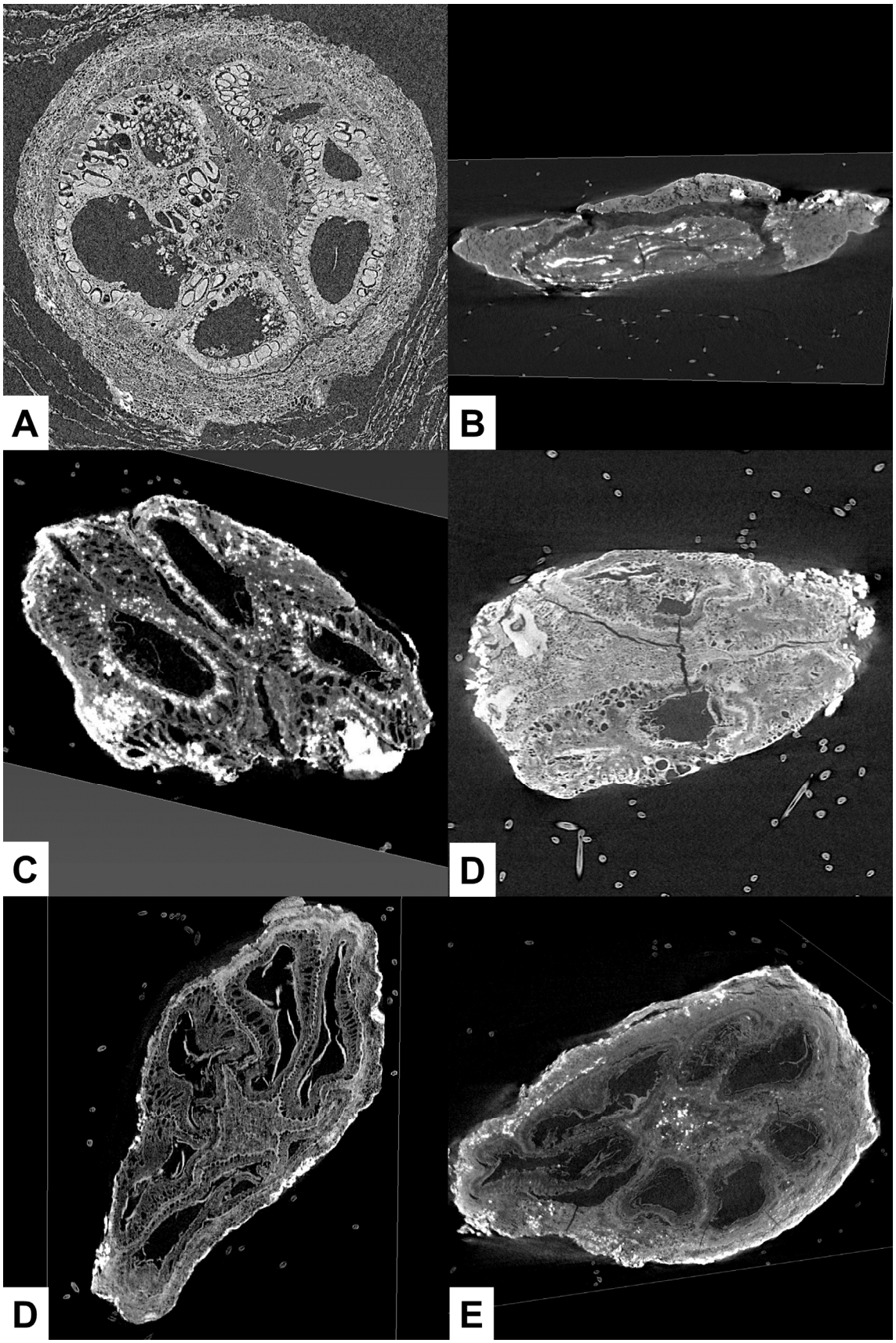

Figure 18. MicroCT images of *Visnea germanica*, transverse view. **A** Type (Late Miocene, Germany); **B** CI1 B5U (Miocene-Pliocene, Italy); **C** SP110 (Miocene-Pliocene, Italy); **D** CV12 A0C (Early Pliocene. Italy); **E** CV (CV12) A0X (Early Pliocene, Italy); **F** BG2A1R (Pliocene, Italy).

3.1.6. Phylogenetic analysis of morphological data: Unresolved relationships

Maximum parsimony analysis and Bayesian analysis recover two clades forming a polytomy with the remainder of taxa (Appendix Figs. S17, S18). The first clade contains *Eurya* and *Freziera*, the second *Visnea mocanera* and *V. germanica* (Appendix Figs. S17, S18). With bootstrap values lower than 70 and posterior probabilities considerably lower than 0.90, neither of these clades is statistically supported. Support values did not improve when taxa with a large amount of missing data were removed from the dataset.

3.1.7. Multivariate statistics on morphological traits: Possible closeness of *Visnea mocanera* and *V. germanica*

Multidimensional scaling analysis of the metric traits indicates that the *Visnea germanica* samples cluster in proximity to each other (Fig. 19). Variation between the samples from different localities is present (Fig. 19). *Anneslea fragrans*, *Ternstroemia gymnanthera*, *Cleyera japonica* and *Adinandra formosana* are rather dissimilar from the *V. germanica* samples (Fig. 19). Less distinct from *V. germanica* is *V. mocanera,* and, also *E. japonica* (Fig 19). In the analysis of the ordinal scaled traits, *V. mocanera* and *V. germanica* are grouped together (Fig. 20). *Adinandra formosana*, *C. japonica* and *T. gymnanthera* are also lumped together and almost indistinct from *Visnea* (Fig. 20). *Anneslea fragrans* and *E. japonica* are quite dissimilar from each other as well as from the other taxa (Fig. 20).

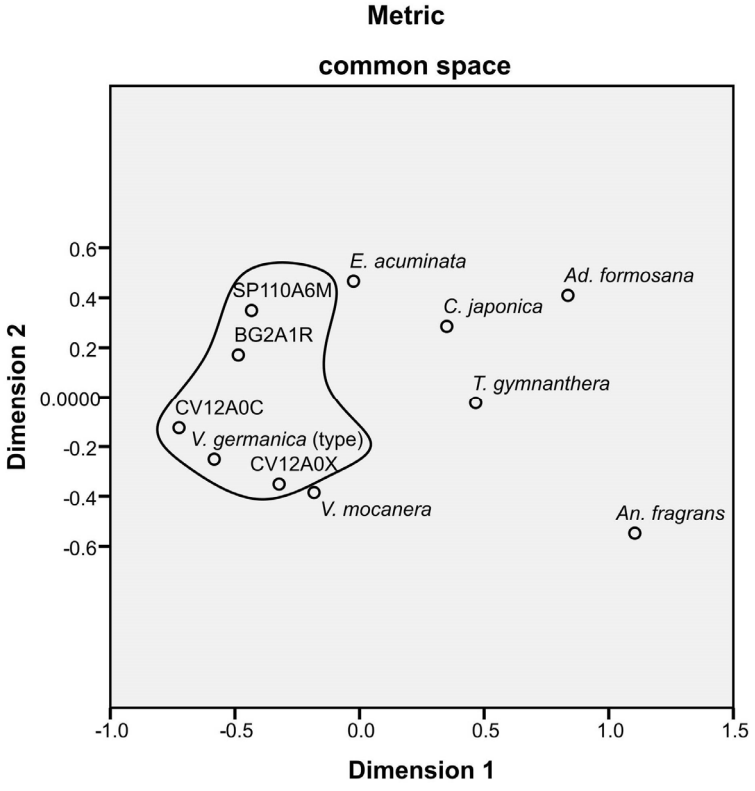

Figure 19. Multidimensional scaling analysis of the metric traits, i.e. fruit diameter, fruit shape, seed shape, seed width. Fossil *Visnea germanica* is circled.

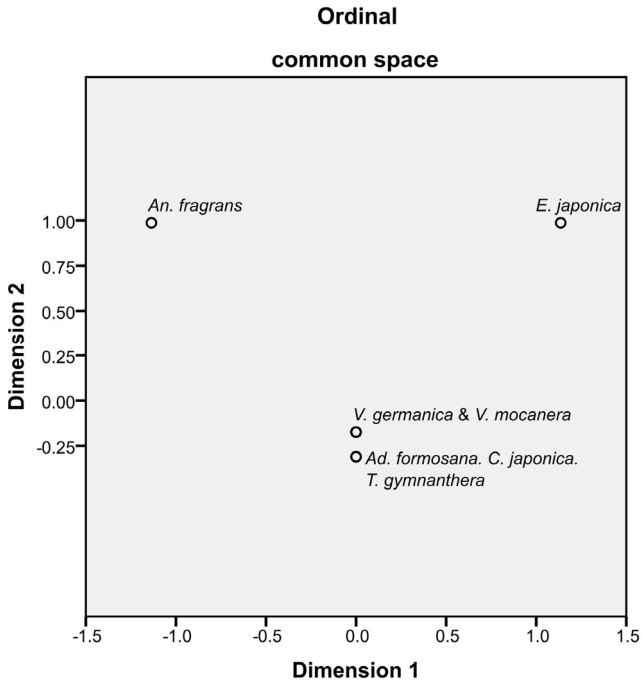

Figure 20. Multidimensional scaling analysis of the ordinal scaled traits, i.e. position of ovary and shape of embryo cavity.

In the hierarchical clustering analyses on the dataset without *Anneslea*, the highest increase in heterogeneity in the dendrogram was found for a two cluster solution when the average linkage, complete linkage, centroid, median or Ward cluster method was used (Fig. 21, Appendix Data). Cluster 1 comprises *Ad. formosana*, *C. japonica* and *T. gymnanthera*, Cluster 2 *E. japonica*, *V. mocanera* and *V. germanica*. Both clusters differ significantly in fruit shape, seed shape, seed width, position of ovary and shape of embryo cavity (Table 12). For the mean fruit diameter, the difference is not significant (Table 12).

Table 12. Clusters indicated by hierarchical (average linkage, complete linkage, centroid, median and Ward) clustering analyses. For the cluster-defining variables, means and standard deviations are given. The results from statistical comparison of the means from the cluster 1 and cluster 2 by independent two-sample t-tests are also indicated. Cluster 1: *Adinandra formosana*, *Cleyera japonica*, *Ternstroemia gymnanthera*; Cluster 2: *Eurya japonica, Visnea mocanera* and *V. germanica*.

Variable	**Name of cluster**	**Mean**	**Standard deviation of mean**	**t-test**		
				T	**df**	**p**
fruit diameter mean	1	7.0 mm	2.4 mm	2.7	2.2	0.11
	2	3.2 mm	0.7 mm			
fruit shape	1	1.0	0.0	4.2	6.0	**0.01**
	2	0.7	0.2			
seed shape	1	0.9	0.1	3.0	8.0	**0.02**
	2	0.7	0.1			
seed width mean	1	2.5 mm	0.9 mm	3.1	8.0	**0.02**
	2	1.3 mm	0.4 mm			
position ovary	1	0.0	0.0	-3.8	8.0	**0.01**
	2	0.9	0.4			
shape embryo cavity	1	0.0	0.0	-5.1	8.0	**0.00**
	2	1.1	0.4			

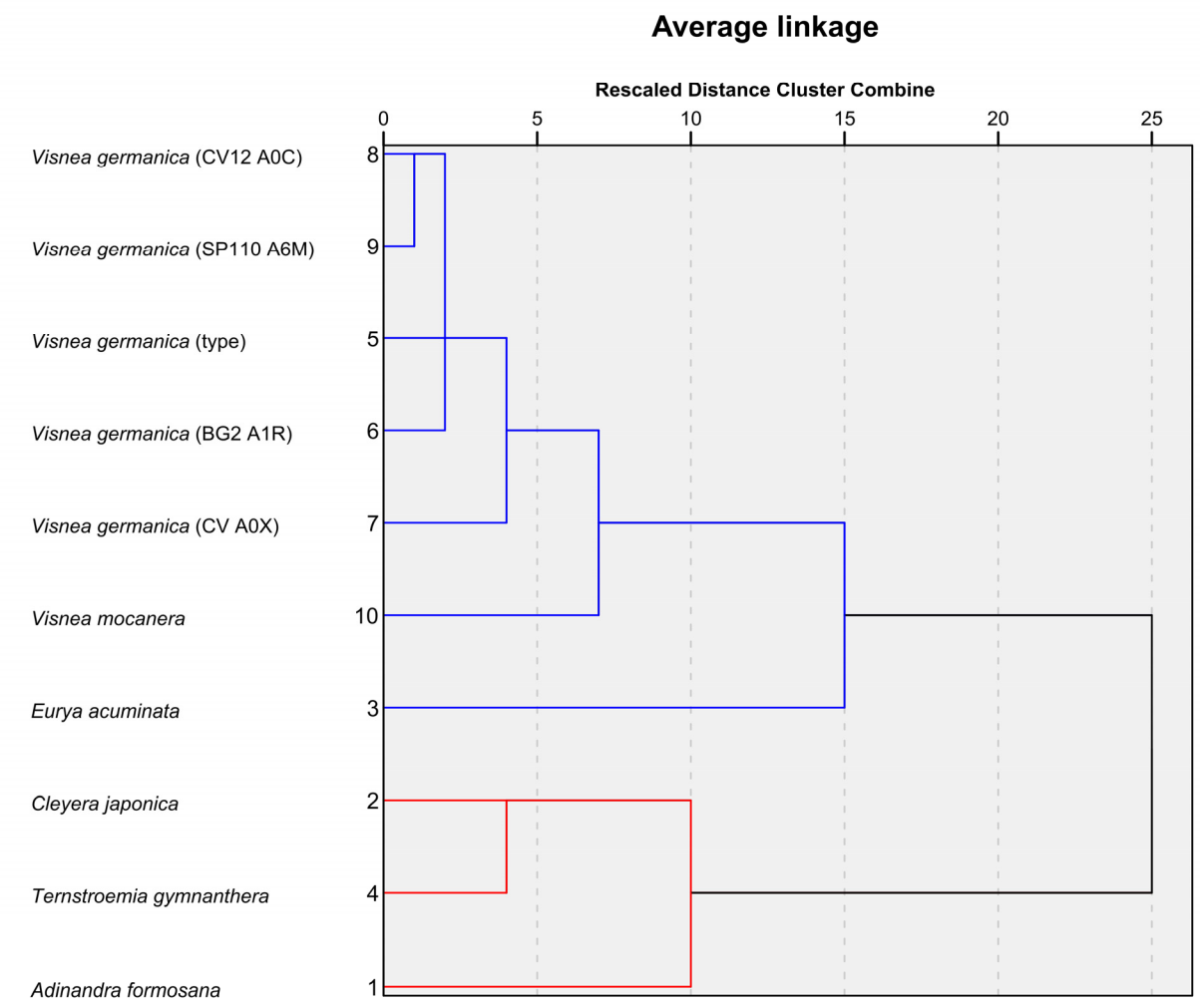

Figure 21. Dendrogram from hierarchical cluster analysis using the average linkage method. Cluster 1 is indicated in red, Cluster 2 in blue.

Hierarchical clustering based on the single linkage method proposes three clusters (Fig. 22). Cluster 1 consists of *Adinandra formosana*, *Cleyera japonica*, *Ternstroemia gymnanthera*, Cluster 2 of *Eurya japonica* and Cluster 3 of *Visnea mocanera* and *V. germanica*. Cluster 1 and 2 as well as Cluster 2 and 3 are significantly different from each other for all variables (Table 13). Between Cluster 1 and 3, significant differences are indicated for all variables except fruit diameter (Table 13).

Two-step cluster analysis determines two clusters as appropriate, with Cluster 1 containing *Adinandra formosana*, *Cleyera japonica*, *Ternstroemia gymnanthera* and *Eurya japonica*. Cluster 2 is constituted by both analyzed species of *Visnea*, *V. mocanera* and *V. germanica*. The clusters are found to significantly differ in fruit shape, seed shape and seed width (Table 14). The position of the ovary and the shape of the embryo cavity also separate both clusters (Table 14).

Table 13. Clusters indicated by hierarchical (single linkage) clustering analysis. For the cluster-defining variables, means and standard deviations are given. The results from statistical comparison of the means from cluster 1, 2 and 3 by independent two-sample t-tests are also indicated. Cluster 1: *Adinandra formosana*, *Cleyera japonica* and *Ternstroemia gymnanthera*; Cluster 2: *Eurya japonica*; Cluster 3: *Visnea mocanera* and *V. germanica*.

Variable	Name of cluster	Mean	Standard deviation of mean	t-test (Clusters: T; df; p)
fruit diameter mean	1	7.0 mm	2.4 mm	1 & 2: 0; 0; **0.00**
	2	2.4 mm	-	1 & 3: 2.6; 2.2; 0.12
	3	3.4 mm	0.7 mm	2 & 3: 0; 0; **0.00**
fruit shape	1	1.0	0.0	1 & 2: 0; 0; **0.00**
	2	1.0	-	1 & 3: 5.8; 5.0; **0.00**
	3	0.7	0.1	2 & 3: 0; 0; **0.00**
seed shape	1	0.9	0.1	1 & 2: 0; 0; **0.00**
	2	0.8	-	1 & 3: 3.2; 7; **0.02**
	3	0.7	0.1	2 & 3: 0; 0; **0.00**
seed width mean	1	2.5 mm	0.9 mm	1 & 2: 0; 0; **0.00**
	2	1.5 mm	-	1 & 3: 2.9; 7; **0.02**
	3	1.3 mm	0.4 mm	2 & 3: 0; 0; **0.00**
position ovary	1	0.0	0.0	1 & 2: 0; 0; 0
	2	0.0	-	1 & 3: -; -; -
	3	1.0	0.0	2 & 3: 0; 0; **0.00**
shape embryo cavity	1	0.0	0.0	1 & 2: 0; 0; 0
	2	2.0	-	1 & 3: -; -; -
	3	1.0	0.0	2 & 3: 0; 0; **0.00**

Table 14. Clusters indicated by two step clustering. For the cluster-defining variables, means and standard deviations are given. The results from independent two-sample t-tests comparing the means from cluster 1 and cluster 2 are also indicated. Cluster 1 *Adinandra formosana*, *Cleyera japonica*, *Ternstroemia gymnanthera*, *Eurya japonica*, Cluster 2 *Visnea mocanera* and *V. germanica*.

	Name of cluster	Mean	Standard deviation of mean	t-test		
				T	df	p
fruit diameter mean	1	5.9 mm	3.0 mm	2.0	8.0	0.08
	2	3.4 mm	0.7 mm			
fruit shape	1	1.0	0.0	5.8	5.0	**0.02**
	2	0.7	0.1			
seed shape	1	0.9	0.1	3.2	8.0	**0.01**
	2	0.7	0.1			
seed width mean	1	2.3 mm	0.9 mm	2.3	8.0	**0.05**
	2	1.3 mm	0.4 mm			
positition ovary	1	0.0	0.0	*	*	*
	2	1.0	0.0			
shape embryo cavity	1	0.5	1.0	*	*	*
	2	1.0	0.0			

* t-test not valid (no interval type data)

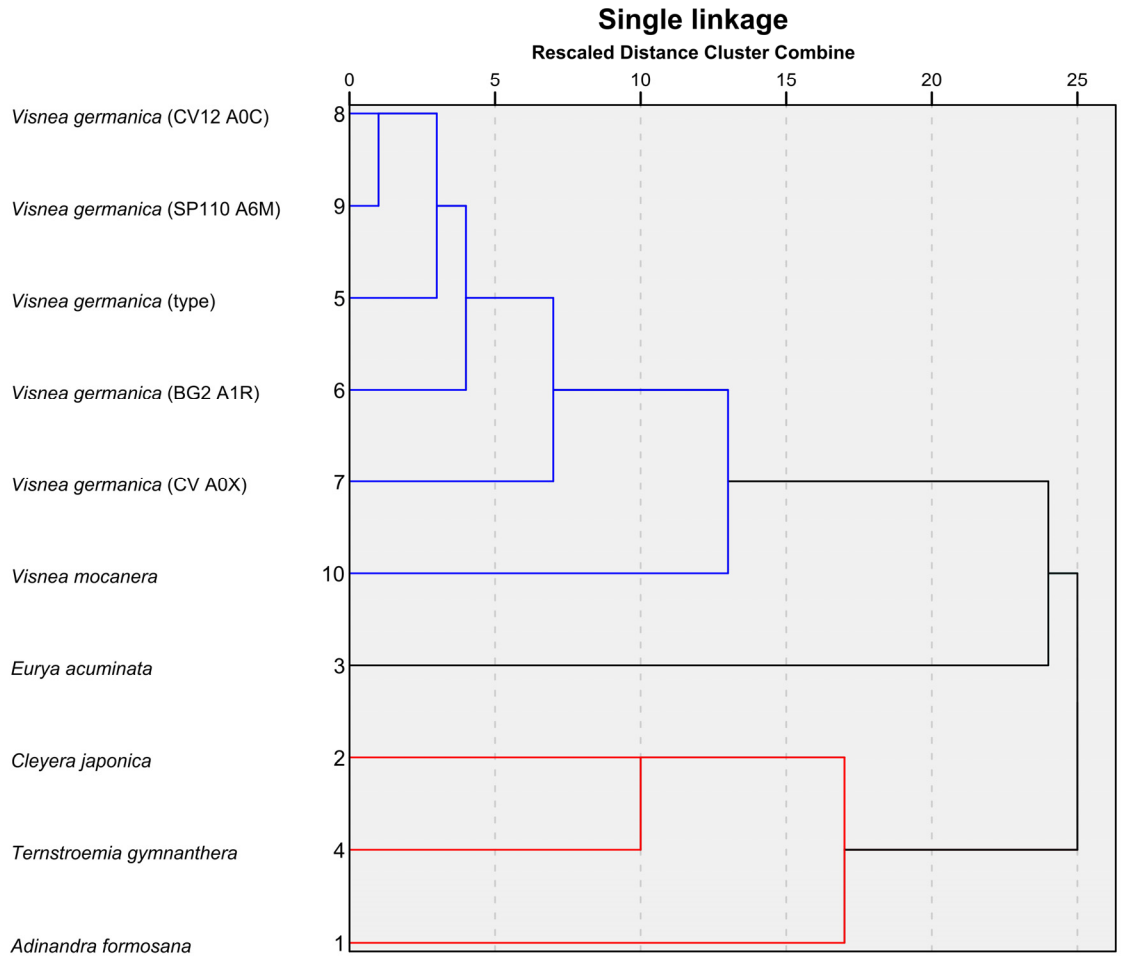

Figure 22. Dendrogram from hierarchical cluster analysis using the single linkage method. Cluster 1 is indicated in red, Cluster 2 (*Eurya* only) is not colored, Cluster 3 is marked in blue.

3.1.8. Discussion

Fruit anatomy: Comparison with literature data

The results on fruit size, seed size, number of seeds, number of locules, position of the ovary, shape of embryo cavity in extant Pentaphylacaceae do not contradict previously published literature, e.g. Corner & Corner (1976) Keng (1962) Kobuski (1941b, 1952), Min & Bartholomew (2007), Schacht (1859) and Weitzman et al. (2004), in most cases. Differences observed in this study will be discussed in the following.

In the analyzed sample of *Adinandra formosana*, the number of locules is higher (six) than the number denoted in Min & Bartholomew (2007; three). Additionally, the fruits are slightly bigger (almost 9 mm) than stated in Min & Bartholomew (2007; 7-8 mm). While the difference in size may be associated by habitat-related factors, drying artifacts in the herbarium specimen or measuring strategies, the deviant number of locules is not so easy to explain. One reason could be that the analyzed fruit belongs to a different species of *Adinandra*. However, the maximum number of locules observed in this genus is five according to Min & Bartholomew (2007) and Weitzman et al. (2004). Another possibility may be that the sample belongs to a different Asian distributed genus, e.g. *Eurya*, *Cleyera*, *Anneslea* or *Ternstroemia*. Yet, in neither of them, a locule number of six is found (Min & Bartholomew, 2007; Weitzman et al., 2004). Furthermore, the rest of the fruit characteristics

match the description for *Adinandra*. Thus, the sample may rather constitute an abnormality of *Ad. formosana* or another *Adinandra* species, or, belong to a new species of *Adinandra*.

The sample of *Adinandra lasiostyla* is significantly smaller than stated in Keng (1962). Yet, its identity is not questioned here as the size still agrees with Min & Bartholomew (2007).

In *Anneslea fragrans* var*. lanceolata*, only one seed is developed instead of two to three (Min & Bartholomew, 2007). This, however, may likely be attributed to chance/intraspecific variation.

The analyzed fruits of *Ternstroemia gymnanthera* and *Cleyera japonica* are smaller than described in Min & Bartholomew (2007) with respect to fruit size and seed size in the first and with respect to fruit size in the latter. Like in the case of *Ad*. *formosana*, this could be related to e.g. habitat-related factors, drying artifacts in the herbarium specimen or measuring strategies.

In consequence, the deviations from literature data or of minor importance here, as most of them may be explained with drying or intra-specific variation. Although the identity of the putative *Ad. formosana* sample is ambiguous, it is still useful as representative of the genus *Adinandra*.

Conflict with previously published results (Knobloch & Mai, 1986; Mai, 1971; Menzel, 1913) is indicated for the Italian fossils as well as the type from Germany.

In the Italian fossils, both average fruit size (ca. 3 mm) and number of seeds developed (min. four, max. eight) rather correspond with *Visnea minima* (fruit size 2-3 mm, number of seeds five to eight) than with *V. germanica* (size 4-11 mm, number of seeds three to five). Still, *V. minima* is only known from the Cretaceous and might be more correctly placed around the stem of Pentaphylacaceae (Magallón et al., 2015). The seed number of the Italian fossils also overlaps with *V. hordwellensis*, but only larger fruits have been reported for this species up to now. It is, however, not clear whether the fruit size is an ideal criterion to delimit the *Visnea* species. The small Italian seeds have already been attributed to *V. germanica* despite their size in previous studies, e.g. Basilici et al. (1997), Kovar-Eder et al. (2006), Martinetto, (1995) and Martinetto & Vassio (2010). It cannot be excluded that these constitute a regional variant. In addition to fruit size and number of seeds, the attachment of the seeds and the seed size compared to locule length were used by Knobloch & Mai (1986) and Mai (1971) to distinguish *V. germanica* from the other fossil species of *Visnea*. The attachment of the seeds can only be interpreted based on the MCT scans, as only one of the seeds was sectioned destructively. The scans suggest that the seeds are likely attached strongly to each other, as described for *V. germanica*. The second characteristic, seed size compared to locule length, also is also recovered according to description.

For the type, most characters, i.e. fruit size (ca. 5 mm), the seeds reaching locule length and probably also the attachment of seeds, match the description of *V. germanica* by Mai (1971). In contrast to that, the number of seeds (six) exceeds the one stated in Mai (1971). This indicates that the maximum number of seeds developed in *V. germanica* should be adjusted to six at least in the description.

In conclusion, the samples from Italy seem to share more characteristics with the type of *V. germanica* than with *V. minima* or *V. hordwellensis*. Thus, their attribution to *V. germanica* cannot be rejected based on the underlying data and the small fruit size may be e.g. a regional variant. Still, the fruits of *V. hordwellensis* and *V. minima* should be re-analyzed to provide more conclusive evidence for species distinction. In this context, it would be also useful to evaluate the identity of the relatively old *V. germanica* samples from the Eocene and Oligocene.

Affinity of the *V. germanica* fossils.

Multivariate statistics places the Italian *V. germanica* samples and the type of *V. germanica* either with *V. mocanera* only (single linkage, Fig. 22; two-step cluster analysis) or with both *V. mocanera* and *Eurya* (average linkage, complete linkage, centroid, median or Ward cluster method; Fig. 21). The first affinity is rather indicated by ordinal data (shape embryo cavity and position of ovary; Fig. 20), the latter by metric data (fruit size, fruit shape, seed size, seed shape, Fig. 19). In all cases of hierarchical analysis, there are hints that *V. germanica* and *V. mocanera* are more similar to each other than *V. germanica* and *Eurya*, as cluster formation first occurs within *V. germanica*. Later on, *V. germanica* and *V. mocanera* are joined, and, in the next step *Eurya* and *Visnea*. Further support for this comes from the structure of the testa of *V. germanica*, *V. mocanera* and *Eurya*. *Eurya* is characterized by the presence of funnel-shaped cells in the testa (Figs. 15D, 16D; Friis, 1985). In the testa of the fossils, elongate, not funnel-shaped cells with thickened cell walls are observed, placing them morphologically closer to *V. mocanera* than to *Eurya*.

Fruits of four genera of Freziereae could not be analyzed here due to the lack of material. Still, none of them seems to be close to *V. mocanera* and *V. germanica* based on previously published data. The first, the New Guinean *Archboldiodendron*, differs from *Visnea* by possessing five to seven locules and a bent embryo according to Weitzman et al. (2004). The second, *Balthasaria*, is distinct from *Visnea* by possessing numerous seeds, rather large fruits of 20-30 mm length and 10 mm width and 4-5 locules (Kobuski, 1956; Weitzman et al., 2004). The third, *Euryodendron*, is close to *Eurya* in the molecular phylogeny. Its seeds are of similar size than the ones of *V. mocanera*, i.e. 3-4 mm (Min & Bartholomew, 2007). Furthermore, it shares the number of locules with *Visnea* (Min & Bartholomew, 2007). Still, its numerous seeds and superior ovary separate it from *Visnea* (Min & Bartholomew, 2007; Weitzman et al., 2004). The last, *Symplococarpon*, shows a tendency to larger fruits than *Visnea*, e.g. 6-8 mm long in *S. brenesii* Kobuski or 13 mm long in *S. airy-shawianum* (Kobuski, 1941a). The seed size is comparable to *V. mocanera*. Nevertheless, the presence of only two seeds, the number of two locules and the inferior ovary do not match *Visnea* (Kobuski, 1941a).

Biogeographical patterns

In accordance with Rose et al. (2018) and the Tertiary relict hypothesis, the stem of *Visnea* dates to this geologic period in all of the three dating approaches tested here. This agrees with the fossil records of *V. germanica* and *V. hordwellensis*, but not with those of *V. minima* (Fig. 23). Hence, this hints that the identity of the latter should be re-checked. In a more direct comparison of the stem ages estimated in the underlying study with those from Rose

et al. (2018), it is noticeable that the estimates by the latter are considerably older (Fig. 23). While Rose et al. (2018) obtain a Late Eocene origin for *Visnea*, an Oligocene origin was suggested here. This was even the case in calibR, where three fossils used by Rose et al. (2018) were assigned to corresponding nodes and the stem of Lecythidaceae was fixed according to estimates from Rose et al. (2018). Possible causes for this discrepancy may be the difference in sampling, the different dating software used and the uncertainty of assigning calibration fossils to nodes. The age of the split of *V. mocanera* from *V. germanica* is estimated to the Miocene in tip-dating. As the analysis did not include trait coding for *V. germanica*, this estimate is deemed to be unreliable. Its age likely falls in the timeframe of the Oligocene (stem *Visnea*, Fig. 23) to the Pliocene (fossil record *V. germanica*, Fig. 23).

Geographically, an Indo-Malaysian-Palearctic origin of *Visnea* was already suggested by Rose et al. (2018). This overlaps with the Asian origin of the genus estimated here (Fig. 12, Appendix Fig. S13). The ancestors of *Visnea* were likely not restricted to Asia. While Pentaphylacaceae are extinct in Europe today, the fossil record indicates that the family was distributed in Europe, Asia and America during the Tertiary (Table 15). The earliest records of Pentaphylacaceae, i.e. *Protovisnea* Knobloch & Mai as well as taxa with affinities to *Pentaphylax*, *Visnea* and *Eurya* (Table 15), are known from the Late Cretaceous of Europe (Knobloch & Mai, 1986). During this time, the primary European flora started to form (Mai, 1989). In the early Tertiary, the European flora was isolated from the Asian flora by the Turgai strait and from America by another flora occupying the land bridge (Mai, 1989). In the Eocene, a belt of laurophyllous vegetation with several interruptions started to form in the northern hemisphere (Mai, 1989). Fossil *Cleyera* and *Ternstroemia* from Northern America date either to this time or are younger (Table 15; Manchester, 1994; Mathewes, Greenwood, & Archibald, 2016; Tiffney, 1994). While a direct connection between Europe and Asia was only established by the closure of the Turgai strait during the Oligocene (Collinson & Hooker, 2003; Mai, 1989), species with affinity to *Ternstroemia* are already known from Asia from the Eocene onwards (Table 15; Huzioka & Takahasi, 1970; Kong, 2000). Thus, floristic exchange between Europe and Asia likely did not rely on the existence of land bridges. Although the decline of laurophyllous taxa in Europe also started in the Oligocene, the break-up of the laurophyllous belt did not occur much later during the climatic and paleogeographic changes of the Late Miocene (Mai, 1989). At the time of the Pleistocene cooling, all laurophyllous elements in Europe were extinct (Mai, 1989). According to the biogeographical analyses (Fig. 12, Appendix Fig. S13), Macaronesia was colonized prior to this, likely in the MRCA of *V. mocanera* and *V. germanica* at latest. Thus, island colonization may fall into the timespan of the Oligocene to the Pliocene (Fig. 23). Although the Oligocene predates the emergence of the extant Canary Islands (21-1.1 mya) and Madeira (14.0-5.0 mya), the islands of Paleo-Macaronesia were already available for colonization (Fernández-Palacios et al., 2011). Still, there is no fossil evidence for the presence of the MRCA of *V. mocanera* and *V. germanica* on the islands as no fossils of *Visnea* are available from Macaronesia at all. Within Pentaphylacaceae, *Visnea* is not the only genus that colonized Macaronesia. Recently, Pleistocene fossils of the European and Asian distributed taxon *Eurya stigmosa* (Ludwig) Mai were reported from Madeira (Góis-Marques et al., 2019). Being a species likely occupying a laurel forest habitat like *Visnea*, the reasons for its extinction in Macaronesia

Table 15. Fossil record of Pentaphylacaceae from literature.

Species	Location	Age	Literature	Remarks
Anneslea? *costata* Chandler	Europe	Upper Eocene	Chandler (1961)	
Cleyera? bartonensis Chandler	Europe	Eocene	Chandler (1960)	
? *Cleyera cooperi* Chandler	Europe	Lower Eocene	Chandler (1964)	
Cleyera grotei Manchester	USA	Middle Eocene	Manchester (1994)	
Cleyera spec.	Europe	Middle Eocene	Collinson, Manchester, & Wilde (2012)	
Cleyera spec.	USA	Lower Miocene	Tiffney (1994)	
Cleyera variabilis Chandler	Europe	Eocene	Chandler (1960)	
Eurya becktonensis Chandler	Europe	Upper Eocene	Chandler (1961); Mai (1971)	probaly syn. *V. hordwellensis*
Eurya boveyana (Chandler) Mai	Europe	Oligocene	Mai (1971); Mai & Walther (1978)	
Eurya carpatica Knobl. & Mai	Europe	Upper Cretaceous	Knobloch & Mai (1986)	
Eurya crassitesta Knobloch	Europe	Upper Cretaceous	Knobloch et al. (1993); Knobloch & Mai (1986); Knobloch & Mai (1991)	
Eurya dubia (Chandler) Mai	Europe	Upper Eocene to Middle Oligocene	Mai (1971)	
Eurya holyi Knobloch	Europe	Upper Cretaceous	Knobloch & Mai (1986)	
Eurya japonica Thunb.	Asia	Pliocene	Yamakawa, Momohara, Saito, & Nunotani (2017)	
Eurya lentiformis (Chandler) Mai	Europe	Upper Eocene	Mai (1971)	
Eurya lusatica Mai	Europe	Miocene	Mai (1971); Van der Burgh (1987)	
Eurya microstigmosa Mai	Europe	Paleocene	Knobloch et al. (1993)	
Eurya obliqua (Chandler) Mai	Europe	Lower to Middle Eocene	Chandler (1962); Mai (1971)	synonymous *Cleyera obliqua*
Eurya poolensis (Chandler) Mai	Europe	Middle Eocene	Mai (1971)	
Eurya spec.	Asia	Oligocene	Tanai & Uemura (1991)	
Eurya spec.	Asia	Late Pliocene	Momohara (1992)	
Eurya stigmosa (Ludwig) Mai	Europe, Asia, Macaronesia	Paleocene to Lower Pleistocene	Basilici et al. (1997); Chandler (1961); Chandler (1963); Friis (1979, 1985); Góis-Marques et al. (2019); Gregor (1978); Gregor (1990); Hastings (1853); Knobloch et al. (1993); Łańcucka-Środoniowa (1984); Mai (1960, 1971, 1997, 2001); Martinetto et al. (2015); Martinetto & Ravazzi (1997); Meller (1998); Van der Burgh (1987); Zhu, Huang, Su, & Zhou (2016)	synonymous *Cleyera stigmosa*

Pentaphylax protogaea Knobl. & Mai	Europe	Upper Cretaceous	Knobloch & Mai (1986)	
Protovisnea cancellata (Vang.) Knobl. & Mai	Europe	Upper Cretaceous	Knobloch & Mai (1986, 1991)	
Protovisnea erinacea Knobl. & Mai	Europe	Upper Cretaceous	Knobloch & Mai (1986)	
Protovisnea maii (Knobl.) Knobl. & Mai	Europe	Upper Cretaceous	Knobloch & Mai (1986)	
Protovisnea reticulata Knobl. & Mai	Europe	Upper Cretaceous	Knobloch & Mai (1986, 1991)	
Protovisnea saxonica Knobl. & Mai	Europe	Upper Cretaceous	Knobloch & Mai (1986)	
Protovisnea tetragonalis Knobl. & Mai	Europe	Upper Cretaceous	Knobloch et al. (1993); Knobloch & Mai (1986)	
Protovisnea zahajensis Knobl. & Mai	Europe	Upper Cretaceous	Knobloch & Mai (1986, 1991)	
Ternstroemia spec.	Europe	Miocene	Ferguson et al. (1998); Friis (1985); Haas et al. (1998)	
Ternstroemia spec.	Northern America	Early Eocene	Mathewes et al. (2016)	
Ternstroemia spec.	Asia	Late Miocene	Huang et al. (2016)	
Ternstroemia spec.	Asia	Upper Eocene	Kong (2000)	
Ternstroemia maekawae Matsuo	Asia	Middle Miocene	Huzioka & Koga (1981)	
Ternstroemia bartonensis (Chandler) Mai	Europe	Upper Eocene	Mai (1971)	
Ternstroemia boveyana (Chandler) Mai	Europe	Upper Oligocene to Upper Miocene	Gregor (1978); Mai (1971, 1997)	
Ternstroemia dorofeevii Geissert, Gregor & Mai	Europe	Miocene to Pliocene	Geissert, Gregor, Mai, Boenigk, & Günther (1990) in PaleoDB (2019)	
Ternstroemia neglecta Mai	Europe	Oligocene	Mai (1971), Mai & Walther (1978) in PaleoDB (2019)	
Ternstroemia radialocarinata Mai	Europe	Upper Eocene	Mai (1971)	
Ternstroemia reniformis (Chandler) Mai	Europe	Lower Eocene to Lower Pliocene	Bertoldi & Martinetto (1995); Gregor (1978); Kovar-Eder, Kvaček, & Meller, (2001); Mai (1971); Martinetto et al. (1997); Meller (1998)	
Ternstroemia sequoioides (Engelhardt) Bůžek & Holý	Europe	Miocene	Kowalski (2008, 2017); Mai (2001)	
Ternstroemia setoi Huzioka & Takahasi	Asia	Eocene	Huzioka & Takahasi (1970) in PaleoDB (2019)	

remain speculative (Góis-Marques et al., 2019). The authors propose volcanic events, the intensification of Pleistocene glaciation cycles, or, the arrival of Portuguese settlers during 15th century as potential causes (Góis-Marques et al., 2019). Overall, an affinity to Asian lineages is not uncommon for Macaronesian laurel forest species. A possible Asian origin was found for e.g. *Apollonias barbujana*, *Heberdenia excelsa*, *Pleiomeris canariensis*, *Prunus lusitanica* and *Hedera canariensis* Willd. (Kondraskov, Schütz, et al., 2015; Valcárcel

et al., 2017). However, colonization of Macaronesia may have occurred more recently than in *Visnea*, dating around the Miocene or Pliocene.

According to Kondraskov, Schütz, et al. (2015), Tertiary relicts have to fulfill the criterion that the MRCA of the taxon and its sister group occupied a laurel forest habitat. The fossil record of *V. germanica* is in favor of that (Table 5). For CI1 B5U and possibly also SP110, occurrence in warm-temperate and probably subhumid gallery forests along rivers was proposed (Kovar-Eder et al., 2006). CV12 A0C and CV (CV12) A0X likely grew in communities resembling the extant evergreen broad-leaved forests in China (Martinetto, 1995). Part of a transported assemblage, the habitat of the *Visnea* samples from BG2A1R is less unambiguous to interpret. Still, *Visnea* from BG2A1R may have been associated with a high number of subtropical species (Basilici et al., 1997). In the open mixed forest flora of Herzogenrath, which contains the type of *V. germanica*, nearly one third of the taxa are tropical or subtropical with affinities to the Mediterranean, Macaronesia, Asia and Northern America (Menzel, 1913). Of Lauraceae, e.g. *Ocotea rhenana* Menzel has also been observed in Herzogenrath (Menzel, 1913). Although the mean annual temperature for this locality is estimated to be slightly colder than in the habitat of CV12 A0C and CV (CV12) A0X (Martinetto, 1995; van der Burgh 1984), the estimates for the mean annual precipitation overlap. Based on climate tolerance and distribution of extant relatives, Martinetto et al. (2017) distinguish three different types of extinct European taxa with Asian affinities, i.e. 1) HUTEA (humid thermophilous extinct European taxa of East Asian Affinity, e.g. *Ternstroemia reniformis* (Chandler) Mai), 2) CTEA (Cool-Tolerant extinct European taxa of East Asian affinity, e.g. *Eurya*) and 3) TEWA (Thermophilous European, West Asian and/or African elements, e.g. *Visnea*). HUTEA, CTEA and TEWA in occurred in the same communities (Martinetto et al., 2017). With the end of the Gelasian (Early Pleistocene) warmth, HUTEA and CTEA became extinct in Europe (Martinetto et al., 2017). Being more drought tolerant, TEWA like *Visnea* survived in refuges, e.g. Macaronesia (Martinetto et al., 2017).

Within *V. mocanera*, intraspecific diversification likely started around the Plio-/Pleistocene transition (ca. 3.6-1.8 mya, Fig. 11), or, alternatively, around the Late Miocene (ca. 11.6-5.3 mya; Appendix Fig. S12). Both Plio-/Pleistocene and Late Miocene patterns were indicated for laurel forest species in previous studies. A Plio-/Pleistocene crown age is found in e.g. in *Prunus lusitanica* (ca. 3.5 mya; Kondraskov, Schütz, et al., 2015). A crown dating to the Late Miocene was recovered for *Ranunculus cortusifolius* (ca. 5.3 mya; Williams et al., 2015). Genetic as well as morphological differentiation between the Macaronesian archipelagos was reported for *Prunus* L. as well as *Ranunculus* L. In contrast to that, genetic differentiation between Madeira and the Canary Islands is only weakly indicated in *V. mocanera* (Fig. 11, Appendix Fig. S11) and no morphological differences have been observed. A lack of morphological variation has also been described by Patiño et al. (2014) for the laurel forest lineages of spore-producing plants. According to Patiño et al. (2014), this may be due to the laurel forest providing a relatively stable habitat during major climate changes. In the study of Kim et al. (2008) on five Macaronesian endemic lineages, the Canary Islands acted as source for the colonization of Madeira during the Plio-/Pleistocene. Here, patterns of inter-archipelago and inter-island dispersal remain mostly unclear. Madeira

was likely colonized in a single event. Furthermore, a relationship between Madeira and Gran Canaria was proposed, but with rather weak statistical support (Appendix Fig. S11).

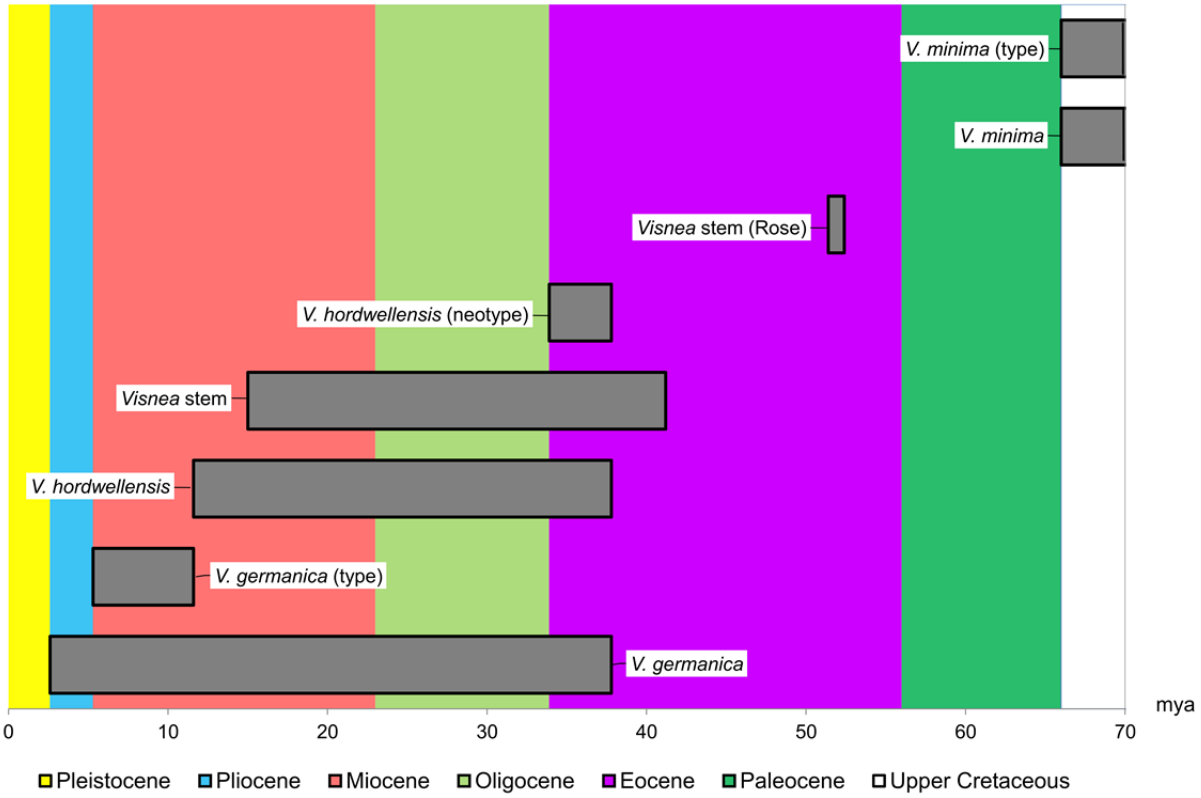

Figure 23. Stem age estimates for *Visnea* (this study, calibM and Rose et al., 2018) as well as occurrence of fossil *Visnea* species.

3.2. *Geranium reuteri*, *G. maderense*, *G. palmatum* and *G.yeoi* (Geraniaceae)

3.2.1. Specific Material and Methods

Phylogenetic sampling

The sampling for the phylogenetic analyses of the Macaronesian laurel forest species in *Geranium* is illustrated in Appendix Table S6. According to the molecular phylogenetic studies by Fiz et al. (2008) and Pokorny et al. (2014) and the morphological study by Yeo (1973), the species are nested within *Geranium* subg. *Robertium* (Picard) Rouy. The sampling of the present study mainly focused on *Geranium* subg. *Robertium* as recovered by Fiz et al. (2008), thus excluding the sections *Polyantha* Reiche, *Divaricata* Rouy and *Batrachioidea* W. D. J. Koch, which were assigned to subgenus *Robertium* based on fruit characteristics by Yeo (1984). All of the species from section *Ruberta* recognized by Aedo (2017) were included in the present study. Of section *Unguiculata* (Boiss.) Reiche, one of the two species listed by Aedo (2017) were sampled and of section *Trilopha* Yeo two of five species (Aedo, Muñoz Garmendia, & Pando, 1998).

Intraspecific sampling of *G. reuteri* consisted of one to three accession from each island of distribution (Gran Canaria, Tenerife, La Gomera, La Palma, El Hierro; Arechavaleta et al., 2010). Of the Madeiran taxa (Borges et al., 2008), three accessions of *G. maderense*, four accessions of *G. palmatum* and two accessions of *G. yeoi* were sampled. Additionally, multiple accessions of the closely related and widespread taxa *G. purpureum* and *G. robertianum* were sampled, in order to represent as many regions of their distribution as possible by at least one sequence (Table 16), see Aedo et al. (1998).

Table 16. Geographic sampling of *Geranium robertianum* and *G. purpureum* for phylogenetic analysis. Native and non-native regions are classified according to Aedo et al. (1998) and Brummitt, Pando, Hollis, & Brummitt (2001).The number of samples analyzed from each region is given in brackets.

Species	Native regions sampled	Native regions (no sample available)	Non-Native regions sampled
G. robertianum	Northern Europe (2) Middle Europe (3) Southwestern Europe (3) Southeastern Europe (3) Eastern Europe (1) Macaronesia (2) Siberia (1) Middle Asia (1) Caucasus (1) Western Asia (1) China (1) Eastern Asia (1)	Northern Africa Northeastern tropical Africa Arabian Peninsula Indian subcontinent	Southwestern USA (1) Northwestern USA (1) Caribbean (1)
G. purpureum	Middle Europe (2) Southwestern Europe (2) Southeastern Europe (3) Macaronesia (4) Northern Africa (1) Western Asia (2) Caucasus (1)	Northern Europe Eastern Europe East Tropical Africa	New Zealand (1) Southern South America (1)

For molecular dating, sequences from the major clades of Geraniaceae, seven species of Francoaceae (incl. Vivianiaceae and Melianthaceae) and two species of Crossosomataceae were retrieved from Fiz et al. (2008; TreeBASE study number S1569) and from GenBank. Francoaceae were included as calibration taxa, whereas Crossosomataceae served as outgroup.

Molecular phylogenetic analyses

Autopolyploidy and hybridization have been suggested for the origin of the Macaronesian *Geranium* species. Thus, plastid and nuclear data were analyzed separately. For plastid data, two different approaches were used: a) *rbcL* (ribulose-1,5-bisphosphate carboxylase/oxygenase large subunit gene) and *trnL-trnF* spacer were analyzed on a dataset containing major clades of Geraniaceae as well as representatives of Francoaceae and, as an outgroup, Crossosomataceae and b) *matK* and *trnL-trnF* spacer were analyzed on a dataset of *Geranium* subgenus *Robertium*, using *G. incanum* as an outgroup. Nuclear data, i.e. ETS (external transcribed spacer) and ITS, were analyzed on a dataset comprising *Geranium* subgenus *Robertium*, using species from *Geranium* subgenus *Geranium* as outgroup. MCMC settings used in BI are given in Table 17. As no statistically well-supported topological incongruences were present, *rbcL* could be combined with *trnL-trnF* (Appendix Figs. S19, S20), *matK* with *trnL-trnF* (Appendix Figs. S21, S22) as well as ITS with ETS (Appendix Figs. S23, S24) in the respective approaches.

In addition to the above mentioned markers, 5S NTS (5S non-transcribed spacer), TOPO6 (Topoisomerase 6 B gene), *3'rps16–5'trnK*$^{(UUU)}$ spacer (3' ribosomal protein S16 and 5' t-RNA Lysine intergenic spacer), *psbA-trnH* spacer and *psbJ-petA* (photosystem II protein J and cytochrome f intergenic spacer) spacer were tested for variability (Appendix Data S2). The markers were discarded for the following reasons: For 5S NTS, the homology of the obtained sequences was doubtful, TOPO6 provided no resolution between *G. reuteri*, *G. robertianum* and *G. purpureum*, *psbJ-petA* and *psbA-trnH* no resolution between *G. robertianum* and *G. purpureum* and *3'rps16–5'trnK*$^{(UUU)}$ spacer was abandoned due to difficulties in amplification and sequencing.

Table 17. MCMC settings for Bayesian analysis of the *Geranium* datasets using MrBayes.

	rbcL [a]	***trnL-trnF*** [a]	***rbcL* & *trnL-trnF*** [a]	**ETS** [b]	**ITS** [b]	**ETS & ITS** [b]	***matK*** [b]	***trnL-trnF*** [b]	***matK* & *trnL-trnF*** [b]
Chain length (million states)	10	10	10	10	10	1	10	10	1
Sample frequency	1000	1000	1000	1000	1000	1000	1000	1000	1000
Number of chains	4	4	4	4	4	4	4	4	4
Number of runs	2	2	2	2	2	2	2	2	2
Heating parameter	0.2	0.2	0.2	0.2	0.2	0.2	0.2	0.2	0.2

[a] Geraniaceae dataset; [b] subg. *Robertium* dataset

Stem age estimation

Analysis was conducted on the *rbcL* and *trnL-trnF* spacer dataset from the study by Fiz et al. (2008), extended by own sequence data and GenBank data. It contained major clades of Geraniaceae, sequences of Francoaceae for rooting, and Crossosomataceae as outgroup. The age of the split of Geraniaceae from Francoaceae was set to 115.2-83.5 mya according to Magallón et al. (2015; calibM). The chain length was set to 70 000 000 and every 7000th state was sampled.

For comparison, a) the same dataset was calibrated setting the crown age of Geraniaceae to 64.2-52.6 mya adding an error margin of 10% to the estimate of 58.4 mya by Landis et al. (2018; calibL), sampling every 5000th state of 50 000 000, and b) a Geraniaceae *rbcL* and *trnL-trnF* spacer dataset was calibrated with the crown age of *Geranium* estimated by Fiz et al. (2008; 23.8-14.5 mya; calibF), sampling every 2000th state of 20 000 000.

Crown age estimation

Analyses were based on three different datasets of the nuclear markers, comprising all species of the *Geranium maderense* clade and the *Geranium robertianum* clade: a) only accessions of which both ITS and ETS could be sequenced, b) ITS sequences only and c) ETS sequences only. The coalescent constant population model was applied as tree prior. The age estimate of 9.7-1.9 mya for the split of section *Ruberta* from section *Anemonifolia*, as estimated in stem node dating (calibM; Appendix Fig. S25), served as calibration point. For the individual ETS dataset, the weight of the BitFlip Operator and the weight of the DeltaExchange Operator were set to 1.0 to increase the otherwise low ESS of the hasEqualFreqs parameter (Bouckaert, 2017). For the combined dataset and ITS, chain length and sampling frequency very set to 80 000 000 and 8000, for ETS to 100 000 000 and 10 000.

Ancestral area estimation

As basis for the biogeographical reconstructions, the dated plastid (*rbcL* and *trnL-trnF* spacer) phylogeny calibrated with the data from Magallón et al. (2015; calibM) was used. Analysis was restricted to *Geranium* subgenus *Robertianum*. The areas coded included the Canary Islands (A), the Mediterranean Region (B), Eurasia (C), Non-Mediterranean Africa (D), Madeira (E) and the Azores (F; Table 18).

The best-scoring model from BioGeoBEARS analysis, DEC, was selected for analysis in RASP (Table 19). To account for topological uncertainty, the analysis was run as S-DEC.

Table 18. Coding for ancestral area estimation in *Geranium* subg. *Robertium*. Canary Islands (A), Mediterranean (B), Eurasia (C), Non-Mediterranean Africa (D), Madeira (E), Azores (F).

Species	Areas	References
Geranium biuncinatum Kokwaro	D	Aedo et al. (1998)
Geranium cataractarum Coss.	B	Aedo et al. (1998)
Geranium glaberrimum Boiss. & Heldr.	B	Aedo et al. (1998)
Geranium lasiopus Boiss. & Heldr.	B	Aedo et al. (1998)
Geranium lucidum L.	BCE	Aedo et al. (1998); Borges et al. (2008)
Geranium macrorrhizum L.	BC	Aedo et al. (1998)
Geranium maderense Yeo	E	Aedo et al. (1998); Borges et al. (2008)
Geranium ocellatum Jacquem. ex Cambess.	C	Aedo, Barberá, & Buira (2016)
Geranium palmatum Cav.	E	Aedo et al. (1998); Borges et al. (2008)
Geranium purpureum Vill.	ABCDEF	Aedo et al. (1998); Arechavaleta et al. (2010); Borges et al. (2008); Silva et al. (2005)
Geranium reuteri Aedo & Muñoz Garm.	A	Aedo et al. (1998); Arechavaleta et al. (2010)
Geranium robertianum L.	ABCDEF	Aedo et al. (1998); Arechavaleta et al. (2010); Borges et al. (2008)
Geranium yeoi Aedo & Muñoz Garm.	E	Aedo et al. (1998); Borges et al. (2008)

Table 19. Biogeographical models tested for the plastid dataset of *Geranium* subg. *Robertium* and their likelihoods, AICs and AICcs as inferred by BioGeoBEARS (Matzke, 2013a; Matzke, 2013b). The best-scoring model is marked in bold.

Model	Likelihood (LnL)	AIC	AICc
DEC	**-39.26**	**82.52**	**83.72**
DEC+J	-39.26	84.52	87.19
DIVALIKE	-50.79	105.6	106.8
DIVALIKE+J	-44.73	95.47	98.13
BAYAREALIKE	-47.94	99.88	101.1
BAYAREALIKE+J	-42.11	90.22	92.89

3.2.2. DNA sequence variation and phylogenies

One hundred and fifty-one newly generated sequences have been uploaded to GenBank (Appendix Table S6). Sequence variation for each alignment is given in Table 20.

The topologies of the Geraniaceae plastid phylogeny (Fig. 24, Appendix Fig. S25) and of the nuclear phylogeny of *Geranium* subg. *Robertium* (Fig. 25) do neither contradict each other nor the previously published phylogenies, e.g. by Fiz et al. (2008) and Pokorny, Oliván, & Shaw, (2011). Within subg. *Robertianum*, sect. *Trilopha* is sister to a clade comprising sect. *Unguiculata* and sect. *Ruberta* (Fig. 24). Sect. *Ruberta* is recovered as paraphyletic with respect to sect. *Unguiculata* and consists of two clades. The first comprises *Geranium lasiopus* Boiss. & Heldr., *G. glaberrimum* Boiss. & Heldr., *G. lucidum* L., and, of sect. *Unguiculata*, *G. macrorrhizum* L. (Fig. 24). The second includes *G. maderense*, *G. palmatum*, *G. robertianum*, *G. purpureum*, *G. reuteri*, *G. yeoi,* and, as sister to the other species, *G. cataractum* (Fig. 24).

Table 20. Sequence characteristics of the *Geranium* subg. *Robertium* and Geraniaceae datasets, i.e. the nuclear and plastid datasets of *Geranium* subg. *Robertium* (ETS, ITS, ETS & ITS, *matK*, *trnL-trnF* spacer, *matK* & *trnL-trnF* spacer) and the plastid datasets (*rbcL*, *trnL-trnF* spacer, *rbcL* & *trnL-trnF* spacer) of Geraniaceae.

	rbcL [a]	***trnL-trnF*** [a]	***rbcL* & *trnL-trnF*** [a]	**ETS** [b]	**ITS** [b]	**ETS & ITS** [b]	***matK*** [b]	***trnL-trnF*** [b]	***matK* & *trnL-trnF*** [b]
Number of accessions	44	90	113	58	65	58	12	28	29
Total number of characters	1408	634	2042	532	713	1258	757	864	1627
Variable characters	25%	47%	32%	48%	22%	26%	9%	13%	11%
Parsimony informative characters	17%	33%	22%	30%	18%	22%	3%	7%	5%
Substitution model (AIC)	GTR+Γ+I	GTR+Γ	GTR+Γ+I	GTR+Γ	GTR+I (MrBayes) GTR+G (RaxML*)	GTR+Γ	GTR+Γ	GTR+Γ	GTR+Γ

* according to PartitionFinder; [a] Geraniaceae dataset; [b] subg. *Robertium* dataset

Canarian endemic *G. reuteri* and Madeiran endemic *G. yeoi* are closely related to *G. robertianum* and *G. purpureum* (*G. robertianum* clade, Fig. 24). The *G. robertianum* clade is significantly supported by plastid data (Fig. 24, Appendix Fig. S26). It is also recovered by nuclear data, but without significant support (Fig. 25). The relationships within the *G. robertianum* clade are not resolved by plastid data (Fig. 24, Appendix Fig. S26). Nuclear data suggests with low support (BS = 88; Fig. 25) that the majority of the accessions of widespread *G. purpureum* are sister to Madeiran *G. yeoi*, Canarian *G. reuteri*, widespread *G. robertianum* and two accessions, which are putatively *G. purpureum*. The three species and the two putative *G. purpureum* accessions form a polytomy, in which the analyzed accessions of *G. reuteri* are weakly indicated as monophyletic (PP = 0.93, Fig. 25). Intraspecific geographic patterns within *G. reuteri* are suggested mainly with low support, i.e. the accessions from El Hierro (BS = 88) as well as the accessions from La Gomera (PP = 0.90, BS = 83) are recovered as distinct by ITS data only (Appendix Fig. S23). A sister group relationship between *G. reuteri* from La Gomera and *G. reuteri* from Gran Canaria is suggested by ETS only (PP = 0.95; Appendix Fig. S24). For Madeiran *G. yeoi* and widespread *G. robertianum*, no intraspecific geographic patterns are supported (Fig. 25). In contrast to that, nuclear data indicates geographic patterns within the widespread *G. purpureum*. The analyzed accessions are found to be intermingled with one accession from the Dominican Republic that is putatively *G. robertianum* (Fig. 25). The sample from Israel is sister to a clade containing all other samples (except SMNS 416 and SMNS 409) of *G. purpureum* (PP = 1.0, BS = 80, Fig. 25). Within this clade, the samples from Sicily and Corsica are closely related to each other (PP = 1.0, BS = 87, Fig. 25). Furthermore, the samples from Greece, mainland Italy and Germany form a clade (PP = 0.97, BS = 82, Fig. 25), which is suggested by ITS data to also comprise a sample from Turkey (PP = 0.98, Appendix Fig. S23). ETS data indicates that the *G. purpureum* sample from the Canary Islands and the *G. purpureum* sample from Madeira are closest relatives (PP = 0.90, BS = 94, Appendix Fig. S24).

According to plastid (Fig. 24, Appendix Fig. S26) and nuclear data (Fig. 25), Madeiran endemic *G. palmatum* and *G. maderense* form a well-supported clade (*G. maderense* clade),

which is sister to the *G. robertianum* clade. In the plastid dataset, both Madeiran endemics are not clearly distinct (Appendix Fig. S26). Nuclear data, however, allows for distinction, albeit with a rather low statistical support (Fig. 25, Appendix Fig. S23). Biogeographic patterns are not resolved within *G. palmatum* (Appendix Fig. S23). Within *G. maderense*, the patterns suggested by ETS differ from those suggested by ITS (Appendix Fig. S23 & S24). A visual check of the alignment, however, showed that the *G. maderense* sequences are almost identical, except for some cases of base ambiguities and a one base pair wide gap.

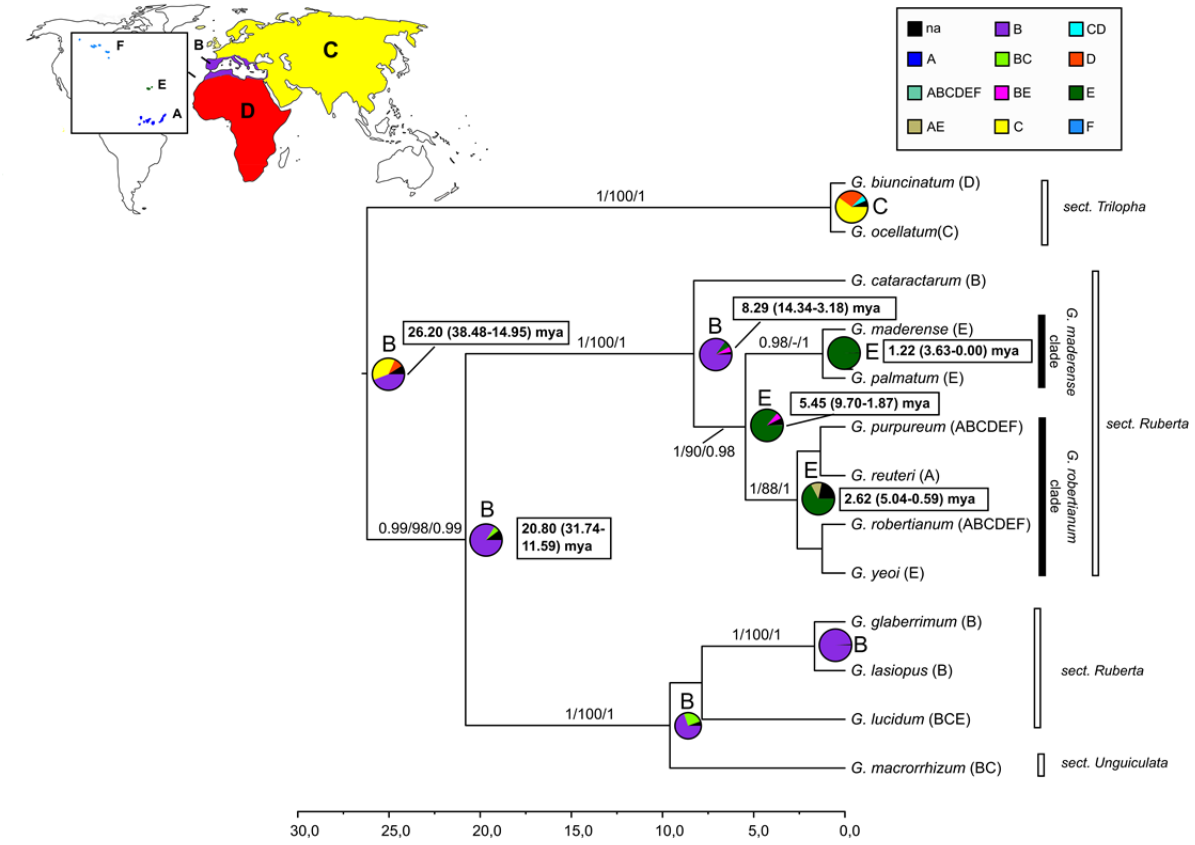

Figure 24. Biogeography of *Geranium* subg. *Robertium* as inferred from BBM analysis in RASP, based on the plastid chronogram. Numbers above branches indicate posterior probabilities from MrBayes analysis, bootstrap values from RAxML analysis and posterior probabilities from BEAST analysis. Only posterior probabilities ≥0.90 and bootstrap values ≥80 are shown. On the nodes, the posterior probabilities of the estimated areas/area combinations are indicated by pie charts. Areas coded include the Canary Islands (A), the Mediterranean (B), Non-Mediterranean Eurasia (C), Non-Mediterranean Africa (D), Madeira (E) and the Azores (F). For nodes of interest, the age estimates from BEAST analysis are given. The world map was modified from https://commons.wikimedia.org/wiki/File:Simplified_blank_world_map_without_Antartica_(no_borders).svg, the map of Macaronesia from A. Platon, https://upload.wikimedia.org/wikipedia/commons/b/b4/Macaronesia_location.svg.

3.2.3. Molecular dating: Late Miocene origin and diversification of the laurel forest lineage

The age estimates based on the calibration data retrieved from Magallón et al. (2015) constitute the oldest (Appendix Fig. S25). In contrast to that, calibrations based on Landis et al. (2018) and Fiz et al. (2008) resulted in younger age estimates (Appendix Figs S27, S28), with the one based on Fiz et al. (2008) providing the youngest. In the following, the results from the calibration based on Magallón et al. (2015; calibM; Fig. 24, Fig. 26, Appendix Fig. S25) and the calibration based on Fiz et al. (2008; calibF; Appendix Fig. S28) are described.

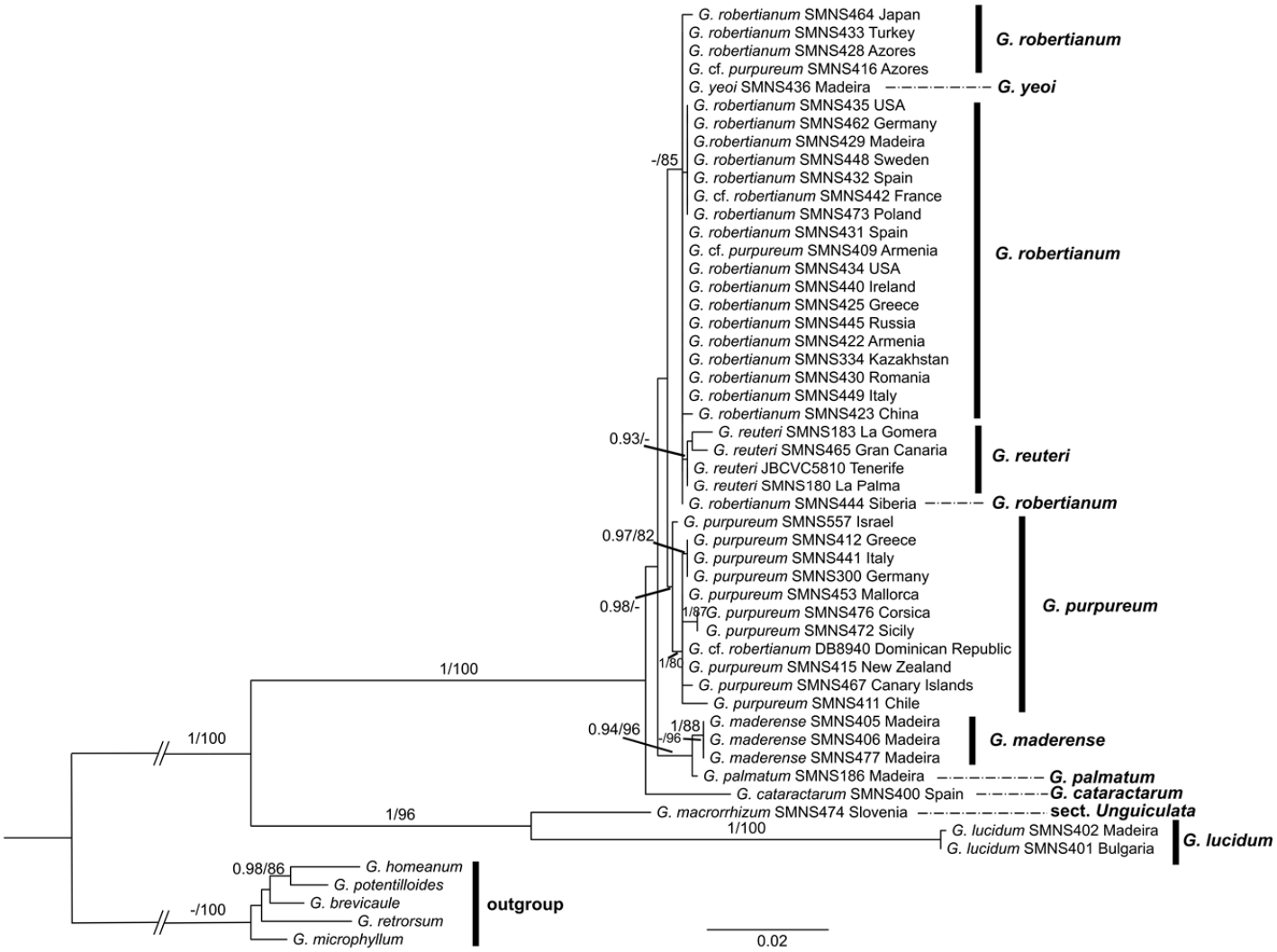

Figure 25. Nuclear phylogeny (ETS & ITS) of *Geranium* sect. *Robertium* and *Geranium* sect. *Unguiculata* from ML analysis. Above the branches, posterior probabilities from Bayesian analysis and bootstrap values from ML analysis are shown.

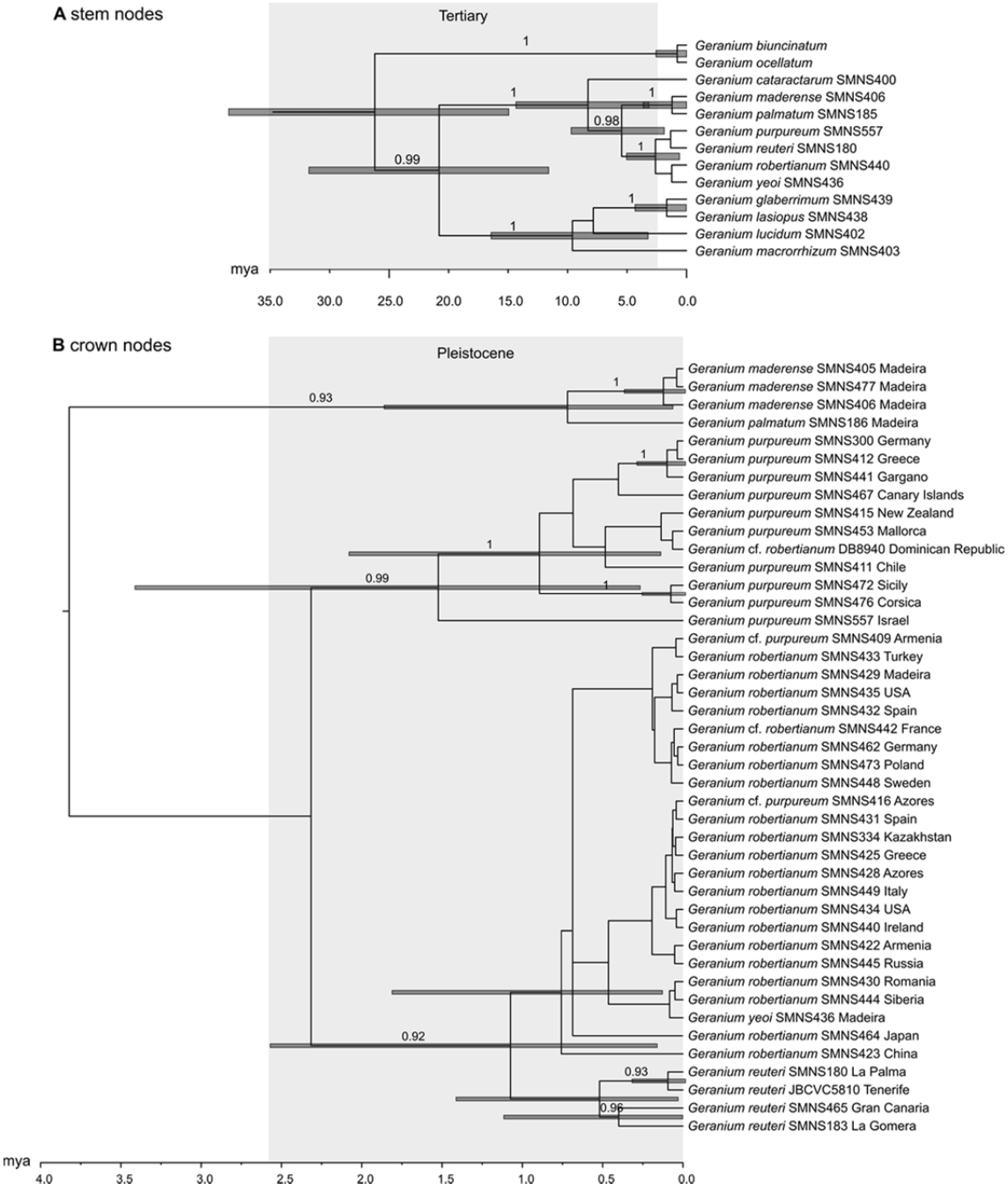

Figure 26. Chronograms from stem node and crown node dating in *Geranium*. Bars at the nodes indicate 95% highest posterior densities; posterior probabilities from BEAST analysis ≥ 0.90 are given above the branches. **A** Stem node dating, plastid data (*rbcL & trnL-trnF*; calibM); **B**, Crown node dating based on nuclear data (ITS & ETS) of the *G. robertianum* clade and the *G. maderense* clade.

The crown of *Geranium* subg. *Robertium* dates to the Late Oligocene (calibM, 26.20 mya, 95% HPD 38.48-14.95 mya; Fig. 24, Fig. 26A) or the Middle Miocene (calibF, 14.95 mya, 95% HPD 20.72-9.58 mya). The MRCA of sect. *Unguiculata* and sect. *Ruberta* is estimated to the Early or Middle Miocene (calibM, 20.80 mya, 95% HPD 31.74-11.59 mya; calibF, 11.81 mya, 95% HPD 17.56-6.91 mya; Fig. 24, Fig. 26A). The split of *G. cataractarum* from the *G. robertianum* clade and the *G. maderense* clade occurred during the Late Miocene (calibM, 8.29 mya, 95% HPD 14.34-3.18 mya; Figs. 24, 26A) or the Early Pliocene (calibF, 5.15 mya, 95% HPD 8.71-1.67 mya). The subsequent divergence of the *G. robertianum*

clade from the *G. maderense* clade dates to the Late Miocene (calibM, 5.45 mya, 95% HPD 9.70-1.87 mya; Figs. 24, 26A) or the Late Pliocene (calibF, 3.43 mya, 95% HPD 6.13-1.07 mya).

Diversification within the *G. robertianum* clade started during the Late Pliocene (calibM, 2.62 mya, 95% HPD 5.04-0.59 mya; Figs. 24, 26A) or the Early Pleistocene (calibF, 1.71 mya, 95% HPD 3.43-0.41 mya). *Geranium robertianum*, *G. reuteri* and *G. yeoi* originated during the Early Pleistocene (1.09 mya, 95% HPD 2.59-0.18 mya) at the earliest (Fig. 26B). The crown of *G. reuteri* dates to the Middle Pleistocene (0.54 mya, 95% HPD 1.83-0.14 mya), whereas the crowns of *G. yeoi* and *G. robertianum* are not recovered (Fig. 26B). The crown age of *G. purpureum* falls into the Early Pleistocene (1.54 mya, 95% HPD 3.43-0.28 mya; Fig. 26B).

Within the *G. maderense* clade, speciation into both Madeiran species *G. maderense* and *G. palmatum* occurred during the Early Pleistocene (calibM, 1.22 mya, 95% HPD 3.63-0.00 mya; calibF, 0.81 mya, 95% HPD 2.44-0.00 mya; Figs. 24, 26A). Intraspecific diversification is dated to the Middle Pleistocene (0.14 mya, 95% HPD 0.38-0.0 mya, Fig. 26B) in *G. maderense* and in *G. palmatum* (ITS data 0.17 mya, 95% HPD 0.40-0.00 mya, Appendix Fig. 29; ETS data 0.13 mya, 95% HPD 0.47-0.00 mya, Appendix Fig. 30).

3.2.4. Biogeographic reconstructions: Mediterranean origin

For the origin of the Macaronesian laurel forest species in *Geranium*, different biogeographical patterns are suggested by BBM and S-DEC analyses. Below, the estimates with the highest probabilities are given.

BBM analysis indicates that the MRCA of *Geranium* subg. *Robertium* was distributed in the Mediterranean region (Fig. 24, PP = 0.44). A Mediterranean origin was also reconstructed for the MRCA of *Geranium* sect. *Unguiculata* and sect. *Ruberta* (Fig. 24, PP = 0.84) as well as for the MRCA of *G. cataractarum*, the *G. maderense* clade and the *G. robertianum* clade (Fig. 24, PP = 0.85). Dispersal to Madeira was found in the MRCA of the *G. maderense* clade and the *G. robertianum* clade (Fig. 24, PP = 0.86). The MRCA of laurel forest taxa *G. palmatum* and *G. maderense* also occurred on Madeira (Fig. 24, PP = 0.99). Within the *G. robertianum* clade, dispersal from Madeira (Fig. 24, PP = 0.67) to different regions is indicated, i.e. to the Canary Islands in the case of *G. reuteri* and a range extension towards a widespread distribution including all coded areas in the case of *G. robertianum* and *G. purpureum* (Fig. 24).

The results from S-DEC analysis in RASP (Appendix Fig. S31) do not contradict the outcome of DEC analysis in BioGeoBEARS (Appendix Fig. S32). S-DEC analysis suggests a Eurasian-Mediterranean distributed MRCA of *Geranium* subg. *Robertium* (p = 0.08; Appendix Fig. S31). A range extension towards a widespread distribution (including all coded areas) was estimated for the MRCA of *Geranium* sect. *Unguiculata* and sect. *Ruberta* (p = 0.17; Appendix Fig. S31). A widespread distribution is also reconstructed for the MRCA of *G. cataractarum*, the *G. maderense* clade and the *G. robertianum* clade (p = 0.88; Appendix Fig. S31), for the MRCA of the *G. maderense* clade and the *G. robertianum* clade (p = 0.73; Appendix Fig. S31) and for the potential origin of the Canarian species *G. reuteri* and the

Madeiran species *G. yeoi* (p = 0.92; Appendix Fig. S31). As origin of both of the Madeiran species *G. maderense* and *G. palmatum*, Madeira was estimated (p = 1.0; Appendix Fig. S31).

3.2.5. Discussion

Hybridization and phylogenetic relationships in *Geranium* subg. *Robertium*

Hybridization has been indicated as a common mode of speciation in Macaronesian taxa (Caujapé-Castells et al., 2017), e.g. *Pericallis*, *Sideritis* and *Argyranthemum* (Barber, Finch, Francisco-Ortega, Santos-Guerra, & Jansen, 2007; Fjellheim, Jørgensen, Kjos, & Borgen, 2009; Jones et al., 2014). In the Macaronesian laurel forest species of *Geranium* and in their closest relatives, cases of hybridization and autopolyploidization have also been suggested, e.g. Yeo (1973). Usually, hybridization is reflected by an incongruence between nuclear (biparental inheritance) and plastid data (uniparental inheritance; see also e.g. Blöch et al., 2009). Although no significantly supported incongruence between the analyzed plastid and nuclear markers was observed here (Fig. 24, Fig. 25), this may be due to biparental inheritance of plastids in Geraniaceae (Weng, Blazier, Govindu, & Jansen, 2013). In consequence, it cannot be rejected that the Madeiran *G. maderense* and *G. palmatum* are the result from hybridization between Mediterranean *G. cataractarum* and widespread *G. purpureum*, as suggested by Widler-Kiefer & Yeo (1987) and Yeo (1973). This event may have occurred within the Mediterranean, where both of the species are distributed. Alternatively, while *G. pupureum* may have been already present in Macaronesia/Madeira, propagules of *G. cataractarum* may have reached Macaronesia from Iberia/Northern Africa. This might have allowed for crossing of both species which enabled the hybrids to colonize new habitats, without a need for permanent establishment of *G. cataractarum* or with later on extinction of the latter (see Caujapé-Castells et al., 2017). A second event of hybridization was proposed for *G. purpureum* and an unknown species, leading to *G. robertianum*. With *G. robertianum* placed close to *G. purpureum* in the molecular phylogeny (Fig. 24, Fig. 25), this may be likely. Autopolyplodization in *G. robertianum* was proposed for the origin of *G. yeoi* and, possibly, in a second independent event, also for the origin of *G. reuteri* (Widler-Kiefer & Yeo, 1987; Yeo, 1973). This is supported by the three species forming a polytomy in the molecular phylogeny (Fig. 24, Fig. 25) and the overlapping distribution of *G. robertianum* and *G. yeoi* and of *G. robertianum* and *G. reuteri*. However, based on the current phylogenetic markers, it cannot be excluded that autopolyploidization occurred only once in a potential MRCA of *G. reuteri* and *G. yeoi*, with subsequent divergence into the Madeiran and the Canarian species.

According to both plastid and nuclear data, sect. *Ruberta* sensu (Aedo, 2017) is recovered as paraphyletic with respect to sect. *Unguiculata.* This suggests that sect. *Ruberta* should probably be extended to *G. macrorrhizum* and, if molecular data is in favor of it, probably also *G. dalmaticum* (Beck) Rech.f.

Tertiary relict hypothesis

Like in *Visnea*, the estimated temporal and biogeographic origin of the laurel forest species containing lineage is in accordance with the Tertiary relict hypothesis. Still, its origin is

estimated to be younger than the one of *Visnea* and overlaps with the Miocene emergence of the oldest Canary Islands. The MRCA of the laurel forest lineage and *G. cataractarum* either occurred in the Mediterranean region (BBM) or was widespread (including Macaronesia and the Mediterranean; S-DEC) during the Late Miocene or Early Pliocene. A Mediterranean distribution of the respective node was also suggested by Pokorny et al. (2014). Further support comes from Fiz et al. (2008), who suggested that the main events of diversification in *Geranium* were located in the Mediterranean region and Eurasia during the late Miocene and the Pliocene. Several Macaronesian laurel forest species are of comparable biogeographic origin, e.g. *Hedera canariensis*, *Ranunculus cortusifolius*, *Ixanthus viscosus*, *Prunus lusitanica*, *Apollonias barbujana*, *Isoplexis* spp. and the *Pericallis hansenii* (G.Kunkel) Sunding lineage (Jones et al., 2014; Kondraskov, Schütz, et al., 2015; Valcárcel et al., 2017; Williams et al., 2015).

The third criterion for Tertiary relicts in laurel forest species, occurrence of the sister group in a laurel forest habitat, cannot be unambiguously inferred for *Geranium*. At the present, laurel forest species are extinct in Europe and surviving lineages may have undergone a change in habitat preference. Furthermore, unlike in *Visnea*, no fossils are available to infer information about the paleo habitat. Nevertheless, the sister *G. cataractarum* grows in rather humid conditions on rocks of higher elevations in Africa and southern Spain, e.g. Aedo (2017). This may indicate a tolerance of humid habitats derived from a laurel forest ancestor. However, Fiz et al. (2008) suggest that the uplift of mountain systems as well as climate changes could have promoted adaptation to disturbed or high and cold Mediterranean and Eurasian habitats in *Geranium*.

Inter- and intra-archipelago patterns

In the Macaronesian distributed taxa studied by e.g. Francisco-Ortega et al. (2002), Jones et al., (2014), Kim et al. (2008), Puppo (2015) and Trusty, Olmstead, Santos-Guerra, Sá-Fontinha, & Francisco-Ortega (2005), Madeira was colonized via a stepping stone scenario from the Canary Islands. Here, the opposite is proposed by BBM analysis. The colonization of Macaronesia may have started with a spread from the Mediterranean to Madeira (Fig. 24). A Madeiran distribution was established in the MRCA of the *G. maderense* and the *G. robertianum* clade during Miocene/Pliocene at latest (Fig. 24). Although probably less common in Macaronesian species, direct dispersal from the mainland to Madeira was also proposed for e.g. *Tolpis* Adans. (Gruenstaeudl, Santos-Guerra, & Jansen, 2013), and, three times independently, for *Scrophularia* L. (Navarro-Pérez et al., 2015). In the latter, dispersal was estimated to the Plio-/Pleistocene and Pleistocene (Navarro-Pérez et al., 2015).

After the distribution on Madeira was established, both colonization of the Canary Islands and back-colonization to the continent are indicated from the Plio-/Pleistocene boundary onwards in the *G. robertianum* clade (Fig. 24). Possible dispersal from Madeira to the Canary Islands was noted for e.g. *Tolpis* (Moore, Francisco-Ortega, Santos-Guerra, & Jansen, 2002), *Festuca* L. (Díaz-Pérez, Sequeira, Santos-Guerra, & Catalán, 2012) and *Scrophularia* (Valtuena, Rodríguez-Riaño, Lopez, Mayo, & Ortega-Olivencia, 2017). However, these scenarios are not regarded as the most likely ones. For example, Gruenstaeudl et al. (2013) suggest that Madeira and the Canary were colonized independently from the mainland in

Tolpis. Thus, it is unclear whether the Canary Islands were directly colonized from Madeira in the *G. robertianum* clade. The opposite direction of inter-archipelago colonization, i.e. from the Canary Islands to Madeira, seems to be the common one (Francisco-Ortega et al., 2002; Jones et al., 2014; Kim et al., 2008; Puppo, 2015; Trusty et al., 2005). Interestingly, the Plio-/Pleistocene timeframe suggested for dispersal from the Canary Islands to Madeira, e.g. *Bystropogon* L'Hér. (Kondraskov, Schütz, et al., 2015), *Scrophularia* (Navarro-Pérez et al., 2015), *Sonchus* L., *Echium*, *Sideritis* and *Crambe* L. (Kim et al., 2008), overlaps with the estimate for the reverse spread. This might indicate that floristic exchange has been facilitated by a reduced distance between the Macaronesian islands during the Pleistocene glaciation cycles (García-Talavera, 1999). Alternatively, the colonization of the Canary Islands could have been preceded by an event of dispersal from Madeira to the mainland. Back dispersal from Macaronesia to the continent was already described for other Macaronesian species, e.g. in *Convolvulus* L. (Carine, 2005; Carine et al., 2004), *Lotus* L. (Allan, Francisco-Ortega, Santos-Guerra, Boerner, & Zimmer, 2004), *Androcymbium* Willd. (Caujapé-Castells, 2004). In *Convolvulus*, it falls in the Pleistocene (Carine, 2005), whereas for *Androcymbium* the Middle or Late Pleistocene were suggested (Caujapé-Castells, 2004).

Another scenario is provided by S-DEC. It suggests that Macaronesia (including Canary Islands, Madeira and Azores) was colonized when a widespread distribution was established in the MRCA of sect. *Unguiculata* and sect. *Ruberta* during the Early Miocene. The Madeiran *G. maderense* clade may have diverged from a widespread ancestor during the Miocene, the Madeiran *G. yeoi* and the Canarian *G. reuteri* from widespread ancestors during the Plio-/Pleistocene. The shrink of distribution in the latter taxa may be associated with the Plio-/Pleistocene climate deteriorations. However, the plausibility of the S-DEC scenario may be questionable. It requires the lineage to maintain a widespread distribution for over 18 my (Appendix Fig. S31). This may be refuted by a decrease of suitable habitat starting with the break-up of the laurophyllous belt from the Late Miocene onwards (Mai, 1989). Although the occurrence of *G. robertianum* and *G. purpureum* in a variety of habitats indicates some plasticity in the lineage, the climatic changes likely should have affected its distribution.

Speciation events in the *G. robertianum* and the *G. maderense* clade overlap with the Pleistocene glaciation cycles, with autopolyploidization and hybridization likely playing a major role for the origin of species within the *G. robertianum* clade. Whether the glaciation cycles functioned as triggers for speciation despite the climatic stability inside the laurel forest proposed by Patiño et al. (2014), cannot be inferred here. Alternative drivers of speciation may have been, e.g. volcanic events. Dispersal within or between islands is poorly resolved within the species, but its timeframe agrees with laurel forest species like *Laurus* and *Canarina* L. (Betzin, Thiv, & Koch, 2016; Mairal, Sanmartín, et al., 2015).

3.3. *Semele androgyna* and *S. gayae* (Asparagaceae)

3.3.1. Specific Material and Methods

Phylogenetic sampling

The taxa incorporated in phylogenetic analysis are given in Appendix Table S7. The sampling of the present study focuses on tribe Rusceae, which comprises *Semele*, *Danae* Medik.and *Ruscus*, according to the phylogenetic studies of Kim et al. (2010) and Chen et al. (2013). For *Semele*, three species are listed as accepted at Plant List (Plant List, 2013) and Plants of the World Online (Royal Botanic Gardens Kew, 2019). Of those, *Semele androgyna* and *S. gayae* could be included here. The specimens of *Semele* from Madeira analyzed in the present study were assigned to *S. androgyna* by their collectors. Due to the lack of inflorescences, unambiguous determination is hampered, and some samples might possibly be *S. menezesii*. Available sequences of *Danae* and *Ruscus* were downloaded from GenBank, covering all species of *Danae* (one) and three of the six species of *Ruscus* (Yeo, 1998).

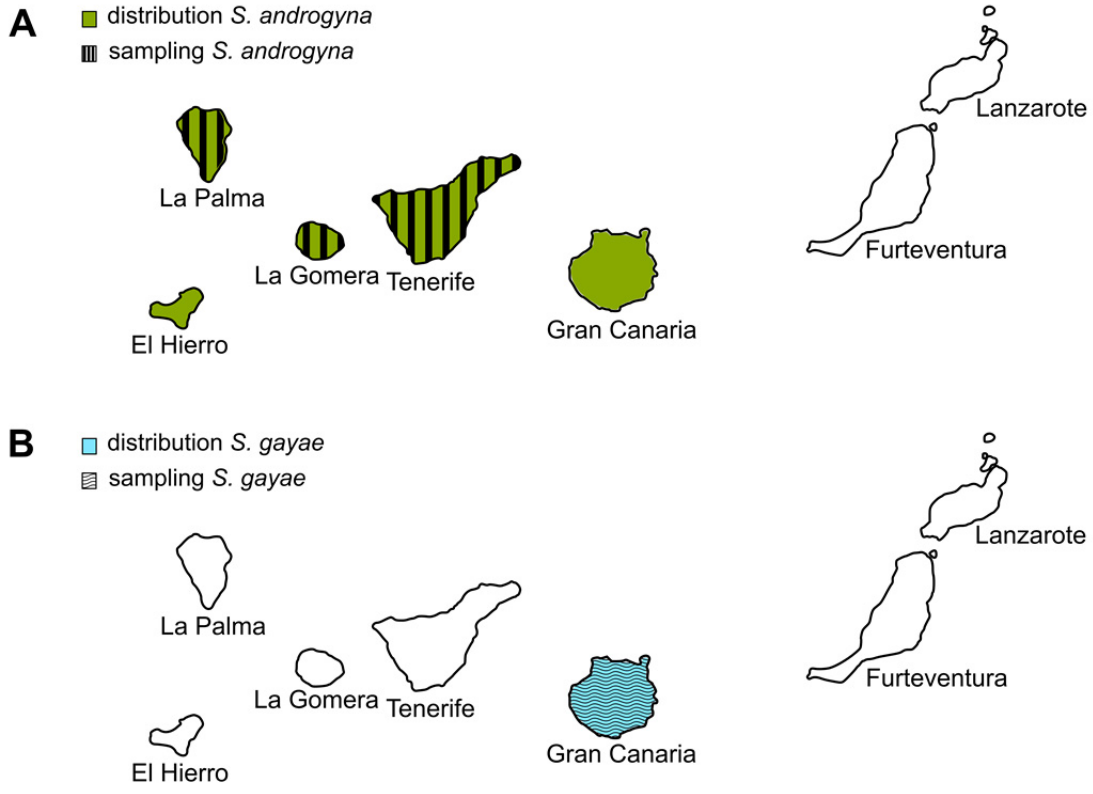

Figure 27. Distribution and sampling of *Semele androgyna* and *S. gayae* on the Canary Islands. **A** *S. androgyna*; **B** *S. gayae*.

Semele androgyna is distributed on the Canary Islands on Gran Canaria, Tenerife, La Gomera, La Palma, El Hierro (Fig. 27A; Arechavaleta et al., 2010) and on the Madeiran archipelago on Madeira, Porto Santo and Desertas (Fig. 28; Borges et al., 2008), whereas *S. gayae* is only found on Gran Canaria (Fig. 27B; Arechavaleta et al., 2010). Of *S. androgyna*, Tenerife, La Gomera, La Palma, Madeira were sampled with one to two accessions (Fig. 27A, Fig. 28), of *S. gayae*, one accession from Gran Canaria was included (Fig. 27B).

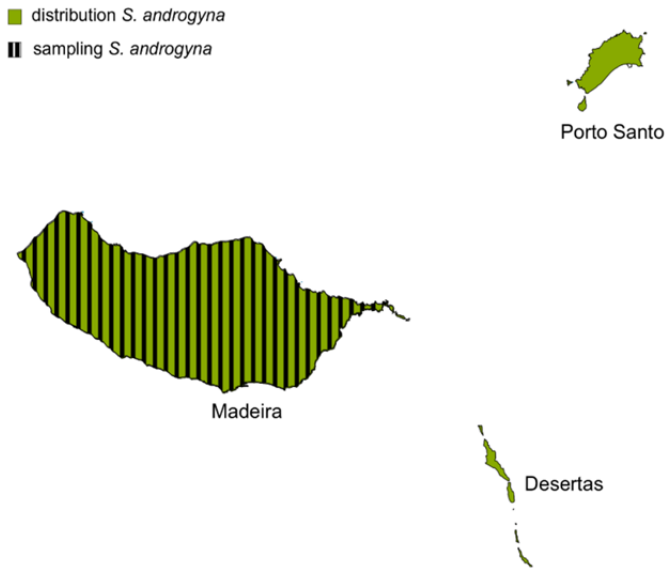

Figure 28. Distribution and sampling of *Semele androgyna* on Madeira.

For dating analyses, sequences of 80 species from the main clades of Asparagaceae as inferred by Chen et al. (2013) were added. Eight species of Amaryllidaceae were retrieved for calibration purpose. Additionally, three species of Xanthorrhoeaceae were added. One species of Xeronemataceae served as outgroup.

Molecular phylogenetic analyses.

Individual phylogenies based on *atpB* (ATPase beta chain gene), *matK*, *ndhF* and *rbcL* were calculated using BI (MrBayes) and ML (RAxML) analyses. MCMC settings for BI are given in Table 21. Topological incongruences were detected for the taxa *Agapanthus africanus* (L.) Hoffmanns., *Anthericum liliago* L., *Camassia cusickii* S.Watson, *Chlorophytum minor* Kativu, *Chlorophytum suffruticosum* Baker, *Cordyline stricta* (Sims) Endl., *Drimia altissima* (L.f.) Ker Gawl., *Echeandia spec.*, *Eriospermum cooperi* Baker, *Eriospermum flagelliforme* (Baker) J.C.Manning, *Eriospermum parvifolium* Jacq., *Hesperocallis undulata* A.Gray, *Hosta plantaginea* (Lam.) Asch., *Leucocrinum montanum* Nutt. ex A.Gray, *Lycoris uydoensis* M.Kim, *Massonia angustifolia* L.f. and *Paradisea liliastrum* (L.) Bertol. (Appendix Figs. S33-S36). According to Pirie (2015), those were removed before concatenating the plastid markers.

For the concatenated plastid dataset, two different partitions were defined for phylogenetic analyses, as suggested by PartionFinder. The first partition consisted of *ndhF* and *matK*, the second partition of *atpB* and *rbcL*.

Table 21. MCMC settings for Bayesian analysis of the *Semele* datasets using MrBayes.

	atpB	***matK***	***ndhF***	***rbcL***	***matK* & *ndhF*, *atpB* & *rbcL***
Chain length	10 000 000	10 000 000	10 000 000	80 000 000	80 000 000
Sample frequency	1000	1000	1000	5000	8000
Number of chains	4	4	4	4	4
Number of runs	2	2	2	2	2
Heating parameter	0.2	0.2	0.2	0.2	0.2

Stem age estimation

Analysis was conducted on the plastid dataset, using the split of Asparagaceae and Amaryllidaceae (49.2-76.7 mya; Magallón et al., 2015) as calibration point. This calibration reference overlaps with the estimates for the respective split by Chen et al. (2013; 67.4-49.9 mya) and Givnish et al. (2018; ca. 55-49 mya). The length of the MCMC chain was set to 100 000 000, the sampling frequency to 10 000.

Crown age estimation

The dataset analyzed consisted of *matK* sequences of *Semele androgyna* and *S. gayae*, as well as six accessions of *Ruscus aculeatus* L. as outgroup. A coalescent constant population tree prior was set up. The split between *Semele* and *R. aculeatus* (9.5-3.6 mya; Appendix Fig. S37) served as calibration point. The length of the MCMC chain equaled 10 000 000, the sampling frequency 1000.

Ancestral area estimation

Biogeographic analyses were based on the dated plastid phylogeny, removing all Non-Rusceae as outgroups. Table 22 illustrates the coding of areas, comprising Canary Islands (A), Madeira (B), Eurasia (including Mediterranean; C).

Table 22. Coding for ancestral area estimation in Rusceae. Canary Islands (A), Madeira (B), Eurasia (including Mediterranean; C).

Species	Areas	References
Danae racemosa (L.) Moench	C	Yeo (1998)
Ruscus aculeatus L.	C	Tutin et al. (1980)
Ruscus hypoglossum L.	C	Tutin et al. (1980)
Ruscus streptophyllus Yeo	B	Borges et al. (2008)
Semele androgyna (L.) Kunth	AB	Arechavaleta et al. (2010); Borges et al. (2008)
Semele gayae (Webb) Sventenius & G.Kunkel	A	Aedo et al. (1998); Arechavaleta et al. (2010); Borges et al. (2008)

Table 23. Biogeographical models tested for the plastid dataset of Ruscaceae and their likelihoods, AICs and AICcs as inferred by BioGeoBEARS (Matzke, 2013a; Matzke, 2013b). The best-scoring models are marked in bold.

Model	Likelihood (LnL)	AIC	AICc
DEC	-9.87	23.74	27.74
DEC+J	**-6.30**	**18.60**	**30.60**
DIVALIKE	**-8.34**	**20.69**	**24.69**
DIVALIKE+J	-6.35	18.71	30.71
BAYAREALIKE	-11.37	26.74	30.74
BAYAREALIKE+J	-6.75	19.49	31.49

BioGeoBEARS suggested DEC+J as best-scoring model based on AIC and likelihood, with the likelihood of the +J model significantly differing from the one of DEC (one-tailed chi-squared test, df = 1, p = 0.01; Table 23). Due to the criticism on DEC+J (see also previous section on *Phyllis*), the best model according to AICc, DIVALIKE, was selected for further analysis (Table 23). Hence, S-DIVA analysis was conducted in RASP.

3.3.2. DNA sequence variation and phylogenies

Seven newly generated *matK* sequences of *Semele androgyna* and *S. gayae* were deposited at GenBank (Appendix Table S7). The sequence characteristics of the plastid marker alignments (*atpB*, *matK*, *ndhF*, *rbcL*, all combined) are given in Table 24.

Table 24. Sequence characteristics of the plastid datasets of Asparagaceae (*atpB*, *matK*, *ndhF*, *rncL*, *matK* & *ndhF* & *atpB* & *rbcL*). The combined dataset comprised two partitions (Partition1: *matK* & *ndhF*, partition 2: *atpB* & *rbcL*).

	atpB	***matK***	***ndhF***	***rbcL***	***matK* & *ndhF*, *atpB* & *rbcL***
Number of accessions	74	108	80	97	81
Total number of characters	1449	1621	2035	1335	6440 (Partition 1: 3656, Partition 2: 2784)
Variable characters	25%	53%	41%	30%	35%
Parsimony informative characters	15%	35%	28%	20%	22%
Substitution model (AIC)	GTR+Γ	GTR+Γ+I	GTR+Γ+I	GTR+Γ+I	Partition 1: GTR+Γ+I Partition 2: GTR+Γ+I

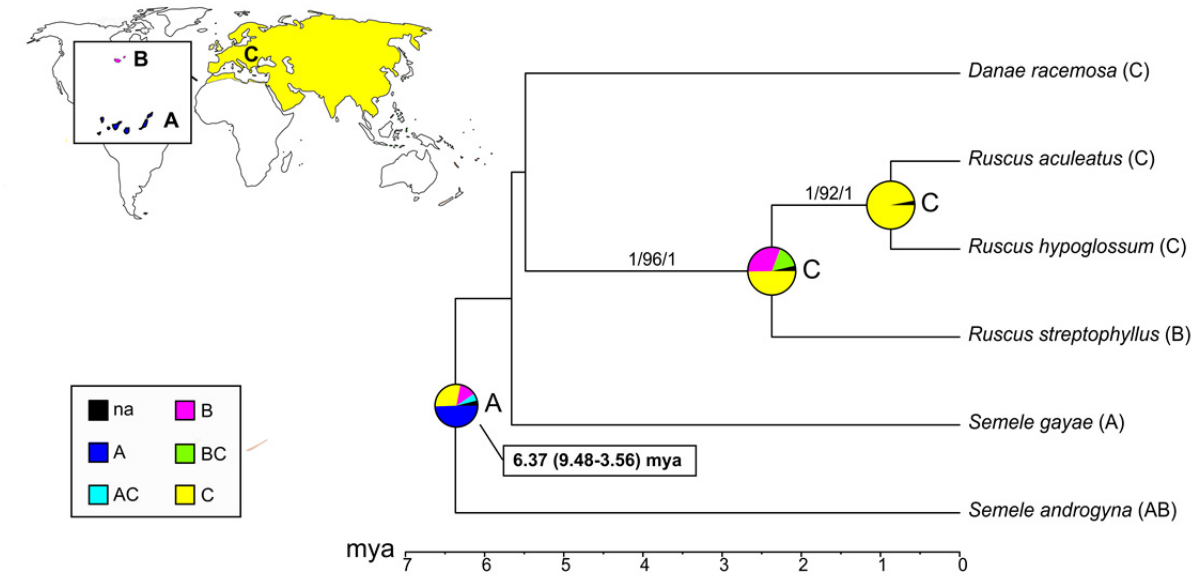

Figure 29. Biogeography of Rusceae as inferred from BBM analysis in RASP, based on the chronogram from plastid data. Numbers above branches indicate posterior probabilities from MrBayes analysis, bootstrap values from RAxML analysis and posterior probabilities from BEAST analysis. Only posterior probabilities ≥0.90 and bootstrap values ≥80 are shown. On the nodes, the posterior probabilities of the estimated areas/area combinations are indicated by pie charts. Areas coded include the Canary Islands (A), Madeira (B), Eurasia (including Mediterranean; C). For nodes of interest, the age estimates from BEAST analysis are also given. The world map was modified from https://commons.wikimedia.org/wiki/File:Simplified_blank_world_map_without_Antartica_(no_borders).svg, the map of Macaronesia from A. Platon, https://upload.wikimedia.org/wikipedia/commons/b/b4/Macaronesia_location.svg.

Some topological conflict was detected between *matK*, *ndhF*, *atpB* and *rbcL* (see Material & Methods section, Appendix Figs. S33-S36). The combined plastid phylogeny with the conflicting taxa removed (Appendix Fig. S37) did not contradict previously published phylogenies, e.g. Chen et al. (2013), Givnish et al. (2018), Kim et al. (2010) and Seberg et al. (2012).

Semele is recovered in subfamily Nolinoideae, tribe Rusceae (Appendix Fig. S37). The relationship between *Semele*, *Danae* and *Ruscus* is unresolved. *Ruscus* is indicated to be monophyletic, with Madeiran *R. streptophyllus* Yeo as sister to Eurasian *R. aculeatus* and *R. hypoglossum* L. (Fig. 29). In *Semele*, *S. androgyna* and *S. gayae* cannot be distinguished by *matK*. No intraspecific geographic patterns are visible either.

3.3.3. Molecular dating: Late Miocene stem and Early Pleistocene crown age

The crown age of Rusceae, which constitutes also the maximum age for the stem of *Semele*, is estimated to the Late Miocene (6.37 mya, 9.48-3.56 mya; Fig. 29, Fig. 30A). The crown of *Semele* dates to the Early Pleistocene (1.51 mya, 3.40-0.24 mya, Fig. 30B).

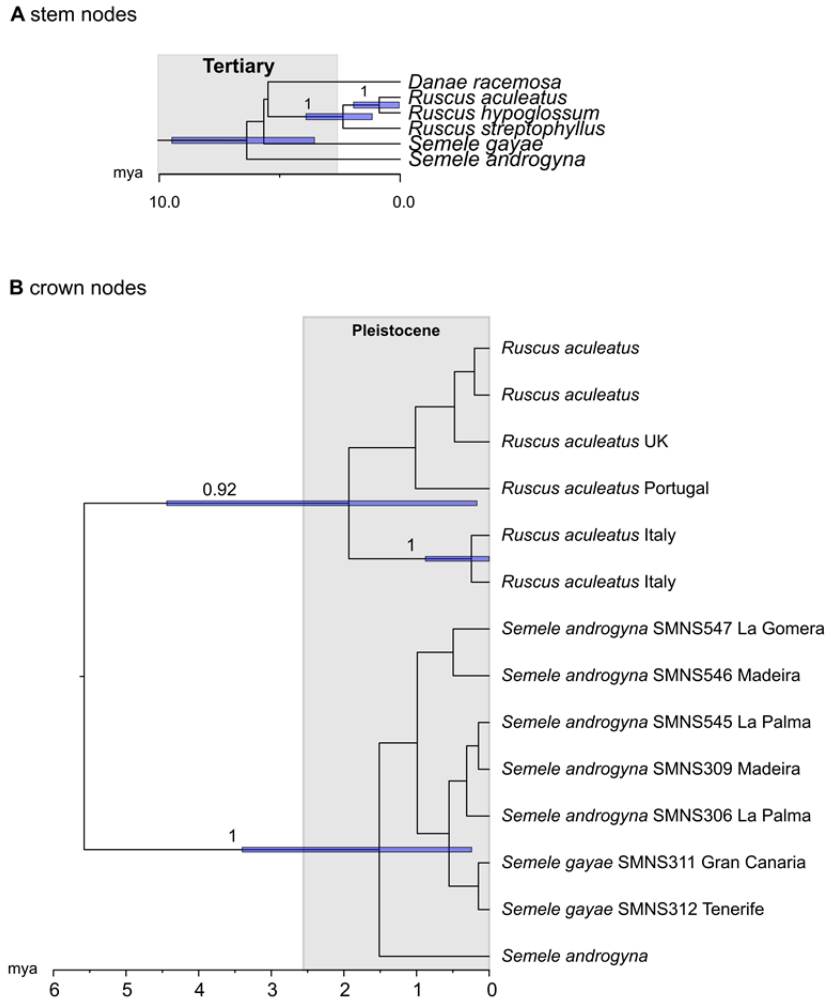

Figure 30. Chronograms from stem node and crown node dating in *Semele*. Bars at the nodes indicate 95% highest posterior densities; posterior probabilities from BEAST analysis ≥ 0.90 are given above the branches. **A** Stem node dating, plastid data (*ndhF* & *rbcL* & *matK* & *atpB*); **B** Crown node dating based on *matK* of *Semele* and *Ruscus aculeatus*.

3.3.4. Biogeograhic reconstruction: Origin in Macaronesia or Eurasia-Macaronesia

BBM analysis reconstructs a Canarian distribution for the MRCA of Rusceae and the ancestor of *Semele* (PP = 0.50, Fig. 29). In contrast to this, DIVA-like and S-DIVA (p = 0.83) suggest a Canarian-Madeiran-Eurasian ancestry of Rusceae and *Semele* (Appendix Figs. S38, S39).

3.3.5. Discussion

The phylogenetic relationships within tribe Rusceae were poorly resolved based on the current marker system (Fig. 29). The study species *S. androgyna* and *S. gayae* could not be distinguished by cp-data (Fig. 29, Fig. 30). Further analyses using more variable markers or a genome approach are needed to establish the identity of *S. gayae*. The nuclear markers ITS and ETS are in general more variable than cp data, but failed to amplify here despite several efforts. Subsequent studies should furthermore try to include the Madeiran taxon *S. menezesii*.

Tertiary relict Hypothesis

By its age and origin, the Tertiary relict hypothesis cannot be unambiguously rejected. The stem of the genus dates around the Late Miocene (Fig. 29, Fig. 30A). However, *Semele* forms a polytomy with *Ruscus* and *Danae* in this study (Fig. 29, Fig. 30A). Kim et al. (2010) found a sister group relationship of *Semele* and *Ruscus,* albeit with low support. Hence, the genus may be younger, with its minimum age predating the Early Pleistocene (crown *Ruscus*, Fig.29, Fig. 30A). Overall, the age estimates obtained in this study agree with previously conducted dating approaches incorporating Asparagaceae. For example, the stem age of Nolinoideae as estimated here agrees with Chen et al. (2013), and the age of split of *Ruscus* from *Sansevieria* Thunb. agrees with Givnish et al. (2018).

As geographical origin of *Semele*, either the Canary Islands or Macaronesia-Eurasia were indicated (Fig. 29, Appendix Fig. S39). Affinity of *Semele* to Mediterranean taxa was already proposed by Schenck & Schimper (1907). This is also suggested by Kim et al. (2010), who recovered Eurasian *Danae* as sister to clade comprising *Ruscus* and *Semele*. Within *Ruscus*, Eurasian taxa are recovered in a sister group relationship to Eurasian species of *Ruscus*. Assuming that the topology provided by Kim et al. (2010) is correct, *Semele* may rather be derived from a Eurasian, Madeiran or Eurasian-Madeiran ancestor. A solely Madeiran distributed ancestor may be unlikely, as dispersal from the Canary Islands to Madeira seems to be more frequent than the opposite scenario (see also *Geranium*, section 3.2.4).

In general, the sister group of a Tertiary relict should occur in a laurel forest habitat. Yet, laurel forest is widely extinct in the distributional area of Rusceae. Despite that, their preference for growing in deep shade of evergreen plants in forests (Yeo, 1998) may hint to a previous affinity to laurel forest-like habitats.

Inter archipelago and inter-Island patterns

Inter-archipelago colonization is inferred for the Early Pleistocene (Fig. 29, Fig. 30B). BBM indicates that the Canary Islands were colonized prior to dispersal to Madeira, whereas S-DIVA does not provide any information about inter-archipelago colonization in *Semele* (Fig. 29, Appendix Fig. S39). Dispersal from the Canary Islands to Madeira during the Plio-/Pleistocene seems to be common and is also found in *Bystropogon* (Kondraskov, Schütz, et al., 2015), *Scrophularia* (Navarro-Pérez et al., 2015), *Sonchus*, *Echium*, *Sideritis* and *Crambe* (Kim et al., 2008; see also *Geranium*, sect. 3.2.4). Inter-island patterns on the Canary Islands are not resolved (Fig. 30B).

3.4. *Daucus elegans* (Apiaceae)

3.4.1. Specific Material and Methods

Phylogenetic sampling

Phylogenetic sampling is given in Appendix Table S8. It concentrates on *Daucus* L. sect. *Daucus* and *Daucus* sect. *Melanoselinum* (Hoffm.) Spalik, Wojew., Banasiak & Reduron, which contain the closest relatives of *Daucus elegans* (Banasiak et al., 2016; Spalik & Downie, 2007).

From each island *D. elegans* occurs on, i.e. El Hierro, La Palma, La Gomera, Tenerife (Hohenester & Welss, 1993), one to three accessions were analyzed here.

For molecular dating, most of the major clades of Apioideae according to Spalik & Downie (2007) could be included with one sequence or more. Subfamilies Mackinlayoideae and Azorelloideae were also represented by one sequence each. One sequence of Myodocarpaceae was added to set the stem of Apiaceae as calibration point, one accession of Araliaceae served as outgroup.

Phylogenetic analyses

Analysis was firstly conducted on an *rps16* dataset of Apiaceae. It included two accessions of Myodocarpaceae, and, as outgroups, two accessions of Araliaceae.

As ITS could not be aligned unambiguously at the family level, analysis of this marker was restricted to *Daucus*. According to Banasiak et al. (2016), one accession of *Laserpitium* L. and one of *Orlaya* Hoffm. were added, with *Orlaya* serving as outgroup.

Topological congruence between ITS and *rps16* datasets of *Daucus* was indicated and these markers were combined accordingly (Appendix Figs. S40, S41). Consistent with PartitionFinder, two partitions were set up, one for each marker.

MCMC settings for BI analyses are given in Table 25.

Table 25. MCMC settings for Bayesian analysis of the *Daucus* datasets using MrBayes.

	rps16 [a]	***rps16*** [b]	**ITS** [b]	**ITS & *rps16*** [b]
Chain length (million states)	70	10	70	50
Sample frequency	7000	1000	7000	5000
Number of chains	4	4	4	4
Number of runs	2	2	2	2
Heating parameter	0.2	0.2	0.2	0.2

[a] Apiaceae dataset [b] Daucus dataset

Stem age estimation

A two-step analysis was performed. Firstly, the Apiaceae *rps16* dataset was calibrated setting the split of Apiaceae from Myodocarpaceae to 71.11-47.38 mya (Magallón et al., 2015). The chain length equaled 50 000 000 and every 5000th state was sampled. Subsequently, the estimate for the stem of *Daucus* from this analysis (15.60-6.24 mya; Appendix Fig. S42) was used to calibrate the concatenated (ITS & *rps16*) *Daucus* dataset. Here, the chain length was set to 70 000 000 and the sampling frequency to 7000.

Table 26. Coding for ancestral area estimation in *Daucus* sect. *Daucus* and *Daucus* sect. *Melanoselinum*. Canary Islands (A), Madeira (B), Cape Verdes (C), Mediterranean (D), Azores (E), Non-Mediterranean Europe (F).

Species	Areas	References
Daucus annuus (Bég.) Wojew., Reduron, Banasiak & Spalik	C	Arechavaleta, Pérez, Gómez, & Esquivel (2005)
Daucus aureus Desf.	AD	Arechavaleta et al. (2010); Tutin et al. (1981)
Daucus biseriatus Murb.	D	Royal Botanic Gardens Kew (2019)
Daucus capillifolius Gilli	D	Laín (1980)
Daucus carota L. subsp. Carota	ABDF	Arechavaleta et al. (2010); Borges et al. (2008); Tutin et al. (1981)
Daucus carota subsp. gummifer (Syme) Hook.f.	F	Aedo et al. (1998); Borges et al. (2008); Tutin et al. (1981)
Daucus carota subsp. maximus (Desf.) Ball	AD	Arechavaleta et al. (2010); Tutin (1981)
Daucus carota subsp. sativus (Hoffm.) Arcang.	DF	Tutin et al. (1981)
Daucus crinitus Desf.	D	Tutin et al. (1981)
Daucus decipiens (Schrad. & J.C.Wendl.) Spalik, Wojew., Banasiak & Reduron	B	Borges et al. (2008)
Daucus della-cellae (Asch. & Barbey ex E.A.Durand & Barratte) Spalik, Banasiak & Reduron	D	Royal Botanic Gardens Kew (2019)
Daucus edulis (Lowe) Wojew., Reduron, Banasiak & Spalik	B	Borges et al. (2008)
Daucus elegans (Webb ex Bolle) Spalik, Banasiak & Reduron	A	Arechavaleta et al. (2010)
Daucus gracilis Steinh.	D	Tutin et al. (1981)
Daucus insularis (Parl. ex Webb) Spalik, Wojew., Banasiak & Reduron	C	Arechavaleta et al. (2005)
Daucus mauritii (Sennen ex Maire) Sennen	D	Royal Botanic Gardens Kew (2019)
Daucus minusculus Pau ex Font Quer	D	Tutin et al. (1981)
Daucus mirabilis (Maire & Pamp.) Reduron, Banasiak & Spalik	D	Royal Botanic Gardens Kew (2019)
Daucus muricatus (L.) L.	DE	Royal Botanic Gardens Kew (2019); Tutin et al. (1981)
Daucus pumilus (L.) Hoffmanns. & Link	AD	Royal Botanic Gardens Kew (2019); Tutin et al. (1981)
Daucus rouyi Spalik & Reduron	D	Banasiak et al. (2016)
Daucus sahariensis Murb.	D	Royal Botanic Gardens Kew (2019); Laín (1980)
Daucus setifolius Desf.	D	Laín (1980); Tutin et al. (1981)
Daucus syrticus Murb.	D	Laín (1980)
Daucus tenuisectus Coss. ex Batt.	D	Laín (1980)
Daucus tenuissimus (A.Chev.) Spalik	C	Arechavaleta et al. (2005)
Daucus virgatus (Poir.) Maire	D	Royal Botanic Gardens Kew (2019)

Crown age estimation

A dataset of ITS and *rps16* was analyzed, comprising six accessions of *Daucus elegans*, three of *D*. *edulis* and eight of *D*. *decipiens*. According to PartitionFinder, the substitution model should not be estimated separately for each marker. Thus, only the clock rates were estimated individually, as the markers are derived from different genetic compartments. For the tree model, coalescent constant populations was selected. The molecular clock was calibrated with the age estimate for the split of *Daucus elegans* from *D. edulis* and *D. decipiens* 8.83-3.22 mya (Appendix Fig. S43). The chain length was set to 10 000 000 and the sampling frequency to 1000.

For comparison, a further analysis was calibrated with the age estimate for the same split (22-11 mya) by Spalik et al. (2010; calibS). The chain length equaled 50 000 000 and every 5000th state was sampled.

Ancestral area estimation

BBM analysis was conducted on the combined *rps16* and ITS phylogeny. The dataset was reduced to only contain *Daucus* sect. *Daucus* and *Daucus* sect. *Melanoselinum*. Areas coded comprised the Canary Islands (A), Madeira (B), Cape Verdes (C), Mediterranean (D), Azores (E), Non-Mediterranean Europe (F; Table 26).

The best-scoring model from BioGeoBEARs analysis according to likelihoods, AICs and AICcs was DEC (Table 27). Thus, S-DEC analysis was run in RASP.

Table 27. Biogeographical models tested for the combined ITS & *rps16* data of *Daucus* sect. *Daucus* and *Daucus* sect. *Melanoselinum* and their likelihoods, AICs and AICcs as inferred by BioGeoBEARS (Matzke, 2013a; Matzke, 2013b). The best-scoring model is marked in bold.

Model	Likelihood (LnL)	AIC	AICc
DEC	-56.11	**116.2**	**116.7**
DEC+J	**-55.39**	116.8	117.8
DIVALIKE	-57.81	119.6	120.1
DIVALIKE+J	-57.28	120.6	121.6
BAYAREALIKE	-68.90	141.8	142.3
BAYAREALIKE+J	-57.04	120.1	121.1

3.4.2. DNA sequence variation and phylogenies

Twelve sequences of *Daucus elegans* have been newly generated and uploaded to GenBank. For sequence variation and characteristics of the alignments, see Table 28.

Table 28. Sequence characteristics of the Apiaceae and *Daucus* datasets, i.e. the plastid dataset of Apiaceae (*rps16*) and the plastid, nuclear and combined datasets of *Daucus* (*rps16*, ITS, *rps16* & ITS). The combined dataset comprised two partitions (Partition1: ITS, partition 2: *rps16*).

	rps16 [a]	***rps16*** [b]	**ITS** [b]	**ITS & *rps16*** [b]
Number of accessions	43	21	38	32
Total number of characters	1256	842	621	1489 (Partition 1: 621, Partition 2: 868)
Variable characters	27%	8%	41%	21%
Parsimony-informative characters	13%	3%	24%	10%
Substitution model (AIC)	GTR+Γ	GTR+ Γ	SYM+Γ (RaxML: GTR+ Γ)	Partition 1: SYM+Γ Partition 2: GTR+Γ

[a] Apiaceae dataset; [b] *Daucus* dataset

The topology of the *rps16*, ITS and concatenated phylogenies (Fig. 31, Appendix Figs. S40-S43) do largely neither contradict each other nor previously published data, e.g. Banasiak et al. (2016), Spalik & Downie (2007) and Spalik et al. (2010). One case of conflict is indicated between the *rps16* Apiaceae phylogeny (Appendix Fig. S42) and the remainder of phylogenies for the relationship of *Silphiodaucus hispidum* (M.Bieb.) Spalik, Wojew., Banasiak, Piwczyński & Reduron and *Daucus muricatus* (L.) L., albeit with low statistical support.

Daucus elegans is placed in *Daucus* and forms a polytomy with the Madeiran endemic *Daucus* sect. *Melanoselinum* as well with accessions of *Daucus* sect. *Daucus* (Fig. 31). Within *D. elegans*, intraspecific patterns are weakly indicated. A clade, in which an accession from Tenerife (SMNS178) is sister to one accession from La Gomera (SMNS176) and one from El Hierro (SMNS174), is recovered for *rps16* data and ML analysis only (Appendix Fig. S41). Furthermore, the two accessions from La Gomera (SMNS175 & SMNS177) are weakly indicated as monophyletic in the ITS as well as in the combined phylogeny (Fig. 32B, Appendix Fig. S40).

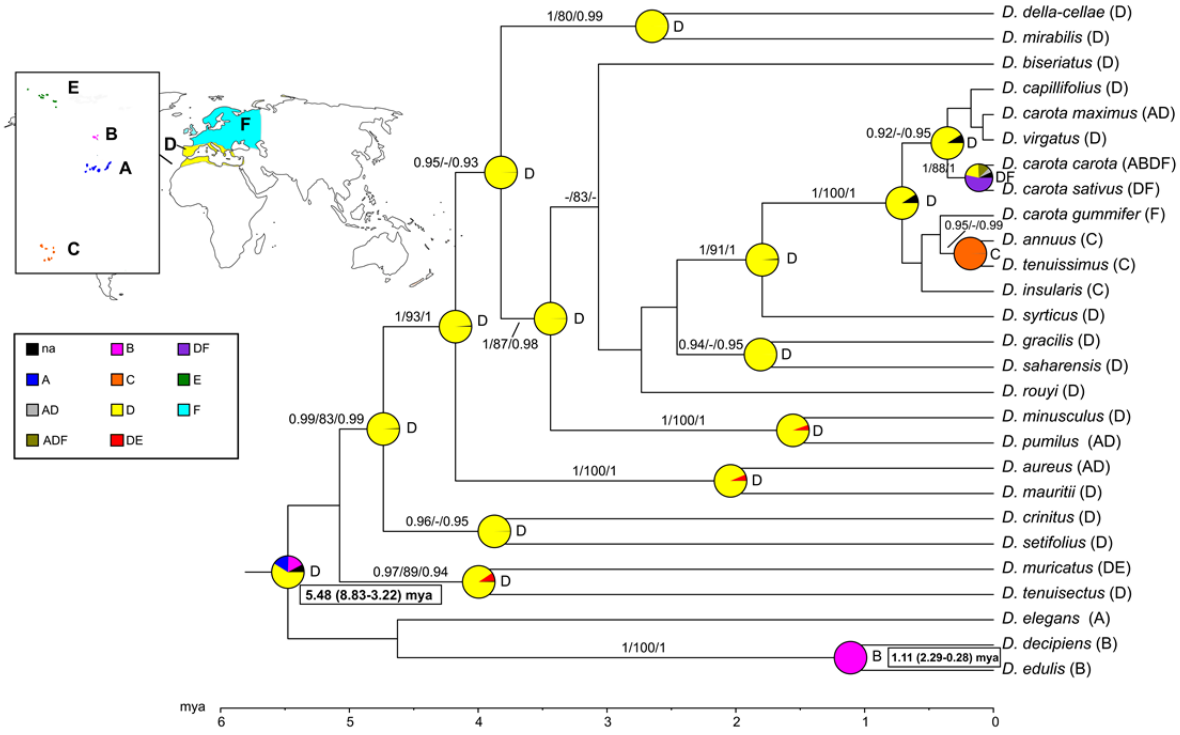

Figure 31. Biogeography of *Daucus* sect. *Daucus* and *Daucus* sect. *Melanoselinum* as inferred from BBM analysis in RASP, based on the chronogram from ITS and *rps16* data. Numbers above branches indicate posterior probabilities from MrBayes analysis, bootstrap values from RAxML analysis and posterior probabilities from BEAST analysis. Only posterior probabilities ≥0.90 and bootstrap values ≥80 are shown. On the nodes, the posterior probabilities of the estimated areas/area combinations are indicated by pie charts. Areas coded include the Canary Islands (A), Madeira (B), Cape Verdes (C), Mediterranean (D), Azores (E), Non-Mediterranean Europe (F). For nodes of interest, the age estimates from BEAST analysis are also given. The world map was modified from https://commons.wikimedia.org/wiki/File:Simplified_blank_world_map_without_Antartica_(no_borders).svg, the map of Macaronesia from A. Platon, https://upload.wikimedia.org/wikipedia/commons/b/b4/Macaronesia_location.svg.

3.4.3. Molecular dating: Late Miocene origin and Middle Pleistocene diversification

The split of *Daucus* sect. *Daucus* from *Daucus* sect. *Melanoselinum* indicates the maximum age for the stem of *D. elegans* and falls into the Late Miocene (5.48 mya, 95% HPD 8.83-3.22 mya, Fig. 31, Fig. 32A; calibM). Intraspecific diversification in *D. elegans* dates to the Middle Pleistocene (0.27 mya, 95% HPD 0.57-0.05 mya, Fig. 32B). The crowns of Madeiran *D. decipiens* and *D. edulis* are also estimated to the Middle Pleistocene (*D. decipiens*: 0.45 mya, 95% HPD 0.91-0.12 mya; *D. edulis*: 0.19 mya, 95% HPD 0.49-0.01 mya, Fig. 32B).

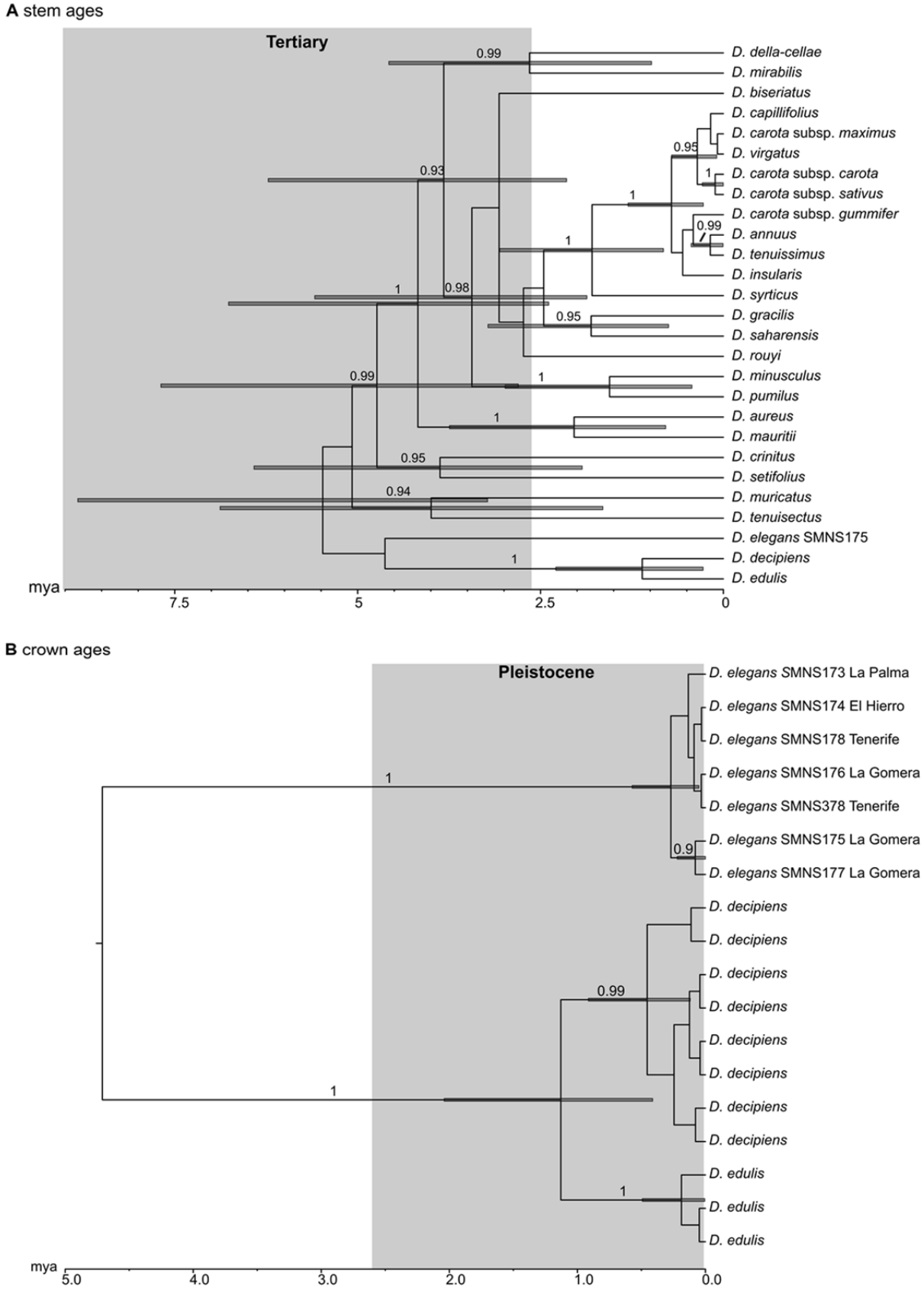

Figure 32. Chronograms from stem node and crown node dating in *Daucus*. Bars at the nodes indicate 95% highest posterior densities; posterior probabilities from BEAST analysis ≥ 0.90 are given above the branches. **A** Stem node dating based on combined ITS & rps16 data (calibM); **B** Crown node dating based on combined ITS & rps16 data of *D. elegans*, *D. edulis* and *D. decipiens*.

The alternative calibration scenario based on Spalik et al. (2010; calibS) proposes that intraspecific diversification in *D. elegans* and *D. decipiens* occurred during the Early Pleistocene (*D. edulis*: 0.82 mya, 95% HPD 1.69-0.16 mya; *D. decipiens*: 1.42 mya,95% HPD 2.72-0.43 mya; Appendix Fig. S44). For *D. edulis*, the Middle Pleistocene is estimated (0.58 mya, 95% HPD 1.48-0.02 mya, Appendix Fig. S44).

3.4.4. Biogeographic reconstruction: Mediterranean or Macaronesian-Mediterranean origin

BBM indicates that the MRCA of *Daucus* sect. *Daucus* and *Daucus* sect. *Melanoselinum*, i.e. the ancestor of *D. elegans*, was distributed in the Mediterranean region (PP = 0.59, Fig. 31). In *D. elegans*, colonization of the Canary Islands occurred.

The BioGeoBEARS DEC and S-DEC results deviate from this, reconstructing a Canarian-Madeiran-Mediterranean distribution for the MRCA of *Daucus* sect. *Daucus* and *Daucus* sect. *Melanoselinum* (p = 0.93; Appendix Fig. S45, S46).

3.4.5. Discussion

Tertiary relict hypothesis

Daucus elegans may be a Tertiary relict by its temporal and spatial origin. Here, its stem age estimated to the Late Miocene. This agrees with the estimates of ca. 16.1 mya by Spalik et al. (2010) and ca. 10.2 mya by Banasiak et al. (2013). However, the genus may be slightly younger. *D. elegans* is recovered in a polytomy with *Daucus* sect. *Melanoselinum* and the rest of *Daucus* sect. *Daucus*. Accordingly, its age may fall into the range from the Late Miocene to Early Pliocene (crown *Daucus* sect. *Daucus* excluding *D. elegans*, Fig. 31). For the spatial origin of *D. elegans*, the Mediterranean or a combination of Macaronesia and the Mediterranean was inferred (Fig. 31, Appendix Fig. S46). This does not contradict the reconstructions by Banasiak et al. (2013) and Spalik & Downie (2007) which recovered Macaronesia, Northern Africa-Macaronesia or Northern Africa. Spalik & Downie (2007) assume the latter with two independent dispersal events to Macaronesia, one to the Canary Islands (*D. elegans*) and one to Madeira (*Daucus* sect. *Melanoselinum*), as the most plausible scenario.

Although the first two criteria for a laurel forest relict by Kondraskov, Schütz, et al. (2015) seem to be fulfilled in *D. elegans,* the third criterion (occurrence of the sister group in a laurel forest habitat) is not. The species of *Daucus* sect. *Daucus* occur in a variety of habitats, many of them ruderal. They are found e.g. in cultivated fields, at sea shores and on dry hills (Tutin et al., 1981). *Daucus* sect. *Melanoselinum* is also not a laurel forest lineage. Both of its species rather occur on shady rocks, cliffs and ravines of Madeira, from sea level up to ca. 800-1000 m elevation (Fernandes & Carvalho, 2014; Press & Dias, 1998). In these surroundings, insular woodiness evolved within the Madeiran lineage, see Góis-Marques, de Nascimento, Fernández-Palacios, Madeira, & Menezes de Sequeira (2020). Even though the habitat affinities of the next relatives does not favor a relict origin, it cannot be rejected based on them. The Mediterranean species of *Daucus* sect. *Daucus* might have originally occupied a laurel forest habitat and undergone a change in habitat preference during the extinction of laurel forest in the Mediterranean region by the end of the Pliocene.

Inter-island patterns

Inter-island patterns are poorly resolved. A sister group relationship between Tenerife and La Gomera/El Hierro has been implied, with the direction of colonization unknown. Furthermore, it is indicated that La Gomera might have been colonized twice. As timeframe for these events, the Middle or the Late Pleistocene was estimated.

3.5. *Phyllis nobla* (Rubiaceae)

3.5.1. Specific Material and Methods

Phylogenetic sampling

Appendix Table S9 lists the taxa sampled for phylogenetic analyses of *Phyllis nobla*. The molecular phylogenetic studies by Anderson et al. (2001), Bremer & Eriksson (2009) and Thureborn et al. (2019) recover *P. nobla* within Rubioideae tribe Anthospermeae, subtribe Anthosperminae. For this reason, the sampling strategy of the present study aimed at including at least one representative from each genus of Anthospermeae. All genera of the predominantly African distributed Anthosperminae were sampled. Of *Anthospermum*, sequences from three of the 39 species listed in Puff (1986) were included here. For *Nenax*, sequences from two of the eight species recognized by Puff (1986) were available. One of the four species in *Galopina* (Puff, 1986) was sampled. *Carpacoce* comprises seven species according to Puff (1986) and is represented by three accessions here, of which two are unspecified. All of the species (two) of Macaronesian genus *Phyllis* (Mendoza Heuer, 1972) were sampled.

Phyllis nobla is distributed on Gran Canaria, Tenerife, La Gomera, La Palma, El Hierro, Madeira, Porto Santo and Desertas (Arechavaleta et al., 2010; Borges et al., 2008). In this study, sequences of two to four accessions from Tenerife, La Gomera, La Palma, El Hierro and Madeira could be included.

For molecular dating, at least one sequence of each tribe of Rubiaceae was added. To use the stem of Rubiaceae as calibration point, sequence data of four species of Loganiaceae, two species of Gelsemiaceae, six species of Apocynaceae and five species of Gentianaceae were included. Two species of Convolvulaceae and two species of Solanaceae served as outgroup.

Phylogenetic analyses

Analysis comprising major clades of Rubiaceae, representatives of Loganiaceae, Gelsemiaceae, Apocynaceae, Gentianaceae, and Convolvulaceae and Solanaceae as outgroups (Rubiaceae dataset), was based on *ndhF* (NADH dehydrogenase subunit 5 gene) only. MCMC settings for BI are given in Table 29.

Table 29. MCMC settings for Bayesian analysis of the *Phyllis* datasets using MrBayes.

	ndhF [a]	***ndhF*** [b]	***rps16*** [b]	***ndhF* & *rps16*** [b]	**ITS** [c]	***rps16*** [c]	**ITS & *rps16*** [c]
Chain length (million states)	10	10	10	10	10	10	50
Sample frequency	1000	1000	1000	1000	1000	1000	5000
Number of chains	4	4	4	4	4	4	4
Number of runs	2	2	2	2	2	2	2
Heating parameter	0.2	0.2	0.2	0.2	0.2	0.2	0.2

[a] Rubiaceae dataset; [b] Anthospermeae dataset; [c] Anthosperminae excl. *Carpacoce*.

Rps16 (ribosomal protein S16 gene) was very variable above tribal level. Therefore, analysis was restricted to Anthospermeae, representatives of the closely related tribes

Paederieae DC., Putorieae Sweet, Theligoneae Wunderlich ex S.P.Darwin, Argostemmateae Bremek. ex Verdc. and Rubieae Baill., and, Knoxieae Hook. f. and Spermacoceae Bercht. & J.Presl as outgroups (Anthospermeae dataset). As the *ndhF* and *rps16* Anthospermeae datasets were not in topological conflict (Appendix Figs. S47, S48), those two markers were combined.

The even more variable ITS was analyzed on a dataset of Anthosperminae, using *Durringtonia* R.J.F.Hend. & Guymer and *Nertera* Banks ex Gaertn. (both tribe Anthospermeae) as outgroups.

Stem age estimation

Analysis consisted of two steps. In the first, the *ndhF* Rubiaceae dataset was calibrated with the stem age of Rubiaceae (87.2-53.8 mya) as estimated by Magallón et al. (2015). The chain length was set to 80 000 000, the sampling frequency to 8000. In the second, the resulting estimate for the split of Anthospermeae from Paederieae, Putorieae, Theligoneae, Argostemmateae and Rubieae from the first analysis (35.3-16.7 mya, Appendix Fig. S49) was used for calibration of the plastid (*rps16* and *ndhF* combined) Anthospermeae dataset. The chain length and sampling frequency were decreased to 50 000 000 and 5000.

For comparison, a further analysis of the plastid Anthospermeae dataset was run, using the much older stem age of Anthospermeae (57.6-38.3 mya) as estimated by Bremer & Eriksson (2009; calibB) as calibration reference. Here, the chain length and sampling frequency were also set to 50 000 000 and 5000.

Crown age estimation

Both ITS and *rps16* indicated intra-species patterns in *P. nobla*. After checking for conflict of data based on Pirie (2015), the markers were combined (Appendix Figs. S50, S51). The resulting dataset comprised *Phyllis nobla* and three accessions of *P. viscosa* as outgroup. As suggested by PartitionFinder, ITS and *rps16* were set up as distinct partitions with unlinked site models and clock models. Analysis was run under a coalescent constant population tree prior. The split of *P. nobla* from *P. viscosa* (6.8-1.1 mya, Appendix Fig. S52) from the analysis based on Magallón et al. (2015) was set as calibration point. Like in *Geranium*, the weight of the BitFlip Operator and the weight of the DeltaExchange Operator needed to be changed for the ITS partition to 1.0 to increase the ESS of the hasEqualFreqs parameter (Bouckaert, 2017).

For comparison, a second analysis was run with the estimate obtained from the stem node analysis calibrated with Bremer & Eriksson (2009; 13.1-2.7 mya). In both cases, the chain length was set to 100 000 000 and the sampling frequency to 10 000.

Ancestral area estimation

The dated plastid (*ndhF* & *rps16*) phylogeny calibrated based on Magallón et al. (2015) served as input for biogeographical analyses, excluding all taxa not assigned to Anthospermeae. Areas were coded as follows: Non-Mediterranean Africa (A), Australasia (B), Pacific Region (C), Antarctic Region (D), New World (E), Asia (F), Canary Islands (G) and Madeira (H; Table 30).

Table 30. Coding for ancestral area estimation in Anthospermeae. Non-Mediterranean Africa (A), Australasia (B), Pacific Region (C), Antarctic Region (D), New World (E), Asia (F), Canary Islands (G), Madeira (H).

Species	Areas	References
Anthospermum aethiopicum L.	A	Puff (1986)
Anthospermum herbaceum L.f.	A	Puff (1986)
Anthospermum tricostatum Sond.	A	Puff (1986)
Carpacoce Sond.	A	Puff (1986)
Carpacoce spermacocea (Rchb. ex Spreng.) Sond.	A	Puff (1986)
Coprosma antipoda W.R.B.Oliv.	B	Breitwieser, Brownsey, Heenan, Nelson, & Wilton (2010)
Coprosma cheesemanii W.R.B.Oliv.	B	Breitwieser et al. (2010)
Coprosma crassifolia Colenso	B	Breitwieser et al. (2010)
Coprosma ernodeoides A.Gray	C	Elliott & Tamashiro (2009)
Coprosma fauriei H.Lév.	C	Royal Botanic Gardens Kew (2019)
Coprosma persicifolia A.Gray	C	Royal Botanic Gardens Kew (2019)
Coprosma pumila Hook.f.	B	Royal Botanic Gardens Victoria (2017)
Coprosma quadrifida B.L.Rob.	B	Royal Botanic Gardens Victoria (2017)
Coprosma repens Hook.f.	B	Breitwieser et al. (2010); Royal Botanic Gardens Victoria (2017)
Coprosma robusta Raoul	B	Breitwieser et al. (2010); Royal Botanic Gardens Victoria (2017)
Coprosma waimeae Wawra	C	Royal Botanic Gardens Kew (2019)
Durringtonia paludosa R.J.F.Hend. & Guymer	B	Royal Botanic Gardens and Domain Trust (2019)
Galopina crocyllioides Bär	A	Puff (1986)
Leptostigma pilosum (Benth.) Fosberg	E	Royal Botanic Gardens Kew (2019)
Leptostigma reptans (F.Muell.) Fosberg	C	Royal Botanic Gardens Victoria (2017)
Nenax acerosa Gaertn.	A	Puff (1986)
Nertera assurgens Thouars	ABCDEF	Royal Botanic Gardens Kew (2019)
Nertera dichondrifolia Hook.f.	B	Breitwieser et al. (2010)
Nertera granadensis Druce	ABCDEF	Royal Botanic Gardens Kew (2019)
Nertera holmboei Christoph.	D	Royal Botanic Gardens Kew (2019)
Normandia neocaledonica Hook.f.	B	Royal Botanic Gardens Kew (2019)
Opercularia aspera Gaertn.	B	Royal Botanic Gardens Victoria (2017)
Opercularia hirsuta F.Muell. ex Benth.	B	Western Australian Herbarium (1998)
Opercularia vaginata Labill.	B	Western Australian Herbarium (1998)
Opercularia varia Hook.f.	B	Royal Botanic Gardens Victoria (2017)
Pomax umbellata Sol. ex A.Rich.	B	Royal Botanic Gardens Victoria (2017)
Phyllis nobla L.	GH	Arechavaleta et al. (2010); Borges et al. (2008)
Phyllis viscosa Christ	G	Arechavaleta et al. (2010)

Although DEC+J was indicated as best-scoring model by BioGeoBEARS (Table 31) and its likelihood was significantly different from DEC according to the likelihood ratio test (one-tailed chi-squared test, df = 1, p = 0.00), this model was discarded due to recent criticism by (Ree & Sanmartín, 2018). The second-best scoring model, DIVALIKE+J, did not significantly

differ from DIVALIKE by its likelihood (one-tailed chi-squared test, df = 1, p = 0.07; Table 31). Accordingly, an S-DIVA analysis was run in RASP.

Table 31. Biogeographical models tested for the plastid dataset of Anthospermeae and their likelihoods, AICs and AICcs as inferred by BioGeoBEARS (Matzke, 2013a; Matzke, 2013b). The best-scoring model is marked in bold, the second best-scoring model with an asterisk (*).

Model	Likelihood (LnL)	AIC	AICc
DEC	-73.09	150.2	150.6
DEC+J	**-68.79**	**143.6**	**144.4**
DIVALIKE	-72.84	149.7	150.1
DIVALIKE+J*	-71.14*	148.3*	149.1*
BAYAREALIKE	-82.41	168.8	169.2
BAYAREALIKE+J	-82.37	170.7	171.5

3.5.2. DNA sequence variation and phylogenies

Twenty-nine newly created sequences of *Phyllis nobla* and *P. viscosa* were uploaded to GenBank (Appendix Table S9). Sequence variation and characteristics of the Rubiaceae *ndhF*, the Anthospermeae plastid datasets and the Anthospermineae ITS dataset are illustrated in Table 32.

Table 32. Sequence characteristics of the Rubiaceae, Anthospermeae and Anthosperminae datasets, i.e. the *ndhF* dataset of Rubiaceae, the Anthospermeae plastid datasets (*ndhF*, r*ps16*, *ndhF* & *rps16*) and the ITS dataset of Anthosperminae.

	ndhF [a]	***ndhF*** [b]	***rps16*** [b]	***ndhF* & *rps16*** [b]	**ITS** [c]	***rps16*** [c]	**ITS & *rps16*** [c]
Number of accessions	64	17	62	53	22	21	26
Total number of characters	2181	2181	1047	3228	637	807	1444 (Partition 1: 637, partition 2: 807)
Variable characters	52%	23%	28%	24%	21%	8%	14%
Parsimony informative characters	38%	11%	16%	12%	13%	5%	8%
Substitution model (AIC)	GTR+Γ+I	GTR+Γ	GTR+Γ	GTR+Γ+I	GTR+Γ	GTR+Γ	Partition 1: GTR+Γ Partition 2: GTR+Γ

[a] Rubiaceae dataset; [b] Anthospermeae dataset; [c] Anthosperminae excl. *Carpacoce* dataset

No contradiction has between found between the topology of the ITS, the plastid and the concatenated phylogenies (Fig. 33, Appendix Figs. S47-S53). The ITS data is also in agreement with Anderson et al. (2001), Bremer & Eriksson (2009) and Thureborn et al. (2019). The topology of the plastid phylogeny does not fully agree with some previously published phylogenies, e.g. Bremer & Eriksson (2009) and Anderson et al. (2001), with respect to the positions of Theligoneae and *Normandia neocaledonica* Hook.f. In this study, Theligoneae is supported as sister to Putorieae (Appendix Fig. S48), Bremer & Eriksson (2009) recover it as sister to Rubieae instead. Additionally, *Normandia neocaledonica* is recovered in a different position than in Bremer & Eriksson (2009) and Anderson et al. (2001). However, the position recovered here is not in conflict with Thureborn et al. (2019).

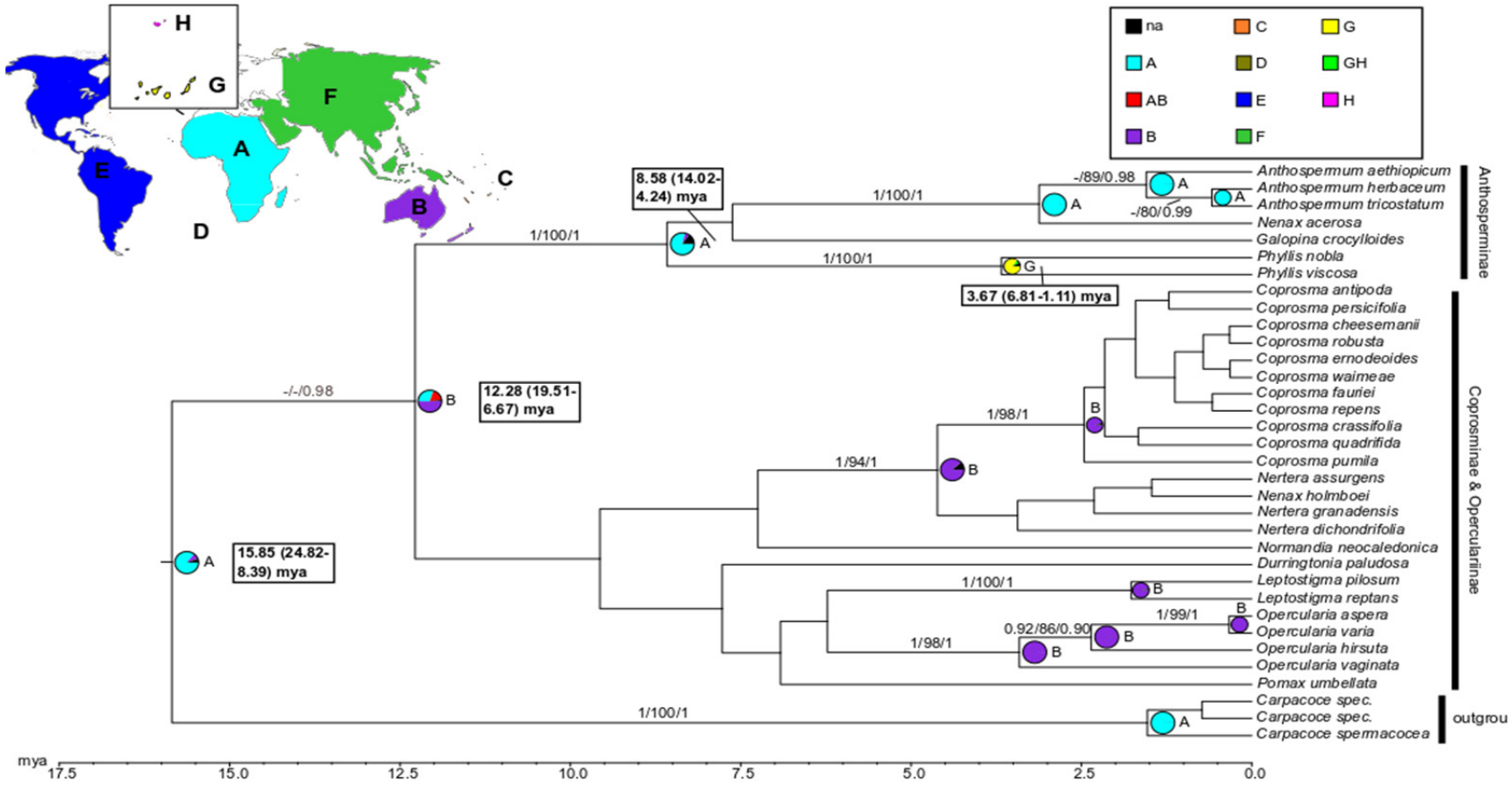

Figure 33. Biogeography of Anthospermeae as inferred from BBM analysis in RASP, based on the plastid chronogram. Numbers above branches indicate posterior probabilities from MrBayes analysis, bootstrap values from RAxML analysis and posterior probabilities from BEAST analysis. Only posterior probabilities ≥0.90 and bootstrap values ≥80 are shown. On the nodes, the posterior probabilities of the estimated areas/area combinations are indicated by pie charts. Areas coded include Africa (A), Australasia (B), Pacific Region (C), Antarctic Region (D), New World (E), Asia (F), Canary Islands (G), Madeira (H). For nodes of interest, the age estimates from BEAST analysis are given. The world map was modified from https://commons.wikimedia.org/wiki/File:Simplified_blank_world_map_without_Antartica_(no_borders).svg, the map of Macaronesia from A. Platon, https://upload.wikimedia.org/wikipedia/commons/b/b4/Macaronesia_locati on.svg.

Phyllis is nested in tribe Anthospermeae, subtribe Anthosperminae (Fig. 33; Appendix Figs. S50, S51, S53). Within the subtribe, the genus forms a polytomy with *Galopina* and a clade of *Nenax* and *Anthospermum* (Fig. 33, Appendix Fig. S50, S51, S53). Laurel forest species *Phyllis nobla* is recovered as sister to Canarian *P. viscosa* (Fig. 33, Appendix Fig. S50, S51, S53). Within *Phyllis nobla*, distinct clades are recovered for a) the Madeiran accessions (Fig. 34B), b) the Tenerife accessions (Fig. 34B) and c) La Palma (Appendix Fig. S48). The relationships between those receive only poor statistical support and remain unresolved.

3.5.3. Molecular dating: Early Pliocene origin and Middle Pleistocene diversification

The analysis based on calibration data derived from Magallón et al. (2015) results in a Mid-Miocene crown age of Anthospermeae (15.85 mya, 95% HPD 24.82-8.39 mya; Fig. 33). The origin of *Phyllis* is estimated to the Late Miocene (8.58 mya, 95% HPD 14.02-4.24 mya; Fig. 33, Fig. 34A) and the split into *P. nobla* and *P. viscosa* to the Early Pliocene (3.67 mya, 95% HPD 6.81-1.11 mya; Fig. 33, Fig. 34A). *Phyllis viscosa* diversified within Tenerife during the Late Pleistocene (0.07 mya, 95% HPD 0.22-0.00 mya; Fig. 34B). The crown of *P. nobla* is dated to the Middle Pleistocene (0.24 mya, 95% HPD 0.52-0.06 mya; Fig. 34B). Diversification of the Madeira accessions of *P. nobla* occurred during the Late Pleistocene (0.03 mya, 95% HPD 0.10-0.00 mya; Fig. 34B). The Tenerife accessions of *P. nobla* also diversified during this time (0.04 mya, 95% HPD 0.10-0.00 mya; Fig. 34B).

The analyses calibrated with data from Bremer & Eriksson (2009) result in much older estimates (Appendix Fig. S54, S55). In this case, the crown of Anthospermeae is dated to the Early Oligocene (32.19 mya, 95% HPD 48.84-19.76 mya), the stem of *Phyllis* to the Early Miocene (17.45 mya, 95% HPD 25.99-10.09 mya) and the origin of *P. nobla* and *P. viscosa* to the Late Miocene (7.40 mya; 95% HPD 13.14-2.69 mya; Appendix Fig. S54). The Tenerife accessions of *P. viscosa* diversified during the Middle Pleistocene (0.16 mya, 95% HPD 0.52-0.00 mya; Appendix Fig. S55). The crown of *P. nobla* is estimated to the Early Pleistocene (0.56 mya, 95% HPD 1.23-0.16 mya; Appendix Fig. S55). Diversification within the Madeiran accessions is dated to the Late Pleistocene (0.08 mya, 0.24-0.00 mya; Appendix Fig. S55). The same is found within the Tenerife accessions (0.09 mya, 95% HPD 0.25-0.00 mya; Appendix Fig. S55).

3.5.4. Biogeography: Macaronesian origin

BBM suggests that the MRCA of Anthospermeae was distributed in Africa (PP = 0.82; Fig. 33). For the MRCA of subtribes Anthosperminae (excl. *Carpacoce*), Opercullariinae Benth. and Coprosminae Fosberg, dispersal to Australasia was indicated (PP = 0.51, Fig. 33). Backdispersal to Africa occurred in the MRCA of Anthosperminae (excl. *Carpacoce*), i.e. the stem of *Phyllis*. *Phyllis nobla* and *P. viscosa* are reconstructed as the result of speciation within the Canary Islands (PP = 0.86; Fig. 33). From the Canary Islands, Madeira was colonized in *Phyllis nobla* (Fig. 33).

The states for some of the nodes reconstructed by S-DIVA are highly ambiguous due to low probabilities (Appendix Fig S56). The overall outcome does not contradict the more unambiguous BioGeoBEARS DIVA-like analysis (Appendix Fig. S57). The MRCA of Antho-

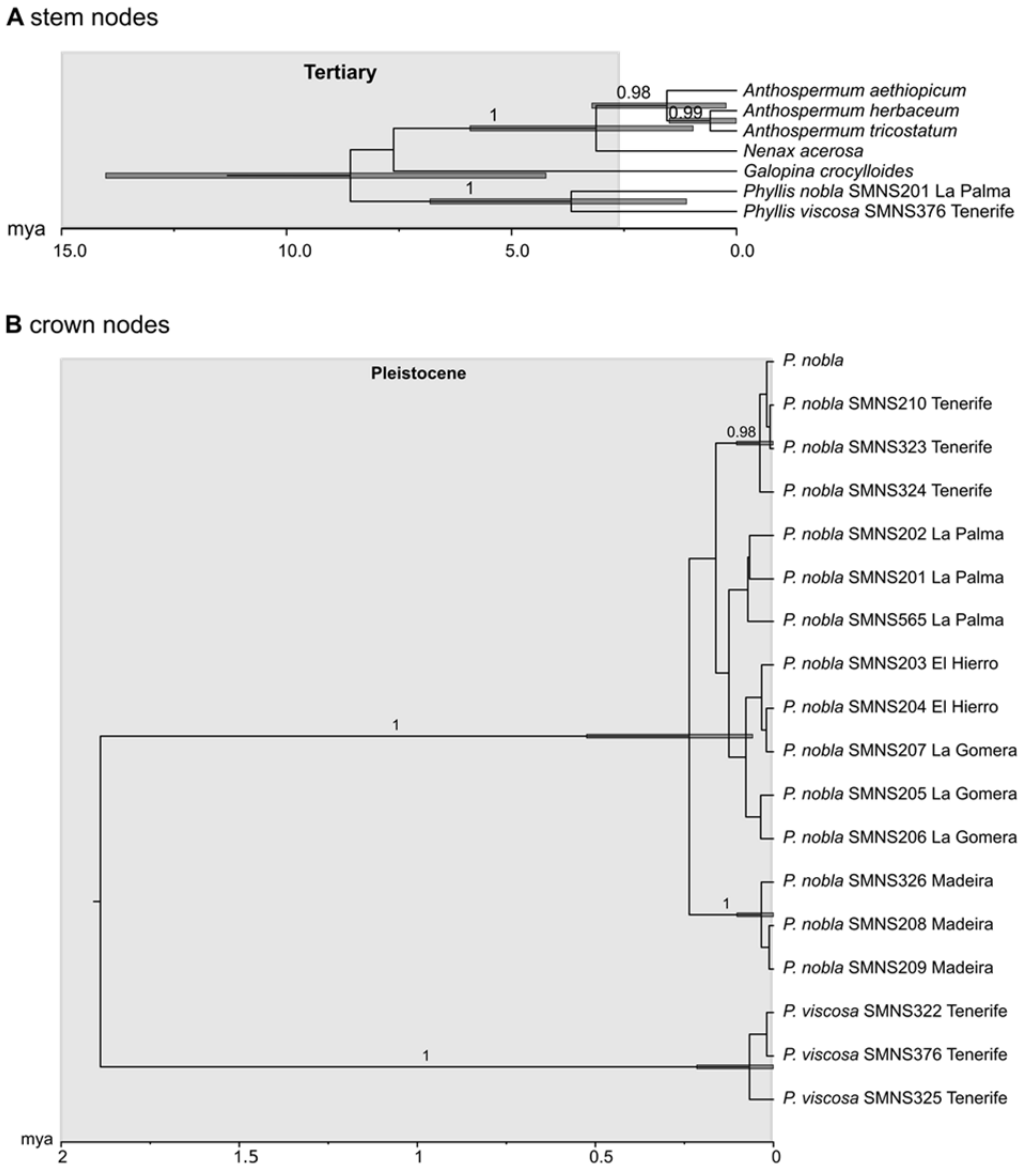

Figure 34. Chronograms from stem node and crown node dating in *Phyllis*. Bars at the nodes indicate 95% highest posterior densities; posterior probabilities from BEAST analysis ≥ 0.90 are given above the branches. **A** Stem node dating, plastid data (*ndhF* & *rps16*, calibM); **B** Crown node dating based on combined ITS & *rps16* data of the *P. nobla* and *P. viscosa*.

spermeae likely occurred in Africa, Australasia and the Canary Islands according to DIVA-like analysis (Appendix Fig. S57). This is also suggested by S-DIVA with $p = 0.14$, with a distribution throughout Africa, Australasia, the Canary Islands and Madeira indicated as equally probable (Appendix Fig. S56). The MRCA of subtribes Anthosperminae (excl. *Carpacoce*), Opercullariinae and Coprosminae was distributed in Australasia and on the Canary Islands according to DIVA-like analysis (Appendix Fig. S57). This is also indicated as one of the most likely distribution by S-DIVA, albeit with low support ($p = 0.08$; Appendix Fig. S56). Alternative distributions suggested for this node by S-DIVA with $p = 0.08$ are a) Africa, Australasia, the Canary Islands and Madeira b) Australasia, the Canary Islands and Madeira or c) Africa, Australasia and the Canary Islands. DIVA-like reconstructs an African-Canarian origin of *Phyllis* (Appendix Fig. S57), whereas S-DIVA is undecided between an

African-Canarian or an African-Canarian-Madeiran origin (both $p = 0.50$; Appendix Fig. S56). Diversification of *Phyllis* occurred within the Canary Islands according to both DIVA-like and S-DIVA ($p = 0.51$; Appendix Figs. S56, S57). Like in BBM, colonization of Madeira from the Canary Islands in *Phyllis nobla* is indicated.

3.5.5. Discussion

Tertiary relict hypothesis

Macaronesian *Phyllis* consists of two species, the laurel forest occupying *P. nobla* and the succulent scrub plant *P. viscosa*. Thus, the whole lineage of *Phyllis* may be relictual or *Phyllis nobla* only. The age criterion for Tertiary relicts (see Kondraskov, Schütz, et al., 2015) is fulfilled by both *Phyllis* and *P. nobla*, with the first dating to the Miocene (Fig. 33, Fig. 34A) and the latter to the Late Miocene or Early Pliocene.

In contrast to that, the geographical origins of both *Phyllis* and *P. nobla* refute a relict origin. Although *Phyllis nobla* was hypothesized to be an ancient Mediterranean laurel forest species by Mendoza-Heuer (1977), with *P. viscosa* having evolved from the laurel forest species, no affinities to the Mediterranean were indicated (Fig. 33). As proposed by Engler (1879), *Phyllis* is likely of tropical or South African origin (Fig. 33). The sister group relationship between *Phyllis* and *Galopina* as suggested by Schenck & Schimper (1907) can neither be confirmed nor rejected due to a lack of resolution (Fig. 33, Appendix Fig. S50, S51, S53). However, the data by Thureborn et al. (2019) suggest that *Phyllis* is rather sister to a clade comprising *Galopina*, *Anthospermum* and *Nenax*. Affinities to South or East Africa have also been shown for other Macaronesian taxa or lineages, e.g. *Canarina*, *Kleinia* Mill., *Plocama* Aiton, *Cicer* L., *Camptoloma* Benth. and *Aeonium* Webb & Berthel. (Pokorny et al., 2014). Like in *Phyllis* and its African relatives, these disjunctions often date to the Mio-/Pliocene (Pokorny et al., 2014). Despite the temporal and spatial homogeneity, the underlying patterns of this divergence are likely not homogenous as the analyzed taxa differ in habitat affinity (Pokorny et al., 2014).

There is no direct evidence for the origin in a laurel forest habitat in *Phyllis* and *P. nobla*. The sister group of *Phyllis* grows predominantly in tropical or subtropical habitats (Puff, 1982). Still, the species are found in wet, moist as well as in dry habitats. Puff (1986) suggests that wet habitats may be ancestral and dry ones more recently colonized, which at least indicates a pre-adaption to a laurel forest type habitat. This would also hint towards a colonization of the succulent scrub from a laurel forest occupying MRCA of *P. nobla* and *P. viscosa.*

Inter-archipelago and inter-island colonization

Inter-archipelago colonization follows the general pattern, i.e. from the Canary Islands to Madeira, e.g. *Bystropogon* (Kondraskov, Schütz, et al., 2015), *Scrophularia* (Navarro-Pérez et al., 2015), *Sonchus*, *Echium*, *Sideritis* and *Crambe* (Kim et al., 2008; see also *Geranium*, sect. 3.2.4). The timeframe from the Late/Middle Pleistocene onwards, also agrees with the previously published data from other Macaronesian taxa.

Within the Canary Islands, both the accessions from Tenerife and the ones from La Palma are distinct and form a polytomy with the remainder (Fig. 34B; Appendix Fig. S51).

This might indicate that *Phyllis nobla* from Tenerife and La Palma are older than the populations from the other islands and point towards Tenerife or La Palma acting as a starting point for Pleistocene inter-island colonization. The most likely starting point may be Tenerife, which has already been indicated as center of diversification by e.g. Mairal, Sanmartín et al. (2015) or in *Euphorbia* subsect. *Macaronesicae* Molero & Barres (Sun, Li, Vargas-Mendoza, Wang, & Xing, 2016). Although Tenerife is derived from three paleo islands and thus has a complex geological history, it is considered to have been geologically stable at least since the Pliocene (Mairal, Sanmartín, et al., 2015). This pre-dates the inter-island spread of *Phyllis nobla*, which occurred not until the Pleistocene.

4. Non-relicts: Pleistocene origin

4.1. *Gesnouinia arborea* (Urticaceae) – An example of an insular woody laurel forest species?

The text, tables and figures of the sections 4.1.1 to 4.1.6 are derived and extended from Schüßler et al. (2019) and have been originally written and created by myself.

4.1.1. Specific Material and Methods

Phylogenetic sampling

Taxa sampled for phylogenetic analyses are listed in Appendix Table S10. According to the molecular phylogeny by Wu et al. (2013) based on seven loci from all three genomic compartments, *Gesnouinia* is nested in tribe Parietarieae. Thus, the sampling strategy focused on including all accepted species of Parietarieae. The tribe comprises three genera, *Gesnouinia*, *Soleirolia* and *Parietaria*. All species of *Soleirolia* (one) and *Gesnouinia* (two) were sampled. *Parietaria* consists of ca. 20 species according to Friis (1993) and Wu et al. (2013), whereas Plants of the World Online (Royal Botanic Gardens Kew, 2019) list 24 species as accepted and Plant List (2013) comprises 14 accepted species. Here, 17 species of *Parietaria* and two unspecified accessions were included, generating 109 new sequences. Those 17 species comprise all species recognized by Weddell (1869), Tutin et al. (1993), Boufford (1997), Jiarui, Qi, Friis, Wilmot-Dear, & Monro (2003) and Robertson, Orchard, & Wilson (1989) as well as one of the two species endemic to tropical Africa (Gebauer, 1994). However, some of the species of the genus are morphologically highly similar. Hence, species identification can be complicated for some of them (Friis, 1993). For example, species of *Parietaria* from tropical Africa were often mistaken for the presumably widespread *Parietaria debilis* (Gebauer, 1994).

Of *G. arborea*, at least two accessions from all islands of its distribution (Gran Canaria, Tenerife, La Gomera, La Palma, El Hierro) according to Arechavaleta et al. (2010) were sampled.

Sequences from the major clades of Urticaceae as recovered by Wu et al. (2013) were downloaded from GenBank for molecular dating. Of each clade, one to three species were included as representatives. In addition to that, sequences of 12 Moraceae were included to calibrate the split between Urticaceae and Moraceae, e.g. Sytsma et al. (2002). Seven Cannabaceae were added as outgroup (Sytsma et al., 2002).

Anatomic sampling

For anatomical analysis, a branch of *Gesnouinia arborea* as well as stems of *G. filamentosa*, *Soleirolia soleirolii* and eight *Parietaria* species were sampled (Appendix Table S10). In most cases, the material was obtained from herbarium specimens. In the case of *Soleirolia* and *P. officinalis*, material immediately stored in alcohol subsequent to collection was available.

Phylogenetic analyses

TrnL-trnF spacer and *matK* Urticaceae datasets were combined removing the only significantly supported conflicting taxon, *Parietaria laxiflora* Engl., from the datasets

according to the criteria listed in Pirie (2015; Appendix Figs. S58, S59). MCMC settings used for BI are listed in Table 33.

ITS was too variable to allow for unambiguous alignment above tribal level. Hence, the analysis was limited to Parietarieae, using four species of the closely related Forsskaoleae (Gaud.) Wedd. (Wu et al., 2013) as outgroup. Although different PCR protocols and primers were tested, ITS1 repeatedly failed to amplify for taxa of the *Parietaria officinalis* clade (*P. judaica*, *P. officinalis*, *P. cretica* L., *P. littoralis* Schchian and *P. elliptica* K.Koch). After testing analysis of the whole ITS region, phylogenetic inference was restricted to ITS2 as the whole region a) included some sites of questionable homology and b) did not significantly improve phylogenetic resolution.

The relationships within the *P. officinalis* clade recovered for ITS data did not agree with those recovered for the plastid data. As the concatenation of the nuclear and the plastid dataset would result in a high amount of missing data due to the reduced sampling of ITS data, nuclear and plastid markers were kept separate.

Table 33. MCMC settings for Bayesian analysis of the *Gesnouinia* datasets using MrBayes.

	trnL-trnF [a]	***matK*** [a]	***trnL-trnF* & *matK*** [a]	**ITS** [b]
Chain length (million states)	1	1	1	1
Sample frequency	1000	1000	1000	1000
Number of chains	4	4	4	4
Number of runs	2	2	2	2
Heating parameter	0.2	0.2	0.2	0.2

[a] Urticaceae dataset; [b] Parietarieae dataset

Stem age estimation

The fossil record of Urticaceae is rather scarce and the available fossils are difficult to assign (Collinson, 1989; Friis, 1993). Thus, the stem age of Urticaceae (57.7—79.0 mya) as estimated by Magallón et al. (2015), was used for calibration. Dating analysis was based on the more reliably aligned concatenated plastid dataset comprising both *matK* and *trnL-trnF* spacer, as ITS was highly variable above tribal level. The length of the MCMC chain was set to 50 000 000 and the sample frequency to 5000.

Crown age estimation

An ITS2 dataset comprising of several accessions of *Gesnouinia*, *Soleirolia* and closely related *Parietaria* species (perennial clade of Parietarieae; see Appendix Fig. S60) was created. A coalescent tree prior with constant populations was set up and the divergence time estimate of the crown age of the perennial clade (4.0—15.6 mya) from the *trnL-trnF* & *matK* analysis (Appendix Fig. S61) was used as a calibration point. Chain length equaled 10 000 000 and sample frequency 1000.

Ancestral area estimation

All taxa not belonging to tribe Parietarieae were removed from the dated plastid (*trnL-trnF* spacer and *matK*) phylogeny prior to analysis. The following areas were coded:

Macaronesia (A), Mediterranean (B), Australia (C), New World (D), Non-Mediterranean Eurasia (E), Non-Mediterranean Africa (F; Table 34). For BBM analysis, the split between the *Parietaria officinalis* clade and *Gesnouinia* (supported with pp < 0.90 in the MCC tree) was not excluded as it is significantly supported in the ITS phylogeny (Appendix Fig. S60; BS = 83; PP = 0.97).

BioGeoBEARS indicated the DEC models as best based on likelihoods, AICs and corrected AICs (AICcs; Table 35). The less complex DEC model was chosen over DEC+J, since the likelihoods of DEC and DEC+J were not significantly different according to the likelihood ratio test (one-tailed chi-squared test, df = 1, p = 0.10). Therefore, S-DEC analysis was run in RASP.

Table 34. Coding for ancestral area estimation and for ancestral character state reconstruction of woodiness in Parietarieae. Areas: Macaronesia (A), Mediterranean (B), Australia (C), New World (D), Non-Mediterranean Eurasia (E), Non-Mediterranean Africa (F). Life-form: Therophyte (0), hemicryptophyte (1), chameophyte (2) and phanerophyte (3). Habit quotient: Herbaceous ≤ 0.28 (0), woody ≥ 0.42 (1). Woodiness stem: Distinct wood cylinder restricted to base (0), distinct wood cylinder in whole stem (1).

Species	**Areas**	**Life form**	**Habit quotient**	**Woodiness stem**	**References**
Gesnouinia arborea (L.f.) Gaudich.	A	3	1	1	this study, Hohenester & Welss (1993)
Gesnouinia filamentosa Wedd.	A	2	1	1	this study, Hohenester & Welss (1993)
Parietaria alsinifolia Delile	BEF	0	0	0	this study, Bobrov et al. (1970)
Parietaria australis Blume	C	0	?	?	Royal Botanic Gardens Victoria (2017)
Parietaria cardiostegia Greuter	C	0	?	?	Robertson et al. (1989)
Parietaria cf. *floridana* Nutt.	D	0/1	?	?	Boufford (1997)
Parietaria cf. *hespera* var. *hespera* B. D. Hinton	D	0	?	?	Boufford (1997)
Parietaria cf. *praetermissa* B.D. Hinton	D	0	?	?	Boufford (1997)
Parietaria cretica L.	B	0/1	1	1	this study, Pignatti (1982)
Parietaria debilis G.Forst.	ABCDEF	0	0	1	this study, Robertson et al. (1989)
Parietaria elliptica K.Koch	E	?	?	?	_
Parietaria hespera var. *californica* B. D. Hinton	D	0	?	?	Boufford (1997)
Parietaria judaica L.	ABE	1	1	0	this study, Pignatti (1982)
Parietaria littoralis Schchian	E	?	?	?	_
Parietaria lusitanica L.	BE	0	0	0	this study, Pignatti (1982)
Parietaria mauritanica Durieu	B	0	0	0	this study, Pignatti (1982)
Parietaria micrantha Ledeb.	E	0	?	?	Bobrov et al. (1970); Jiarui et al. (2003)
Parietaria officinalis L.	BE	1	0	0	this study, Pignatti (1982)
Parietaria pensylvanica Muhl. ex Willd.	D	0	0	0	this study, Boufford (1997)
Soleirolia soleirolii (Req.) Dandy	B	1	0	0	this study, Pignatti (1982)

Table 35. Biogeographical models tested for the Parietarieae plastid dataset and their likelihoods, AICs and AICcs as inferred by BioGeoBEARS (Matzke, 2013a; Matzke, 2013b). Best-scoring models are marked in bold.

Model	Likelihood (LnL)	AIC	AICc
DEC	−50.79	105.6	**106.2**
DEC+J	**−49.44**	**104.9**	106.3
DIVALIKE	−55.00	114	114.7
DIVALIKE+J	−54.87	115.7	117.1
BAYAREALIKE	−51.34	106.7	107.3
BAYAREALIKE+J	−51.34	108.7	110.1

Microtome sections

The lower stems (0—1 cm above the ground, in the lower third of the stem) and the upper stems (upper third of the stem) of *Gesnouinia arborea*, *G. filamentosa*, *Soleirolia soleirolii* (Req.) Dandy and eight *Parietaria* species (Appendix Table S10) were sectioned transversely and, in the case broad wood cylinders were present, also longitudinally. In this study, no material from the lower stem was available for *G. arborea*. Hence, only the lower part of a branch was sectioned here. For further information on the stem anatomy of *G. arborea*, the data from the study by Bonsen & ter Welle (1984) was consulted.

Wood anatomical characteristics, e.g. vessel diameter, vessel element length, ray height, cf. Wheeler, Baas, & Gasson (1989), were measured for the species with a broad wood cylinder in the stem basis (*G. arborea*, *G. filamentosa*, *P. cretica* and *P. judaica*). In this study, sections were measured instead of macerations. Therefore, all measurements of vessel element and fiber length in this study provide minimum values, as the tails cannot be measured precisely from sections (Carlquist, 2001). At least 25 measurements were conducted for each character. In addition to that, wood cylinder thickness and stem diameter of the basal stem were determined based on Lens et al. (2012).

Ancestral character state optimization

Three different characteristics were coded, i.e. a) Raunkiær perennation strategy: Therophyte (0), hemicryptophyte (1), chameophyte (2) and phanerophyte (3); b) Presence of distinct wood cylinder throughout stem: Distinct wood cylinder restricted to base (0), distinct wood cylinder in whole stem (1); c) habit quotient stem basis [$\frac{double\ wood\ cylinder\ thickness}{average\ stem\ diameter}$]: Herbaceous ≤ 0.28 (0), woody ≥ 0.42 (1; Table 34). The habit quotient was coded on the basis of two different classes observed in this study. These classes are mainly agree with Lens et al. (2012). In their study, herbaceousness ranged to at least 0.24 and woodiness started at 0.3 at least. Character states of woodiness were optimized on the outgroup-reduced pt phylogeny generated by RASP (see Ancestral area reconstruction).

4.1.2. DNA sequence variation and phylogenies

One hundred and nine sequences have been newly created and uploaded to GenBank (cf. Appendix Table S10), the alignments and phylogenies are available at TreeBase (http://purl.org/phylo/treebase/phylows/study/TB2:S22751). Sequence variation for the analyzed ITS, *matK* and *trnL-trnF* spacer and combined plastid datasets is given in Table 36.

Table 36. Sequence characteristics of the Parietarieae and Urticaceae datasets, i.e. the Parietarieae ITS dataset and the Urticaceae *trnL-trnF*, *matK* and combined plastid datasets.

	trnL-trnF [a]	***matK*** [a]	***trnL-trnF* & *matK*** [a]	**ITS** [b]
Number of accessions	101	77	94	58
Total number of characters	1219	765	1984	472
Variable characters	44%	57%	49%	33%
Parsimony-informative characters	29%	41%	33%	27%
Substitution model (AIC)	GTR+Γ+I	GTR+Γ+I	GTR+Γ+I	GTR+Γ

[a] Urticaceae dataset [b] Parietarieae dataset

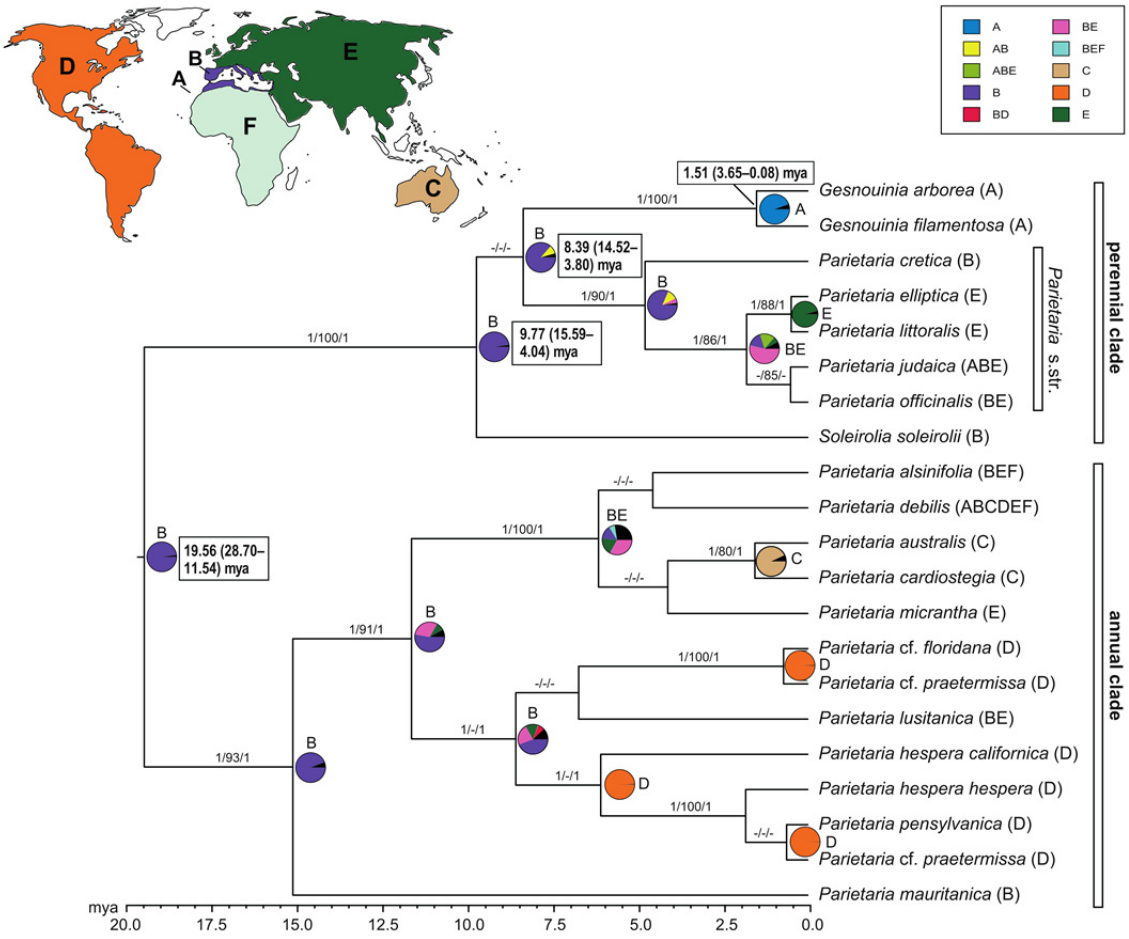

Figure 35. Biogeography of Parietarieae as inferred from BBM analysis in RASP, based on the plastid chronogram. Numbers above branches indicate posterior probabilities from MrBayes analysis, bootstrap values from RAxML analysis and posterior probabilities from BEAST analysis. Only posterior probabilities ≥0.90 and bootstrap values ≥80 are shown. On the nodes, the posterior probabilities of the estimated areas/area combinations are indicated by pie charts. Areas coded include Macaronesia (A), Mediterranean (B), Australia (C), New World (D), Non-Mediterranean Eurasia (E), Non-Mediterranean Africa (F). For nodes of interest, the age estimates from BEAST analysis are also given. The world map was modified from https://commons.wikimedia.org/wiki/File:Simplified_blank_world_map_without_Antartica_(no_borders).svg.

There is no topological conflict between the phylogeny by (Wu et al., 2013) and the Urticaceae plastid phylogeny (Appendix. Fig. S61) as well as the Parietarieae ITS phylogeny (Appendix. Fig. S60). Parietarieae are recovered as monophyletic, genus *Parietaria* as paraphyletic with respect to *Gesnouinia* and *Soleirolia* (Fig. 35, Appendix. Fig. S61). The tribe comprises two well-supported main clades (Fig. 35, Appendix. Fig. S61). One clade consists of annual *Parietaria* species from all over the world (annual clade; Fig. 35,

Appendix. Fig. S61). The second clade contains perennial Mediterranean-Eurasian-distributed species of *Parietaria* s.str. and the perennial genera *Gesnouinia* and *Soleirolia* and (perennial clade; Fig. 35, Appendix. Fig. S61). The relationship between *Gesnouinia*, *Soleirolia* and *Parietaria* s.str. is unresolved by plastid data (Fig. 35), whereas ITS data reveals *Soleirolia* as sister to *Gesnouinia* and *Parietaria* s.str. (Appendix. Fig. S60).

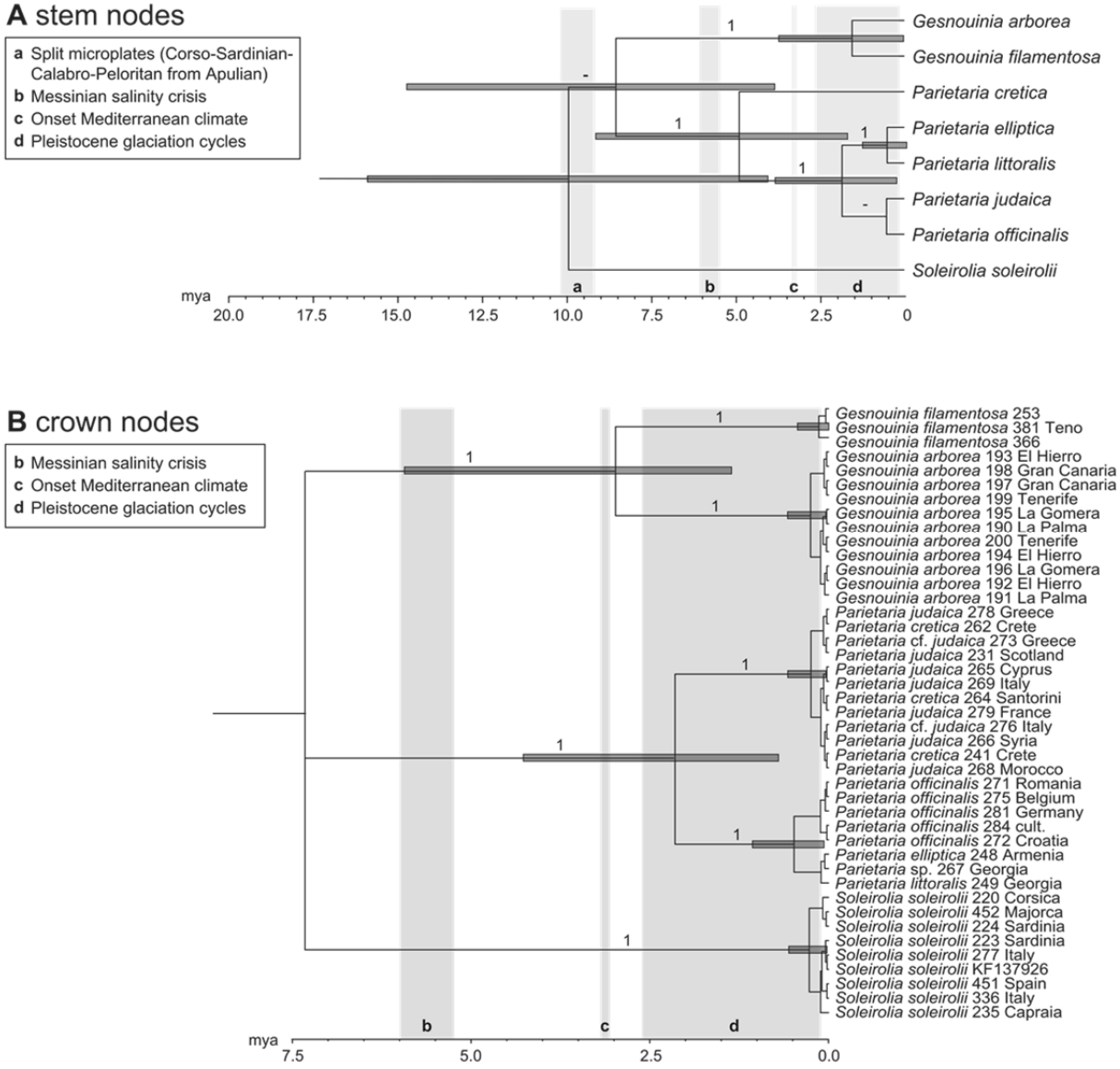

Figure 36. Chronograms of the perennial clade of Parietarieae with important tectonic and climatic events indicated in gray and by letters (a: split of Corso-Sardinian–Calabro-Peloritan microplate from Apulian microplate, b: Messinian salinity crisis, c: onset of Mediterranean climate, d: Pleistocene glaciation cycles). Bars at the nodes indicate 95% highest posterior densities; posterior probabilities from BEAST analysis ≥ 0.90 are given above the branches. **A** Stem node dating from Urticaceae plastid dataset (*matK* & *trnL-trnF*); **B** Crown node dating based on ITS data of perennial clade.

There is some topological conflict indicated between the individual datasets. For instance, African perennial *P. laxiflora* is either sister to the annual *Parietaria* clade according to *matK* and ITS data (Appendix Figs. S58, S60) or sister to all other Parietarieae according to *trnL-trnF* spacer (Appendix Fig. S59). Also, the species within *Parietaria* s.str. are positioned differently to each other in plastid and in nuclear data (Fig. 35, Appendix Fig. S60).

4.1.3. Molecular dating: Early Pleistocene origin and Middle Pleistocene diversification

Parietarieae diversified in the Early Miocene (19.56 mya, 95% highest posterior density [HPD] 28.70–11.54 mya; Fig. 35), the perennial clade in the Late Miocene (9.77 mya, 95% HPD 15.59–4.04 mya; Figs. 35, 36A). The subsequent split of *Gesnouinia* from *Parietaria* s.str. occurred during the Late Miocene (8.39 mya, 95% HPD 14.52–3.80 mya; Figs. 35, 36A). Speciation into *G. arborea* and *G. filamentosa* is dated to the Early Pleistocene (1.51 mya, 95% HPD 3.65–0.08 mya; Figs. 35, 36A). Diversification within *Gesnouinia arborea* is dated around the Middle Pleistocene (0.25 mya, 95% HPD 0.61–0.03 mya; Fig. 36B), in the Tenerife populations of *G. filamentosa* around the Late Pleistocene (0.14 mya, 95% HPD 0.37–0.01 mya; Fig. 36B).

4.1.4. Biogeographic reconstructions: Macaronesian origin

BBM and S-DEC analyses propose different biogeographical patterns for the origin of Macaronesian endemic *Gesnouinia*. Below, the estimates with the highest probabilities are described in detail.

BBM suggests that the MRCA of Parietarieae (Fig. 35, PP = 0.98) and the MRCA of the perennial clade were distributed in the Mediterranean region (Fig. 35; PP = 0.98). For the origin of *Gesnouinia*, dispersal from the Mediterranean to Macaronesia is estimated (Fig. 35, PP = 0.86).

The results from S-DEC analysis in RASP (Appendix Fig. S62) do not contradict the BioGeoBEARS DEC analysis (Appendix Fig. S63). Similar to BBM, S-DEC indicates a Mediterranean-distributed MRCA of Parietarieae (p = 0.18; Appendix Fig. S62). For the MRCA of the perennial clade, a Mediterranean-Macaronesian distribution is inferred (p = 0.62, Appendix Fig. S62). *Gesnouinia* is estimated to be the result of vicariance in a Mediterranean-Macaronesian-distributed ancestor (p = 0.63, Appendix Fig. S62).

4.1.5. Stem sections: Derived woodiness in *G. arborea* and *G. filamentosa*

The wood cylinders of the basal stems were continuous in all analyzed taxa of Parietarieae (see also Appendix. Fig. S64A–F; appendix) but differed in extent. The wood cylinders found in *P. officinalis*, *P. debilis*, *P. pensylvanica* Muhl. ex Willd., *P. mauritanica* Durieu, *P. alsinifolia* Delile, *P. lusitanica* L. and *S. soleirolii* were short (habit quotient 0.21–0.28; Table 37), whereas the wood cylinders in *G. filamentosa*, *P. cretica* and *P. judaica* were broad (habit quotient ≥0.42; Table 37). For *G. arborea*, no stem basis was available for sectioning. In this case, the habit quotient was approximated using the section of a branch basis. Here, a broad wood cylinder was recovered (habit quotient = 0.42; Table 37).

In the taxa with broad wood cylinders in the stem basis, rays with mostly square to upright cells in proximity of the cambium were present in the basal stems of *G. arborea* and *G. filamentosa* (see also Appendix. Fig. S64B). Although areas with ray or ray-like cells were visible in the transverse sections of *P. judaica*, no ray cells were detected in the longitudinal and radial sections. In *P. cretica*, no ray cells were observed either. In all of the four taxa, intervessel pits were alternate to scalariform and perforation plates were simple. Libriform fibers ranging from very thin to thin were found in *P. cretica* and very thin libriform fibers in

the other species. For a more detailed wood description, see Table 37.

Distinct continuous wood cylinders were also observed in the upper part of the stem respectively in the branches of *G. arborea*, *G. filamentosa*, *P. cretica* and *P. debilis* (cf. Appendix Fig. S65A,E,F). The other analyzed taxa showed no distinct wood cylinder in the upper part of the stem (cf. Appendix Fig. S65B-D) but the interfascicular cambium was already developed or in some cases starting to form.

4.1.6. Character state optimization of woodiness: Woody traits already present prior to colonization of Macaronesia

ML and MP character state optimization agreed in the pattern proposed for the evolution of the perennation strategy (Fig. 37, Appendix Fig. S66). The reconstruction for MRCA of Parietarieae was ambiguous, inferring it either to be a therophyte (ML proportional likelihood 0.65, Fig. 37) or a hemicryptophyte (ML proportional likelihood 0.28, Fig. 37). For the MRCA of the annual clade, a therophyte life-form (ML proportional likelihood 0.96, Fig. 37) was indicated. The most likely state of MRCA of the perennial clade as well as the most likely state of the MRCA of *Parietaria* s.str. and *Gesnouinia* was estimated to be a hemicryptophyte (both ML proportional likelihood 0.92, Fig. 37). The ancestral character state for the genus *Gesnouinia* could not be reconstructed conclusively and may be hemicryptophyte, chameophyte or phanerophytes (Fig. 37). At the latest, chameophytes evolved in *G. filamentosa* and phanerophytes in *G. arborea* (Fig. 37).

The ML character state optimization of woodiness as indicated by the habitat quotient was ambiguous for most nodes (Appendix Fig. S67). The MP optimization was unambiguous, estimating the MRCA of Parietarieae to be herbaceous (Fig. 37). In the MRCA of *Gesnouinia* and *Parietaria* s.str., woodiness evolved (Fig. 37). In *P. officinalis*, a reversal to herbaceousness is implied (Fig. 37).

For the continuity of the wood cylinder throughout the stem, ML optimization again was equivocal for most nodes (Appendix Fig. S68) and MP optimization more unambiguous (Fig. 37). According to MP, the ancestor of Parietarieae lacked a continuous wood cylinder in the upper stem (Fig. 37). The evolution of wood cylinders in the upper stems either occurred in the MRCA of *Parietaria* s.str. and *Gesnouinia* (reconstructions ambiguous) or within *Gesnouinia* (Fig. 37).

Table 37. Stem anatomy of Parietarieae. Detailed measurements and descriptions are given for species with a broad wood cylinder (habit quotient, i.e., ratio of double wood cylinder/average stem diameter > 0.3). For intervessel pit size, vessel diameter, vessels per mm^2, mean vessel element length, mean fiber length and ray height, mean values and ranges (minimum and maximum measured) are given according to Wheeler et al. (1989). * The asterisk marks data obtained from Bonsen & ter Welle (1984), and constitute the lowest and highest mean values per specimen and the range (minimum and maximum value measured).

	***G. arborea* (twig)**	***G. arborea* (stem)***	***G. filamentosa***	***P. cretica***	***P. judaica***	***S. soleirolii***	***P. officinalis***	***P. debilis***	***P. pensylvanica***	***P. mauritanica***	***P. alsinifolia***	***P. lusitanica***
Distinct wood cylinder	Present	Present	present	Present	present	present	present	present	present	present	present	present
Growth rings	Absent	Absent	absent	Absent	absent	Absent	absent	absent	absent	absent	absent	absent
Porosity	wood diffuse-porous	wood diffuse-porous	wood diffuse-porous	wood diffuse-porous	wood diffuse-porous	–	–	–	–	–	–	–
Vessel arrangement	vessels mainly solitary, sometimes in short radial multiples	solitary and in radial multiples and irregular clusters	vessels mainly solitary, sometimes in short radial multiples	vessels mainly solitary, sometimes in short radial or tangential multiples	vessels mainly solitary, sometimes in short radial multiples	–	–	–	–	–	–	–
Perforation plates	Simple	Simple	simple	Simple	simple	–	–	–	–	–	–	–
Intervessel pit arrangement	alternate or scalariform	alternate or scalariform	alternate or scalariform	alternate or scalariform	alternate or scalariform	–	–	–	–	–	–	–
Intervessel pit size [µm]	5 (3–7)	6–12	4 (3–8)	5 (2–8)	3 (2–8)	–	–	–	–	–	–	–
Vessel diameter [tangential; µm]	37 (18–68)	45–70 (25–95)	23 (8–39)	25 (15–39)	27 (16–45)	–	–	–	–	–	–	–
Vessels per mm2	86 (16–176)	20–70	71 (0–240)	163 (112–224)	71 (0–192)	–	–	–	–	–	–	–
Mean vessel element length [µm]	204 (130–276)	195–275 (130–370)	124 (54–207)	100 (64–131)	135 (92–219)	169 (98–228)	–	–	–	–	–	–
Ground tissue fibers	libriform fibers, pits in mainly in radial walls	fibers with with simple pits in the radial and tangential walls	libriform fibers	libriform fibers	libriform fibers	–	–	–	–	–	–	–
Fiber wall thickness	very thin	very thin	very thin	ranging from very thin to thin walled	very thin	–	–	–	–	–	–	–
Mean fiber length [µm]	388 (193–388)	425–575 (265–755)	238 (138–307)	154 (85–235)	231(169–275)	–	–	–	–	–	–	–
Axial parenchyma	scanty paratracheal	paratracheal, vasicentric	scanty paratracheal	scanty paratracheal	scanty paratracheal	–	–	–	–	–	–	–
Ray width	1–2 cells	3–5 (8) cells	1–2 (3) cells	not observed	not observed	–	–	–	–	–	–	–

Ray height [µm]	195 (58–390)	600–1940 (420–2850)	221 (106–407)	not observed	not observed	–	–	–	–	–	–	–
Rays: cellular composition	mainly square to upright cells	mainly square to upright cells	mainly square to upright	not observed	not observed	not observed						
Thickness double wood cylinder [mm]	1.53	Na	1.31	0.91	0.75	0.12	0.25	0.37	0.52	0.57	0.27	0.44
Average stem diameter [mm]	3.67	Na	2.67	2.05	1.54	0.58	3.94	1.49	1.88	2.68	1.23	2.14
Ratio double wood cylinder/average stem diameter	0.42	Na	0.49	0.44	0.49	0.21	0.06	0.25	0.28	0.21	0.21	0.21
upper stem	–	–	short continuous wood cylinder (ca. 6 layers)	very narrow wood cylinder (2–3 layers)	interfascicular cambium present, no wood cylinder	start formation interfascicular cambium, no wood cylinder	start formation interfascicular cambium, no wood cylinder	short continuous wood cylinder (~3 layers)	information about interfascicular cambium not available, no wood cylinder	start of wood cylinder formation	information about interfascicular cambium not available, no wood cylinder	start of wood cylinder formation

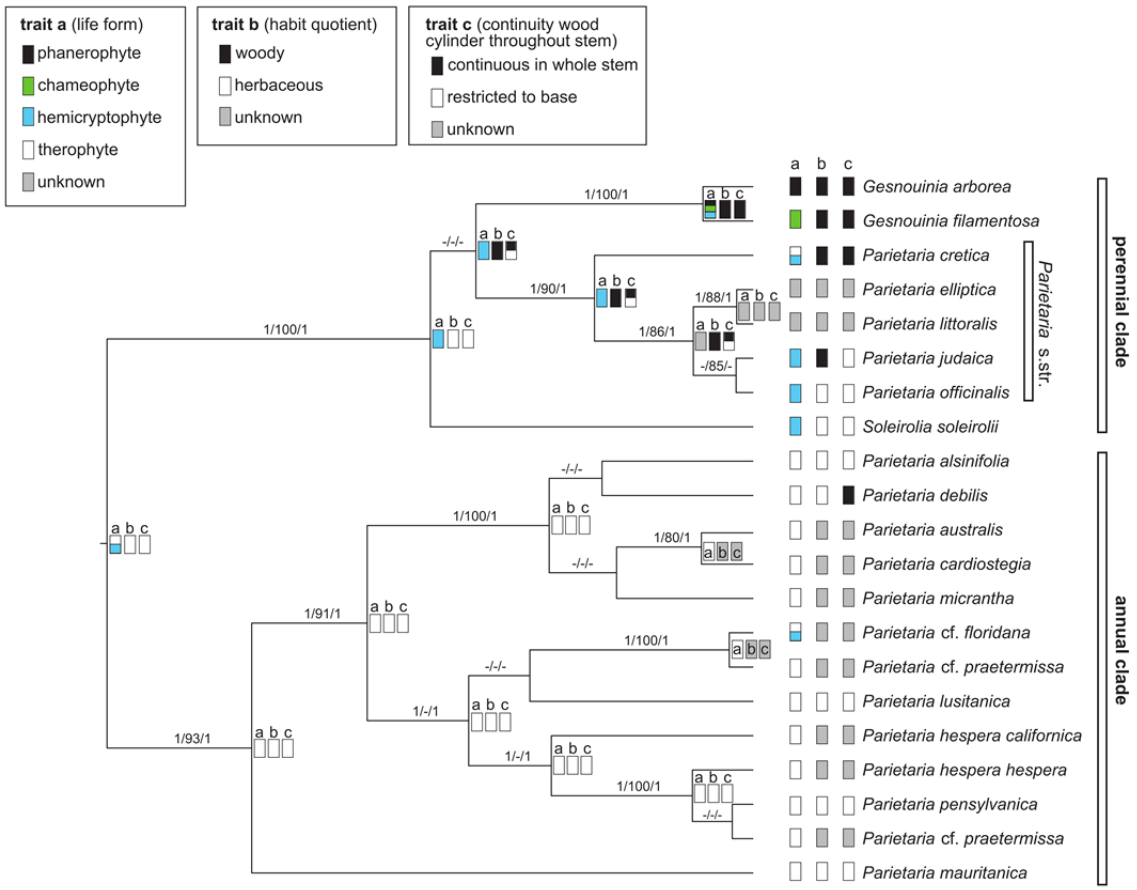

Figure 37. Evolution of woody traits (life-form, habit quotient, continuity of wood cylinder throughout the stem) in Parietarieae, based on the plastid chronogram. For the life-form, the outcome of the maximum likelihood reconstruction in Mesquite is shown at the nodes; for habit quotient and continuity of wood cylinder, the results from maximum parsimony reconstruction are given. Numbers above branches indicate (from left to right) posterior probabilities from MrBayes analysis, bootstrap values from RAxML analysis and posterior probabilities from BEAST analysis. Only posterior probabilities ≥0.90 and bootstrap values ≥80 are shown.

4.1.7. Discussion

Parietaria is recognized as a paraphyletic group when considering *Gesnouinia* and *Soleirolia* as distinct genera (Fig. 35, Appendix Fig. S60). Consequently, these two genera should either be included in *Parietaria* or parts of *Parietaria* should be attributed to a different genus. In this study, *Soleirolia* and *Gesnouinia* are treated as separate genera since morphological differences warrant a generic treatment. *Parietaria officinalis* L., the type of the genus *Parietaria* L., is nested within *Parietaria* s.str. in our phylogeny (Fig. 35, Appendix Fig. S60). Thus, the annual clade of *Parietaria* should probably be attributed to a different genus, which is, however, not implemented here.

Biogeographical patterns in Macaronesian *Gesnouinia* and the Tertiary relict hypothesis

The occurrence of *Gesnouinia* on Macaronesia is very likely the result of long-distance dispersal as the Canary Islands were formed by a volcanic hotspot system and have never been connected to the main land (Fernández-Palacios et al., 2011). This raises the question whether *Gesnouinia* is a Tertiary relict.

According to Kondraskov, Schütz, et al. (2015), taxa should meet the following criteria to be considered Tertiary laurel forest relicts: (1) Their stem age should fall into the Tertiary,

i.e., the timespan of Paleocene to Pliocene (66.0–2.6 mya), (2) their biogeographic origin should be Europe or the Mediterranean and (3) the MRCA of the taxon and its sister group should have occurred in a laurel forest habitat.

Two taxonomic levels need to be considered regarding this problem. The Macaronesian endemic genus *Gesnouinia* may be a Tertiary laurel forest relict or only the laurel forest species *G. arborea*. For *Gesnouinia* the first two relict criteria are clearly fulfilled. For its temporal and spatial origin, the Mediterranean region (BBM) or the Mediterranean and Macaronesia (S-DEC) during the Late Miocene (8.4 mya, 95% HPD 14.5–3.8 mya; Fig. 35) were inferred. This emphasizes the close links between the Mediterranean and Macaronesian flora as indicated previously by, e.g., Hooker (1867), Engler (1879), Schenck & Schimper (1907) and Sunding (1979). It also shows that *Gesnouinia* evolved after the formation of the oldest of the extant Canary Islands ca. 21 mya (Fernández-Palacios et al., 2011). The third criterion, however, may not be fulfilled because the genus likely did not originally inhabit laurel forests. Only *G. arborea* occurs in laurel forests. Whether this is also its ancestral habitat is doubtful (see below). *Gesnouinia filamentosa* is found in the drier infra-canarian zone as a rupicolous taxon growing in shady cliffs. The sister group of the genus *Gesnouinia*, *Parietaria* s.str., is also not associated with laurel forest and tends to occur in a range of habitats from relatively humid and shady forest margins to open and relatively dry ruderal places in the Mediterranean and Eurasia. Nevertheless, the occurrence of a sister group in a laurel forest habitat may be not an ideal relict criterion. Although laurel forest is still found in, e.g., China and the Himalaya, this vegetation type is largely extinct in Eurasia by now. Surviving species of a previously laurel-forest-associated lineage are likely to have undergone a change in habitat preference. In the case of *Gesnouinia,* this scenario is rather unlikely, as the evolutionary path usually goes in the direction from generalists, e.g., *Parietaria* s.str., to specialists, e.g., the laurel forest species *G. arborea*.

Gesnouinia arborea itself is most likely not a Tertiary relict from European laurel forests by age and geographic origin. Biogeographical analyses indicate that it split from the more xeric and lower altitude occupying *G. filamentosa* within Macaronesia (BBM, S-DEC) around the Early Pleistocene (1.5 mya, 95% HPD 3.7–0.1 mya; Figs. 35, 36A). A Macaronesian origin has also been found for other laurel forest taxa, e.g., *Bystropogon* sect. *Canariense* La Serna, *Picconia excelsa*, the *Aichryson pachycaulon* Bolle group, *Aeonium cuneatum* Webb & Berthel. as well as those of *Pericallis* and *Crambe* sect. *Dendrocrambe* DC. (Jones et al., 2014; Kondraskov, Schütz, et al., 2015). Of these, the *Aichryson pachycaulon* group, *Aeonium cuneatum* and some laurel forest species of *Pericallis* are also of Pleistocene age. Proposed triggers of Pleistocene speciation events within Macaronesia are range shifts during the climate changes associated with Pleistocene glacials and interglacials (Steinbauer et al., 2016).

In the case of *G. arborea*, at least three range shift scenarios are possible. In the first, the MRCA of *G. arborea* and *G. filamentosa* occurred in laurel forest and secondarily colonized lower-elevation habitats during a cooling phase, leading to separation of more dry- and of more wet-adapted populations during the following warming phase. The second is reverse to the first, with wet habitats being colonized from dry ones. In the third, intermediate-height habitats are the basis for colonization of the drier infra-canarian zone and the laurel forest. In

the second and the third cases, *G. arborea* cannot be interpreted as Tertiary laurel forest relict. The most likely scenario out of these three is not easy to determine as it is not clear which kind of habitat is ancestral for *Gesnouinia*. The close relatives from the perennial clade comprise rather wet-adapted taxa like *S. soleirolii* as well as the ecologically broader *Parietaria* s.str. However, habitat shift may have occurred in *Parietaria* s.str. after the decline of laurel forests in Eurasia. Furthermore, different patterns of habitat shifts have been indicated for other Macaronesian laurel forest taxa. Colonization from dry habitats to the laurel forest has been indicated for *Crambe* sect. *Dendrocrambe* (Francisco-Ortega et al., 2002). The laurel forest habitat of *Aeonium cuneatum*, *Bystropogon* sect. *Canariense* and the lineage comprising *Pericallis lanata* (L'Hér.) B.Nord., *P. appendiculata* (L.f.) B.Nord. and *Pericallis aurita* (L'Hér.) B.Nord. may also be secondary. Most of them occur along paths in rather open conditions and their closest relatives occur outside the laurel forest, indicating that these species are pioneer species that may have evolved from lower open habitats into the laurel forest (Jones et al., 2014; Kondraskov, Schütz, et al., 2015). The reverse, a shift from the laurel forest to a dry habitat, is reported for *Pericallis lanata* (Jones et al., 2014). *Gesnouinia arborea* often grows in rather open areas, e.g., paths, of the laurel forest. This may be an argument that it joins the mentioned examples (*Aeonium cuneatum*, *Bystropogon* sect. *Canariense* and the lineage comprising *Pericallis lanata*, *P. appendiculata* and *Pericallis aurita*) for a secondary colonization of the laurel forest. The diversification within *Gesnouinia* overlaps with the Pleistocene glaciations cycles. They may have acted as triggers for the speciation. However, an alternative scenario where the MRCA of *G. filamentosa* and *G. arborea* evolved gradually without any trigger for speciation from higher-altitude populations (level of thermophilous woodlands) into the laurel forest habitat cannot be ruled out.

Divergence between the populations of *G. arborea* on the islands of Gran Canaria, Tenerife, La Gomera, La Palma and El Hierro seems not to have occurred immediately after speciation and to be quite recent. The crown node of the species is dated to the Middle Pleistocene (0.3 mya, 95% HPD 0.6–0.0 mya; Fig. 36B) and may be putatively linked with the Pleistocene climate fluctuations which might have pushed the species through bottlenecks. Pleistocene inter-island dispersal has also been indicated for the laurel forest taxon *Canarina canariensis* with Tenerife as a starting point for an East-West pattern of differentiation (Mairal, Sanmartín, et al., 2015). Another biogeographic pattern of Pleistocene or even younger inter-island differentiation has been indicated for *Laurus novocanariensis* Rivas Mart. & al., where distinct gene pools were indicated (a) for Central Tenerife, (b) for Tenerife, part of La Palma and Gran Canaria and (c) for El Hierro, La Gomera, part of La Palma and Gran Canaria (Betzin et al., 2016). In contrast to those species, the biogeographical inter-island dispersal patterns for *G. arborea* were unresolved in this study.

Derived woodiness in Macaronesian *Gesnouinia*

A feature traditionally often associated with a relict status is (ancestral) woodiness. Yet, woodiness may also be non-relictual and derived, i.e., it evolved from herbaceous ancestors. If the evolution of derived woodiness within a lineage occurs on an island, this lineage is considered to be insular woody. *Gesnouinia* is proposed as such an insular woody lineage by

Carlquist (1974). In contrast to that, Lens et al. (2013) suggest it is possibly ancestrally woody instead.

Anatomical features of derived woodiness are found in both *G. arborea* and *G. filamentosa*. They possess wood with mainly square to upright ray cells at the basis of the stem, very thin-walled libriform fibers, transitions to scalariform intervessel pits and simple perforation plates (Table 37, Appendix Fig. S64A,B; Bonsen & ter Welle, 1984). The most indicative feature of those is the shape of the ray cells (Carlquist, 1974; Dulin & Kirchoff, 2010; Lens et al., 2013). In contrast to that, the presence of libriform fibers and simple perforation plates is likely not related to derived woodiness (Dulin & Kirchoff, 2010). Still, there are some pitfalls to interpret *Gesnouinia* as insular woody based on all of the recovered anatomical features. First of all, derived woodiness is not exclusive to insular woody taxa as it can also evolve in non-island species (Carlquist, 1974; Lens et al., 2013). In the closest relatives of *Gesnouinia* from the perennial clade, broad wood cylinders are present in *P. judaica* and *P. cretica* (cf. Appendix. Fig. S64C), but not in the remainder. The amount of wood in those two species is, however, smaller than the amount of wood in a tree or shrub. This indicates that *P. judaica* and *P. cretica* might exhibit intermediary life-forms between herbaceous and woody. No ray cells were found in the longitudinal sections of both species. Absence of rays is a characteristic of derived woodiness (Carlquist, 1974). However, the underlying study refrains from interpreting those species as derived woody based on the absence of those cells as ray cells or ray-like cells were observed in the transverse sections. Thus, they simply might have not been detected in the longitudinal sections due to, e.g., scarcity or obscurity. A second pitfall for the interpretation of the stem anatomy of *Gesnouinia* as derived woody is that woody intermediates like half shrubs, e.g., *G. filamentosa*, are difficult to interpret (Lens et al., 2013). The third and most important pitfall is that some ancestrally woody species have been shown to exhibit derived woody features like square to upright ray cells (Carlquist, 2009; Lens et al., 2013). Consequently, although the anatomical observations hint towards the presence of derived woodiness in *Gesnouinia* and probably also in at least some species of *Parietaria* s.str., derived woodiness cannot be inferred from those characteristics alone.

The phylogeny needs also to be taken into account when evaluating the woodiness of a lineage. As Parietarieae are found in a clade containing both herbaceous and woody species with the ancestrally woody Cecropieae Gaudich. at its base, *Gesnouinia* is assumed to be possibly ancestrally, i.e., relictually woody by Lens et al. (2013). This contradicts with the ancestral character state estimation conducted for Urticaceae by Wu et al. (2015). Based on an incomplete sampling of Parietarieae (four species, *G. filamentosa* not included), they found the MRCA of Parietarieae to be herbaceous and a shift from herbaceousness to woodiness in *Gesnouinia*. An herbaceous MRCA of Parietarieae is also suggested by the underlying study's ancestral character state reconstructions based on three indicators of woodiness, i.e., perennation strategy (Dulin & Kirchoff, 2010), habit quotient (Lens & al., 2012) and continuity of wood cylinder throughout the stem (Kidner et al., 2015; Lens et al., 2013). The MRCA of Parietarieae is reconstructed as hemicryptophyte or therophyte with no or narrow wood cylinder that, if present, was limited to the lower part of the stem (Fig. 37). The nodes indicated for shifts towards woodiness vary between the analyzed indicators. The

shift towards broad wood cylinders in the stem bases is estimated for the MRCA of *Gesnouinia* and *Parietaria* s.str. around the Miocene (Figs. 35, 37). Continuous distinct wood cylinders extending into the upper part of the stem evolved either at the same point or in *Gesnouinia* around the Pleistocene at the latest (Fig. 35, 37). This character, however, should probably be interpreted with caution as the comparability of wood samples from the upper third of the stem, used to code this character, might not be truly warranted between the species. Concerning the perennation strategy, chameophytes and phanerophytes likely evolved once within *Gesnouinia* on the Canary Islands around the Pleistocene, probably from continental hemicryptophytes (Figs. 35, 37). Accordingly, all analyzed indicators of woodiness suggest that woodiness in *Gesnouinia* is not ancestral and relictual but derived instead. Whether derived woodiness in *Gesnouinia* evolved on an island cannot be inferred from the underlying data. The evolution of broad wood cylinders in the stem basis is likely not solely related to an island habitat. BBM suggests the Mediterranean (Figs. 35, 37), S-DEC Macaronesia and the Mediterranean as locality for the respective shift. In contrast to that, the change in perennation strategy is clearly linked with the Macaronesian islands in our analyses (Figs. 35, 37). In conclusion, the derived woodiness of *Gesnouinia* may be the result of graduated evolutionary processes and exemplifies that the transition from herbaceousness to woodiness may be rather continuous than abrupt. Further hints towards the presence of derived woodiness in *G. arborea* come from many other species occupying open areas of the Macaronesian laurel forest. For example, *Bencomia caudata* (Aiton) Webb & Berthel., *Echium pininana* Webb & Berthel., *Isoplexis sceptrum* (L.f.) Steud., *Marcetella moquiniana* (Webb & Berthel.) Svent., *Musschia wollastonii* Lowe and *Sonchus fruticosus* L.f. are woody species within clades with herbaceous ancestors. As pioneers, they colonize open areas of the laurel forest after a collapse of the canopy caused by catastrophic events and are locally outcompeted when the gaps close (Capelo, Sequeira, Jardim, & Mesquita, 2007; Fernández-Palacios et al., 2017). Although ancestral character state analyses reconstructed the MRCA of Parietarieae as herbaceous, there is also evidence for ancestral woodiness in the tribe. Urticaceae are sister to Moraceae which comprise mainly ancestrally woody taxa (Sytsma et al., 2002). Thus, Urticaceae are likely ancestrally woody. This contrasts (Wu et al., 2015) who reconstructed Urticaceae as herbaceous. However, this conflict may be caused by the outgroups used in their study (one herbaceous species from Moraceae and two species from Cannabaceae) and poor sampling of the early diverging lineages. Lens et al. (2013) regarded Parietarieae as an early diverging clade within Urticaceae and closely related to presumably ancestrally woody clades (e.g., Boehmerieae (Gaud.) Wedd., Cecropieae). Consequently, Parietarieae could be interpreted as ancestrally woody with several shifts towards herbaceousness. Yet, the putative sister of Parietarieae is Forsskaoleae (Wu et al., 2013), a tribe regarded as predominantly herbaceous, e.g., by Friis (1993). In addition to the nested position of *Gesnouinia* in an otherwise herbaceous tribe, this may favor a shift from herbaceousness towards woodiness as more parsimonious and seems to be more likely than multiple shifts from woodiness to herbaceousness within Parietarieae. However, for more conclusive evidence, e.g., a detailed anatomical and phylogenetic study of Forsskaoleae would be needed.

5. Conclusions

Model taxa

The Macaronesian laurel forest is traditionally considered to be a Tertiary relict (Engler, 1879; Mai, 1989), whereas Kondraskov, Schütz, et al. (2015) found a rather heterogeneous origin of eighteen characteristic laurel forest taxa. In this thesis, further hints towards a heterogeneous origin of this vegetation type are recovered. Four of the six analyzed laurel forest taxa/lineages, *Visnea*, *Geranium*, *Semele*, *Daucus*, are potential relicts by their stem ages and geographic origin. Using the crown age as criterion (see García-Verdugo et al., 2019), only *Geranium* may be seen as relictual. Still, the crown age is likely not optimal for evaluating the relict status of a lineage, as it does not consider e.g. extinction. This is exemplified by *Visnea*, which is a relict according to the fossil record, whereas the crown age estimate suggests the opposite. The laurel forest species of *Phyllis* and *Gesnouinia* contradict a relict origin by stem age and/or geographic affinity and likely do not exhibit primary woodiness, a trait often associated with relicts. Instead, secondary woodiness is indicated. Whether the shift towards woodiness is linked to islands in this case, however, cannot be inferred here.

Molecular dating conducted analogously for the six species/lineages indicates two waves of colonization to the islands of Macaronesia: 1) the Oligocene (e.g. *Visnea*) and 2) the Late Miocene (*Geranium*, *Semele*, *Daucus*, *Phyllis*, and *Gesnouinia*). The first has not been reported by previous studies, the latter was also recovered in e.g. *Canarina*, *Hedera* L., *Ixanthus*, *Arbutus* L. and *Prunus* (Kondraskov, Schütz, et al., 2015; Mairal, Pokorny, et al., 2015; Valcárcel et al., 2017). Yet, it is possible that the time of colonization in *Visnea*, *Daucus* and *Semele* may be younger. While the ancestors of laurel forest *Visnea*, *Daucus*, *Semele* and *Geranium* likely directly colonized the Macaronesian laurel forest from the mainland, laurel forest *Gesnouinia* and *Phyllis* have sister species in the drier infra-canarian zone. The ancestral Macaronesian habitat cannot be unambiguously identified in both cases, although there are hints towards dispersal from the drier infra-canarian zone to the laurel forest in *Gesnouinia* and for dispersal in the opposite direction in *Phyllis*. Different processes for the spread between the vegetation zones in *Gesnouinia* and *Phyllis* are also supported by the different windows of time estimated, i.e. the Early Pliocene in *Phyllis* and the Early Pleistocene in the case of *Gesnouinia*.

The inter-archipelago patterns between the Canary Islands and Madeira largely agree with the ones recovered for the whole Macaronesian flora. Predominantly, colonization of Madeira from the Canary Islands during the Plio-/Pleistocene is found and may have been facilitated by reduced distances between islands linked with the glaciation cycles, e.g. Kim et al. (2008). Exceptions to this may be *Daucus* and *Geranium*. In *Daucus*, the Canary Islands and Madeira might each have been colonized in an individual event with the mainland acting as source region, as already proposed by Spalik & Downie (2007). In *Geranium*, the opposite of the usual inter-archipelago pattern is indicated and the Canary Islands might have been colonized from Madeira. Still, alternative scenarios, e.g. involving back-colonization to the mainland, cannot be excluded. Consequently, the laurel forest is likely no endpoint of colonization. In *Geranium robertianum* and *G. purpureum*, the continent was back-colonized

at the latest within the *Geranium* lineage. Back-colonization may overlap with the Pleistocene glaciation cycles that provided periods of time with reduced distances between Macaronesia and mainland.

Dispersal patterns within the archipelagos are of recent nature and poorly resolved. They may be subject to further studies, using more variable marker systems or genomic data.

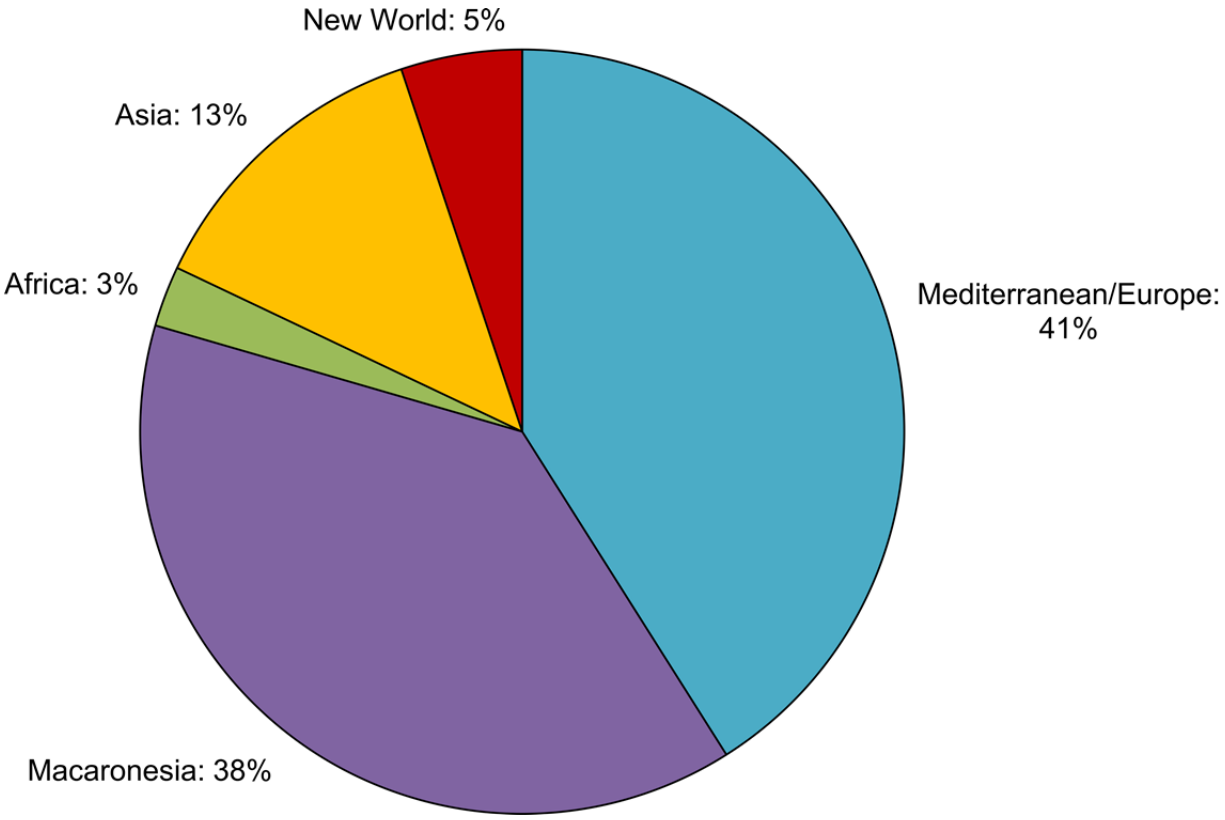

Figure 38. Biogeographic affinity of Macaronesian laurel forest as inferred from 36 species/lineages. Geographic origins were either inferred in the underlying thesis or obtained from literature (Appendix Table S11), i.e. Barber et al. (2007), Carine et al. (2004), Cubas et al. (2010), Francisco-Ortega, Jansen, & Santos-Guerra (1996), Jones et al. (2014), Kim et al. (2008), Kondraskov, Schütz, et al. (2015), Mairal, Pokorny, et al. (2015), Percy et al. (2004), Särkinen, Bohs, Olmstead, & Knapp (2013), Valcárcel et al. (2017) and Williams et al. (2015).

Implications for the Macaronesian laurel forest

For the Macaronesian laurel forest as a whole, a continuous influx of taxa during the Late Miocene to the Middle Pleistocene is indicated (Fig. 38), with *Visnea* being the only species of potential Oligocene origin. While the climate was likely relatively stable and humid from the Oligocene to the Early Pliocene, afterwards several climate changes took place within Macaronesia (Table 38). In the humid climate of the Oligocene to Early Pliocene, 49% of taxa arrived. The climatic deteriorations of the Late Pliocene and Pleistocene have been previously suggested as drivers of extinction within the laurel forest, providing colonization opportunities for external species. Accordingly, 21% of taxa colonized the Macaronesian laurel forest during the Late Pliocene change towards a colder, more arid and increasingly seasonal climate. 30% of taxa established during the climate fluctuations of the Pleistocene glaciation cycles. As regards the life-form and ecological preference of the colonizers, no obvious time windows are indicated. No specific time frames for the colonization of the herb, shrub and tree layer of the laurel forest are visible, despite a gap in colonization of the herb

layer during the Late Pliocene (Appendix Table S 11). This, however, might be associated with sampling bias, as e.g. woody taxa were previously preferred for analysis, and may change with an increasing numbers of taxa studied. Likewise, for the habitats occupied within the laurel forest (lower dry zone, open, closed canopy, Fayal Brezal), a gap of laurel forest colonization is only recovered for the Fayal Brezal during the Early Pliocene and for the thermophilous lower edge in the Late Pliocene. Still, the extant ecological niches recovered in the laurel forest may not reflect the previous ones, as the ancient laurel forests likely were more humid than the ones of the present day, see e.g. Nogue, de Nascimento, Fernández-Palacios, Whittaker, & Willis (2013).

Based on geographical origin, the largest proportion of Macaronesian laurel forest taxa, i.e. 41%, is descendant from Mediterranean/European ancestors (Fig. 38, Appendix Table S11). 56% of those Mediterranean/European taxa dispersed likely habitat conservatively during the Oligocene, Late Miocene or Early Pliocene, when the Macaronesian climate was humid and laurel forests were still widely distributed in Europe. Oligocene colonization is very rare (only recovered for *Visnea*) and may have occurred to the Paleo-Macaronesian islands. In contrast to that, establishment during the Late Miocene is common, with the colonizers likely benefiting from new habitat opening up during the Early to Late Miocene emergence of the oldest extant Canary Islands. Furthermore, landslides and collapses during the Late Miocene, e.g. Acosta et al., (2005), Ancochea, Hernán, Huertas, Brändle, & Herrera (2006), Cantagrel, Arnaud, Ancochea, Fúster, & Huertas (1999), Emerson (2003) and Stillman (1999), likely aided new species to establish. Although catastrophic events also took place in the Early Pliocene, e.g. Ancochea et al. (2006), Emerson (2003) and Walter et al. (2005), and the emergence of Madeira dates to this time, colonization of the Macaronesian laurel forest by taxa with Mediterranean/European affinity is very rare. Dispersal during the Late Pliocene and Early Pleistocene is found for 44% of the taxa of Mediterranean/European origin. During this time, the Mediterranean/European laurel forest was reduced to a few patches or extinct. Thus, dispersal into the Macaronesian laurel forest likely occurred from non-laurel forest communities, i.e. non-habitat conservatively. Compared to the Early Pliocene, the number of colonizers from the Mediterranean increased during the climate changes of the Late Pliocene. This could be related to the postulated extinction of the more tropical Macaronesian laurel forest species (see above). Furthermore, the emergence of La Palma as well as the onset of the trade winds and the Canarian current might have facilitated dispersal. Late Pliocene catastrophic events have been reported from e.g. Gran Canaria (Emerson, 2003), but probably played a minor role. The amount of colonizers from the Mediterranean/Europe to the Macaronesian laurel forest slightly decreased during the Early Pleistocene, although the distance to mainland decreased during the glaciation cycles. Moreover, new ecological opportunities might have opened during the climate fluctuations of the glaciation cycles, the emergence of El Hierro or due to Pleistocene landslides or volcanism, e.g. Cantagrel et al. (1999), Dóniz et al. (2008) and Krastel et al. (2001).

The second largest proportion of Macaronesian laurel forest taxa, i.e. 38%, continuously colonized the Macaronesian laurel forest from other Macaronesian habitats during the Late Miocene to the Middle Pleistocene (Fig. 38, Appendix Table S11). Almost half of these intra-

Macaronesian colonizations (42%) are linked to the humid climate, island emergence and catastrophic events of the Late Miocene to the Early Pliocene, with Late Miocene patterns being slightly less frequent than Early Pliocene ones. In absence of climatic speciation triggers, the emergence of new habitat in form of the extant Canary Islands and Madeira and catastrophic events (as mentioned above) may have played a major role. More than half of the intra-Macaronesian laurel forest colonizations (58%) overlap with the Late Pliocene to Middle Pleistocene climate changes, whereas Late Pliocene colonization is very rare. For the remaining considerable amount of species (50% of all the intra-Macaronesian colonizations into the laurel forest), the climatic oscillations of the Pleistocene and the range shifts associated with the glaciation cycles may have played an important role for dispersal into a different vegetation type.

The lowest proportions of Macaronesian laurel forest taxa constitute such with affinity to more distant areas, i.e. Asia (13%), the New World (5%) and Africa (3%; Fig. 38, Appendix Table S 11). Their arrival and establishment mainly overlaps with the Late Mio-/Early Pliocene emergence of the oldest extant Canaries and of Madeira, as well as catastrophic events within Macaronesia. Furthermore, some fall into the timeframe of the Late Pliocene climate deterioration and the emergence of La Palma. The taxa of Asian affinity dispersed to the Macaronesian laurel forest during the Late Miocene (40%), the Early (40%) and the Late Pliocene (20%). The Late Miocene is associated with the breaking up of the laurophyllous belt connecting Europe and Asia. Taxa postdating this may have maintained their European-Asian distribution and become extinct in Europe later on. Alternatively, they may have reached Macaronesia by stepping stone dispersal from Asia to Europe. During the Late Pliocene, when laurel forest was already very scarce in Europe, taxa may have either been derived from one of the habitat patches or have reached Macaronesia by LDD from Asia.

Colonizers from the New World reached the Macaronesian laurel forest during the Late Miocene (50%) and the Late Pliocene (50%). They may have dispersed via Asia, as the North Atlantic and Beringian land bridges connected America and Asia several times, e.g. during the Paleocene/Eocene, Late Miocene and Pleistocene glaciation cycles (Denk, Grímsson, & Zetter, 2010; Elias, Short, Nelson, & Birks, 1996; Viruel et al., 2016).

Dispersal from (Eastern) Africa into the Macaronesian laurel forest is relatively rare and has been only recovered for *Canarina* until now. It occurred during the humid Late Miocene and may be explained by climatic vicariance, i.e. formation of the Sahara desert (Mairal, Pokorny, et al., 2015).

In consequence, the species composition of the Macaronesian laurel forest likely changed several times from at least the Late Miocene to the Mid-Pleistocene. In the humid climate of the Late Miocene, habitat conservative dispersal from the Mediterranean/Europe to newly emerged islands and habitat space created by catastrophic events likely played an important role. Intra-Macaronesian colonization of the laurel forest was also present, but to a lower extent. In contrast to that, almost all new colonizers arrived from within Macaronesia in the still humid Early Pliocene. During this time, new habitat became available as Madeira emerged and catastrophic events occurred. The Late Pliocene climatic deterioration mainly favored the establishment of incoming Mediterranean taxa, which may have dispersed non-habitat conservatively and thus were probably rather euryoecious. Alternatively, they may

Table 38. Climatic history of the Canary Islands.

Time	Climate	Source
Late Oligocene and Mio-/Pliocene (25-5 mya)	Tropical	Fernández-Palacios et al. (2011) and references therein
Mio-/Pliocene transition	Tropical or subtropical	Betancort, Lomoschitz, & Meco (2014)
Early Pliocene	Tropical to equatorial	Betancort, Lomoschitz, & Meco (2016)
Early Pliocene	Lanzarote warm and dry	Lécuyer et al. (2020)
Early-Late Pliocene (4.2-2.9 mya)	Onset Canarian current and trade winds	Meco, Koppers, Miggins, Lomoschitz, & Betancort (2015)
Late Pliocene	Shift from tropical to a more arid, Mediterranean type climate (humid periods interspersed), onset Canarian current	Fernández-Palacios et al. (2011) and references therein
Late Pliocene (3.0-2.8 mya)	Strong seasonality	Meco et al. (2015)
Late Pliocene	Cooling	Meco et al. (2011)
Plio-/Pleistocene (3-2 mya)	Deterioration leads to extinction in laurel forest taxa	Fernández-Palacios et al. (2011) and references therein
Plio/Pleistocene, Early Pleistocene	Similar to extant	Meco et al. (2002)
Pleistocene	Cycles of 1) glacial, aridity 2) early inter-glacial, aridity with humid periods 3) interglacial, humid and warm 4) transitional arid and temperate	Meco et al. (2011)
Middle Pleistocene (Interglacial, ca. 424-374 kya)	Similar to extant	Meco et al. (2002)
Middle Pleistocene (ca. 300 kya)	More humid than extant	Pannell, Gray, Zalasiewicz, Branney, & Curry (2011)
Late Pleistocene (Last interglacial, 125 kya)	Tropical	Fernández-Palacios et al. (2011) and references therein
Late Pleistocene (Last interglacial, 125 kya)	Warmer than extant	Meco et al. (2002)
Late Pleistocene to extant (50-0 kya)	Decline in humidty	Yanes et al. (2011)
Late Pleistocene (End of last glacial, 14-13 kya)	Humid	Fernández-Palacios et al. (2011) and references therein
Beginning Holocene (8 kya)	Humid	Fernández-Palacios et al. (2011) and references therein
Middle Holocene (5.5 kya)	Decrease in hygrophilous forest species	Nogue et al. (2013)

have colonized another Macaronesian habitat first (in which they are presently extinct) and subsequently evolved into the laurel forest. In the course of the Pleistocene (Early and Middle), mainly Macaronesian taxa arrived in the laurel forest, probably facilitated by range shifts associated with the glaciation cycles. A larger amount of taxa of Mediterranean/Eurasian origin also reached the islands during the Pleistocene, but is restricted to the Early Pleistocene. Their arrival may have been supported by the decreased distance between Macaronesia and the mainland during the glaciation cycles. Colonization events from Asia, the New World and (Eastern) Africa are rare and occurred prior to the Pleistocene. In these cases, dispersal was probably aided by the absence of e.g. climatic,

tectonic or marine barriers during certain periods of time. Although no colonization events have been recovered for more recent times in this study, the composition of the laurel forest likely was also subject to change subsequent to the Pleistocene. For example, the Middle Holocene extinction of hygrophilous taxa (Table 38) and the human settlement between 3 and 2 kya (thousand years ago) on the Canary Islands and ca. 600 years ago on the Azores and Madeira possibly had their share in shaping the plant community.

References

Acosta, J., Uchupi, E., Muñoz, A., Herranz, P., Palomo, C., Ballesteros, M., & Group, Z. W. (2005). Geologic evolution of the Canarian Islands of Lanzarote, Fuerteventura, Gran Canaria and La Gomera and comparison of landslides at these islands with those at Tenerife, La Palma and El Hierro. In *Geophysics of the Canary Islands* (pp. 1-40). Dordrecht: Springer.

Aedo, C. (2017). Taxonomic Revision of *Geranium* Sect. *Ruberta* and *Unguiculata* (Geraniaceae). *Annals of the Missouri Botanical Garden, 102*(3), 409-466.

Aedo, C., Barberá, P., & Buira, A. (2016). Taxonomic revision of *Geranium* sect. *Trilopha* (Geraniaceae). *Systematic Botany, 41*(2), 354-377.

Aedo, C., Muñoz Garmendia, F., & Pando, F. (1998). World checklist of *Geranium* L. (Geraniaceae). *Anales del Jardín Botánico de Madrid, 56*(2), 211-252.

Allan, G. J., Francisco-Ortega, J., Santos-Guerra, A., Boerner, E., & Zimmer, E. A. (2004). Molecular phylogenetic evidence for the geographic origin and classification of Canary Island *Lotus* (Fabaceae: Loteae). *Molecular Phylogenetics and Evolution, 32*(1), 123-138.

Ancochea, E., Hernán, F., Huertas, M., Brändle, J., & Herrera, R. (2006). A new chronostratigraphical and evolutionary model for La Gomera: implications for the overall evolution of the Canarian Archipelago. *Journal of volcanology and geothermal research, 157*(4), 271-293.

Anderson, C. L., Rova, J. H., & Andersson, L. (2001). Molecular phylogeny of the tribe Anthospermeae (Rubiaceae): systematic and biogeographic implications. *Australian Systematic Botany, 14*(2), 231-244.

Andrus, N., Trusty, J., Santos-Guerra, A., Jansen, R. K., & Francisco-Ortega, J. (2004). Using molecular phylogenies to test phytogeographical links between East/South Africa–Southern Arabia and the Macaronesian islands—a review, and the case of *Vierea* and *Pulicaria* section *Vieraeopsis* (Asteraceae). *Taxon, 53*(2), 333-347.

Arber, A. (1924). *Danae*, *Ruscus*, and *Semele*: a morphological study. *Annals of Botany, 38*(150), 229-260.

Arechavaleta, M., Pérez, N. Z., Gómez, M. M., & Esquivel, J. M. (2005). *Lista preliminar de especies silvestres de Cabo Verde. Hongos, Plantas y Animales Terrestres*. La Laguna: Consejería de Medio Ambiente y Ordenación Territorial, Gobierno de Canarias.

Arechavaleta, M., Rodríguez, S., Zurita, N., & García, A. (2010). *Lista de especies silvestres de Canarias. Hongos, plantas y animales terrestres*. *2009*. Santa Cruz de Tenerife: Gobierno de Canarias.

Banasiak, Ł., Piwczyński, M., Uliński, T., Downie, S. R., Watson, M. F., Shakya, B., & Spalik, K. (2013). Dispersal patterns in space and time: a case study of Apiaceae subfamily Apioideae. *Journal of Biogeography, 40*(7), 1324-1335.

Banasiak, Ł., Wojewódzka, A., Baczyski, J., Reduron, J.-P., Piwczyński, M., Kurzyna-Młynik, R., . . . Spalik, K. (2016). Phylogeny of Apiaceae subtribe Daucinae and the taxonomic delineation of its genera. *Taxon, 65*(3), 563-585.

Barber, J. C., Finch, C. C., Francisco-Ortega, J., Santos-Guerra, A., & Jansen, R. K. (2007). Hybridization in Macaronesian *Sideritis* (Lamiaceae): evidence from incongruence of multiple independent nuclear and chloroplast sequence datasets. *Taxon, 56*(1), 74-88.

Barry, A. R. (1977). Epidermis foliar y venación en *Gesnouinia arborea* (L. fil) Gaudich.(Urticaceae). *Botanica Macaronesica, 4*, 55-68.

Basilici, G., Martinetto, E., Pavia, G., & Violanti, D. (1997). Paleoenvironmental evolution in the Pliocene marine-coastal succession of Val Chiusella (Ivrea, NW Italy). *Bollettino della Società Paleontologica Italiana, 36*, 23-52.

Beaulieu, J. M., Tank, D. C., & Donoghue, M. J. (2013). A Southern Hemisphere origin for campanulid angiosperms, with traces of the break-up of Gondwana. *BMC Evolutionary Biology*, *13*(1), 80.

Donoghue, Michael J.Bertoldi, R., & Martinetto, E. (1995). Ricerche paleobotaniche (palinologiche e paleocarpologiche) sulla successione villafranchiana del Rio Ca'Viettone. *Il Quaternario, 8*, 403-422.

Betancort, J., Lomoschitz, A., & Meco, J. (2016). Early Pliocene fishes (Chondrichthyes, osteichthyes) from Gran Canaria and Fuerteventura (Canary Islands, Spain). *Estudios Geológicos, 72*(2), e054.

Betancort, J. F., Lomoschitz, A., & Meco, J. (2014). Mio-Pliocene crustaceans from the Canary Islands, Spain. *Rivista Italiana di paleontologia e Stratigrafia, 120*(3), 337-349.

Betzin, A., Thiv, M., & Koch, M. A. (2016). Diversity hotspots of the laurel forest on Tenerife, Canary Islands: a phylogeographic study of *Laurus* and *Ixanthus*. *Annals of Botany, 118*(3), 495-510.

Blattner, F. (1999). Direct amplification of the entire ITS region from poorly preserved plant material using recombinant PCR. *BioTechniques, 27*(6), 1180-1186.

Blattner, F. R. (2016). TOPO6: a nuclear single-copy gene for plant phylogenetic inference. *Plant systematics and evolution, 302*(2), 239-244.
Blöch, C., Weiss-Schneeweiss, H., Schneeweiss, G. M., Barfuss, M. H., Rebernig, C. A., Villaseñor, J. L., & Stuessy, T. F. (2009). Molecular phylogenetic analyses of nuclear and plastid DNA sequences support dysploid and polyploid chromosome number changes and reticulate evolution in the diversification of *Melampodium* (Millerieae, Asteraceae). *Molecular Phylogenetics and Evolution, 53*(1), 220-233.
Bobrov, E. G., Fedchenko, B. A., Grigor'ev, Y. S., Ivanova, N. A., Komarov, V. L., Krishtofovich, A. N., . . . Yarmolenko, A. V. (1970). *Flora of the USSR. - 5*. Jerusalem: Israel Program for Scientific Translations.
Boieiro, M., Carvalho, J. C., Cardoso, P., Aguiar, C. A., Rego, C., e Silva, I. d. F., . . . Borges, P. A. (2013). Spatial factors play a major role as determinants of endemic ground beetle beta diversity of Madeira Island Laurisilva. *PloS one, 8*(5), e64591.
Bonsen, K., & ter Welle, B. (1984). Systematic wood anatomy and affinities of the Urticaceae. *Mededelingen van het Botanisch Museum en Herbarium van de Rijksuniversiteit te Utrecht, 541*(1), 49-71.
Borges, P. A., Abreu, C., Aguiar, A. M. F., Carvalho, P., Jardim, R., Melo, I., . . . Vieira, P. (2008). *Listagem dos fungos, flora e fauna terrestres dos arquipélagos da Madeira e Selvagens: A list of the terrestrial fungi, flora and fauna of Madeira and Selvagens archipelagos*. Funchal: Direcçao regional do ambiente, Governo regional da Madeira.
Bouckaert, R. (2015). bModelTest: Bayesian site model selection for nucleotide data. *bioRxiv*, 020792.
Bouckaert, R. (2017, 18.5.2017). bModelTest Wiki - Trouble shooting. Retrieved 18th May, 2017 from https://github.com/BEAST2-Dev/bModelTest/wiki/Trouble-shooting
Bouckaert, R., Heled, J., Kühnert, D., Vaughan, T., Wu, C.-H., Xie, D., . . . Drummond, A. J. (2014). BEAST 2: a software platform for Bayesian evolutionary analysis. *PLoS Comput Biol, 10*(4), e1003537.
Boufford, D. E. (1997). Urticaceae. In Flora of North America Editorial Committee (Ed.), Flora of North America North of Mexico, Magnoliophyta: Magnoliidae and Hamamelidae (Vol. 3). New York and Oxford. Retrieved 15th Februar, 2019 from http://www.efloras.org/florataxon.aspx?flora_id=1&taxon_id=10931.
Bramwell, D., & Bramwell, Z. I. (1974). *Wild flowers of the Canary Islands*. London: Burford, Thornes.
Breitwieser, I., Brownsey, P.J., Heenan, P.B., Nelson, W.A., Wilton, A.D. (2010). Flora of New Zealand Online. Retrieved 2nd August, 2019 from www.nzflora.info
Bremer, B., & Eriksson, T. (2009). Time tree of Rubiaceae: phylogeny and dating the family, subfamilies, and tribes. *International Journal of Plant Sciences, 170*(6), 766-793.
Brummitt, R. K., Pando, F., Hollis, S., & Brummitt, N. (2001). *World geographical scheme for recording plant distributions*. Pittsburgh: Hunt Institute for Botanical Documentation, Carnegie Mellon University.
Cantagrel, J. M., Arnaud, N. O., Ancochea, E., Fúster, J. M., & Huertas, M. a. J. (1999). Repeated debris avalanches on Tenerife and genesis of Las Canadas caldera wall (Canary Islands). *Geology, 27*(8), 739-742.
Capelo, J., Menezes de Sequeira, M., Jardim, R., & Mesquita, S. (2007). Biologia e Ecologia das florestas das Ilhas–Madeira. In: J. Sande Silva (Ed.), *Açores e Madeira: A floresta das ilhas* (pp. 81-134). Lisbon: Público, Comunicaçao Social.
Capelo, J., Sequeira, M., Jardim, R., Mesquita, S., & Costa, J. C. (2005). The vegetation of Madeira Island (Portugal). A brief overview and excursion guide. *Quercetea, 7*, 95-122.
Carine, M. A. (2005). Spatio-temporal relationships of the Macaronesian endemic flora: a relictual series or window of opportunity? *Taxon, 54*(4), 895-903.
Carine, M. A., Russell, S. J., Santos-Guerra, A., & Francisco-Ortega, J. (2004). Relationships of the Macaronesian and Mediterranean floras: molecular evidence for multiple colonizations into Macaronesia and back-colonization of the continent in *Convolvulus* (Convolvulaceae). *American Journal of Botany, 91*(7), 1070-1085.
Carlquist, S. (1974). *Island biology*. New York & London: Columbia University Press.
Carlquist, S. (2001). *Comparative wood anatomy: systematic, ecological, and evolutionary aspects of dicotyledon wood.* Springer Series in Wood Science (2nd ed.). Berlin Heidelberg: Springer-Verlag.
Carlquist, S. (2009). Xylem heterochrony: an unappreciated key to angiosperm origin and diversifications. *Botanical Journal of the Linnean Society, 161*(1), 26-65.
Caujapé-Castells, J. (2004). Boomerangs of biodiversity?: the interchange of Biodiversity between mainland north Africa and the Canary islands as inferred from cpDNA RFLPs in genus *Androcymbium*. *Bot Macaronesica, 25*, 53-69.

Caujapé-Castells, J., García-Verdugo, C., Marrero-Rodríguez, Á., Fernández-Palacios, J. M., Crawford, D. J., & Mort, M. E. (2017). Island ontogenies, syngameons, and the origins and evolution of genetic diversity in the Canarian endemic flora. *Perspectives in Plant Ecology, Evolution and Systematics, 27*, 9-22.
Chandler, M. E. J. (1964). The Lower Tertiary Floras of Southern England. IV. A Summary and Survey of Findings in the Light of Recent botanical observations. *Botanical Observations*.
Chandler, M. E. J. (1925). The Upper Eocene Flora of Hordle, Hants. Part I. Pages 1–32; Plates I–IV. *Monographs of the Palaeontographical Society, 77*(360), 1-32.
Chandler, M. E. J. (1960). Plant remains of the Hengistbury and Barton Beds. *Bulletin of the British Museum (Natural History), 4*(6), 191-238.
Chandler, M. E. J. (1961). Flora of the Lower Headon beds of Hampshire and the Isle of Wight. *Bulletin of the Natural History Museum: Geology Series, 5*(5), 93-157.
Chandler, M. E. J. (1962). *The Lower Tertiary Floras of Southern England. II. Flora of the Pipe-Clay Series of Dorset (Lower Bagshot)*. London: Trustees of the British Museum.
Chandler, M. E. J. (1963). *The Lower Tertiary Floras of Southern England. III. Flora of the Bournemouth Beds, The Boscombe, and the Highcliff Sands*. London: Trustees of the British Museum.
Chen, S., Kim, D.-K., Chase, M. W., & Kim, J.-H. (2013). Networks in a large-scale phylogenetic analysis: reconstructing evolutionary history of Asparagales (Lilianae) based on four plastid genes. *PloS one, 8*(3), e59472.
Claudino-Sales, V. (2019). Laurisilva of Madeira, Portugal. In *Coastal World Heritage Sites* (pp. 243-249). Dordrecht: Springer.
Collinson, M. (1989). The fossil history of the Moraceae, Urticaceae (including Cecropiaceae), and Cannabaceae. In: P. R. Crane & S. Blackmore (Eds.), *Evolution, systematics, and fossil history of the Hamamelidae* (Vol. 2, pp. 319-339). Oxford: Oxford University Press.
Collinson, M. E., & Hooker, J. J. (2003). Paleogene vegetation of Eurasia: framework for mammalian faunas. *Deinsea, 10*(1), 41-84.
Collinson, M. E., Manchester, S. R., & Wilde, V. (2012). Fossil fruits and seeds of the Middle Eocene Messel biota, Germany. *Abhandlungen der Senckenberg Gesellschaft für Naturforschung, 570*, 1-249.
Corner, E. J. H., & Corner, E. J. H. (1976). *The seeds of dicotyledons* (Vol. 1): Cambridge University Press.
Cox, A. V., Bennett, M. D., & Dyer, T. A. (1992). Use of the polymerase chain reaction to detect spacer size heterogeneity in plant 5S-rRNA gene clusters and to locate such clusters in wheat (*Triticum aestivum* L.). *Theoretical and Applied Genetics, 83*(6), 684-690.
Cubas, P., Pardo, C., Tahiri, H., & Castroviejo, S. (2010). Phylogeny and evolutionary diversification of *Adenocarpus* DC.(Leguminosae). *Taxon, 59*(3), 720-732.
Darriba, D., Taboada, G. L., Doallo, R., & Posada, D. (2012). jModelTest 2: more models, new heuristics and parallel computing. *Nature methods, 9*(8), 772.
Denk, T., Grímsson, F., & Zetter, R. (2010). Episodic migration of oaks to Iceland: Evidence for a North Atlantic “land bridge” in the latest Miocene. *American Journal of Botany, 97*(2), 276-287.
Dias, E., Mendes, C., Melo, C., Pereira, D., & Elias, R. (2005). Azores central islands vegetation and flora field guide. *Quercetea, 7*, 123-173.
Díaz-Pérez, A., Sequeira, M., Santos-Guerra, A., & Catalán, P. (2012). Divergence and biogeography of the recently evolved Macaronesian red *Festuca* (Gramineae) species inferred from coalescence-based analyses. *Molecular Ecology, 21*(7), 1702-1726.
Dóniz, J., Romero, C., Coello, E., Guillén, C., Sánchez, N., García-Cacho, L., & García, A. (2008). Morphological and statistical characterisation of recent mafic volcanism on Tenerife (Canary Islands, Spain). *Journal of Volcanology and Geothermal Research, 173*(3-4), 185-195.
Drummond, A. J., & Bouckaert, R. R. (2015). *Bayesian evolutionary analysis with BEAST.* Cambridge: Cambridge University Press.
Dulin, M. W., & Kirchoff, B. K. (2010). Paedomorphosis, secondary woodiness, and insular woodiness in plants. *The Botanical Review, 76*(4), 405-490.
Edgar, R. C. (2004). MUSCLE: multiple sequence alignment with high accuracy and high throughput. *Nucleic acids research, 32*(5), 1792-1797.
Ehrig, F. R. (1998). Die Hauptvegetationseinheiten der Kanarischen Inseln im bioklimatischen Kontext. *Kieler Geographische Schriften, 97*, 67-115.
Elias, S. A., Short, S. K., Nelson, C. H., & Birks, H. H. (1996). Life and times of the Bering land bridge. *Nature, 382*(6586), 60-63.
Elliott, D. D., & Tamashiro, S. Y. (2009). Native Plants Hawai‘i. Retrieved 2nd August, 2019 from http://nativeplants.hawaii.edu/index/

Emerson, B. C. (2003). Genes, geology and biodiversity: faunal and floral diversity on the island of Gran Canaria. *Animal Biodiversity and Conservation, 26*(1), 9-20.
Engler, A. (1879). *Versuch einer Entwicklungsgeschichte der Pflanzenwelt: insbesondere der Florengebiete seit der Tertiärperiode*. Leipzig: W. Engelmann.
Ferguson, D. K., Pingen, M., Zetter, R., & Hofmann, C.-C. (1998). Advances in our knowledge of the Miocene plant assemblage from Kreuzau, Germany. *Review of Palaeobotany and Palynology, 101*(1-4), 147-177.
Fernandes, F., & Carvalho, J. A. (2014). An historical review and new taxa in the Madeiran endemic genus *Monizia* (Apiaceae, Apioideae). *Webbia, 69*(1), 13-37.
Fernández-Palacios, J., Arévalo, J., Balguerías, E., Barone, R., Delgado, J., De Nascimento, L., . . . Naranjo Cigala, A. (2017). La Laurisilva. *Canarias, Madeira y Azores.* Santa Cruz de Tenerife: Macaronesia Editorial.
Fernández-Palacios, J., & Whittaker, R. (2010). El ciclo de la isla. In: J. L. Martín-Esquivel (Ed.), *Atlas de la biodiversidad de Canarias* (pp. 18-27). Las Palmas de Gran Canaria: Gobierno de Canarias.
Fernández-Palacios, J. M., de Nascimento, L., Otto, R., Delgado, J. D., García-del-Rey, E., Arévalo, J. R., & Whittaker, R. J. (2011). A reconstruction of Palaeo-Macaronesia, with particular reference to the long-term biogeography of the Atlantic island laurel forests. *Journal of Biogeography, 38*(2), 226-246.
Fernández-Palacios, J. M., Rijsdijk, K. F., Norder, S. J., Otto, R., Nascimento, L., Fernández-Lugo, S., . . . Whittaker, R. J. (2015). Towards a glacial-sensitive model of island biogeography. *Global Ecology and Biogeography*, *25*(7), 817-830.
Ferrero, E., Merlino, B., Provera, A., & Martinetto, E. (2005). Associazione a molluschi marini e vegetali terrestri del Pliocene di Castellengo (Biella, Italia NW). *Rendiconti della Società Paleontologica Italiana, 2*, 87-106.
Fiz, O., Vargas, P., Alarcón, M., Aedo, C., García, J. L., & Aldasoro, J. J. (2008). Phylogeny and historical biogeography of Geraniaceae in relation to climate changes and pollination ecology. *Systematic Botany, 33*(2), 326-342.
Fjellheim, S., Jørgensen, M. H., Kjos, M., & Borgen, L. (2009). A molecular study of hybridization and homoploid hybrid speciation in *Argyranthemum* (Asteraceae) on Tenerife, the Canary Islands. *Botanical Journal of the Linnean Society, 159*(1), 19-31.
Francisco-Ortega, J., Fuertes-Aguilar, J., Kim, S.-C., Santos-Guerra, A., Crawford, D. J., & Jansen, R. K. (2002). Phylogeny of the Macaronesian endemic *Crambe* section *Dendrocrambe* (Brassicaceae) based on internal transcribed spacer sequences of nuclear ribosomal DNA. *American Journal of Botany, 89*(12), 1984-1990.
Francisco-Ortega, J., Jansen, R. K., & Santos-Guerra, A. (1996). Chloroplast DNA evidence of colonization, adaptive radiation, and hybridization in the evolution of the Macaronesian flora. *Proceedings of the National Academy of Sciences, 93*(9), 4085-4090.
Freitas, R., Romeiras, M., Silva, L., Cordeiro, R., Madeira, P., González, J. A., . . . Floeter, S. R. (2019). Restructuring of the 'Macaronesia'biogeographic unit: A marine multi-taxon biogeographical approach. *Scientific Reports, 9*(1), 1-18.
Friis, E. M. (1979). The Damgaard flora: a new Middle Miocene flora from Denmark. *Bulletin of the Geological Society of Denmark, 27*, 117-142.
Friis, E. M. (1985). *Angiosperm fruits and seeds from the Middle Miocene of Jutland (Denmark)*.
Friis, I. (1993). Urticaceae. In *Flowering Plants· Dicotyledons* (pp. 612-630): Springer.
García-Talavera, F. (1999). La Macaronesia: consideraciones geológicas, biogeográficas y paleoecológicas. In: J. M. Fernández-Palacios, J. J. Bacallado, & J. A. Belmonte (Eds.), *Ecología y cultura en Canarias* (pp. 39-64). La Laguna: Organismo Autónomo, Complejo Insular de Museos y Centros.
García-Verdugo, C., Caujapé-Castells, J., & Sanmartín, I. (2019). Colonization time on island settings: lessons from the Hawaiian and Canary Island floras. *Botanical Journal of the Linnean Society, 191*(2), 155-163.
Gavryushkina, A. (2015). Dating with FBD model tutorial. Retrieved 26th September, 2019 from http://beast2-dev.github.io/beast-docs/beast2/FBDDating/tutorial.html
Gavryushkina, A., Welch, D., Stadler, T., & Drummond, A. J. (2014). Bayesian inference of sampled ancestor trees for epidemiology and fossil calibration. *PLoS computational biology, 10*(12), e1003919.
Gebauer, R. (1994). Some taxa of *Parietaria* (Urticaceae) from tropical Africa. *Nordic journal of botany, 14*(5), 501-514.
Geissert, F., Gregor, H.-J., Mai, D. H., Boenigk, W., & Günther, T. (1990). Die Saugbaggerflora: eine Frucht-und Samenflora aus dem Grenzbereich Miozän-Pliozän von Sessenheim im Elsass (Frankreich). *Documenta naturae*, 57, 1-207.

Geldmacher, J., Hoernle, K., Bogaard, P., Duggen, S., & Werner, R. (2005). New 40 Ar/39 Ar age and geochemical data from seamounts in the Canary and Madeira volcanic provinces: Support for the mantle plume hypothesis. *Earth and Planetary Science Letters, 237*(1), 85-101.

Geldmacher, J., Hoernle, K., van den Bogaard, P., Zankl, G., & Garbe-Schönberg, D. (2001). Earlier history of the≥ 70-Ma-old Canary hotspot based on the temporal and geochemical evolution of the Selvagen Archipelago and neighboring seamounts in the eastern North Atlantic. *Journal of volcanology and geothermal research, 111*(1), 55-87.

Geldmacher, J., van den Bogaard, P., Hoernle, K., & Schmincke, H. U. (2000). The 40Ar/39Ar age dating of the Madeira Archipelago and hotspot track (eastern North Atlantic). *Geochemistry, Geophysics, Geosystems, 1*(2), 1008.

Givnish, T. J., Zuluaga, A., Spalink, D., Soto Gomez, M., Lam, V. K., Saarela, J. M., . . . Leebens-Mack, J. (2018). Monocot plastid phylogenomics, timeline, net rates of species diversification, the power of multi-gene analyses, and a functional model for the origin of monocots. *American Journal of Botany, 105*(11), 1888-1910.

Góis-Marques, C. A., Mitchell, R. L., de Nascimento, L., Fernández-Palacios, J. M., Madeira, J., & de Sequeira, M. M. (2019). *Eurya stigmosa* (Theaceae), a new and extinct record for the Calabrian stage of Madeira Island (Portugal): 40Ar/39Ar dating, palaeoecological and oceanic island palaeobiogeographical implications. *Quaternary Science Reviews, 206*, 129-140.

Góis-Marques, C. A., de Nascimento, L., Fernández-Palacios, J. M., Madeira, J., & Menezes de Sequeira, M. (2020). Tracing insular woodiness in giant *Daucus* (sl) fruit fossils from the Early Pleistocene of Madeira Island (Portugal). *Taxon*. doi:10.1002/tax.12175

Gravendeel, B., Chase, M. W., de Vogel, E. F., Roos, M. C., Mes, T. H., & Bachmann, K. (2001). Molecular phylogeny of *Coelogyne* (Epidendroideae; Orchidaceae) based on plastid RFLPs, matK, and nuclear ribosomal ITS sequences: evidence for polyphyly. *American Journal of Botany, 88*(10), 1915-1927.

Gregor, H.-J. (1978). Die miozänen Frucht-und Samen-Floren der Oberpfälzer Braunkohle. I. Funde aus den sandigen Zwischenmitteln. *Palaeontographica Abteilung B*, *167*, 8-103.

Gregor, H.-J. (1990). Contributions to the Late Neogene and Early Quaternary floral history of the Mediterranean. *Review of Palaeobotany and Palynology, 62*(3-4), 309-338.

Grehan, J. R. (2017). Biogeographic relationships between Macaronesia and the Americas. *Australian Systematic Botany, 29*(6), 447-472.

Gruenstaeudl, M., Santos-Guerra, A., & Jansen, R. K. (2013). Phylogenetic analyses of *Tolpis* Adans.(Asteraceae) reveal patterns of adaptive radiation, multiple colonization and interspecific hybridization. *Cladistics, 29*(4), 416-434.

Haas, M., Daxner-Höck, G., Decker, K., Kolcon, I., Kovar-Eder, J., Meller, B., & Sachsenhofer, R. (1998). Palaeoenvironmental Studies in the Early Miocene Lignite Opencast Mine Oberdorf (N Voitsberg, Styria, Austria). *Jahrbuch der Geologischen Bundesanstalt, 140*(4), 483-490.

Hastings, B. (1853). On the tertiary beds of Hordwell, Hampshire. *Philosophical Magazine and Journal of Science, Fourth Series, 6*(36), 1-11.

Hess, J., Kadereit, J., & Vargas, P. (2000). The colonization history of *Olea europaea* L. in Macaronesia based on internal transcribed spacer 1 (ITS-1) sequences, randomly amplified polymorphic DNAs (RAPD), and intersimple sequence repeats (ISSR). *Molecular Ecology, 9*(7), 857-868.

Hohenester, A., & Welss, W. (1993). *Exkursionsflora für die Kanarischen Inseln: mit Ausblicken auf ganz Makaronesien*. Stuttgart: Ulmer.

Hooker, J. (1867). On insular floras: a lecture. *Journal of Botany, 5*, 23-31.

Huang, Y., Jia, L., Wang, Q., Mosbrugger, V., Utescher, T., Su, T., & Zhou, Z. (2016). Cenozoic plant diversity of Yunnan: a review. *Plant Diversity, 38*(6), 271-282.

Huzioka, K., & Koga, T. (1981). The Middle Miocene Daijima-type floras in southwestern border of northeast Honshu, Japan. *Journal of Geography (Chigaku Zasshi), 90*(4), 235-246.

Huzioka, K., & Takahasi, E. (1970). The Eocene flora of Ube coal-field, southwest Honshu, Japan. *Journal of the Mining College, Akita University, Series A: Mining Geology, 4*, 1-88.

Ivanova, N. V., Fazekas, A. J., & Hebert, P. D. (2008). Semi-automated, membrane-based protocol for DNA isolation from plants. *Plant Molecular Biology Reporter, 26*(3), 186-198.

Jiarui, C., Qi, L., Friis, I., Wilmot-Dear, C. M., & Monro, A. K. (2003). Urticaceae. In W. Zhengyi, P. H. Raven, & H. Deyuan (Eds.), *Flora of China* (Vol. 5, pp. 76-189). Beijing & St. Louis: Science Press & Missouri Botanical Garden.

Jones, K. E., Reyes-Betancort, J. A., Hiscock, S. J., & Carine, M. A. (2014). Allopatric diversification, multiple habitat shifts, and hybridization in the evolution of *Pericallis* (Asteraceae), a Macaronesian endemic genus. *American Journal of Botany, 101*(4), 637-651.

Keng, H. (1962). Comparative morphological studies in the Theaceae. *University of California Publications in Botany, 33*, 269-384.

Keng, H. (1990). *The concise flora of Singapore: gymnosperms and dicotyledons* (Vol. 1). Singapore: Singapore University Press, National University of Singapore.
Kidner, C., Groover, A., Thomas, D. C., Emelianova, K., Soliz-Gamboa, C., & Lens, F. (2015). First steps in studying the origins of secondary woodiness in *Begonia* (Begoniaceae): combining anatomy, phylogenetics, and stem transcriptomics. *Biological Journal of the Linnean Society, 117*(1), 121-138.
Kim, J.-H., Kim, D.-K., Forest, F., Fay, M. F., & Chase, M. W. (2010). Molecular phylogenetics of Ruscaceae sensu lato and related families (Asparagales) based on plastid and nuclear DNA sequences. *Annals of Botany, 106*(5), 775-790.
Kim, S.-C., McGowen, M. R., Lubinsky, P., Barber, J. C., Mort, M. E., & Santos-Guerra, A. (2008). Timing and tempo of early and successive adaptive radiations in Macaronesia. *PloS one, 3*(5), e2139.
Knobloch, E., Kvaček, Z., Bůžek, Č., Mai, D., & Batten, D. (1993). Evolutionary significance of floristic changes in the Northern Hemisphere during the Late Cretaceous and Palaeogene, with particular reference to Central Europe. *Review of Palaeobotany and Palynology, 78*(1-2), 41-54.
Knobloch, E., & Mai, D. (1986). *Monographie der Früchte und Samen in der Kreide Mitteleuropas.* Rozpravy Ustredního Ustavu Geologickêho (Vol. 47). Prague: Ústředni ústav geologický v Academii, Československé academie věd.
Knobloch, E., & Mai, D. H. (1991). Evolution of Middle and Upper Cretaceous Floras in Central and Western Europe. *Jahrbuch der Geologischen Bundesanstalt, 134*(2), 257-270.
Kobuski, C. E. (1941a). Studies in the Theaceae, VI The genus *Symplococarpon* Airy–Shaw. *Journal of the Arnold Arboretum, 22*(2), 188-196.
Kobuski, C. E. (1941b). Studies in the Theaceae, VIII A synopsis of the genus *Freziera*. *Journal of the Arnold Arboretum, 22*(4), 457-496.
Kobuski, C. E. (1942). Studies in the Theaceae, XIII: Notes on the Mexican and Central American species of *Ternstroemia*. *Journal of the Arnold Arboretum, 23*(4), 464-478.
Kobuski, C. E. (1952). Studies in the Theaceae, XXVI The genus *Visnea*. *Journal of the Arnold Arboretum, 33*(2), 188-191.
Kobuski, C. E. (1956). Studies in the Theaceae, XXVIII *Melchiora*, a new genus in Africa. *Journal of the Arnold Arboretum, 37*(2), 153-159.
Koek-Noorman, J., & Puff, C. (1983). The wood anatomy of Rubiaceae tribes Anthospermeae and Paederieae. *Plant Systematics and Evolution, 143*(1-2), 17-45.
Kondraskov, P., Koch, M. A., & Thiv, M. (2015). *How did Lauraceae colonise Macaronesia?* Conference paper presented at the Flora Mac 2015, Gran Canaria.
Kondraskov, P., Schütz, N., Schüßler, C., Menezes de Sequeira, M., Santos Guerra, A., Caujapé-Castells, J., . . . Thiv, M. (2015). Biogeography of Mediterranean Hotspot Biodiversity: Re-Evaluating the'Tertiary Relict'Hypothesis of Macaronesian Laurel Forests. *PloS one, 10*(7), e0132091.
Kong, W. S. (2000). Vegetational history of the Korean Peninsula. *Global Ecology and Biogeography, 9*(5), 391-402.
Kovar-Eder, J. (2003). Vegetation dynamics in Europe during the Neogene. *Deinsea, 10*(1), 373-392.
Kovar-Eder, J., Kvaček, Z., Martinetto, E., & Roiron, P. (2006). Late Miocene to Early Pliocene vegetation of southern Europe (7–4 Ma) as reflected in the megafossil plant record. *Palaeogeography, Palaeoclimatology, Palaeoecology, 238*(1-4), 321-339.
Kovar-Eder, J., Kvaček, Z., & Meller, B. (2001). Comparing early to middle Miocene floras and probable vegetation types of Oberdorf N Voitsberg (Austria), Bohemia (Czech Republic), and Wackersdorf (Germany). *Review of Palaeobotany and Palynology, 114*(1-2), 83-125.
Kowalski, R. (2008). Contribution to the knowledge of the Middle Miocene flora from Konin brown coal basin (central Poland). *Acta Palaeobotanica, 48*(2), 277-299.
Kowalski, R. (2017). Miocene carpological floras of the Konin region (Central Poland). *Acta Palaeobotanica, 57*(1), 39-100.
Krastel, S., Schmincke, H. U., Jacobs, C. L., Rihm, R., Le Bas, T. P., & Alibés, B. (2001). Submarine landslides around the Canary Islands. *Journal of Geophysical Research: Solid Earth, 106*(B3), 3977-3997.
Kunkel, G. (1993). *Die Kanarischen Inseln und ihre Pflanzenwelt* (3rd ed.). Stuttgart, Jena, New York: Gustav Fischer Verlag.
Laenen, B., Désamoré, A., Devos, N., Shaw, A. J., González-Mancebo, J. M., Carine, M. A., & Vanderpoorten, A. (2011). Macaronesia: a source of hidden genetic diversity for post-glacial recolonization of western Europe in the leafy liverwort *Radula lindenbergiana*. *Journal of Biogeography, 38*(4), 631-639.

Laín, C. S. (1980). Research on "*Daucus*" L.(" Umbelliferae"). *Anales del Jardin Botanico de Madrid*, *37*(2), 481-534.
Łańcucka-Środoniowa, M. (1984). The results obtained hitherto in studies on the Miocene macroflora from the salt-mine at Wieliczka. *Acta Palaeobotanica, 24*(1,2), 3-26.
Landis, J. B., Soltis, D. E., Li, Z., Marx, H. E., Barker, M. S., Tank, D. C., & Soltis, P. S. (2018). Impact of whole-genome duplication events on diversification rates in angiosperms. *American Journal of Botany, 105*(3), 348-363.
Lanfear, R., Frandsen, P. B., Wright, A. M., Senfeld, T., & Calcott, B. (2016). PartitionFinder 2: new methods for selecting partitioned models of evolution for molecular and morphological phylogenetic analyses. *Molecular biology and evolution, 34*(3), 772-773.
Lécuyer, C., Marco, A. S., Lomoschitz, A., Betancort, J.-F., Fourel, F., Amiot, R., . . . Meco, J. (2020). δ18O and δ13C of diagenetic land snail shells from the Pliocene (Zanclean) of Lanzarote, Canary Archipelago: Do they still record some climatic parameters? *Journal of African Earth Sciences, 162*, 103702.
Lens, F., Davin, N., Smets, E., & del Arco, M. (2013). Insular woodiness on the Canary Islands: a remarkable case of convergent evolution. *International Journal of Plant Sciences, 174*(7), 992-1013.
Lens, F., Eeckhout, S., Zwartjes, R., Smets, E., & Janssens, S. B. (2012). The multiple fuzzy origins of woodiness within Balsaminaceae using an integrated approach. Where do we draw the line? *Annals of Botany, 109*(4), 783-799.
Losos, J. B., & Ricklefs, R. E. (2009). Adaptation and diversification on islands. *Nature, 457*(7231), 830-836.
Lucas, I. C. V., Pinheiro de Carvalho, M. Â. A., & Paiva, J. A. (1998). Morphological and anatomical characterization of the genus *Semele* (Lilliaceae) in the island of Madeira.
Luna, I., & Ochoterena, H. (2004). Phylogenetic relationships of the genera of Theaceae based on morphology. *Cladistics, 20*(3), 223-270.
Lüpnitz, D. (1995). *Kanarische Inseln, Florenvielfalt auf engem Raum: Begleitheft zur gleichnamigen Ausstellung im Palmengarten der Stadt Frankfurt am Main*. Frankfurt: Stadt Frankfurt am Main.
MacArthur, R. H., & Wilson, E. O. (2001). *The Theory of Island Biogeography - with a new preface by Edward O. Wilson*. Princeton, Oxford: Princeton University Press.
Maddison, W. P., & Maddison, D. R. (2006). StochChar: A package of Mesquite modules for stochastic models of character evolution (Version Version 1.1.).
Maddison, W. P., & Maddison, D. R. (2017). Mesquite: a modular system for evolutionary analysis (Version 3.2). Available at http://mesquiteproject.org
Magallón, S., Gómez-Acevedo, S., Sánchez-Reyes, L. L., & Hernández-Hernández, T. (2015). A metacalibrated time-tree documents the early rise of flowering plant phylogenetic diversity. *New Phytologist, 207*(2), 437-453.
Mai, D. H. (1960). Über neue Früchte und Samen aus dem deutschen Tertiär. *Paläontologische Zeitschrift, 34*(1), 73-90.
Mai, D. H. (1971). Über fossile Lauraceae und Theaceae in Mitteleuropa. *Feddes Repertorium, 82*(5), 313-342.
Mai, D. H. (1989). Development and regional differentiation of the European vegetation during the Tertiary. *Plant Systematics and Evolution, 162*(1-4), 79-91.
Mai, D. H. (1997). Die oberoligozänen Floren am Nordrand der sächsischen Lausitz. *Palaeontographica Abteilung B*, *244*, 1-124.
Mai, D. H. (1998). Contribution to the flora of the middle Oligocene Calau Beds in Brandenburg, Germany. *Review of Palaeobotany and Palynology, 101*(1-4), 43-70.
Mai, D. H., & Walther, H. (1978). *Die Floren der Haselbacher Serie im Weißelster-Becken (Bezirk Leipzig, DDR).* Leipzig: Deutscher Verlag für Grundstoffindustrie.
Mai, D. H. (2001). Die mittelmiozänen und obermiozänen Floren aus der Meuroer und Raunoer Folge in der Lausitz. Teil III: Fundstellen und Paläobiologie. *Palaeontographica Abteilung B*, *258*, 1-85.
Mairal, M., Pokorny, L., Aldasoro, J. J., Alarcón, M., & Sanmartín, I. (2015). Ancient vicariance and climate-driven extinction explain continental-wide disjunctions in Africa: the case of the Rand Flora genus *Canarina* (Campanulaceae). *Molecular Ecology, 24*(6), 1335-1354.
Mairal, M., Sanmartín, I., Aldasoro, J., Culshaw, V., Manolopoulou, I., & Alarcón, M. (2015). Palaeo-islands as refugia and sources of genetic diversity within volcanic archipelagos: the case of the widespread endemic *Canarina canariensis* (Campanulaceae). *Molecular Ecology, 24*(15), 3944-3963.
Manchester, S. R. (1994). Fruits and seeds of the Middle Eocene nut beds flora, Clarno Formation, Oregon. *Paleontographica Americana, 58*, 1-205.

Martín Osorio, V. E., Wildpret de la Torre, W.; Alcántara Vernet, E. (2008). *Gesnouinia arborea* (L. f.) Gaud. In: Á. Bañarea Baudet, G. Blanca, J. Güemes, J. C. Moreno Saiz, & S. Ortiz (Eds.), *Atlas y Libro Rojo de la Flora Vascular Amenazada de España - Adenda 2008* (pp. 98-99). Madrid: Dirección General de Medio Natural y Política Forestal (Ministerio de Medio Ambiente, y Medio Rural y Marino)-Sociedad Española de Biología de la Conservación de Plantas.

Martinetto, E. (1995). *Significato cronologico e paleoambientale dei macrofossili vegetali nell'inquadramento stratigrafico del" Villafranchiano" di alcuni settori del Piemonte (Italia NW).* Unpublished PhD Thesis, University of Torino.

Martinetto, E., Momohara, A., Bizzarri, R., Baldanza, A., Delfino, M., Esu, D., & Sardella, R. (2017). Late persistence and deterministic extinction of "humid thermophilous plant taxa of East Asian affinity"(HUTEA) in southern Europe. *Palaeogeography, Palaeoclimatology, Palaeoecology, 467*, 211-231.

Martinetto, E., Monegato, G., Irace, A., Vaiani, S. C., & Vassio, E. (2015). Pliocene and Early Pleistocene carpological records of terrestrial plants from the southern border of the Po Plain (northern Italy). *Review of Palaeobotany and Palynology, 218*, 148-166.

Martinetto, E., Pavia, G., & Bertoldi, R. (1997). *Fruit and seed floras rich in exotic and subtropical elements from two Lower Pliocene successions of Italy.* Paper presented at the 4th EPPC.

Martinetto, E., & Ravazzi, C. (1997). Plant biochronology of the Valle della Fornace succession (Varese) based on the Plio-Pleistocene record in northern Italy. *Geologia Insubrica*, *2* (2), 81-98

Martinetto, E., Scardia, G., & Varrone, D. (2007). Magnetobiostratigraphy of the Stura di Lanzo fossil forest succession (Piedmont, Italy). *Rivista Italiana di Paleontologia e Stratigrafia (Research In Paleontology and Stratigraphy), 113*(1), 109-125.

Martinetto, E., & Vassio, E. (2010). Reconstructing "Plant Community Scenarios" by means of palaeocarpological data from the CENOFITA database, with an example from the Ca'Viettone site (Pliocene, Northern Italy). *Quaternary International, 225*(1), 25-36.

Mathewes, R. W., Greenwood, D. R., & Archibald, S. B. (2016). Paleoenvironment of the Quilchena flora, British Columbia, during the Early Eocene Climatic Optimum. *Canadian Journal of Earth Sciences, 53*(6), 574-590.

Matzke, N. (2013a). BioGeoBEARS: BioGeography with Bayesian (and Likelihood) Evolutionary Analysis in R Scripts. Berkeley, CA: University of California, Berkeley. Available at http://CRAN.R-project.org/package=BioGeoBEARS

Matzke, N. J. (2013b). Probabilistic historical biogeography: new models for founder-event speciation, imperfect detection, and fossils allow improved accuracy and model-testing. *Frontiers of Biogeography, 5*(4), 242-248.

Matzke, N. J. (2014). Model selection in historical biogeography reveals that founder-event speciation is a crucial process in island clades. *Systematic Biology, 63*(6), 951-970.

Meco, J., Koppers, A. A., Miggins, D. P., Lomoschitz, A., & Betancort, J.-F. (2015). The Canary record of the evolution of the North Atlantic Pliocene: New 40Ar/39Ar ages and some notable palaeontological evidence. *Palaeogeography, Palaeoclimatology, Palaeoecology, 435*, 53-69.

Meco, J., Muhs, D. R., Fontugne, M., Ramos, A. J., Lomoschitz, A., & Patterson, D. (2011). Late pliocene and quaternary eurasian locust infestations in the Canary archipelago. *Lethaia, 44*(4), 440-454.

Meco, J., Guillou, H., Carracedo, J.-C., Lomoschitz, A., Ramos, A.-J. G., & Rodríguez-Yánez, J.-J. (2002). The maximum warmings of the Pleistocene world climate recorded in the Canary Islands. *Palaeogeography, Palaeoclimatology, Palaeoecology, 185*(1-2), 197-210.

Meiri, S., Cooper, N., & Purvis, A. (2008). The island rule: made to be broken? *Proceedings of the Royal Society of London B: Biological Sciences, 275*(1631), 141-148.

Meller, B. (1998). Diaspore assemblages from the Early Miocene lignite opencast mine Oberdorf (N Voitsberg, Styria, Austria). *Jahrbuch der Geologischen Bundesanstalt*, *140*(4), 453-460.

Mendoza-Heuer, I. (1977). Die Rubiaceen der Kanarischen Inseln. *Berichte der Deutschen Botanischen Gesellschaft, 90*(1), 211-217.

Mendoza Heuer, I. (1972). Datos para la determinacion de especies en el genero *Phyllis* (Rubiaceae). *Cuadernos de botanica Canaria*, *14/15*, 5-9.

Menzel, P. (1913). Beitrag zur Flora der Niederrheineschen Braunkohlenformation. *Jahrbuch der Königlich Preussischen Geologischen Landesanstalt, 34*(1), 1-98.

Miller, M. A., Pfeiffer, W., & Schwartz, T. (2010). *Creating the CIPRES Science Gateway for inference of large phylogenetic trees.* Paper presented at the Gateway Computing Environments Workshop (GCE), 2010.

Min, T., & Bartholomew, B. (2007). Theaceae. In Flora of China (Vol. 12, pp. 366-478). Retrieved 30th September, 2019 from http://www.efloras.org/florataxon.aspx?flora_id=2&taxon_id=10882.

Mitchell, A., Heenan, P., & Paterson, A. (2009). Phylogenetic relationships of Geranium species indigenous to New Zealand. *New Zealand Journal of Botany, 47*(1), 21-31.
Momohara, A. (1992). Late Pliocene plant biostratigraphy of the lowermost part of the Osaka Group, southwest Japan, with reference to extinction of plants. *The Quaternary Research (Daiyonki-Kenkyu), 31*(2), 77-89.
Moore, M. J., Francisco-Ortega, J., Santos-Guerra, A., & Jansen, R. K. (2002). Chloroplast DNA evidence for the roles of island colonization and extinction in *Tolpis* (Asteraceae: Lactuceae). *American Journal of Botany, 89*(3), 518-526.
Müller, K., Quandt, D., Müller, J., & Neinhuis, C. (2005). PhyDE 0.9971: phylogenetic data editor. Available at http://www.phyde.de/
Navarro-Pérez, M. L., Vargas, P., Fernández-Mazuecos, M., López, J., Valtuena, F. J., & Ortega-Olivencia, A. (2015). Multiple windows of colonization to Macaronesia by the dispersal-unspecialized *Scrophularia* since the Late Miocene. *Perspectives in Plant Ecology, Evolution and Systematics, 17*(4), 263-273.
Navarro J., N. J., Navarro B. . (2004). *Semele gayae* (Webb & Berthel.) Svent. & G. Kunkel. In: Á. Bañares Baudet, G. Blanca, J. Güemes Heras, J. C. Moreno Saiz, & S. Ortiz (Eds.), *Atlas y libro rojo de la flora vascular amendanza de España* (p. 911). Madrid: Ministerio de Medio Ambiente.
Nishida, S., Azuma, H., Naiki, A., & Ogawa, M. (2012). Molecular Phylogenetic Analyses of Geranium robertianum Populations Recently Found in Japan. *APG: Acta phytotaxonomica et geobotanica, 62*(2), 79-87.
Nogue, S., de Nascimento, L., Fernández-Palacios, J. M., Whittaker, R. J., & Willis, K. J. (2013). The ancient forests of La Gomera, Canary Islands, and their sensitivity to environmental change. *Journal of Ecology, 101*(2), 368-377.
Nürk, N. M., Atchison, G. W., & Hughes, C. E. (2019). Island woodiness underpins accelerated disparification in plant radiations. *New Phytologist*, *224*(1), 518–531.
Otto, R., Whittaker, R. J., Gaisberg, M., Stierstorfer, C., Naranjo-Cigala, A., Steinbauer, M. J., . . . Arco, M. (2016). Transferring and implementing the general dynamic model of oceanic island biogeography at the scale of island fragments: the roles of geological age and topography in plant diversification in the Canaries. *Journal of Biogeography*, *43*(5), 911-922.
PaleoDB (2019). Paleobiology Database. Retrieved 22th October, 2019 https://paleobiodb.org/classic
Pannell, C. L., Gray, A., Zalasiewicz, J. A., Branney, M. J., & Curry, G. B. (2011). Pleistocene forest on Tenerife's southern coast: a case study of Montaña Negra. *Journal of Quaternary Science, 26*(5), 485-490.
Patiño, J., Carine, M., Fernández-Palacios, J. M., Otto, R., Schaefer, H., & Vanderpoorten, A. (2014). The anagenetic world of spore-producing land plants. *New Phytologist, 201*(1), 305-311.
Percy, D. M., Page, R. D., & Cronk, Q. C. (2004). Plant–insect interactions: double-dating associated insect and plant lineages reveals asynchronous radiations. *Systematic Biology, 53*(1), 120-127.
Pignatti, S. (1982). Flora d'Italia (1st ed.). Bologna: Edagricole.
Pinheiro de Carvalho, P., Almeida, M. Â., Wilcock, C. C., Dos Santos, T., Marques, M., Vale Lucas, I. C., . . . Freitas Sousa, N. (2004). A review of the genus *Semele* (Ruscaceae) systematics in Madeira. *Botanical Journal of the Linnean Society, 146*(4), 483-497.
Pirie, M. D. (2015). Phylogenies from concatenated data: Is the end nigh? *Taxon, 64*(3), 421-423.
Plant List (2013). The Plant List Version 1.1. Retrieved 9th November, 2016 http://www.theplantlist.org/
Pokorny, L., Oliván, G., & Shaw, A. (2011). Phylogeographic patterns in two southern hemisphere species of *Calyptrochaeta* (Daltoniaceae, Bryophyta). *Systematic Botany, 36*(3), 542-553.
Pokorny, L., Riina, R., Mairal, M., Meseguer, A. S., Culshaw, V., Cendoya, J., . . . Heuertz, M. (2014). Living on the edge: timing of Rand Flora disjunctions congruent with ongoing aridification in Africa. *Frontiers in Genetics, 6*, 154.
Pott, R. (2005). *Allgemeine Geobotanik: Biogeosysteme und Biodiversität*: Berlin, Heidelberg: Springer-Verlag.
Press, J. R., & Dias, E. (1998). The genera *Melanoselinum* Hoffm. and *Angelica* L.(Umbelliferae) in Macaronesia. *ARQUIPÉLAGO. Life and Marine Sciences, 16*, 1-10.
Press, J. R., & Short, M. (1994). *Flora of Madeira*. London: The Natural History Museum.
Puff, C. (1982). The delimitation of the tribe Anthospermeae and its affinities to the Paederieae (Rubiaceae). *Botanical Journal of the Linnean Society, 84*(4), 355-377.
Puff, C. (1986). *A biosystematic study of the African and Madagascan Rubiaceae-Anthospermeae.* Plant Systematics and Evolution – Supplementum 3. Wien, New York: Springer Verlag.

Puppo, P. (2015). *Diversification patterns of Micromeria Benth.(Lamiaceae) in the Canary Islands: Genetic and morphological implications of inter-island colonization.* PhD thesis, Universidade do Porto (Portugal).
Rambaut, A., & Drummond, A. (2013). TreeAnnotator. Version 1.8. 0. MCMC Output Analysis. Available at https://code.google.com/archive/p/beast-mcmc/downloads
Rambaut, A., Suchard, M., Xie, W., & Drummond, A. (2014). Tracer v. 1.6. . Available at http://beast.bio.ed.ac.uk/Tracer
Ree, R. H., & Sanmartín, I. (2018). Conceptual and statistical problems with the DEC+ J model of founder-event speciation and its comparison with DEC via model selection. *Journal of Biogeography, 45*(4), 741-749.
Renvoize, S. (1979). The origins of Indian Ocean island floras. *Plants and islands. Academic Press, London*, 107-129.
Robertson, R., Orchard, A. E., & Wilson, A. (1989). *Hamamelidales to Casuarinales* (R. Robertson, A. E. Orchard, & A. Wilson Eds.). Canberra: Australian Government Public Service.
Rohwer, J. G. (2000). Toward a phylogenetic classification of the Lauraceae: evidence from matK sequences. *Systematic Botany, 25*(1), 60-71.
Ronquist, F., & Huelsenbeck, J. P. (2003). MrBayes 3: Bayesian phylogenetic inference under mixed models. *Bioinformatics, 19*(12), 1572-1574.
Ronquist, F., Teslenko, M., Van Der Mark, P., Ayres, D. L., Darling, A., Höhna, S., . . . Huelsenbeck, J. P. (2012). MrBayes 3.2: efficient Bayesian phylogenetic inference and model choice across a large model space. *Systematic Biology, 61*(3), 539-542.
Rose, J. P., Kleist, T. J., Löfstrand, S. D., Drew, B. T., Schönenberger, J., & Sytsma, K. J. (2018). Phylogeny, historical biogeography, and diversification of angiosperm order Ericales suggest ancient Neotropical and East Asian connections. *Molecular Phylogenetics and Evolution, 122*, 59-79.
Royal Botanic Gardens and Domain Trust (2019). PlantNET (The NSW Plant Information Network System). Retrieved 2nd August, 2019 from http://plantnet.rbgsyd.nsw.gov.au/floraonline.htm
Royal Botanic Gardens Kew (2019). Plants of the World Online. Retrieved 2nd August, 2019 from http://plantsoftheworldonline.org/
Royal Botanic Gardens Victoria (2017). Flora of Victoria. Retrieved 2nd August, 2019, from Royal Botanic Gardens Victoria https://vicflora.rbg.vic.gov.au/flora
Sang, T., Crawford, D., & Stuessy, T. (1997). Chloroplast DNA phylogeny, reticulate evolution, and biogeography of *Paeonia* (Paeoniaceae). *American Journal of Botany, 84*(8), 1120-1120.
Särkinen, T., Bohs, L., Olmstead, R. G., & Knapp, S. (2013). A phylogenetic framework for evolutionary study of the nightshades (Solanaceae): a dated 1000-tip tree. *BMC Evolutionary Biology, 13*(1), 214.
Schacht, H. (1859). *Zur Kenntniss der Visnea mocanera Linn. fil - der Königl. Bayer. Akad. d. Wissenschaften zur Feier ihres 100 jährigen Jubiläums dargebracht von der Königl. Bayer. Botanischen Gesellschaft zu Regensburg*. Regensburg: Julius Heinrich Demmler.
Schaefer, H., Moura, M., Belo Maciel, M. G., Silva, L., Rumsey, F. J., & Carine, M. A. (2011). The Linnean shortfall in oceanic island biogeography: a case study in the Azores. *Journal of Biogeography, 38*(7), 1345-1355.
Schäfer, H. (2005). *Flora of the Azores: a field guide.* Weikersheim: Margraf Verlag.
Schenck, H., & Schimper, A. F. (1907). Beiträge zur Kenntnis der Vegetation der Canarischen Inseln: mit Einfügung hinterlassener Schriften AFW Schimpers. In: C. Chun (Ed.), *Wissenschaftliche Ergebnisse der Deutschen Tiefsee-Expedition auf dem Dampfer "Valdivia" 1898–1899* (vol. 2, pp. 225–406). Jena: G. Fischer.
Schönfelder, P., & Schönfelder, I. (1997). *Die Kosmos-Kanarenflora.* Stuttgart: Kosmos.
Schüßler, C., Bräuchler, C., Reyes-Betancort, J. A., Koch, M. A., & Thiv, M. (2019). Island biogeography of the Macaronesian *Gesnouinia* and Mediterranean *Soleirolia* (Parietarieae, Urticaceae) with implications for the evolution of insular woodiness. *Taxon*, *68*(3), 537-556.
Schweingruber, F. H. (2007). *Wood structure and environment.* Berlin, Heidelberg : Springer Science & Business Media.
Seberg, O., Petersen, G., Davis, J. I., Pires, J. C., Stevenson, D. W., Chase, M. W., . . . Sytsma, K. J. (2012). Phylogeny of the Asparagales based on three plastid and two mitochondrial genes. *American Journal of Botany, 99*(5), 875-889.
Shaw, J., Lickey, E. B., Beck, J. T., Farmer, S. B., Liu, W., Miller, J., . . . Small, R. L. (2005). The tortoise and the hare II: relative utility of 21 noncoding chloroplast DNA sequences for phylogenetic analysis. *American Journal of Botany, 92*(1), 142-166.
Shaw, J., Lickey, E. B., Schilling, E. E., & Small, R. L. (2007). Comparison of whole chloroplast genome sequences to choose noncoding regions for phylogenetic studies in angiosperms: the tortoise and the hare III. *American Journal of Botany, 94*(3), 275-288.

Silva, L., N., P., Press, B., Rumsey, F., Carine, M., Henderson, S., & Sjögren, E. (2005). List of Vascular Plants (Pteridophyta and Spermatophyta). In: P. A. V. Borges, R. Cunha, R. Gabriel, A. F. Martins, L. Silva, & V. Vieira (Eds.), *A list of the terrestrial fauna (Mollusca and Arthropoda) and flora (Bryophyta, Pteridophyta and Spermatophyta) from the Azores* (pp. 131-156). Horta, Angra do Heroísmo and Ponta Delgada: Direcção Regional do Ambiente and Universidade dos Açores.

Silvertown, J. (2004). The ghost of competition past in the phylogeny of island endemic plants. *Journal of Ecology, 92*(1), 168-173.

Silvertown, J., Francisco-Ortega, J., & Carine, M. (2005). The monophyly of island radiations: an evaluation of niche pre-emption and some alternative explanations. *Journal of Ecology, 93*(4), 653-657.

Spalik, K., & Downie, S. R. (2007). Intercontinental disjunctions in *Cryptotaenia* (Apiaceae, Oenantheae): an appraisal using molecular data. *Journal of Biogeography, 34*(12), 2039-2054.

Spalik, K., Piwczyński, M., Danderson, C. A., Kurzyna-Młynik, R., Bone, T. S., & Downie, S. R. (2010). Amphitropic amphiantarctic disjunctions in Apiaceae subfamily Apioideae. *Journal of Biogeography, 37*(10), 1977-1994.

Stamatakis, A. (2014). RAxML version 8: a tool for phylogenetic analysis and post-analysis of large phylogenies. *Bioinformatics, 30*(9), 1312-1313.

Stearn, W. T. (1973). Philip Barker Webb and Canarian Botany. In: G. Kunkel (Ed.), *Proceedings of the I International Congress pro Flora Macaronesica*. Monographiae Biologicae Canariensis (Vol. 4, pp. 15-29). Las Palmas de Gran Canaria: Cabildo Insular de Gran Canaria.

Steinbauer, M. J., Field, R., Fernández-Palacios, J. M., Irl, S. D., Otto, R., Schaefer, H., & Beierkuhnlein, C. (2016). Biogeographic ranges do not support niche theory in radiating Canary Island plant clades. *Global Ecology and Biogeography*, *25*(7), 792-804.

Stillman, C. (1999). Giant Miocene landslides and the evolution of Fuerteventura, Canary Islands. *Journal of Volcanology and Geothermal Research, 94*(1-4), 89-104.

Stuessy, T. F., Jakubowsky, G., Gómez, R. S., Pfosser, M., Schlüter, P. M., Fer, T., . . . Kato, H. (2006). Anagenetic evolution in island plants. *Journal of Biogeography, 33*(7), 1259-1265.

Su, Y., Liao, W., Wang, T., Sun, Y., Wei, Q., & Chang, H. (2011). Phylogeny and evolutionary divergence times in *Apterosperma* and *Euryodendron*: Evidence of a Tertiary origin in south China. *Biochemical Systematics and Ecology, 39*(4), 769-777.

Sun, Y., Li, Y., Vargas-Mendoza, C. F., Wang, F., & Xing, F. (2016). Colonization and diversification of the *Euphorbia* species (sect. *Aphyllis* subsect. *Macaronesicae*) on the Canary Islands. *Scientific Reports, 6*, 34454.

Sunding, P. (1979). Origins of the Macaronesian flora. In: D. Bramwell (Ed.), *Plants and Islands* (pp. 13-40). London, New York, Toronto, Sydney, San Francisco: Academic Press.

Sytsma, K. J., Morawetz, J., Pires, J. C., Nepokroeff, M., Conti, E., Zjhra, M., . . . Chase, M. W. (2002). Urticalean rosids: circumscription, rosid ancestry, and phylogenetics based on *rbcL*, *trnL-F*, and *ndhF* sequences. *American Journal of Botany, 89*(9), 1531-1546.

Taberlet, P., Gielly, L., Pautou, G., & Bouvet, J. (1991). Universal primers for amplification of three non-coding regions of chloroplast DNA. *Plant Molecular Biology, 17*(5), 1105-1109.

Takhtajan, A. (1986). *Floristic regions of the world*. Berkeley: University of California Press.

Tanai, T., & Uemura, K. (1991). The Oligocene Noda flora from the Yuya-wan area of the western end of Honshu, Japan. Part 1. *Bulletin of the National Science Museum Tokyo Series C, 17*(2), 57-80.

Tate, J. A., & Simpson, B. B. (2003). Paraphyly of *Tarasa* (Malvaceae) and diverse origins of the polyploid species. *Systematic Botany, 28*(4), 723-737.

Thureborn, O., Razafimandimbison, S. G., Wikström, N., Khodabandeh, A., & Rydin, C. (2019). Phylogeny of Anthospermeae of the Coffee Family Inferred Using Clock and Nonclock Models. *International Journal of Plant Sciences, 180*(5), 386-402.

Tiffney, B. H. (1994). Re-evaluation of the age of the Brandon Lignite (Vermont, USA) based on plant megafossils. *Review of Palaeobotany and Palynology, 82*(3-4), 299-315.

Trusty, J. L., Olmstead, R. G., Santos-Guerra, A., Sá-Fontinha, S., & Francisco-Ortega, J. (2005). Molecular phylogenetics of the Macaronesian-endemic genus *Bystropogon* (Lamiaceae): palaeo-islands, ecological shifts and interisland colonizations. *Molecular Ecology, 14*(4), 1177-1189.

Tsou, C.-H., Li, L., & Vijayan, K. (2016). The intra-familial relationships of Pentaphylacaceae sl as revealed by DNA Sequence Analysis. *Biochemical Genetics, 54*(3), 270-282.

Tutin, T., Burges, N., Chater, A., Edmondson, J., Heywood, V., Moore, D., . . . Webb, D. (1981). *Flora Europaea. Vol. 2 Rosaceae to Umbelliferae* (3rd ed.). Cambridge: Cambridge University Press.

Tutin, T., Burges, N., Chater, A., Edmondson, J., Heywood, V., Moore, D., . . . Webb, D. (1993). *Flora Europaea*. *Vol. 1 Psilotaceae to Platanaceae* (2nd ed.). Cambridge: Cambridge University Press.
Tutin, T., Heywood, V., Burges, N., Moore, D., Valentine, D., Walters, S., & Webb, D. (1980). *Flora Europaea. Vol. 5. Alismataceae to Orchidaceae*. Cambridge: Cambridge University Press.
Ulloa Ulloa, C., & Jørgensen, P. M. (2004). Árboles y arbustos de los Andes del Ecuador. Retrieved 30th September, 2019 from http://www.efloras.org/flora_page.aspx?flora_id=201
Vaidya, G., Lohman, D. J., & Meier, R. (2011). SequenceMatrix: concatenation software for the fast assembly of multi-gene datasets with character set and codon information. *Cladistics, 27*(2), 171-180.
Valcárcel, V., Guzmán, B., Medina, N., Vargas, P., & Wen, J. (2017). Phylogenetic and paleobotanical evidence for late Miocene diversification of the Tertiary subtropical lineage of ivies (*Hedera* L., Araliaceae). *BMC Evolutionary Biology, 17*(1), 146.
Valtuena, F. J., Rodríguez-Riaño, T., Lopez, J., Mayo, C., & Ortega-Olivencia, A. (2017). Peripatric speciation in an endemic Macaronesian plant after recent divergence from a widespread relative. *PloS one, 12*(6), e0178459.
Van der Burgh, J. (1973). Hölzer der niederrheinischen Braunkohlenformation, 2. Hölzer der Braunkohlengruben “Maria Theresia” zu Herzogenrath, “Zukunft West” zu Eschweiler und “Victor” (Zülpich Mitte) zu Zülpich. Nebst einer systematisch-anatomischen Bearbeitung der Gattung *Pinus* L. *Review of Palaeobotany and Palynology*, *15*, 73-275.
Van der Burgh, J. (1984). Some palms in the Miocene of the Lower Rhenish Plain. *Review of Palaeobotany and Palynology, 40*, 359-374.
Van der Burgh, J. (1987). Miocene floras in the lower Rhenish Basin and their ecological interpretation. *Review of Palaeobotany and Palynology, 52*(4), 299-366.
Van Loon, J. C. (1984). Hybridization experiments in Geranium. *Genetica, 65*(2), 167-171.
Vasilevskaya, V. K., & Oganesyan, M. E. (1978). Leaf anatomy and some questions on ecology of representatives of the genus *Parietaria* L. (Urticaceae) from the flora of the Armenian SSR. *Vestnik Leningradskogo universiteta Biologiia, 1,* 51-55.
Viruel, J., Segarra-Moragues, J. G., Raz, L., Forest, F., Wilkin, P., Sanmartín, I., & Catalán, P. (2016). Late Cretaceous–Early Eocene origin of yams (*Dioscorea*, Dioscoreaceae) in the Laurasian Palaearctic and their subsequent Oligocene–Miocene diversification. *Journal of Biogeography, 43*(4), 750-762.
Wallace, A. R. (1902). *Island life, or, the phenomena and causes of insular faunas and floras: including a revision and attempted solution of the problem of geological climates* (3rd and rev. ed.). London: Macmillan.
Walter, H., & Breckle, S.-W. (1999). *Vegetation und Klimazonen*. Stuttgart: Ulmer.
Walter, T. R., Troll, V. R., Cailleau, B., Belousov, A., Schmincke, H.-U., Amelung, F., & v. d. Bogaard, P. (2005). Rift zone reorganization through flank instability in ocean island volcanoes: an example from Tenerife, Canary Islands. *Bulletin of Volcanology, 67*(4), 281-291.
Weddell, H. (1857). Monographie de la familie des Urticées. *Archives du Muséum d'Histoire Naturelle*, *9*, 1–592.
Weddell, H. A. (1869). Urticacées. In: A. D. Candolle (Ed.), *Prodromus Systematis Naturalis Regni Vegetabilis* (Vol. 16,1, pp. 32–235). Paris: Victoris Masson et Filii.
Weitzman, A., Dressler, S., & Stevens, P. (2004). Ternstroemiaceae. In: K. Kubitzki (Ed.), *Flowering Plants. Dicotyledons - Celastrales, Oxalidales, Rosales, Cornales, Ericales* (Vol. 6, pp. 450-460). Berlin, Heidelberg: Springer.
Weng, M.-L., Blazier, J. C., Govindu, M., & Jansen, R. K. (2013). Reconstruction of the ancestral plastid genome in Geraniaceae reveals a correlation between genome rearrangements, repeats and nucleotide substitution rates. *Molecular Biology and Evolution*, *31*(3), 645–659.
Western Australian Herbarium (1998). FloraBase—the Western Australian Flora. Retrieved 2nd August, 2019 from https://florabase.dpaw.wa.gov.au/
Wheeler, E. A., Baas, P., & Gasson, P. E. (1989). IAWA list of microscopic features for hardwood identification. *IAWA Bulletin, 10*(3): 219–332
White, T. J., Bruns, T., Lee, S., & Taylor, J. (1990). Amplification and direct sequencing of fungal ribosomal RNA genes for phylogenetics. *PCR protocols: a guide to methods and applications, 18*(1), 315-322.
Whittaker, R. J., & Fernández-Palacios, J. M. (2007). *Island biogeography: ecology, evolution, and conservation*. Oxford: Oxford University Press.
Whittaker, R. J., Triantis, K. A., & Ladle, R. J. (2008). A general dynamic theory of oceanic island biogeography. *Journal of Biogeography, 35*(6), 977-994.

Widler-Kiefer, H., & Yeo, P. F. (1987). Fertility relationships of *Geranium* (Geraniaceae): sectt. *Ruberta*, *Anemonifolia*, *Lucida* and *Unguiculata*. *Plant Systematics and Evolution, 155*(1-4), 283-306.

Williams, B. R., Schaefer, H., de Sequeira, M. M., Reyes-Betancort, J. A., Patiño, J., & Carine, M. A. (2015). Are there any widespread endemic flowering plant species in Macaronesia? Phylogeography of *Ranunculus cortusifolius*. *American Journal of Botany, 102*(10), 1736-1746.

Wright, S. D., Yong, C. G., Wichman, S. R., Dawson, J. W., & Gardner, R. C. (2001). Stepping stones to Hawaii: a trans-equatorial dispersal pathway for *Metrosideros* (Myrtaceae) inferred from nrDNA (ITS+ ETS). *Journal of Biogeography, 28*(6), 769-774.

Wu, C.-C., Hsu, Z.-F., & Tsou, C.-H. (2007). Phylogeny and taxonomy of *Eurya* (Ternstroemiaceae) from Taiwan, as inferred from ITS sequence data. *Botanical Studies, 48*, 97-116.

Wu, Z.-Y., Milne, R. I., Chen, C.-J., Liu, J., Wang, H., & Li, D.-Z. (2015). Ancestral state reconstruction reveals rampant homoplasy of diagnostic morphological characters in Urticaceae, conflicting with current classification schemes. *PloS one, 10*(11), e0141821.

Wu, Z.-Y., Monro, A. K., Milne, R. I., Wang, H., Yi, T.-S., Liu, J., & Li, D.-Z. (2013). Molecular phylogeny of the nettle family (Urticaceae) inferred from multiple loci of three genomes and extensive generic sampling. *Molecular Phylogenetics and Evolution, 69*(3), 814-827.

Yamakawa, C., Momohara, A., Saito, T., & Nunotani, T. (2017). Composition and paleoenvironment of wetland forests dominated by *Glyptostrobus* and *Metasequoia* in the latest Pliocene (2.6 Ma) in central Japan. *Palaeogeography, Palaeoclimatology, Palaeoecology, 467*, 191-210.

Yanes, Y., Yapp, C. J., Ibáñez, M., Alonso, M. R., De-la-Nuez, J., Quesada, M. L., . . . Delgado, A. (2011). Pleistocene–Holocene environmental change in the Canary Archipelago as inferred from the stable isotope composition of land snail shells. *Quaternary Research, 75*(3), 658-669.

Yeo, P. (1973). The biology and systematics of Geranium, sections *Anemonifolia* Knuth and *Ruberta* Dum. *Botanical Journal of the Linnean Society, 67*(4), 285-346.

Yeo, P. (1984). Fruit-discharge-type in *Geranium* (Geraniaceae): its use in classification and its evolutionary implications. *Botanical Journal of the Linnean Society, 89*(1), 1-36.

Yeo, P. (1998). Ruscaceae. In *Flowering Plants. Monocotyledons - Lilianae (except Orchidaceae)* (Vol. 3, pp. 412-416). Berlin, Heidelberg: Springer.

Yu, Y., Harris, A., Blair, C., & He, X. (2014). *A Rough Guide to RASP 3.1 05/15/2014*. Retrieved from http://mnh.scu.edu.cn/soft/blog/RASP/RASP_Win_20170501.zip

Yu, Y., Harris, A., & He, X. (2010). S-DIVA (Statistical Dispersal-Vicariance Analysis): a tool for inferring biogeographic histories. *Molecular Phylogenetics and Evolution, 56*(2), 848-850.

Yu, Y., Harris, A. J., Blair, C., & He, X. (2015). RASP (Reconstruct Ancestral State in Phylogenies): a tool for historical biogeography. *Molecular Phylogenetics and Evolution, 87*, 46-49.

Zhang, R.-J., & Schönenberger, J. (2014). Early floral development of Pentaphylacaceae (Ericales) and its systematic implications. *Plant Systematics and Evolution, 300*(6), 1547-1560.

Zhu, H., Huang, Y.-J., Su, T., & Zhou, Z.-K. (2016). New fossil seeds of *Eurya* (Theaceae) from East Asia and their paleobiogeographic implications. *Plant Diversity, 38*(3), 125-132.

Appendix

Appendix Datasets, Figures and Tables are included on DVD. Photographs of the *Visnea* and *Gesnouinia* sections as well as MCT data has been deposited at Wserver04\Amira\Schüßler and Wserver02\botanik\Schüßler of the State Museum of Natural History Stuttgart.

List of Appendix Datasets

Data S1. *Visnea* datasets. Input and output files for/from phylogenetic analyses, molecular dating, ancestral area estimation, ancestral character state estimation and multivariate statistics.

Data S2. *Geranium* datasets. Input and output files for/from phylogenetic analyses, molecular dating and ancestral area estimation.

Data S3. *Semele* datasets. Input and output files for/from phylogenetic analyses, molecular dating and ancestral area estimation.

Data S4. *Daucus* datasets. Input and output files for/from phylogenetic analyses, molecular dating and ancestral area estimation.

Data S5. *Phyllis* datasets. Input and output files for/from phylogenetic analyses, molecular dating and ancestral area estimation.

Data S6. *Gesnouinia* datasets. Input and output files for/from phylogenetic analyses, molecular dating, ancestral area estimation and ancestral character state estimation.

List of Appendix Figures

Appendix Figure S1. Maximum likelihood *matK* phylogeny of Ericales using balsaminoids as outgroup. Numbers above branches indicate posterior probabilities from MrBayes analysis (left) and bootstrap values from RAxML analysis (right). Only posterior probabilities ≥0.90 and bootstrap values ≥80 are given.

Appendix Figure S2. Maximum likelihood *trnL-trnF* phylogeny of Ericales using balsaminoids as outgroup. Numbers above branches indicate posterior probabilities from MrBayes analysis (left) and bootstrap values from RAxML analysis (right). Only posterior probabilities ≥0.90 and bootstrap values ≥80 are given.

Appendix Figure S3. Maximum likelihood *trnL-trnF* and *matK* phylogeny of the subset of Ericales (Pentaphylacaceae, Theaceae, styracoids, ericoids and sarracenioids) using Primulaceae, Sapotaceae and Ebenaceae as outgroup. Numbers above branches indicate posterior probabilities from MrBayes analysis (left) and bootstrap values from RAxML analysis (right). Only posterior probabilities ≥0.90 and bootstrap values ≥80 are given.

Appendix Figure S4. Maximum likelihood *psbA-trnH* phylogeny of the subset of Ericales (Pentaphylacaceae, Theaceae and ericoids) using Primulaceae, Sapotaceae and Ebenaceae as outgroup. Numbers above branches indicate posterior probabilities from MrBayes analysis (left) and bootstrap values from RAxML analysis (right). Only posterior probabilities ≥0.90 and bootstrap values ≥80 are given.

Appendix Figure S5. Maximum likelihood *psbA-trnH*, *trnL-trnF* and *matK* phylogeny of Pentaphylacaceae s.str. using tribe Pentaphylaceae as outgroup. Numbers above branches indicate posterior probabilities from MrBayes analysis (left) and bootstrap values from RAxML analysis (right). Only posterior probabilities ≥0.90 and bootstrap values ≥80 are given.

Appendix Figure S6. Maximum likelihood ITS phylogeny of Pentaphylacaceae s.str. using tribe Pentaphylaceae as outgroup. Numbers above branches indicate posterior probabilities from MrBayes

analysis (left) and bootstrap values from RAxML analysis (right). Only posterior probabilities ≥0.90 and bootstrap values ≥80 are given.

Appendix Figure S7. Plastid chronogram (*trnL-trnF* spacer, *psbA-trnH* spacer & *matK*) of the subset of Ericales from BEAST analysis (calibM). Primulaceae, Ebenaceae and Sapotaceae served as outgroups. The calibration point based on Magallon et al. (2015; stem Pentaphylacaceae) is indicated by a black star. Bars at the nodes indicate 95% highest posterior densities, bold numbers at nodes the estimated mean ages. Numbers above branches represent posterior probabilities from MrBayes analysis, bootstrap values from RAxML analysis and posterior probabilities from BEAST analysis. Only posterior probabilities ≥0.90 and bootstrap values ≥80 are shown.

Appendix Figure S8. Dendrogram from hierarchical cluster analysis using the average linkage method. Approach with *Anneslea fragrans* included.

Appendix Figure S9. Plastid chronogram (*trnL-trnF* spacer & *matK*) from BEAST analysis (calibL) using balsaminoids as outgroup. The calibration point based on Landis et al. (2018; split of Ericaceae from Fouquieriaceae) is indicated by a black star. Bars at the nodes indicate 95% highest posterior densities, bold numbers at nodes the estimated mean ages. Numbers above branches represent posterior probabilities from MrBayes analysis, bootstrap values from RAxML analysis and posterior probabilities from BEAST analysis. Only posterior probabilities ≥0.90 and bootstrap values ≥80 are shown.

Appendix Figure S10. Plastid chronogram (*trnL-trnF* spacer & *matK*) of Ericales from BEAST analysis (calibR) using balsaminoids as outgroup. The calibration points based on Rose et al. (2018; i.e. a: stem Lecythidaceae, b: split of Eriaceae from Clethraceae, c: MRCA of Diapensiaceae and Styracaceae and d: MRCA of *Actinidia* and *Roridula*) are indicated by black stars. Bars at the nodes indicate 95% highest posterior densities, bold numbers at nodes the estimated mean ages. Numbers above branches represent posterior probabilities from MrBayes analysis, bootstrap values from RAxML analysis and posterior probabilities from BEAST analysis. Only posterior probabilities ≥0.90 and bootstrap values ≥80 are shown.

Appendix Figure S11. Maximum likelihood ITS, *psbA-trnH*, *trnL-trnF* and *matK* phylogeny of Pentaphylacaceae s.str. using tribe Pentaphylaceae as outgroup. Numbers above branches indicate posterior probabilities from MrBayes analysis (left) and bootstrap values from RAxML analysis (right). Only posterior probabilities ≥0.90 and bootstrap values ≥80 are given. Asterisks denote (statsically supported) differences in topology in the MrBayes phylogeny.

Appendix Figure S12. Chronogram from crown node dating based on ITS data of *Visnea* and *Euryodendron*. As calibration point, the age estimate for *Visnea* from Rose et al. (2018) was used. Bars at the nodes indicate 95% highest posterior densities; posterior probabilities from BEAST analysis ≥ 0.90 are given above the branches.

Appendix Figure S13. Ancestral Area Estimation in Pentaphylacaceae s.str. under the DIVALIKE+J model in BioGeoBEARS; based on the chronogram (ITS, *psbA-trnH*, *trnL-trnF*, *matK*) from tip-dating. On the nodes, the probabilities of the estimated areas/area combinations are indicated by pie charts/letters. Areas coded include Macaronesia (A), Asia (B), Europe and the Mediterranean (C), New World (D).

Appendix Figure S14. Longitudinal microtome sections of fruits of *Visnea mocanera*. Abbreviations: ca: central axis, ec: embryo cavity, em: embryo, en: endosperm, ext: exotesta, mt: mesotesta, p: pericarp, r: raphe, sp: sepals.

Appendix Figure S15. Longitudinal section (by hand) of *Visnea germanica* from the Miocene-Pliocene of Scipione Ponte, Italy (SP110). The sample was fixed with pink plasticine to facilitate sectioning. S: Seed.

Appendix Figure S16. MicroCT images of extant Pentaphylacaceae s.str. and fossil *Visnea germanica*. Exterior of the fruits, reconstruction of seeds and of embryo as well as raphe cavities.

Appendix Figure S17. Phylogeny of Pentaphylacaceae s.str. including fossil *Visnea germanica* based on analysis of morphological data in MrBayes. Posterior probabilities are given above branches.

Appendix Figure S18. Phylogeny of Pentaphylacaceae s.str. including fossil *Visnea germanica* based on analysis of morphological data in PAUP. Bootstrap support is given above the branches. Branch lengths are drawn to scale with bootstrap support.

Appendix Figure S19. Maximum likelihood *rbcL* phylogeny of Geraniaceae using Crossosomataceae as outgroup. Numbers above branches indicate posterior probabilities from MrBayes analysis (left) and bootstrap values from RAxML analysis (right). Only posterior probabilities ≥0.90 and bootstrap values ≥80 are given.

Appendix Figure S20. Maximum likelihood *trnL-trnF* spacer phylogeny of Geraniaceae using Crossosomataceae as outgroup. Numbers above branches indicate posterior probabilities from MrBayes analysis (left) and bootstrap values from RAxML analysis (right). Only posterior probabilities ≥0.90 and bootstrap values ≥80 are given.

Appendix Figure S21. Maximum likelihood *matK* phylogeny of *Geranium* subg. *Robertium* using *Geranium incanum* (*Geranium* subg. *Geranium*) as outgroup. Numbers above branches indicate posterior probabilities from MrBayes analysis (left) and bootstrap values from RAxML analysis (right). Only posterior probabilities ≥0.90 and bootstrap values ≥80 are given.

Appendix Figure S22. Maximum likelihood *trnL-trnF* spacer phylogeny of *Geranium* subg. *Robertium* using *Geranium incanum* (*Geranium* subg. *Geranium*) as outgroup. Numbers above branches indicate posterior probabilities from MrBayes analysis (left) and bootstrap values from RAxML analysis (right). Only posterior probabilities ≥0.90 and bootstrap values ≥80 are given.

Appendix Figure S23. Maximum likelihood ITS phylogeny of *Geranium* subg. *Robertium* using *Geranium* subg. *Geranium* as outgroup. Numbers above branches indicate posterior probabilities from MrBayes analysis (left) and bootstrap values from RAxML analysis (right). Only posterior probabilities ≥0.90 and bootstrap values ≥80 are given.

Appendix Figure S24. Maximum likelihood ETS phylogeny of *Geranium* subg. *Robertium* using *Geranium* subg. *Geranium* as outgroup. Numbers above branches indicate posterior probabilities from MrBayes analysis (left) and bootstrap values from RAxML analysis (right). Only posterior probabilities ≥0.90 and bootstrap values ≥80 are given.

Appendix Figure S25. Plastid (*rbcL* & *trnL-trnF* spacer) chronogram of Geraniaceae from BEAST analysis (calibM) using Crossosomataceae as outgroup. The calibration points based on Magallon et al. (2015; stem Geraniaceae) is indicated by a black star. Bars at the nodes indicate 95% highest posterior densities, bold numbers at nodes the estimated mean ages. Numbers above branches represent posterior probabilities from MrBayes analysis, bootstrap values from RAxML analysis and posterior probabilities from BEAST analysis. Only posterior probabilities ≥0.90 and bootstrap values ≥80 are shown.

Appendix Figure S26. Maximum likelihood *matK* & *trnL-trnF* spacer phylogeny of *Geranium* subg. *Robertium* using *Geranium incanum* (*Geranium* subg. *Geranium*) as outgroup. Numbers above branches indicate posterior probabilities from MrBayes analysis (left) and bootstrap values from RAxML analysis (right). Only posterior probabilities ≥0.90 and bootstrap values ≥80 are given.

Appendix Figure S27. Plastid (*rbcL* & *trnL-trnF* spacer) chronogram of Geraniaceae from BEAST analysis (calibL) using Crossosomataceae as outgroup. The calibration point based on Landis et al. (2018; crown Geraniaceae) is indicated by a black star. Bars at the nodes indicate 95% highest posterior densities, bold numbers at nodes the estimated mean ages. Numbers above branches represent posterior probabilities from BEAST analysis. Only posterior probabilities ≥0.90 are shown.

Appendix Figure S28. Plastid (*rbcL* & *trnL-trnF* spacer) chronogram of *Geranium* from BEAST analysis (calibF) using *Erodium* and *California* as outgroups. The calibration point based on Fiz et al. (2008; crown *Geranium*) is indicated by a black star. Bars at the nodes indicate 95% highest posterior densities, bold numbers at nodes the estimated mean ages. Numbers above branches represent posterior probabilities from BEAST analysis. Only posterior probabilities ≥0.90 are shown.

Appendix Figure S29. Chronogram from crown node dating based on ITS data of the *Geranium robertianum* clade and the *G. maderense* clade. As calibration point, the age estimate for the split

between both clades from stem node dating (calibM) was used. Bars at the nodes indicate 95% highest posterior densities; posterior probabilities from BEAST analysis ≥ 0.90 are given above the branches.

Appendix Figure S30. Chronogram from crown node dating based on ETS data of the *Geranium robertianum* clade and the *G. maderense* clade. As calibration point, the age estimate for the split between both clades from stem node dating (calibM) was used. Bars at the nodes indicate 95% highest posterior densities; posterior probabilities from BEAST analysis ≥ 0.90 are given above the branches.

Appendix Figure S31. Ancestral area reconstruction in *Geranium* subg. *Robertium* as inferred from S-DEC analysis in RASP, based on the plastid chronogram (*rbcL* & *trnL-trnF* spacer; calibM). Numbers at the nodes indicate posterior probabilities from BEAST analysis. Only posterior probabilities ≥0.90 are shown. On the nodes, the posterior probabilities of the estimated areas/area combinations are indicated by pie charts. Areas coded include the Canary Islands (A), the Mediterranean (B), Non-Mediterranean Eurasia (C), Non-Mediterranean Africa (D), Madeira (E) and the Azores (F).

Appendix Figure S32. Ancestral Area Estimation in *Geranium* subg. *Robertium* under the DEC model in BioGeoBEARS; based on the plastid chronogram (*rbcL* & *trnL-trnF* spacer; calibM). On the nodes, the probabilities of the estimated areas/area combinations are indicated by pie charts/letters. Areas coded include the Canary Islands (A), the Mediterranean (B), Non-Mediterranean Eurasia (C), Non-Mediterranean Africa (D), Madeira (E) and the Azores (F).

Appendix Figure S33. Maximum likelihood *atpB* phylogeny of Asparagaceae using Xeronemataceae as outgroup. Numbers above branches indicate posterior probabilities from MrBayes analysis (left) and bootstrap values from RAxML analysis (right). Only posterior probabilities ≥0.90 and bootstrap values ≥80 are given.

Appendix Figure S34. Maximum likelihood *matK* phylogeny of Asparagaceae using Xeronemataceae as outgroup. Numbers above branches indicate posterior probabilities from MrBayes analysis (left) and bootstrap values from RAxML analysis (right). Only posterior probabilities ≥0.90 and bootstrap values ≥80 are given.

Appendix Figure S35. Maximum likelihood *ndhF* phylogeny of Asparagaceae using Xeronemataceae as outgroup. Numbers above branches indicate posterior probabilities from MrBayes analysis (left) and bootstrap values from RAxML analysis (right). Only posterior probabilities ≥0.90 and bootstrap values ≥80 are given.

Appendix Figure S36. Maximum likelihood *rbcL* phylogeny of Asparagaceae using Xeronemataceae as outgroup. Numbers above branches indicate posterior probabilities from MrBayes analysis (left) and bootstrap values from RAxML analysis (right). Only posterior probabilities ≥0.90 and bootstrap values ≥80 are given.

Appendix Figure S37. Plastid (*atpB*, *matK*, *ndhF* & *rbcL*) chronogram of Asparagaceae from BEAST analysis (calibM) using Xeronemataceae as outgroup. The calibration point based on Magallon et al. (2015; split Asparagaceae from Amaryllidaceae) is indicated by a black star. Bars at the nodes indicate 95% highest posterior densities, bold numbers at nodes the estimated mean ages. Numbers above branches represent posterior probabilities from MrBayes analysis, bootstrap values from RAxML analysis and posterior probabilities from BEAST analysis. Only posterior probabilities ≥0.90 and bootstrap values ≥80 are shown.

Appendix Figure S38. Ancestral Area Estimation in Rusceae under the DIVALIKE model in BioGeoBEARS; based on the plastid chronogram (*atpB*, *matK*, *ndhF* & *rbcL*; calibM). On the nodes, the probabilities of the estimated areas/area combinations are indicated by pie charts/letters. Areas coded include the Canary Islands (A), Madeira (B), Eurasia (including Mediterranean; C).

Appendix Figure S39. Ancestral area reconstruction in Rusceae as inferred from S-DIVA analysis in RASP, based on the plastid chronogram (*rbcL* & *trnL-trnF* spacer; calibM). Numbers at the nodes indicate posterior probabilities from BEAST analysis. Only posterior probabilities ≥0.90 are shown. On the nodes, the posterior probabilities of the estimated areas/area combinations are indicated by pie

charts. Areas coded include the Canary Islands (A), Madeira (B), Eurasia (including Mediterranean; C).

Appendix Figure S40. Maximum likelihood ITS phylogeny of *Daucus* using *Orlaya* as outgroup. Numbers above branches indicate posterior probabilities from MrBayes analysis (left) and bootstrap values from RAxML analysis (right). Only posterior probabilities ≥0.90 and bootstrap values ≥80 are given.

Appendix Figure S41. Maximum likelihood *rps16* phylogeny of *Daucus* using *Orlaya* as outgroup. Numbers above branches indicate posterior probabilities from MrBayes analysis (left) and bootstrap values from RAxML analysis (right). Only posterior probabilities ≥0.90 and bootstrap values ≥80 are given.

Appendix Figure S42. Plastid (*rps16*) chronogram of Apiaceae from BEAST analysis (calibM) using Araliaceae as outgroup. The calibration point based on Magallon et al. (2015; stem Apiaceae) is indicated by a black star. Bars at the nodes indicate 95% highest posterior densities, bold numbers at nodes the estimated mean ages. Numbers above branches represent posterior probabilities from MrBayes analysis, bootstrap values from RAxML analysis and posterior probabilities from BEAST analysis. Only posterior probabilities ≥0.90 and bootstrap values ≥80 are shown.

Appendix Figure S43. Chronogram (*rps16* & ITS) of *Daucus* from BEAST analysis using *Orlaya* as outgroup. The calibration point based on the estimate from *rps16* stem node dating (calibM, stem *Daucus*) is indicated by a black star. Bars at the nodes indicate 95% highest posterior densities, bold numbers at nodes the estimated mean ages. Numbers above branches represent posterior probabilities from MrBayes analysis, bootstrap values from RAxML analysis and posterior probabilities from BEAST analysis. Only posterior probabilities ≥0.90 and bootstrap values ≥80 are shown.

Appendix Figure S44. Chronogram from crown node dating based on ITS and *rps16* data of *Daucus elegans*, *D. edulis* and *D. decipiens*. As calibration point, the age estimate for the split of *Daucus elegans* from *D. edulis* and *D. decipiens* according to Spalik et al. (2010; calibS) was used. Bars at the nodes indicate 95% highest posterior densities; posterior probabilities from BEAST analysis ≥ 0.90 are given above the branches.

Appendix Figure S45. Ancestral Area Estimation in *Daucus* under the DEC model in BioGeoBEARS; based on the ITS & *rps16* chronogram (calibM). On the nodes, the probabilities of the estimated areas/area combinations are indicated by pie charts/letters. Areas coded include the Canary Islands (A), Madeira (B), Cape Verdes (C), Mediterranean (D), Azores (E), Non-Mediterranean Europe (F).

Appendix Figure S46. Ancestral area reconstruction in *Daucus* as inferred from S-DEC analysis in RASP, based on the chronogram (ITS & *rps16*; calibM). Numbers at the nodes indicate posterior probabilities from BEAST analysis. Only posterior probabilities ≥0.90 are shown. On the nodes, the posterior probabilities of the estimated areas/area combinations are indicated by pie charts. Areas coded include the Canary Islands (A), Madeira (B), Cape Verdes (C), Mediterranean (D), Azores (E), Non-Mediterranean Europe (F).

Appendix Figure S47. Maximum likelihood *ndhF* phylogeny of Anthospermeae using Knoxieae and Spermacoceae as outgroups. Numbers above branches indicate posterior probabilities from MrBayes analysis (left) and bootstrap values from RAxML analysis (right). Only posterior probabilities ≥0.90 and bootstrap values ≥80 are given.

Appendix Figure S48. Maximum likelihood *rps16* phylogeny of Anthospermeae using Knoxieae and Spermacoceae as outgroups. Numbers above branches indicate posterior probabilities from MrBayes analysis (left) and bootstrap values from RAxML analysis (right). Only posterior probabilities ≥0.90 and bootstrap values ≥80 are given.

Appendix Figure S49. Plastid (*ndhF*) chronogram of Rubiaceae from BEAST analysis (calibM) using Convolvulaceae and Solanaceae as outgroups. The calibration point based on Magallon et al. (2015; stem Rubiaceae) is indicated by a black star. Bars at the nodes indicate 95% highest posterior densities, bold numbers at nodes the estimated mean ages. Numbers above branches represent posterior probabilities from MrBayes analysis, bootstrap values from RAxML analysis and posterior

probabilities from BEAST analysis. Only posterior probabilities ≥0.90 and bootstrap values ≥80 are shown.

Appendix Figure S50. Maximum likelihood ITS phylogeny of Anthosperminae using *Durringtonia* and *Nertera* as outgroups. Numbers above branches indicate posterior probabilities from MrBayes analysis (left) and bootstrap values from RAxML analysis (right). Only posterior probabilities ≥0.90 and bootstrap values ≥80 are given.

Appendix Figure S51. Maximum likelihood *rps16* phylogeny of Anthosperminae using *Durringtonia* and *Nertera* as outgroups. Numbers above branches indicate posterior probabilities from MrBayes analysis (left) and bootstrap values from RAxML analysis (right). Only posterior probabilities ≥0.90 and bootstrap values ≥80 are given.

Appendix Figure S52. Plastid (*ndhF* & *rps16*) chronogram of Anthospermeae from BEAST analysis (calibM) using Knoxieae and Spermacoceae as outgroups. The calibration point based on Magallon et al. (2015; stem Anthospermeae) is indicated by a black star. Bars at the nodes indicate 95% highest posterior densities, bold numbers at nodes the estimated mean ages. Numbers above branches represent posterior probabilities from MrBayes analysis, bootstrap values from RAxML analysis and posterior probabilities from BEAST analysis. Only posterior probabilities ≥0.90 and bootstrap values ≥80 are shown.

Appendix Figure S53. Maximum likelihood *rps16* and ITS phylogeny of Anthosperminae using *Durringtonia* and *Nertera* as outgroups. Numbers above branches indicate posterior probabilities from MrBayes analysis (left) and bootstrap values from RAxML analysis (right). Only posterior probabilities ≥0.90 and bootstrap values ≥80 are given.

Appendix Figure S54. Plastid (*ndhF* & *rps16*) chronogram of Anthospermeae from BEAST analysis (calibB) using Knoxieae and Spermacoceae as outgroups. The calibration point based on Bremer et al. (2009; stem Anthospermeae) is indicated by a black star. Bars at the nodes indicate 95% highest posterior densities, bold numbers at nodes the estimated mean ages. Numbers above branches represent posterior probabilities from MrBayes analysis, bootstrap values from RAxML analysis and posterior probabilities from BEAST analysis. Only posterior probabilities ≥0.90 and bootstrap values ≥80 are shown.

Appendix Figure S55. Chronogram from crown node dating based on ITS and *rps16* data of *Phyllis*. As calibration point, the age estimate for the split of *Phyllis nobla* from *P. viscosa* according to stem node dating based on Bremer et al. (2009; calibB) was used. Bars at the nodes indicate 95% highest posterior densities; posterior probabilities from BEAST analysis ≥ 0.90 are given above the branches.

Appendix Figure S56. Ancestral area reconstruction in Anthospermeae as inferred from S-DIVA analysis in RASP, based on the plastid chronogram (*ndhF* & *rps16*; calibM). Numbers at the nodes indicate posterior probabilities from BEAST analysis. Only posterior probabilities ≥0.90 are shown. On the nodes, the posterior probabilities of the estimated areas/area combinations are indicated by pie charts. Areas coded include Africa (A), Australasia (B), Pacific Region (C), Antarctic Region (D), New World (E), Asia (F), Canary Islands (G), Madeira (H).

Appendix Figure S57. Ancestral Area Estimation in Anthospermeae under the DIVALIKE model in BioGeoBEARS; based on the *ndhF* & *rps16* chronogram (calibM). On the nodes, the probabilities of the estimated areas/area combinations are indicated by pie charts/letters. Areas coded include Africa (A), Australasia (B), Pacific Region (C), Antarctic Region (D), New World (E), Asia (F), Canary Islands (G), Madeira (H).

Appendix Figure S58. Maximum likelihood *matK* phylogeny of Urticaceae using Cannabaceae as outgroup. Numbers above branches indicate posterior probabilities from MrBayes analysis (left) and bootstrap values from RAxML analysis. Only posterior probabilities ≥0.90 and bootstrap values ≥80 are shown.

Appendix Figure S59. Maximum likelihood *trnL-trnF* spacer phylogeny of Urticaceae using Cannabaceae as outgroup. Numbers above branches indicate posterior probabilities from MrBayes analysis (left) and bootstrap values from RAxML analysis. Only posterior probabilities ≥0.90 and bootstrap values ≥80 are shown.

Appendix Figure S60. Maximum likelihood ITS phylogeny of Parietarieae using Forsskaoleae as outgroup. Numbers above branches indicate posterior probabilities from MrBayes analysis (left) and bootstrap values from RAxML analysis. Only posterior probabilities ≥0.90 and bootstrap values ≥80 are shown.

Appendix Figure S61. Plastid chronogram (*trnL-trnF* spacer & *matK*) of Urticaceae from BEAST analysis using Cannabaceae as outgroup. The calibration point based on Magallon et al. (2015; stem Urticaceae) is indicated by a black star. Bars at the nodes indicate 95% highest posterior densities, bold numbers at nodes the estimated mean ages. Numbers above branches represent posterior probabilities from MrBayes analysis, bootstrap values from RAxML analysis and posterior probabilities from BEAST analysis. Only posterior probabilities ≥0.90 and bootstrap values ≥80 are shown.

Appendix Figure S62. Ancestral area reconstruction in Parietarieae as inferred from S-DEC analysis in RASP, based on the plastid chronogram (*trnL-trnF* spacer *& matK*). Numbers at the nodes indicate posterior probabilities from BEAST analysis. Only posterior probabilities ≥0.90 are shown. On the nodes, the posterior probabilities of the estimated areas/area combinations are indicated by pie charts. Areas coded include Macaronesia (A), Mediterranean (B), Australia (C), New World (D), Non-Mediterranean Eurasia (E), Non-Mediterranean Africa (F).

Appendix Figure S63. Ancestral Area Estimation in Parietarieae under the DEC model in BioGeoBEARS; based on the *trnL-trnF* spacer & *matK* chronogram. On the nodes, the probabilities of the estimated areas/area combinations are indicated by pie charts/letters. Areas coded include Macaronesia (A), Mediterranean (B), Australia (C), New World (D), Non-Mediterranean Eurasia (E), Non-Mediterranean Africa (F).

Appendix Figure S64. Sections of lower stems of selected representatives of Parietarieae. **A** *Gesnouinia filamentosa* (transverse); **B** *G. filamentosa* (longitudinal); **C** *Parietaria judaica* (transverse); **D** *P. officinalis* (transverse); **E** *Soleirolia soleirolii* (transverse); **F** *P. debilis* (transverse).

Appendix Figure S65. Transverse sections of upper stems of selected representatives of Parietarieae (basis of a branch for *Gesnouinia arborea*): **A** *Gesnouinia filamentosa*; **B** *Parietaria judaica*; **C** *P. officinalis*; **D** *Soleirolia soleirolii*; **E** *P. debilis*; **F** *G. arborea*.

Appendix Figure S66. Maximum parsimony reconstruction (unordered) of the perennation strategy in Parietarieae using Mesquite. Coding: Therophyte (0), hemicryptophyte (1), chameophyte (2) and phanerophyte (3).

Appendix Figure S67. Maximum likelihood reconstruction (Mk1) of the habit quotient in Parietarieae using Mesquite. Coding: Herbaceous ≤ 0.28 (0), woody ≥ 0.42 (1).

Appendix Figure S68. Maximum likelihood reconstruction (Mk1) of the presence of the wood cylinder throughout the stem in Parietarieae using Mesquite. Coding: Distinct wood cylinder restricted to base (0), distinct wood cylinder in whole stem (1).

List of Appendix Tables

Appendix Table S1. Uncategorized (phylogenetically relevant) Pentaphylacaceae s.str. fruit and seed traits for statistical analysis in SPSS.

Appendix Table S2. Sampling for molecular and anatomical analyses of *Visnea*. Given is: taxon name, family, country, collector and collection number, herbarium code, lab number of the DNA (SMNS/other), GenBank accession number (ITS, *matK*, *trnL-trnF* spacer, *psbA-trnH* spacer) and the availability of MCT, microtome and hand sections (including file/sample names). Data newly generated in this study is marked in bold. Hyphens indicate missing data.

Appendix Table S3. SkyScan 1272 settings tested for the *Visnea germanica* fossils.

Appendix Table S4. Fruit and seed traits for each Pentaphylacaceae sample analyzed.

Appendix Table S5. Fruit and seed traits of Pentaphylacaceae s.str., summarized (means, minimum and maximum values, ranges of values) for each species (extant taxa) or fossil locality (*Visnea germanica* fossils). The number of fruit samples analyzed is also given.

Appendix Table S6. Sampling for molecular and anatomical analyses of *Geranium*. Given is: taxon name, family, country, collector and collection number, herbarium code, lab number of the DNA (SMNS/other), GenBank accession number (ITS, ETS, *rbcL*, *matK*, *trnL-trnF* spacer). Data newly generated in this study is marked in bold. Hyphens indicate missing data.

Appendix Table S7. Sampling for molecular and anatomical analyses of *Semele*. Given is: taxon name, family, country, collector and collection number, herbarium code, lab number of the DNA (SMNS/other), GenBank accession number (*atpB*, *ndhF*, *rbcL*, *matK*). Data newly generated in this study is marked in bold. Hyphens indicate missing data.

Appendix Table S8. Sampling for molecular and anatomical analyses of *Daucus*. Given is: taxon name (most recent and synonym), family, Apiaceae subfamily, Apiaceae tribe, clade within *Daucus*, country, collector and collection number, herbarium code, lab number of the DNA (SMNS/other), GenBank accession number (*rps16*, ITS). Data newly generated in this study is marked in bold. Hyphens indicate missing data.

Appendix Table S9. Sampling for molecular and anatomical analyses of *Phyllis*. Given is: taxon name, family, tribe within Rubiaceae, country, collector and collection number, herbarium code, lab number of the DNA (SMNS/other), GenBank accession number (*ndhF*, *rps16*, ITS). Data newly generated in this study is marked in bold. Hyphens indicate missing data.

Appendix Table S10. Sampling for molecular and anatomical analyses of *Gesnouinia*. Taxon name, country, collector and collection number, herbarium code, DNA (SMNS) and/or section number, GenBank accession numbers (ITS, *matK*, *trnL-trnF* spacer) and the part of the stem sectioned. GenBank numbers of sequences newly generated in this study are marked with an asterisk. Hyphens indicate missing data.

Appendix Table S11. Stem ages, crown ages and geographical affinities of Macaronesian laurel forest lineages based on literature and this study.

Acknowledgements

This thesis would not have been possible without the help of many people. I want to thank:

Professor Dr. Marcus A. Koch for the supervision of this thesis and for providing guidance, encouragement and support.

PD Dr. Mike Thiv for providing the opportunity to conduct this thesis at the State Museum of Natural History Stuttgart, for sharing his knowledge on the Macaronesian laurel forests and for his encouragement and advice.

Dr. Andreas Franzke, for being my third TAC member and for his feedback.

Several colleagues from the State Museum of Natural History, especially the Botany department. Many thanks to Dr. Holger Thues for advising on statistical analyses, to Paulina Kondraskov for introducing me to the lab, collecting samples and discussing laurel forest topics, to Dr. Nicole Schütz and Dr. Ursula Eberhardt for their help, company and support, to Cornelia Krause for sample collection and advice, to Dr. Arno Wörz for his counsel on identification of *Parietaria* and to Anette Rosenbauer, Christiane Dalitz and Diana Körner for preparation of the material from the fieldtrips. Furthermore, I want to thank Christiane Zeitler, Annette Schultheiss and Daniel Dick for helping with the use of the SkyScan MCT. Peter Pogoda introduced me to Stratovan and advised me on Amira. I am also grateful to PD Dr. Anita Roth-Nebelsick and Milan Pallmann for their advice on microtome sections, to Dr. Joerg Lange for setting up BEAST on the Linux server, to Anne Schilling for the lab work on *Visnea* from Madeira, to Dr. Rena Schott and Michael Haas for helping with the use of the Keyence microscope and to Raffalele Gamba for the company during many of my Keyence sessions.

Dr. Edoardo Martinetto (Torino) for providing the Italian material of *V. germanica* and for advice regarding sampling and experimental setup.

Professor Dr. Jürg Schönenberger for offering the use of his MCT to scan difficult samples, Dr. Yannick Staedler for conducting and providing the scans and Susanne Pamperl (all Vienna) for explaining Amira.

Dr. Stephan Schultka for providing me with a scan of the type specimen of *Visnea germanica* and Kerstin Mahlow (both Berlin), who conducted the scan and advised on MCT scanning of difficult objects.

Dr. Christian Bräuchler (Vienna), for providing material of *Gesnouinia* and *Parietaria* and for his input on the paper.

Dr. Alfredo Reyes-Betancort (Tenerife), for his help with the collection of *Gesnouinia filamentosa* and his advice on the paper.

Dr. Carlos Aedo (Madrid), for providing samples of and advice on *Geranium*.

Dr. Anne Heller and Erika Rücker (both Hohenheim) for the use of their facilities and providing reagents as well as protocols for embedding and sectioning.

Prof. Dr. Frederic Lens (Leiden) for discussing problems on the evolution of woodiness.

Lisa Kretz (Heidelberg), Dr. Fred Stauffer (Geneva) and Dr. Michael Gudo (Morphisto) for their suggestions to improve the micromtome sections and Technovit embedding.

Dr. Arnoldo Santos-Guerra (Tenerife), Desiree Braun, Professor Dr. Ulrich Kull (both Stuttgart) Rainer Schulz (Heidelberg), Professor Dr. Severin Irl (Frankfurt), Professor Dr. Manuel Steinbauer (Bayreuth), Dr. Alexander Seregin (Moscow), Professor Dr. Arne

Anderberg (Stockhom), Dr. Sachiko Nishida (Nagoya), Dr. Eileen Power (Dublin), Professor Dr. Miguel Menez de Sequeira (Madeira) and Victoria Troschkina (Novosibirsk) for collecting or helping to collect samples and the local authorities on the Canary Islands for providing collection permits.

Dr. Mario Mairal (Stellenbosch), Professor Dr. Gudrun Kadereit (Mainz) and her working group, especially Dr. Maximilian Lauterbach and Dr. Katharina Bohley, and several people I met at conferences for their company, advice and input.

The curators of the herbaria B, BR, CAS, FI, FTG, JVC, M, MA, MEL, RO, STU and W as well as the Botanical Garden Rome Material for providing material.

A lot of people accompanied me on my way and cheered me up during hard times. I want to thank all of you. To my friends from school (Claudia, Eva, Katharina, Kristin, Sabine, Sibylle, Michael): You are amazing! Thank you so much for being still there after all those years! To all of my friends from Stuttgart, especially Lisa, Sara and Lennart: Thank you for being there, believing in me and motivating me! I am truly glad that we met!

And last but not least my family (my parents Hans-Dieter and Gabi, my siblings Eva and Michael). I could not have done this without you. Thank you for your constant love and support! To my mother, who did not get to see the end of this journey: This one is for you.